The clinical relevance of pigment epithelium-derived factor (PEDF) in wound healing and colorectal cancer

Rhiannon Harries

Thesis submitted to Cardiff University for the degree of

Doctor of Medicine (MD)

Acknowledgements

Firstly, I am extremely grateful to both the Royal College of Surgeons of England and the Welsh Wound Innovation Centre for kindly support the work undertaken within this MD, through a research grant. Huge thanks to Professor Jared Torkington and Professor Keith Harding, two of my research supervisors for starting this journey with me so many years ago and for their unwavering mentorship throughout. A special thank you to Mr Martyn Coomer, Head of Royal College of Surgeons of England Research Department for affording me this incredible opportunity as Royal College of Surgeons of England research fellowship.

I would also like to thank my research supervisors, Dr Jun Cai and Professor Wen Jiang for all their support. Thank you to Dr Sioned Owen, Dr Andy Sanders and Miss Fiona Ruge for continual helping a 'non-scientist' out when I was lost in the lab. To John Watkins, Statistician for statistical advice. To Dr Meleri Morgan, Consultant Pathologist for her kind guidance with the reviewing of immunohistochemical staining of the colorectal tissues.

To Aled, my fellow Research buddy, for all the entertainment and for keeping me sane!

And finally, to my grandmother Jean, who has always been my biggest supporter, and to my parents for always being there.

Publications

RL Harries, KG Harding. Management of Diabetic Foot Ulcers. Curr Geri Rep 2015. DOI 10.1007/s13670-015-0133-x

RL Harries, J Torkington, KG Harding. Advances in Acellular Extracellular Dermal Matrices in Wound Healing. In Skin Tissue Engineering and Regenerative Medicine, Academic Press, Elsevier. 2015. ISBN 978-0-12-801654-1

RL Harries, D Bosanquet, KG Harding. Wound Bed Preparation; TIME for an update. Int Wound J 2016; 13 Suppl 3:8-14.

RL Harries, S Owen, F Ruge, J Li, Z Zhang, M Morgan, KG Harding, J Torkington, J Cai, W Jiang. Impact of Pigment epithelial derived factor (PEDF) on colorectal cancer *in vitro* and *in vivo.* Oncotarget 2017; in submission

RL Harries, R Jones, J Torkington. A review of the role of target therapies in the management of colorectal cancer. Colorectal Dis 2017; in submission

Presentations

RL Harries, J Cai, J Li, S Owen, K Harding, J Torkington, W Jiang. Expression of pigment epithelium-derived factor in colorectal cancer. Gut 2015; 64(Suppl 1): A554.1-A554. DOI:10.1136/gutjnl-2015-309861.1215

Poster presentation at Digestive Disorders Federation 2015, London, June 2015.

RL Harries, S Owen, F Ruge, J Cai, J Torkington, K Harding, W Jiang. Expression of PEDF in wound healing cells. Anticancer Research 2015; 35: 4366.

Poster presentation at China- UK Cancer Conference, Cardiff, July 2015

Poster presentation at Wound Healing Society International Congress, San Antonio, Texas April 2015

RL Harries, F Ruge, S Owen, J Cai, J Torkington, W Jiang, K Harding. The role of pigment epithelium-derived factor in wound healing.

Oral presentation at Welsh Surgical Society Spring Meeting 2016, Bangor, April 2016

RL Harries, J Cai, F Ruge, M Morgan, KG Harding, J Torkington, WG Jiang. Expression of pigment epithelium derived factor (PEDF) within colorectal cancer tissue using immunohistochemistry. Colorectal Dis 2016; 18(S1):80

Poster presentation at European Society of Coloproctology 2016 Conference, Milan, Sept 2016

RL Harries, J Cai, S Owen, KG Harding, J Torkington, WG Jiang. The role of pigment epithelium derived factor (PEDF) on cellular function in colorectal cancer cells. Colorectal Dis 2016; 18(S1):80

Poster presentation at European Society of Coloproctology 2016 Conference, Milan, Sept 2016

RL Harries. Essential genetics for colorectal surgeons.

Invited Speaker at International Colorectal Forum, Villars Switzerland, January 2017

Abbreviations

ABS- antibiotics

Bps- base pairs

BSS- balanced saline solution

cDNA- complementary deoxyribonucleic acid

CI- confidence intervals

c-Mi- c-Met inhibitor

DEPC- diethyl pyrocarbonate

DF- primary dermal fibroblasts

DMEM- Dulbecco's modified eagles medium

DMSO- dimethyl sulpoxide

DNA- Deoxyribonucleic acid

ECIS- electric cell-substrate impedance sensing

ECM- extracellular matrix

EDTA- ethylenediaminetetracetic acid

ECOG- Eastern Cooperative Oncology Group

EGF- epidermal growth factor

EGFR- epidermal growth factor receptor

EGTA- ethylene glycol-bis(2-aminoethylether)-N,N,N',N'-tetraacetic acid

ELISA- enzyme-linked immunosorbent assay

EPC1- early population double level cDNA-1

FAK- focal adhesion kinase

FAKi- focal adhesion kinase inhibitor

FCS- foetal calf serum

FGFb- basic fibroblast growth factor

FGFR- fibroblast growth factor receptor

FITC- fluorescein isothiocyanate

FOLFIRI- 5-Fluorouracil (5-FU), combined Leucovorin, and Irinotecan chemotherapy regime

FOLFOX- 5-Fluorouracil (5-FU), Folinic acid and Oxaliplatin chemotherapy regime

FU/LV- 5-Fluorouracil (5-FU) and Leucovorin chemotherapy regime

HASC- human adipose-derived stem cells

HECV- human endothelial vascular cell line

HGF- hepatocyte growth factor

HR- hazard ratio

H_20_2- hydrogen peroxide

IQR- interquartile range

KCl- potassium chloride

KH_2PO_4- potassium phosphate monobasic

KRAS- kirsten rat sarcoma

Met- hepatocyte growth factor receptor

mIFL- Bolus 5-Fluorouracil (5-FU), Leucovorin, and Irinotecan chemotherapy regime

MMPs- matrix metalloproteinases

mRNA- messenger ribonucleic acid

MVD- microvessel density

NaCl- sodium chloride

Na_2HPO_4- sodium phosphate dibasic

NaOH- sodium hydroxide

NHS- National Healthcare System

OR- odds ratio

PCR- polymerase chain reaction

PDGF- platelet derived growth factor

PDGFR- platelet derived growth factor receptor

PEDF-pigment epithelium derived factor

PLGF- placental growth factor

PLGFR- placenta growth factor receptor

PMSF- phenylmethylsulfonyl fluoride

PPAR- peroxisome proliferator-activated receptor

PVDF- polyvinylidene difluoride

QoL- quality of life

qPCR- quantitative polymerase chain reaction

RNA- ribonucleic acid

RT-PCR- reverse transcription polymerase chain reaction

RT- reverse transcription

SDS- sodium dodecyl sulphate

SDS-PAGE- sodium dodecyl sulphate polyacrylamide gel electrophoresis

SEM- standard error of the mean

TBE- tris-boric acid EDTA

TBS- tris buffered saline

TBST- tris buffered saline with Tween 20

TEMED- tetramethylethylenediamine

TIE-2- angiopoietin 1 receptor

TNF- α- tumour necrosis factor - α

TGF- β- transforming growth factor- β

VEGF- vascular endothelial growth factor

VEGFR- vascular endothelial growth factor receptor

XELOX- Capecitabine and Oxaliplatin chemotherapy regime

Summary

There are similarities between tissue repair and cancer development. Epithelial tumours promote the formation of the stroma by activation of the wound healing process, but unlike healing wounds the process is not self-limiting. Pigment epithelium derived factor (PEDF) is a secreted glycoprotein that has been shown to exhibit multiple biological properties including anti-angiogenesis, anti-tumorigenesis and immune-modulation. Previous studies demonstrated that PEDF expression is downregulated as prognostic factors worsen in a range of cancers and chronic inflammatory conditions and treatment with recombinant PEDF has showed some benefit in cellular functional models. However, there has been little evidence to date to assess the role of PEDF in colorectal cancer and wound healing. The aims of this study were to elucidate more detailed regulatory mechanisms of PEDF in wound healing, and tumour angiogenesis in colorectal cancer and provide evidence to develop PEDF or its fragments as therapeutics for wound healing or colorectal cancer treatment.

This study found that PEDF expression was downregulated in colorectal cancer cell lines and tissue and that treatment with recombinant PEDF resulted in significant decreases in the rate of colorectal cancer cellular migration and invasion and an increase in cellular adhesion in some colorectal cancer cell lines examined, suggesting a promising role of the treatment of PEDF in the prevention of colorectal cancer metastatic spread.

Within wound healing, our results indicated that PEDF expression was high amongst dermal fibroblasts but less so in keratinocytes and endothelial cell lines, suggesting

that fibroblasts are responsible for secretion of PEDF in response to inflammation. In cellular functional models, recombinant PEDF treatment significantly increased the migration of keratinocytes, suggesting a possible role as a chronic wound treatment.

Further studies are warranted to assess the role of PEDF in a range of colorectal cancer subsets, other wound healing cells and animal models to identify a suitable delivery vector.

List of Figures

List of Tables

Contents

Chapter 1

General Introduction

1.1 The similarities between wound repair and cancer development

1.1.1 Wound healing process

The wound healing process takes place as a series of complex interactions between epidermal cells, dermal cells, the extracellular matrix (ECM) and plasma controlled proteins and is controlled by cytokines and growth factors (Harding et al. 2002; Gurtner et al. 2008; Haertel et al. 2014). The stages of the wound healing process, which often overlap in time and space, are described below and summarised in Figure 1.1.

1. Injury and Coagulation Stage.

Initial injury causes leakage of blood constituents to fill the wound space. Neuronal reflex mechanisms cause rapid constriction of injured vessels by contraction of vascular smooth muscle cells, and endothelial cells, platelets and coagulation factors interact, to achieve haemostasis. Platelets trapped within the fibrin rich wound clot, composed of fibronectin, vitronectin, fibrin and thrombospondin, trigger an inflammatory response by the release of vasodilators, (e.g. serotonin), cytokines, (e.g. tumour necrosis factor- α (TNF- α), transforming growth factor- β (TGF- β)), and growth factors, (e.g. vascular endothelial growth factor (VEGF), platelet-derived growth factor (PDGF), and basic fibroblast growth factor (FGFb)), and finally, activation of the complement cascade (Coppinger et al. 2004; Golebiewska & Poole. 2015).

2. Inflammation Stage.

Within a few hours following injury, various leukocytes infiltrate the wound space. Polymorphonuclear neutrophils, activated by pro-inflammatory cytokines such as TGF- β, remove bacteria and debride devitalised tissue, via a release of antimicrobial substances and proteases (Weiss. 1989; Su & Richmond. 2015). Polymorphonuclear neutrophils are also responsible for the release of pro-angiogenic factors such as VEGF-A, and therefore are an important trigger for wound angiogenesis (Schruefer et al. 2006). Following this, macrophages, the majority recruited from blood, predominate in the wound regulated by a number of different chemotactic factors including growth factors, chemokines and pro-inflammatory cytokines, which are all released by platelets, hyperproliferative keratinocytes, fibroblasts and leukocytes subsets themselves (Wetzler et al. 2000; Bodnar. 2015). Macrophages in turn, release soluble mediators including the growth factors VEGF-A, PDGF, FGFb and TGF- β, to promote angiogenesis, cellular proliferation and synthesis of the extra cellular matrix (ECM) (DiPietro & Polverini. 1993; Eming et al. 2017). Mast cells are also an important source of pro-inflammatory mediators and cytokines in wound healing (Reed et al. 1995; Haertel et al. 2014; Eming et al. 2017).

3. Proliferation Stage.

Neovascularisation begins to occur in the fibrin rich wound clot. This is in direct response to soluble mediators being released by macrophages during the inflammation stage as described above. Activated endothelial cells respond by retracting and reducing cell junctions, and escaping from their embedded endothelium (Greaves et al. 2013). The macrophages, mast cells and endothelial cells themselves secrete proteases to break down existing basal lamina. The breakdown

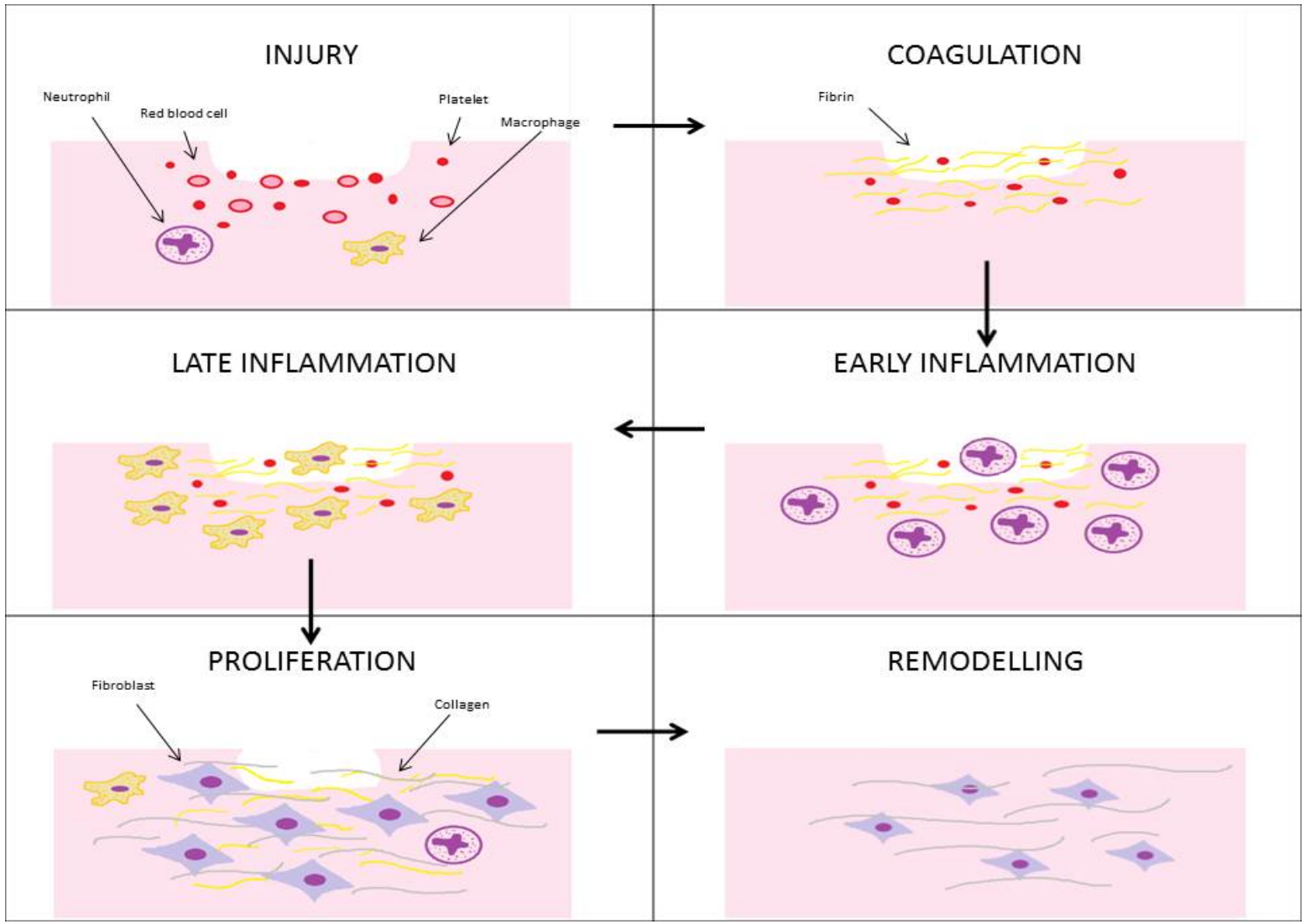

Figure 1.1. Wound healing process. Diagrammatic representation of the phases of wound healing.

of the endothelial basement membrane allows detached endothelial cells from pre-existing capillaries to migrate chemotactically towards the wound and lay down new vessels (Greaves et al. 2013). The wound microenvironment of hypoxia and acidosis aids this process. Following angiogenesis, fibroblasts contribute to the production of the ECM and ultimately differentiate into myofibroblasts; this stage is characterised clinically with the formation of granulation tissue (Greaves et al. 2013). Matrix metalloproteinases (MMP's) are responsible for the degradation of the existing ECM (Eming et al. 2014). However excessive protease levels can lead to degradation of the same growth factors that are required to stimulate keratinocytes and is a common reason for chronicity of a wound. Keratinocytes proliferate and migrate across the wound bed resulting in re-epithelialisation, via synthesis of proteases and components of the basal lamina (Gurtner et al. 2008).

4. Remodelling Stage.

After closure of the wound, remodelling of the resulting scar takes place over a number of months (Gurtner et al. 2008).

1.1.2. Angiogenesis

Angiogenesis is a complex process through which new blood vessels form from pre-existing vessels and is regulated by an interacting balance between pro-angiogenic and anti-angiogenic molecules (Ribatti. 2006; Carmeliet & Jain 2011). The two main forms of angiogenesis are sprouting and intussuscepting.

Sprouting angiogenesis occurs when angiogenic growth factors, such as vascular endothelial growth factor (VEGF), activate receptors on endothelial cells present in

pre-existing blood vessels (Figure 1.2) (Ribatti & Crivellato. 2012). The activated endothelial cells release proteases that degrade the basement membrane to allow the endothelial cells to escape vessel walls. Endothelial cells then proliferate into the surrounding matrix and form solid sprouts connecting neighbouring vessels. As sprouts extend towards the source of the angiogenic stimulus, endothelial cells migrate in tandem and the sprouts form the vessel lumen.

Intussuscepting (or splitting) angiogenesis occurs when a new blood vessel is formed by splitting an existing one (Figure 1.3) (Makanya et al. 2009). Essentially this consists of opposing capillary walls protruding into the lumen of the vessel and creation of a contact zone between the endothelial cells. Following the central perforation of the cellular bilayer, the fused endothelial cells form a transluminal cuff, which become invaded by myofibroblasts and pericytes.

In normal physiological conditions, angiogenesis occurs primarily in embryonic development, in response to ovulation and in the normal wound healing process (Folkman 1971). However, in pathological conditions the steady state of the angiogenesis system is disrupted and endothelial cells of the microvasculature proliferate, migrate, and form new but leaky vessels that can invade the tissue (Folkman 1971; Carmeliet & Jain 2011). Pathological angiogenesis has been implicated in a range of diseases including psoriasis, age-related macular degeneration, diabetic retinopathy and in particular cancer (Heidenreich et al. 2009; Ng et al. 2005; Crawford et al. 2009; Folkman 1971; Carmeliet & Jain 2011). Angiogenesis is a crucial.

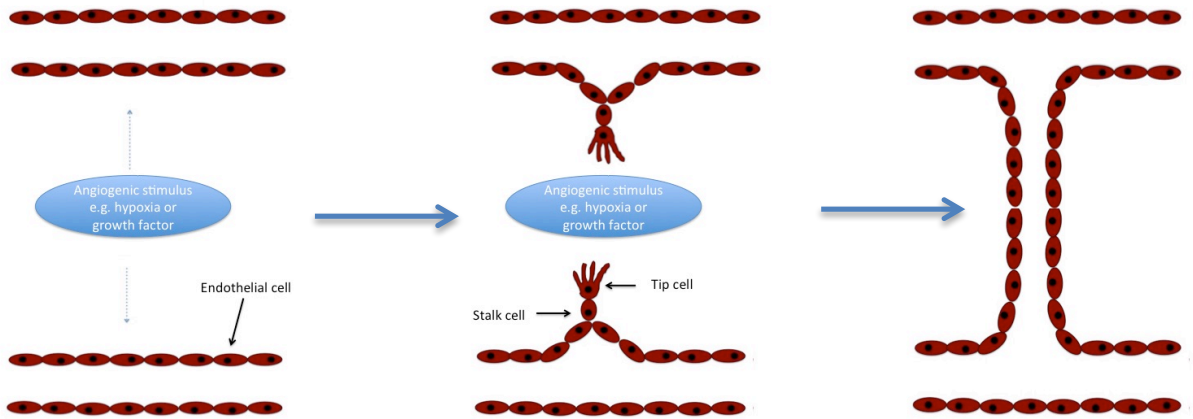

Figure 1.2 Sprouting angiogenesis

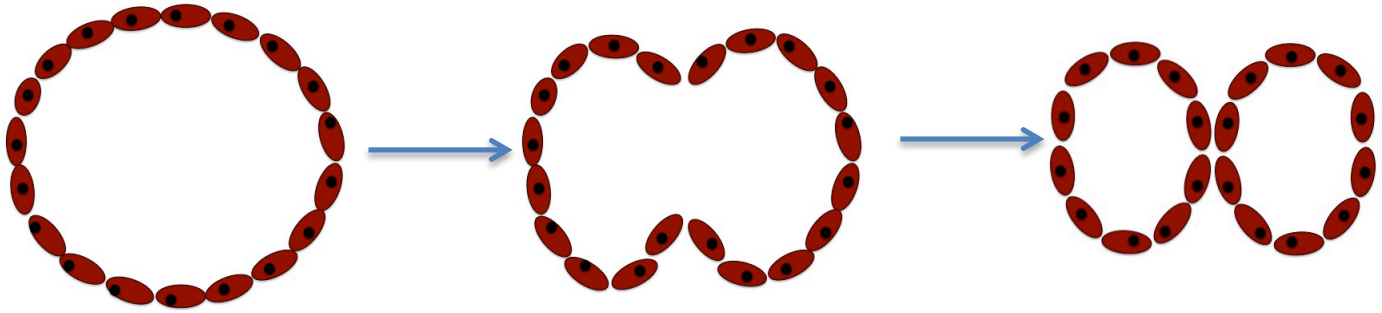

Figure 1.3 Intussuscepting angiogenesis

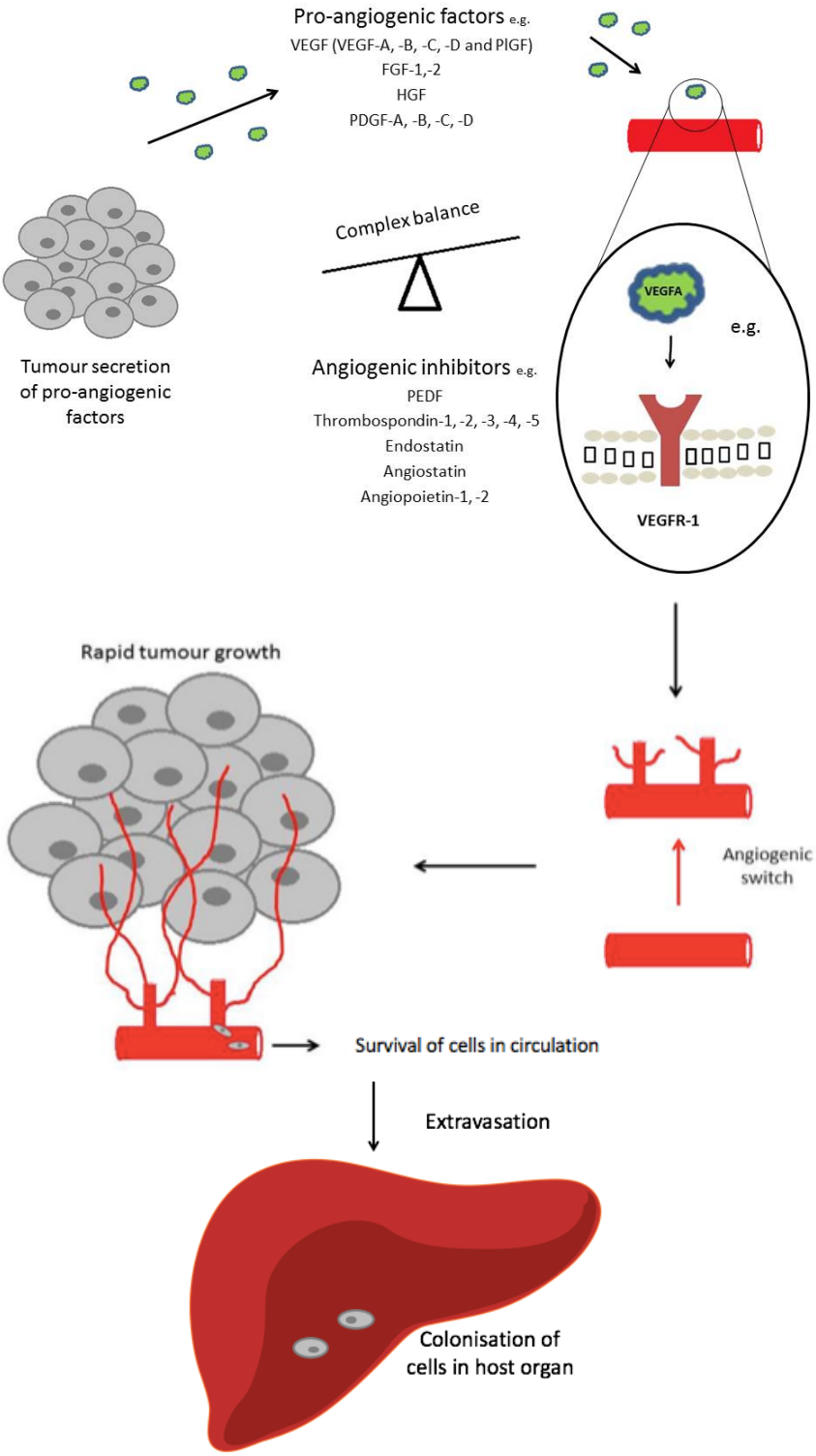

Figure 1.4 Endogenous regulating factors of angiogenesis in tumour growth and metastases

event necessary for the growth and invasion of solid tumours and subsequent metastatic spread (Figure 1.4) (Folkman 1995; Carmeliet & Jain 2011)

1.1.3 Cancer as an over-healing wound

It has long been acknowledged that there is a link between chronic inflammation and malignant transformation (Virchow. 1863), with a variety of clinical observations that malignant changes can occur in the presence of chronic inflammatory conditions, such as *Helicobacter pylori* related oesphagogastric inflammation, ulcerative colitis and chronic hepatitis (Dunham. 1972). These clinical observations reinforced the hypothesis that there must be similar cellular mechanisms in both tissue repair and cancer development. In 1972, Haddow postulated that 'tumour production is a possible over-healing' (Haddow. 1972). It was later recognised that the composition of the stroma of a tumour was remarkably similar, to the granulation tissue of healing skin wounds (Dvorak. 1986). Both skin wounds and tumour tissue are characterised by the presence of a fibrin clot, inflammatory cells, newly formed blood vessels and high number of migrating and proliferating fibroblasts (Schäfer et al. 2008). The deposition of fibrin and fibronectin matrix is an acute event within normal wound healing related to mechanically injured blood vessels. In contrast it is a chronic event in tumour proliferation secondary to hyper-permeability of tumour vessels releasing plasma proteins (Dvorak. 1986; Hanahan & Weinburg. 2011). Inflammatory cells such as macrophages, produce inflammatory cytokines during both wound repair and tumorigenesis. In established tumours, these tumour derived cytokines promote the differentiation of macrophages to the M2 phenotype, which stimulate both angiogenesis and ECM breakdown by producing growth factors and MMPs, which in

turn further induce tumorigenesis (Allavena et al. 2008; Hanahan & Weinburg. 2011). They also release mediators, such as reactive oxygen species and reactive nitrogen species that can directly damage DNA and alter proteins that regulate cell cycle control and apoptosis (Allavena et al. 2008; Hanahan & Weinburg. 2011). However, the main contrast between tumours and wounds is related to the invasive growth of the transformed keratinocytes (Schäfer et al. 2008). As discussed in section 1.1.2, angiogenic processes are also similar between both wound repair and tumorigenesis, however the tight control regulating the balance of pro- and anti-angiogenic molecules is disrupted. It is also accepted that the prolonged presence of myofibroblasts at wound sites can result in the formation of hypertrophic or keloid scars, and that large numbers of myofibroblasts are found in tumours at advanced stages, reinforcing the link between exaggerated healing and cancer (Radisky et al. 2007; Albini & Sporn. 2007; Schäfer et al. 2008).

In summary, epithelial tumours promote the formation of the stroma by activation of the wound healing process but, unlike healing wounds, the process is not self-limiting in tumour formation and results in uncontrolled cell proliferation, invasion and metastasis.

1.2 PEDF

Pigment epithelium-derived factor (PEDF), also known as early population double level cDNA-1 (EPC1), is a secreted glycoprotein. It was first identified when Tombrank-Tink's group were studying human retinal cell development. They found a factor that was secreted by the human foetal retinal pigment epithelial cells and

showed it to be a potent neurite promoting factor (Tombran-Tink et al. 1991). The identified 50kDa neurotrophic protein was first referred to as RPE-54 (retinal pigmented epithelium-54) before officially being named PEDF.

Subsequently, the same group performed laboratory sequencing and found PEDF to be a member of the serpin gene family (Steele et al. 1993). Serpins, with most being serine protease inhibitors are a group of proteins that have a common three-dimensional structure which act by inhibiting proteolysis action (Carrell & Travis. 1985). However, some members of the serpin gene family, including PEDF, do not have demonstrable serpin protease inhibitory activity and belong to a sub-group of non-inhibitory serpins. It is hypothesised that this sub-group have lost the protease inhibitory actions but gained additional properties via evolution, many of which have been demonstrated to exhibit neurotrophic effects.

Tombran-Tink later localised the gene encoding PEDF (SERPINF1) to the chromosome 17p13.1 (Tombran-Tink et al. 1994). The gene encodes a 418-amino acid protein, consisting of 8 exons and 7 introns, with an mRNA transcript of approximately 1.5kb (Tombran-Tink et al. 1994; Xu et al. 2006). PEDF was found to be closely related to several cancer genes including the tumour suppressor gene p53 (Tombran-Tink et al. 1994), which is the most frequent target gene for genetic alterations in human cancers (Hollstein et al. 1997). To date, the PEDF gene has only been detected in vertebrates. Tombran-Tink's group suggested their findings of the expression and lack of expression in undifferentiated and differentiated human retinoblastoma cells, respectively, alongside neurotrophic activity, may mean that PEDF might be linked to proliferative events resulting in final phenotypic determination. There has since been

evidence that PEDF is pleotropic with multiple biological properties including neuroprotective, anti-angiogenic, anti-tumorigenic and immune-modulating (Becerra et al. 2013; Zhang et al. 2006b).

1.3 The role of PEDF in angiogenesis

PEDF has been demonstrated to be one of the most potent natural inhibitors of angiogenesis, more so than angiostatin, endostatin and thrombospondin-1 (Dawson et al. 1999; Duh et al. 2002). PEDF exerts anti-angiogenic activities by arresting endothelial cell proliferation and migration, and has been shown to occur even in the presence of VEGF (Dawson et al. 1999; Volpert et al. 2002; Bouck 2002). The mechanisms of action appear to be multifactorial (Figure 1.5). It is suggested that the underlying mechanism of PEDF biological effects on endothelial cells involve a complex cross talk between the signal events triggered by both pro-angiogenic and anti-angiogenic molecules. It has been proven that PEDF upregulates gamma secretase effects, which in turn leads to cleavage of the vascular endothelial growth factor receptor (VEGFR) transmembrane domain, thereby limiting VEGF signalling and inhibiting angiogenesis (Cai et al. 2006). Evidence also supports the concept that PEDF upregulates thrombospondin-1 and thrombospondin-2 and downregulates basic fibroblast growth factor (FGFb) and MMP-9 (Guan et al. 2004), and finally that PEDF expression is upregulated by angiostatin and downregulated by hypoxia (Yang et al. 2006; Gao et al. 2002). Interestingly, PEDF's activity appears to be selective in targeting only new vessel growth and spares the pre-existing vasculature (Bouck 2002). It also appears to induce peroxisome proliferator-activated receptor (PPAR)-gamma expression, which downstream induces p53, which is involved in cell cycle

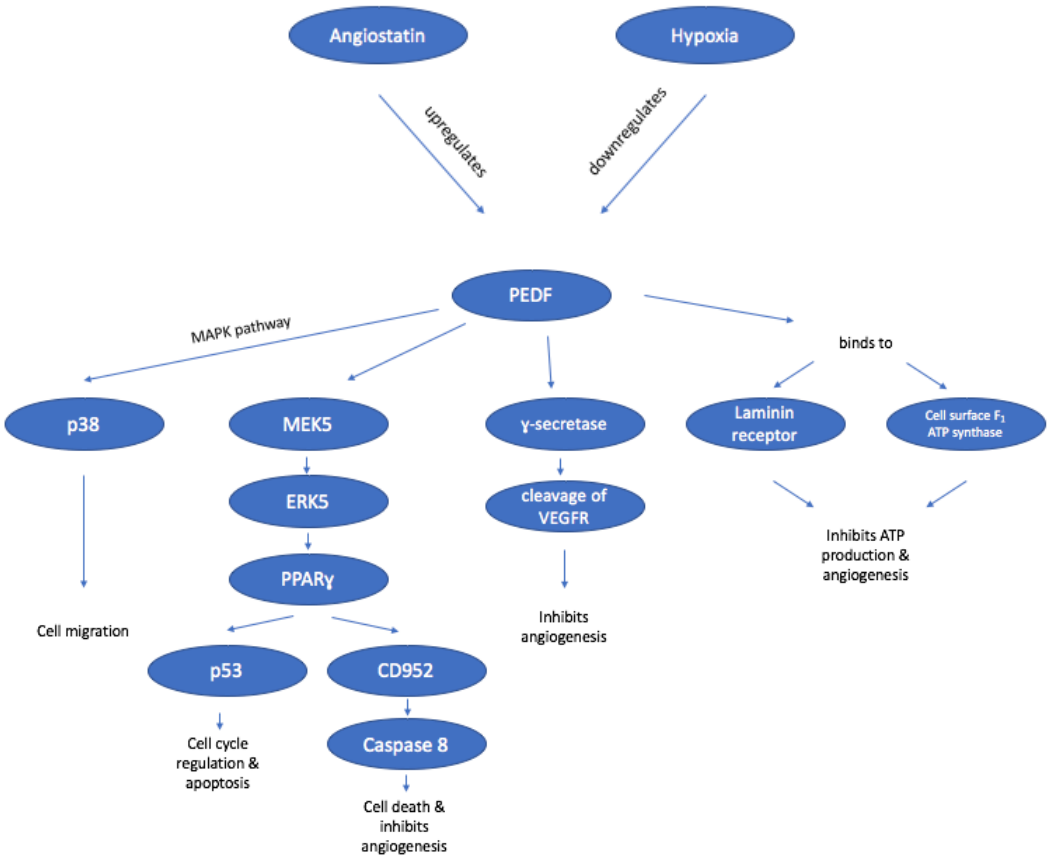

Figure 1.5. Mechanisms of action of PEDF

regulation and apoptosis (Ho et al. 2007). PEDF selectively induces endothelial cell apoptosis in actively remodelling vessels via Fas/FasL death receptor signalling (Zaichuk et al. 2004; Elayappan et al. 2009).

It has been demonstrated that the 34-mer fragment of PEDF (residues 24-57) exhibits the anti-angiogenic effects and the 44-mer fragment (residues 58-101) the neurotrophic effects (Filleur et al. 2005), highlighting that different fragments of PEDF seem to be responsible for different activities.

To date, the anti-angiogenic activity of PEDF has been largely studied in ocular neovascularization. However, PEDF has been found to be expressed extracellularly in blood and cerebrospinal fluid (Petersen et al. 2003; Kuncl et al. 2002), and a range of other tissues including the central nervous system, skeletal muscle, liver, heart, testis, stomach, ovaries, prostate, colon (Rychil et al. 2010; Matsumoto et al. 2004; Tombran-Tink et al. 1996; Sawant et al. 2004; Browne et al. 2006; Cheung et al. 2006; Bilak et al. 1999). Moreover, PEDF has been implicated in a plethora of pathological conditions including diabetic complications, psoriasis, liver cirrhosis and cancer (Matsumoto et al. 2004; Abe et al. 2010; Ogata et al. 2007; Zhu et al. 2012; Becerra et al. 2013).

1.4 Colorectal Cancer

1.4.1 The role of anti-angiogenic therapies in colorectal cancer

Colorectal cancer is the fourth commonest cancer in the UK, with an incidence of approximately 41,000 new cases in 2013 and an estimated 1.36 million diagnosed globally in 2012 (Cancer Research UK. 2016; http://www.cancerresearchuk.org).

There have been many advances in both the detection and management of colorectal cancer over recent decades, including the improvement of radiological imaging, bowel cancer screening programmes, chemotherapy and radiotherapy regimes and surgical techniques, such as total mesorectal excision for low rectal tumours. Despite these improvements in management the overall 5 year survival rate in the UK is only 58.7% (Cancer Research UK. 2016; http://www.cancerresearchuk.org). It is for this reason that the search for novel therapies for the treatment of colorectal cancer is imperative.

As the role of angiogenesis was established in tumour proliferation and metastasis, Folkman proposed the concept that proteins that display anti-angiogenic actions, may have a potential role in cancer therapeutics (Folkman. 1995). This subsequently led to the development of a range of agents targeting differing factors or pathways in the complex balance of angiogenic promoters and inhibitors (Table 1.1).

It is recognised that primary colonic tumours with metastasis are associated with increased expression of VEGF and increased vascular density when compared to those without metastasis or benign adenomas, and that the invasive edge of the colonic tumour contains a higher vascular density than other areas of the tumour indicating the role of VEGF in tumour metastatic spread (Takahashi et al. 1995). It was initially recognised that the VEGF ligand VEGF-A is a key driver of sprouting angiogenesis and can be overexpressed in a number of solid tumours, and in particular, colorectal cancer (Ellis et al. 2008). Early work involving a murine monoclonal antibody directed against VEGF proved that it recognised all VEGF isoforms and potently and reproducibly inhibited the proliferation of human tumour

Table 1.1 Anti-angiogenic therapies proposed in the treatment of metastatic colorectal cancer and their mechanisms of action

Anti-angiogenic therapy	Mechanism of action
Aflibercept	Binds to VEGF ligands (VEGF-A, VEGF-B and PLGF))
Bevacizumab	Binds to VEGF ligand (VEGF-A)
Brivanib	VEGFR and FGFR tyrosine kinase inhibitor
Cediranib	VEGFR tyrosine kinase inhibitor
Cetuximab	EGFR inhibitor
Erolotinib	EGFR tyrosine kinase inhibitor
Panitumumab	EGFR inhibitor
Ramucirumab	Binds to VEGFR2
Regorafenib	VEGFR, PDGFR, FGFR and TIE-2 tyrosine kinase inhibitor
Sunitinib	VEGFR and PDGFR tyrosine kinase inhibitor
Vatalanib	VEGFR and PLGFR tyrosine kinase inhibitor

EGFR- epidermal growth factor receptor; PDGFR- platelet derived growth factor receptor; PLGFR- placenta growth factor receptor; FGFR- fibroblast growth factor receptor; TIE-2- angiopoietin 1 receptor; VEGF- vascular endothelial growth factor; VEGFR- vascular endothelial growth factor receptor

cell lines in nude mice (Kim et al. 1992; Warren et al. 1995; Borgstrom et al. 1996). However the significant immune response elicited with murine antibodies prevented its use in humans (Schroff et al. 1985). In 1997, Presta *et al* (1997) reported on their work on a humanised monoclonal antibody directed against VEGF, in order to limit the anti-human globulin response. Few of these humanised monoclonal antibody anti-angiogenic therapies have been proven to have clinical benefit in colorectal cancer patients. One of the first reported randomised clinical trial of the use of the anti-VEGF-A therapy Bevacizumab (Avastin®) in humans was published in 2003 (Kabbinavar et al. 2003). This phase II trial randomised metastatic colorectal cancer patients to receive either treatment with Bevacizumab 10mg/kg every two weeks plus chemotherapy (FU/LV), Bevacizumab 5mg/kg every two weeks plus chemotherapy or chemotherapy alone. Their results demonstrated a significantly higher response rate with the 5mg/kg treatment dose of Bevacizumab plus chemotherapy when compared to chemotherapy alone, and an increased progression-free survival in both of the Bevacizumab treatment groups. The authors did however note the side effects seen in the patient group including thromboembolic complications and bleeding, but concluded that the safety profile was acceptable as a therapeutic option. The findings of increased progression-free survival with the combined use of Bevacizumab plus chemotherapy when compared to chemotherapy alone, as well as overall survival, were confirmed in a Phase III randomised control trial the following year (Hurwitz et al. 2004). Following these publications, Bevacizumab in combination with Fluoropyrimidine-based chemotherapy was given a UK marketing authorisation for the treatment of patients with metastatic carcinoma of the colon or the rectum. More recently, there has been

a plethora of evidence to support the use of Bevacizumab in combination with standard chemotherapy, in selected patients for the treatment of metastatic colorectal cancer (Table 1.3 and 1.4), as well as metastatic breast cancer, (Miller et al. 2005), renal cancer (Yang et al. 2003) and non-small cell lung cancer (Sandler et al. 2006). However, there is currently a lack of evidence to support the use of Bevacizumab as an adjuvant treatment in non-metastatic colorectal cancer (Table 1.2).

Despite the increasing publication of evidence for the use of Bevacizumab in the treatment of metastatic colorectal cancer, in 2010 the National Institute of Health and Care Excellence (NICE) issued guidance that did not support the use of Bevacizumab in colorectal cancer within the UK (NICE. 2010). This decision was based on several criteria. Firstly, the use of FOLFIRI as first line chemotherapy has declined within the UK, in favour of chemotherapy agents with better clinical efficacy and lower adverse effects; therefore, studies using FOLFIRI should not been considered as gold standard as a comparator to novel therapies. Secondly, concerns arose over the robustness of the NO16966 study design which included only patients with Eastern Cooperative Oncology Group (ECOG) performance status of 0 or 1, therefore making difficulties in comparing with the UK metastatic colorectal cancer cohort who are typical older and frailer, and when performing a secondary analysis of the data it showed only a statistical significant increase in progression-free survival but not overall survival (Saltz et al. 2008). NICE concluded that whilst the first-line treatment of metastatic colorectal cancer, Bevacizumab in combination with Oxaliplatin-containing regimens gave a modest clinical benefit compared with regimens without

Table 1.2 Phase III randomised controlled trials assessing the use of anti-angiogenic agents in adjuvant treatment of non-metastatic colorectal cancer

Bevacizumab

Trial identifier and reference	Treatment	Trial results
AVANT (de Gramont et al. 2012)	Bevacizumab + FOLFOX-4 vs. Bevacizumab + XELOX vs. FOLFOX-4 Adjuvant treatment in patients with high-risk Stage 2 or curatively resected Stage 3 colon cancer N=3451	No difference in disease-free survival Potential detrimental effect on overall survival seen with Bevacizumab treatment arms compared to control
NSABP C-08 (Allegra et al. 2013)	Bevacizumab + FOLFOX-6 vs. FOLFOX-6 Adjuvant treatment in patients with Stage 2-3 colon cancer N=2673	No difference in disease-free or overall survival
QUASAR 2 (Kerr et al. 2016)	Bevacizumab + Capecitabine vs. Capecitabine Adjuvant treatment in patients with high-risk Stage 2 or curatively resected Stage 3 colon cancer N=1941	No difference in disease-free survival

Cetuximab

Trial identifier and reference	Treatment	Trial results
N0147 (Alberts et al. 2012)	Cetuximab + mFOLFOX-6 vs. mFOLFOX-6 Adjuvant treatment in patients with curatively resected Stage 3 wild-type KRAS colon cancer N=2686	No difference in disease-free or overall survival
PETACC-8 (Taieb et al. 2014)	Cetuximab + FOLFOX-4 vs. FOLFOX-4 Adjuvant treatment in patients with curatively resected Stage 3 colon cancer N=2559	No difference in disease-free or overall survival

FOLFOX- Fluorouracil (5-FU), Folinic acid and Oxaliplatin; XELOX- Capecitabine and Oxaliplatin

Table 1.3 Phase III randomised controlled trials assessing the use of anti-angiogenic agents in the first line treatment of metastatic colorectal cancer

Bevacizumab

Trial identifier and reference	Treatment	Trial results
AVF2107 (Hurwitz et al. 2004)	Bevacizumab + FOLFIRI vs. FOLFIRI N=813	Increased progression-free survival in favour of Bevacizumab arm (median 10.6 vs. 6.2 months, HR 0.54; p<0.001) Increased overall survival in Bevacizumab arm (median 20.3 vs. 15.6 months, HR 0.66; p<0.001) Increased response rate in favour of Bevacizumab arm (44.8% vs. 32.6%; p=0.004)
NO16966 (Saltz et al. 2008)	Bevacizumab vs. placebo combined with XELOX or FOLFOX-4 N=1401	Increased progression-free survival in favour of the Bevacizumab arm (median 9.4 vs. 8.0 months, HR 0.83 97.5% CI 0.72-0.95; p=0.0023) No difference in overall survival or response rate
(Stathopoulos et al. 2010)	Bevacizumab + FOLFIRI vs. FOLFIRI N= 222	No difference in overall survival or response rate
MAX (Tebbutt et al. 2010)	Capecitabine vs. Bevacizumab + Capecitabine vs. Mytomycin + Bevacizumab + Capecitabine N=471	Increased progression-free survival with the addition of Bevacizumab (with or without the addition of Mytomycin (Median 8.5 (CB)/. 8.4 (CBM) vs. 5.7 (C) months, HR 0.61 95% CI 0.50-0.72, p<0.001) No difference in overall survival or response rate with the addition of Bevacizumab
ARTIST (Guan et al. 2011)	Bevacizumab + mIFL vs. mIFL N=214	Increased progression-free survival in favour of the treatment arm (median 8.3 vs. 4.2 months, HR 0.44 95% CI 0.31-0.63; p<0.001) Increased overall survival in favour of treatment arm (median 18.7 vs. 13.4 months, HR 0.62 95% CI 0.41-0.95; p=0.014) Increased response rate with treatment arm (35% vs. 17%, p=0.013)
AIO KRK-0306 (Stintzing et al. 2012)	Bevacizumab + FOLFIRI vs. Cetuximab + FOLFIRI Mutant KRAS tumours N=96	No difference in progression-free or overall survival, or response rate.
(Saltz et al. 2012)	Bevacizumab + mFOLFOX-6 vs. Cetuximab + Bevacizumab + FOLF N=247	No difference in progression-free or overall survival, or response rate
AVEX (Cunningham et al. 2013a)	Bevacizumab + Capecitabine vs. Capecitabine Patients not suitable for Oxaliplatin or Irinotecan N=280	Increased progression-free survival in favour of the Bevacizumab arm (median 9.1 vs. 5.1 months, HR 0.53 95% CI 0.41-0.69; p<0.0001) Increased response rate in favour of t Bevacizumab arm (19% vs. 10%; p=0.04) No difference seen in overall survival
FIRE-3 (Heinemann et al. 2014)	Bevacizumab + FOLFIRI vs. Cetuximab + FOLFIRI Wild-type KRAS tumours N=592	Increased overall survival in favour of Cetuximab arm (median 28.7 vs. 25.0 months, HR 0.77 (95% CI 0.62-0.96; p=0.017) No difference in progression-free survival or response rate

ITACa (Passardi et al. 2015)	Bevacizumab +FOLFIRI/FOLFOX4 vs. FOLFIRI/FOLFOX4 N= 376	No difference in progression-free or overall survival, or response rate
80405 (Venook et al. 2017)	Bevacizumab + mFOLFOX-6/FOLFIRI vs. Cetuximab + mFOLFOX-6/FOLFIRI Wild-type KRAS tumours N=1137	No difference in progression-free or overall survival, or response rate

Cediranib

Trial identifier and reference	**Treatment**	**Trial results**
HORIZON II (Hoff et al. 2012)	Cediranib + FOLFOX/XELOX vs. placebo + FOLFOX/XELOX N=860	No difference in progression-free or overall survival, or response rate
HORIZON III (Schmoll et al. 2012)	Cediranib 20mg + FOLFOX6 vs. Cediranib 30mg + FOLFOX6 vs. Bevacizumab + FOLFOX6 N= 1422	No difference in progression-free or overall survival, or response rate Patient reported outcomes less favourable with Cediranib

Cetuximab

Trial identifier and reference	**Treatment**	**Trial results**
CRYSTAL (Van Cutsem et al. 2009)	Cetuximab + FOLFIRI vs. FOLFIRI N=599	Increased progression-free survival in Cetuximab arm (Median 8.9 vs. 8.0 months, HR 0.85 95% CI 0.72-0.99; p=0.048) Increased response rate in favour of Cetuximab arm (46.9% vs. 38.7%, p=0.004) No difference in overall survival
CAIRO2 (Tol et al. 2009)	Cetuximab + Capecitabine + Oxaliplatin + Bevacizumab vs. Capeciabine + Oxaliplatin + Bevacizumab N=755	Decreased progression-free survival in Cetuximab arm (Median 9.4 vs. 10.7 months, HR 1.22 95% CI 1.04-1.43; p=0.01) No difference in overall survival or response rate.
MRC COIN (Maughan et al. 2011)	Cetuximab + oxaliplatin + fluoropyrimidine vs. oxaliplatin + fluoropyrimidine N=1630	No difference in progression-free or overall survival in either all patients or patients with KRAS wild –type tumours Increased response rate in favour of Cetuximab group in KRAS wild-type patients (57% vs. 64%; p=0.049)
NORDIC-VII (Tveit et al. 2012)	Cetuximab + intermittent FLOX vs. Cetuximab + FLOX vs. FLOX N=571	No difference in progression-free or overall survival, or response rate
AIO KRK-0306 (Stintzing et al. 2012)	Bevacizumab + FOLFIRI vs. Cetuximab + FOLFIRI Patients with KRAS mutations on codon 12 0r 13 N=96	No difference in progression free or overall survival, or response rate.
FIRE-3 (Heinemann et al. 2014)	Bevacizumab + FOLFIRI vs. Cetuximab + FOLFIRI Patients without KRAS exon 2 mutations N=592	Increased overall survival in favour of Cetuximab arm (median 28.7 vs. 25.0 months, HR 0.77 (95% CI 0.62-0.96; p=0.017) No difference in response rate and progression-free survival

80405 (Venook et al. 2017)	Bevacizumab + mFOLFOX-6/FOLFIRI vs. Cetuximab + mFOLFOX-6/FOLFIRI Patient with KRAS wild-type tumours N=1137	No difference in progression-free or overall survival, or response rate

Panitumumab

Trial identifier and reference	Treatment	Trial results
PACCE (Hecht et al. 2009)	Panitumumab + Oxaliplatin + Bevacizumab vs. Oxaliplatin + Bevacizumab vs. Panitumumab + Irinotecan + Bevacizumab vs. Irinotencan + Bevacizumab N=1183	Trial discontinued early due to decreased progression-free survival and increased toxicity with panitumumab arm
PRIME (Douillard et al. 2014)	Panitumumab + FOLFOX-4 vs. FOLFOX-4 N=1183	Increased progression-free survival seen in wild-type KRAS patients in favour of Panitumumab arm (Median 10 vs. 8.6 months, HR 0.80 95% CI 0.67-0.95; p=0.01). Decreased progression-free survival seen in mutation KRAS patients in favour of Panitumumab arm (Median 7.4 vs. 9.2 months, HR 1.27 95% ci 1.04-1.55; p=0.02) Increased response rate seen in wild-type KRAS oatients in favour of Panitumumab arm (57% vs.48%; p=0.02 No difference in response rate in mutation KRAS patients No difference in overall survival in either wild-type or mutation KRAS patients

Sunitinib

Trial identifier and reference	Treatment	Trial results
SUN1122 (Carrato et al. 2013)	Sunitinib +FOLFIRI vs. placebo + FOLFIRI N=768	Trial discontinued early due to poorer safety profile with Sunitinib

Vatalanib (PTK/ZK)

Trial identifier and reference	Treatment	Trial results
CONFIRM 1 (Hecht et al. 2011)	(PTK/ZK) Vatalanib + FOLFOX-4 vs. placebo + FOLFOX-4 N=1168	No difference in progression-free or overall survival, or response rate

FLOX- Fluorouracil (5-FU), Leucovorin and Oxaliplatin; FOLF- Fluorouracil (5-FU), Oxaliplatin and Leucovorin; FOLFIRI- Fluorouracil (5-FU), combined Leucovorin and Irinotecan; FOLFOX- Fluorouracil (5-FU), Folinic acid and Oxaliplatin; mIFL- Bolus Fluorouracil (5-FU), Leucovorin and Irinotecan; XELOX- Capecitabine and Oxaliplatin

Table 1.4 Phase III randomised controlled trials assessing the use of anti-angiogenic agents in the second line treatment of metastatic colorectal cancer

Aflibercept

Trial identifier and reference	Treatment	Trial results
VELOUR (Van Cutsem et al. 2012)	Aflibercept + FOLFIRI vs. placebo + FOLFIRI Patients previously treated with Oxaliplatin N=1226	Increased progression-free survival in favour of the Aflibercept arm (median 6.9 vs. 4.67 months, HR 0.76 95% CI 0.66-0.87; p<0.0001) Increased overall survival in favour of the Aflibercept arm (median 13.50 vs. 12.06 months, HR 0.81 95% CI 0.71-0.93 p=0.0032) Increased response rate in favour of the Aflibercept arm (19.8% vs. 11.1%, p=0.0001)

Bevacizumab

Trial identifier and reference	Treatment	Trial results
E3200 (Giantonio et al. 2007)	Bevacizumab +FOLFOX-4 vs. FOLFOX-4 vs. Bevacizumab Patients previously treated with Fluorouracil and Irinotecan N=829	Increased overall survival in favour of Bevacizumab +FOLFOX-4 arm (Median 12.9 vs. 10.8 (FOLFOX-4 alone) vs. 10.2 (Bevacizumab alone) months, HR 0.75; p=0.0011) Increased progression-free survival in favour of Bevacizumab +FOLFOX-4 arm (Median 7.3 vs. 4.7 (FOLFOX-4) vs. 2.7 (Bevacizumab alone), HR 0.61; p<0.001)
ML18 147 (Bennouna et al. 2013)	Bevacizumab + standard second-line chemotherapy (Oxaliplatin or Irinotecan) vs. standard second-line chemotherapy Patients who progressed after first-line Bevacizumab N=409	Increased overall survival in favour of the Bevacizumab arm (Median 11.2 vs. 9.8 months, HR 0.81 95% CI 0.69-0.94 p=0.0062) Increased progression-free survival in favour of the Bevacizumab arm (Median 5.7 VS. 4.1 months, HR 0.68 95% CI 0.59-0.78; p<0.0001) No difference seen in response rate
EAGLE (Iwamoto et al. 2015)	Bevacizumab 5mg/kg + FOLFIRI vs. Bevacizumab 10mg/kg + FOLFIRI Patients who progressed after first-line Bevacizumab N=387	No difference seen in progression-free survival or response rate Overall survival not reported
BEBYP (Masi et al. 2015)	Bevacizumab + mFOLFOX-6/FOLFIRI vs. mFOLFOX-6/FOLFIRI Patients who progressed after or during first-line Fluoropyrimidine N=185	Increased overall survival in favour of Bevacizumab arm (Median 14.1 vs.15.5 months, but due to curves intersection in favour of Bevacizumab arm HR 0.77 95% CI 0.56-1.06; p=0.043) Increased progression-free survival in favour of Bevacizumab arm (Median 6.8 vs. 5.0 months, HR 0.70 95% CI 0.52-0.95; p=0.010) No difference in response rate
AIO 0207 (Hegewisch-Becker et al. 2015)	Bevacizumab + Fluoropyrimidine vs. Bevacizumab vs. No treatment Patients who oreviously received Fluoropyrimidine, Oxaliplatin,and Bevacizumab and neither progressed or had option for resection after 24 weeks treatment N=472	Increased progression-free survival in favour of the Bevacizumab + Fluoropyrimidine arm (Median 11.7 (BF) vs. 10.0 (B) vs. 9.0 (no treatment) months; B vs. BF HR 1.34 95% CI 1.06-1.70; p=0.015, no treatment vs. BF HR 2.09 95% CI 1.64-2.67; p<0.0001, no treatment vs. B HR 1.45 95% CI 1.15-1.82; p0.0018 No difference seen in overall survival or response rate

SAKK 41/06 (Koeberle et al. 2015)	Bevacizumab vs. no treatment Patients without disease progression after 4-6 months of standard first-line chemotherapy plus Bevacizumab N=262	No difference seen in progression-free or overall survival, or response rate
Nordic ACT2 (Hagman et al. 2016)	Bevacizumab vs. Capecitabine Patients who previously had Bevacizumab and chemotherapy with Mutant KRAS tumours N=67	No difference was seen in progression-free or overall survival

Brivanib

Trial identifier and reference	**Treatment**	**Trial results**
CO.20 (Siu et al. 2013)	Brivanib + Cetuximab + vs. placebo + Cetuximab Patients with wild-type KRAS. Previously treated with Fluoropyrimidine, and treated but discontinued Irinotecan and Oxaliplatin due to adverse events with disease progression within 6 months N=750	Increased progression-free survival in favour of Brivanib group (Median 5.0 vs. 3.4 months, HR 0.88 95% ci 0.74-1.03; p<0.001) Increased response rate in favour of Brivanib group (13.6% vs. 7.2%; p=0.004) No difference in overall survival Increased toxicity seen with Brivanib

Cediranib

Trial identifier and reference	**Treatment**	**Trial results**
HORIZON I (Cunningham et al. 2013b)	Cediranib 20mg + FOLFOX-6 vs. Cediranib 30mg + FOLFOX-6 vs. Bevacizumab + FOLFOX-6 N=215	No difference in progression-free or overall survival

Cetuximab

Trial identifier and reference	**Treatment**	**Trial results**
CO.17 (Jonker et al. 2007)	Cetuximab vs. best supportive care Patients previously treated with Fluoropyrimidine N=572	Increased progression-free survival in Cetuximab arm (Median months not reported, HR 0.68 95% CI 0.57-0.80;p<0.001) Increased overall survival in favour of the Cetuximab arm (median 6.1 vs. 4.6 months, HR 0.77 95% CI 0.64-0.92; p=0.005) Increased response rate in favour of the Cetuximab arm (8% vs. 0%; p<0.001
EPIC (Sobrero et al. 2008)	Cetuximab + Irinotecan vs. Irinotecan Patients previously failed treatment with Fluoropyrimidine and Oxaliplatin N=1298	Increased progression-free survival in Cetuximab arm (median 4.0 vs. 2.6 months, HR 0.69 95% CI 0.61-0.77; p<0.001) Increased response rate with Cetuximab arm (16.4% vs. 4.2%, p<0.001) No difference in overall survival

Erlotinib

Trial identifier and reference	Treatment	Trial results
Nordic ACT Johnson et al. 2013)	Erlotinib + Bevacizumab vs. Bevacizumab N=159	No difference was seen in progression-free or overall survival
GRECOR DREAM; OPTIMOX3 (Tournigand et al. 2015)	Erlotinib + Bevacizumab vs. Bevacizumab N=452 After Bevacizumab induction therapy	Increased progression-free survival in favour of Erlotinib arm (Median 5.4 vs. 4.9 months, HR 0.78 95% CI 0.63-0.96; p=0.019) Increased overall survival in favour of Erlotinib arm (Median 24.9 vs. 22.1 months, HR 0.79 95% CI 0.64-0.98; p=0.035) Increased response rate in favour of Erlotinib arm (11% vs. 22%, OR 2.23 95% CI 1.27-3.98; p=0.0029)
Nordic ACT2 (Hagman et al. 2016)	Erlotinib + Bevacizumab vs. Bevacizumab N=67 Wild-type KRAS tumours	No difference was seen in progression-free or overall survival, or response rate

Panitumumab

Trial identifier and reference	Treatment	Trial results
(Van Cutsem et al. 2007)	Panitumumab vs. best supportive care N=463	Increased progression-free survival in favour of Panitumumab arm (Median 8 weeks vs. 7.3 weeks, HR 0.54 95% CI 0.44-0.66; p<0.0001) No difference in overall survival Increased response rate in favour of Panitumumab arm (10% vs. 0%; p<0.0001)
(Amado et al. 2008)	Panitumumab vs. best supportive care N=427	Increased progression-free survival in favour of the Panitumumab arm in wild-type KRAS patients (Median 12.3 vs. 7.3 weeks, HR 0.45 95%CI 0.34-0.59; p<0.0001) No difference in progression-free survival seen in mutant KRAS patients No difference in overall survival seen for all patients or between wild-type KRAS or mutant KRAS patients
PICCOLO (Seymour et al. 2013)	Panitumumab + Irinotecan vs. Irinotecan N=460 Wild-type KRAS tumours	Increased progression-free survival in favour of Panitumumab arm (Median months not reported, HR 0.78 95% CI 0.64=0.95; p=0.015) Increased response rate in favour of Panitumumab arm (34% vs. 27%, p<0.0001) No difference in overall survival
ASPECTT (Price et al. 2014)	Panitumumab vs. Cetuximab N=999 Wild-type KRAS tumours	No difference in progression-free or overall survival, or response rate
20050181 (Peeters et al. 2014)	Panitumumab + FOLFIRI vs. FOLFIRI N=1186 Wild-type KRAS tumours	Increased progression-free survival in favour of the Panitumumab arm (Median 6.7 vs. 4.9 months, HR 0.82 95% CI 0.69-0.97 p=0.023) Increased response rate in favour of Panitumumab arm (36% vs. 10%, p<0.0001) No difference in overall survival

20100007 (Kim et al. 2016)	Panitumumab vs. best supportive care N=377 Wild-type KRAS tumours	Increased overall survival in favour of Panitumumab arm (Median 10.0 vs. 7.4 months, HR 0.73 95% CI 0.57-0.93; p=0.0096) Increased progression-free survival in favour of Panitumumab arm (Median3.6 vs. 1.7 months, HR 0.51 95% CI 0.41-0.64; p=<0.0001) Increased response rate in favour of Panitumumab arm (27% vs. 1.6% p<0.0001)

Ramucirumab

Trial identifier and reference	**Treatment**	**Trial results**
RAISE (Tabernero et al. 2015)	Ramucirumab + FOLFIRI vs. placebo + FOLFIRI N=1072	Increased overall survival in favour of treatment arm (Median 13.3 vs. 11.7 months, HR 0.84 95% CI 0.73-0.97; p=0.0219) Increased progression-free survival in favour of treatment arm (Median 5.7 vs. 4.5 months, HR 0.79 95% CI 0.69-0..90; p=0.0005 No difference was seen in response rate

Regorafenib

Trial identifier and reference	**Treatment**	**Trial results**
CORRECT (Grothey et al. 2013)	Regorafenib vs. placebo N=1052	Increased progression-free survival in favour of the Regorafenib arm (Median 1.9 vs. 1.7 months, HR 0.49 95% CI 0.42-0.58; p<0.0001) Increased overall survival in favour of the Regorafenib arm (median 6.4 vs. 5.0 months, HR 0.77 95% CI 0.64-0.94 p=0.0052) No difference seen in response rate
CONCUR (Li et al. 2015)	Regorafenib vs. placebo N=204	Increased progression-free survival in favour of the Regorafenib arm (Median 3.2 vs. 1.7 months, HR 0.31 95% CI 0.22-0.44; p<0.0001) Increased overall survival in favour of the Regorafenib arm (median 8.8 vs. 6.3 months, HR 0.55 95% CI 0.40-0.77 p=0.00016) Increased response rate seen in the Regorafenib arm (4% vs. 0%; p<0.0001)

Vatalanib (PTK/ZK)

Trial identifier and reference	**Treatment**	**Trial results**
CONFIRM 2 (Van Cutsem et al. 2011)	(PTK/ZK) Vatalanib + FOLFOX-4 vs. placebo + FOLFOX-4 N=855	Increased progression-free survival in favour of treatment arm (Median 13.1 vs. 11.9 months, HR 0.83 95% CI 0.71-0.96; p=0.013) No difference in overall survival and response rate

FOLFIRI- Fluorouracil (5-FU), combined Leucovorin and Irinotecan; FOLFOX- Fluorouracil (5-FU), Folinic acid and Oxaliplatin; KRAS- Kirsten rat sarcoma

Bevacizumab, benefits from Bevacizumab were achieved at the expense of small but definite increases in adverse events and that it was deemed to not be cost-effective within the NHS setting. Later NICE issued further guidance to not recommend the use of Bevacizumab for second-line treatment of metastatic colorectal cancer (NICE. 2012).

A further anti-VEGF therapy has been proposed for use in colorectal cancer; Aflibercept (Zaltrap®) is a novel fusion protein that binds to three VEGF ligands (VEGF-A, VEGF-B and placental growth factor (PlGF)). As Aflibercept also targets VEGF-B and PlGF, not just VEGF-A like Bevacizumab, it has been hypothesised that it may confer additional anti-angiogenic effects (Fischer et al. 2008). A Phase III randomised trial in 2012 investigated the benefit of the addition of Aflibercept given with chemotherapy (FOLFIRI) compared to chemotherapy alone in patients with metastatic colorectal cancer (Van Cutsem et al. 2012). The results showed an extension of both progression-free survival and overall survival, and with a 2-year survival significantly higher in the Aflibercept/chemotherapy group compared to the chemotherapy alone group (28% vs. 18.7%). However, at time of print, NICE has not reviewed its widespread use within the NHS setting.

Cetuximab (Erbitux®) is an epidermal growth factor receptor (EGFR) inhibitor and works as a chimeric monoclonal antibody. The CRYSTAL study, a Phase III randomised clinical trial, published in 2009, compared the use of Cetuximab plus FOLFIRI vs. FOLFIRI alone as first-line treatment for metastatic carcinoma of the colon and rectum (Van Cutsem et al. 2009). Their results demonstrated an increased progression-free survival in the treatment arm (median 8.9 vs. 8.0 months, HR 0.85,

p=0.048), with an increased response rate (46.9% vs. 38.7%, p=0.004), but did not prove an overall survival benefit. Sub-group analysis of patients with wild-type KRAS tumours showed a hazard ratio of 0.68 when comparing progression-free survival between the two groups, therefore concluded that the benefit of Cetuximab as first-line treatment for metastatic colorectal cancer was more so in these patients. The OPUS Trial, a Phase II randomised clinical trial also published in 2009, found an increase in both progression-free survival (HR 0.567, p=0.0064) and response rate (OR 2.551, p=0.0027) with the addition of Cetuximab to FOLFOX in wild-type KRAS tumours in the first-line treatment of metastatic colorectal cancer (Bokemeyer et al. 2009). Shortly after these publications, the FDA approved Cetuximab for the treatment of colorectal cancer with wild-type KRAS (USFDA. 2010). In the UK, NICE recommended the use of Cetuximab in combination with FOLFOX (or FOLFIRI if intolerant of Oxaliplatin) for the first-line treatment of patients with EGFR-expressing KRAS wild-type metastatic colorectal cancer with the following criteria; Primary (completely resected or potentially operable) colorectal tumour with unresectable metastasis confined to the liver and the patient is deemed fit enough for primary colorectal tumour and hepatic resections if the metastases become resectable following Cetuximab treatment (NICE. 2009). However NICE did not support its use for second-line treatment of metastatic colorectal cancer (NICE. 2012).

A further anti-angiogenic agent, which targets EGFR is Panitumumab (Vectibix®), a fully human monoclonal antibody. One Phase III randomised control trial has demonstrated an increase in progression-free survival in the first-line treatment for metastatic colorectal cancer in wild-type KRAS tumours (Douillard et al. 2014),

however NICE has not yet assessed its use for this indication. Whilst three Phase III randomised control trials have shown an increase in progression-free survival and response rate in second-line treatment for metastatic colorectal cancer in wild-type KRAS tumours (Amado et al. 2008; Seymour et al. 2013; Peeters et al. 2014), to date NICE has not recommended its use for this indication (NICE. 2012). Clearly the KRAS gene status appears to be a predictive marker of the anti-EGFR monoclonal antibodies, with evidence supporting that mutant KRAS does not confer a clinical benefit of anti-EGFR therapies (Amado et al. 2008) (Figure 1.6).

Several other anti-angiogenic agents have been proposed for the treatment of metastatic colorectal cancer by mono- or poly-receptor tyrosine kinase inhibition (i.e. inhibit downstream receptor signalling); Cediranib (AZD2171, Recentin™), Vatalanib (PTK 787/ZK22584), Regorafenib (Stivarga), Brivanib and Sunitinib (Sutent®). However apart from Regorafenib, results from Phase III randomised control trials do not currently support their use in the treatment of metastatic colorectal cancer (Table 1.3 and 1.4).

Clearly these anti-angiogenic therapies show promise for treatment of colorectal cancer, nevertheless the outcomes discussed in this section highlight some disappointing results within phase III clinical trials, with only one anti-angiogenic therapy (Cetuximab) recommended to date for use in metastatic colorectal KRAS wild-type tumours in the UK. Therefore, there is a desperate need to seek out alternative anti-angiogenic therapies that are both clinically effective and cost effective, with an acceptable side-effect profile.

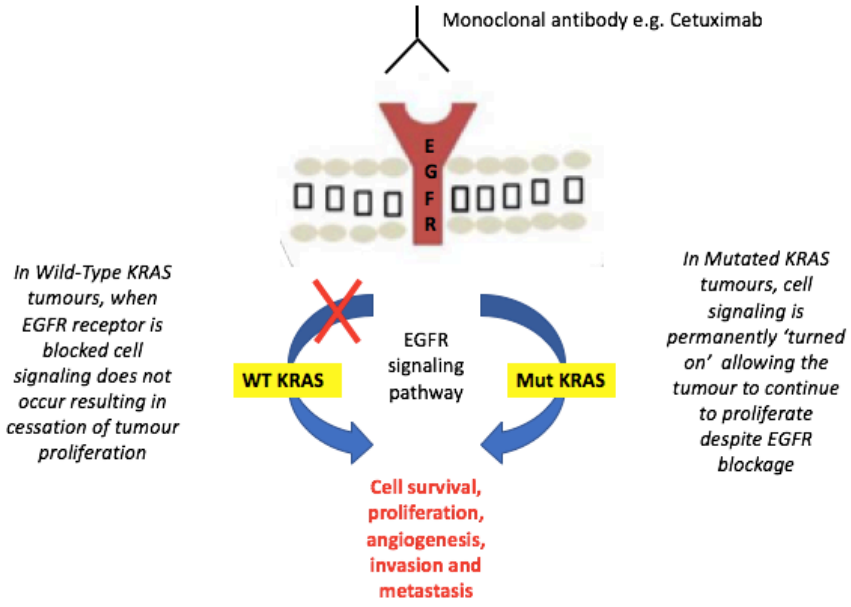

Figure 1.6. KRAS status and mechanism of anti-EGFR therapies

EGFR- epidermal growth factor receptor; KRAS- Kirtsen Rat Sarcoma; Mut- mutated; WT- wild-type

1.4.2 The role of PEDF in solid tumours

There is a plethora of evidence to support that a decline in the expression of PEDF can be found in a range of cancers, with a direct correlation associated with several poorer prognostic clinical features. Comparing cancer tissue specimens to normal tissue from the same organ, PEDF expression has been found to be significantly decreased in breast cancer tissue (Cai et al. 2006b; Zhou et al. 2010), non-small cell lung cancer tissue (Zhang et al. 2006a), ovarian cancer tissue (Cheung et al. 2006), glioma tissue (Guan et al. 2003) and malignant melanoma tissue (Zhang et al. 2009).

A significant correlation between low PEDF expression and increased microvessel density (MVD) was found in breast adenocarcinoma (Zhou et al. 2010), hepatoblastoma (Browne et al. 2006) and osteosarcoma (Dass et al. 2008). High microvessel density is a parameter for the degree of angiogenesis and has previously been found to be a predictor of high risk of metastasis and shorter survival in solid tumours (Guang-Wu et al. 2000; Ohta et al. 2003; Seo et al. 2000). Decreased levels of PEDF were found to significantly correlate with increased tumour size in breast cancer (Zhou et al. 2010) as well as increasing grade of tumour in glioma (Guan et al. 2003). A decline in the PEDF expression was also found to be a marker of tumour cellular invasion and migration; with studies confirming lower PEDF expression levels in cases of lymph node involvement, in breast cancer (Cai et al. 2006b) and lung cancer (Fitzgerald et al. 2012). There is evidence to support that this expression pattern is similar in the presence of metastasis within breast cancer (Cai et al. 2006b; Zhou et al. 2010; Fitzgerald et al. 2012), pancreatic cancer (Uehara et al. 2004), osteosarcoma (Dass et al. 2008) and prostate cancer (Halin et al. 2004). Increased

rate of local recurrence was found to correlate with low PEDF expression in breast cancer (Cai et al. 2006b; Zhou et al. 2010).

Low levels of PEDF expression directly correlate with overall and disease -free survival, in breast cancer (Zhou et al. 2010), pancreatic cancer (Seo et al. 2000) and lung cancer (Chen et al. 2009). Zhou *et al* (2010) demonstrated that multivariate analysis of overall survival using Cox regression confirmed PEDF positivity to be an independent favourable prognostic factor in breast cancer (risk ratio 2.203, P=0.0062).

PEDF is thought to inhibit tumour growth and metastasis by suppressing angiogenesis, inhibiting tumour cell proliferation, increasing tumour cell apoptosis, and/or decreasing tumour cell migration and invasion. Several studies have investigated the effects of the administration of recombinant PEDF (rhPEDF) on tumour cellular function. A reduction in tumour cellular proliferation was found in a range of cancers upon administration of recombinant PEDF, including lung cancer (Chen et al. 2009), breast cancer (Hong et al. 2014), ovarian cancer (Cheung et al. 2006), osteosarcoma (Dass et al. 2008), hepatocellular cancer (Matsumoto et al. 2004), prostate cancer (Guan et al. 2007), glioma (Zhang et al. 2007) and malignant melanoma (Abe et al. 2004). Treatment with recombinant PEDF has also been shown to induce apoptosis in ovarian cancer cells (Cheung et al. 2006), prostate cancer cells (Doll et al. 2003), chondrosarcoma cells (Tan et al. 2010) and osteosarcoma cells (Takenda et al. 2005), and resulted in inhibition of tumour cell migration and invasion in breast cancer cells (Hong et al. 2014), and chondrosarcoma cells (Tan et al. 2010).

1.4.3 The role of PEDF in colorectal cancer

There are limited studies to date, which have examined either PEDF expression or the effects of PEDF on functional cellular outcomes and the clinical significance in colorectal cancer. mRNA expression of PEDF was first reported as being detected in two human colorectal cancer cell lines, with HT115 (colonic adenocarcinoma cell line) showing strong expression and HRT-18 (rectal adenocarcinoma cell line) showing weak expression (Cai et al. 2006b).

Wågsäter *et al* (2010) analysed serum samples for PEDF expression in 80 colorectal cancer patients compared to 72 healthy controls (Wågsäter et al. 2010)**.** There was no difference found in gender distributions between the colorectal cancer patients and the healthy controls. They found a significant reduction in serum PEDF levels in colorectal cancer patients compared to healthy controls (median 1.6μg/ml (range 0.1-4.8μg/ml) *cf.* 3.6μg/ml (range 1.1-7.2μg/ml) respectively, $p<0.001$). Interestingly, the results also revealed that plasma PEDF levels were significantly lower in healthy female controls compared to healthy male controls (median 3.1μg/ml (range 1.5-7.2μg/ml) *cf.* 4.3μg/ml (range 1.1-6.5μg/ml) respectively, $p<0.01$); a finding which was previously noted by Yamagishi *et al* (2006). However, this gender difference was not observed in colorectal cancer patients ($p=0.113$). The plasma PEDF levels were not associated with patient age, tumour location or Duke's stage.

Ji *et al* also studied serum samples from patients with colorectal cancer, patients with colorectal adenoma and healthy controls (Ji et al. 2013). All serum samples were collected pre-operatively and none of the patients had received neoadjuvant chemoradiotherapy or had evidence of other causes of malignancy. Similar to

findings of Wågsäter *et al* (2010), serum levels of PEDF were significantly decreased in patients with colorectal cancer compared to normal subjects ($p<0.0001$). No difference was found between patients with colorectal adenoma and healthy subjects or between preoperative and postoperative serum PEDF levels in patients with colorectal cancer. Serum PEDF levels decreased significantly with increased TNM colorectal tumour staging and low serum PEDF levels were observed in the presence of liver metastases ($p<0.0001$). Of interest, cases of mucinous adenocarcinomas had significantly higher levels of PEDF compared with adenocarcinomas ($p=0.0127$). Receiver-operating characteristic (ROC) curve analyses revealed that the ROC curve area for serum level of PEDF was 0.5744 (95% CI= 0.52-0.63), with a cut-off value of 4323ng/ml the sensitivity and specificity was 34% and 96% respectively; unfortunately, dispelling theories that PEDF could be used as a useful biomarker for the screening of colorectal cancer.

Ji *et al* (2013) analysed 225 patients for correlation between clinical outcomes and levels of PEDF protein. Kaplan-Meier analyses were performed for overall survival using the median levels of protein as the cut-off for the definition of subgroups. Patients with lower PEDF levels were associated with significantly shorter overall survival than those with higher PEDF levels ($p=0.003$), but no significant difference was observed in disease-free survival. This was also confirmed on a further training set of 180 patients in the same study (Ji et al. 2013). On multivariate analysis, decreased PEDF levels were found to be an independent risk factor for prognosis in colorectal cancer patients (HR for death= 0.42, 95% CI= 0.221-0.801, $p=0.008$).

Expression of PEDF in colorectal cancer tissue determined by qPCR and western blot analysis at mRNA and protein levels revealed significant decrease in PEDF expression in tumour tissue compared to matched adjacent normal tissue, confirming the serum level findings (Ji et al. 2013). The results showed that downregulation of PEDF significantly correlated with advanced clinical stage, lymph node metastasis, distant metastasis and shorter disease-free survival time, supporting the evidence of this association in other solid tumours (as discussed in section 1.4.2).

Díaz *et al* (2008) reported that mRNA expression of PEDF in colorectal cancer tissue has a significant difference dependent on the tumour location (geometric averages for PEDF levels were 1.5, 0.71 and 0.68 for rectum, right-sided colonic and left-sided colonic tumour locations, respectively; p=0.05) and that low expression level (using median transcript copy number (0.87) as cut-off) of PEDF correlated with microvessel density (p=0.028).

Wågsäter *et al* (2010) also examined protein levels of PEDF in colorectal tissue compared to paired normal tissue using ELISA (enzyme-linked immunosorbent assay). They found no significant difference in PEDF protein levels in colorectal cancer tissue samples compared to the paired normal tissue samples and there was no association found between either plasma levels and tissue levels of PEDF or clinicopathological characteristics including patient age, patient gender, tumour locations and Dukes's stage.

In immunohistochemistry studies, colorectal cancer showed strong nuclear staining in large atypical cancer cells as well as in mesenchymal cells of cancer stroma (Uhlen. 2005). The authors hypothesise that expression may have appeared stronger in

cancer cells as it reflects that cancer cell nuclei are larger and contain more nucleic acids and have a higher rate of transcription and metabolism. In contrast, Ji *et al* (2013) found that PEDF was expressed in the cytoplasm and cell membrane in normal colorectal mucosa, primary cancer and adenoma cells, with expression of PEDF in cancer cells being weaker than in normal mucosa.

The interactions between PEDF and other angiogenic regulators in the context of colorectal cancer has been studied by Díaz *et al* (2008). They examined colorectal cancer specimens from 112 patients for expression of and correlation between PEDF, VEGF, p53, p73 isoforms and KRAS status. p73 is a protein related to p53, which has a complex number of isoforms with both tumour suppressor (TAp73) and oncogenic properties (ΔTAp73); its interaction with VEGF remains unclear. The results of the study found that median mRNA geometric average for the colorectal cancer specimen cohort was -0.06 (IQR -0.36-0.47). A direct statistically significant correlation between VEGF and PEDF mRNA levels in their cohort was noted ($p=0.04$, $r=0.2$), reinforcing evidence of the interplay between VEGF and PEDF. However, the authors noted that when they used primers that amplified for both VEGF and VEGFb variants, this association was lost and they commented that previous work on this area may have led to confusing results dependent on the primers used. The association between KRAS mutations and decrease in PEDF expression was statistically significant ($p=0.04$), with a geometric average for PEDF levels of 0.6 when KRAS was mutated and 1.1 when wild type KRAS. This suggests that oncogenic KRAS may downregulate PEDF expression *in vivo*.

Díaz *et al* (2008) found a direct correlation between VEGF and PEDF in the group that had high levels of ΔEx2p73 (defined as transcript copy number higher than 0.66, based on the median value) (p=0.005, r=0.463), and an inverse correlation between PEDF and ΔEx2p73 (p=0.04, r=-0.33). These findings suggest that p73 might negatively regulate PEDF. No observed association was seen between p53 and PEDF. These findings were comparable to those of Sasaki *et al* (2005), who concluded that both p63 and p73 but not p53 induced PEDF expression through direct binding to the PEDF gene in colorectal cancer cell lines.

There have been some concerns raised regarding the instability of recombinant PEDF, which has led some studies to investigate possible vector delivery of PEDF. Jia & Waxman (2013) investigated the effects of endogenous PEDF in colorectal cancer by comparing wild-type KM12 colonic cancer cells (KM12/WT) with KM12 cells infected with retroviral vector encoding PEDF cDNA (KM12/PEDF) in colon adenocarcinoma xenografts. The KM12/PEDF tumours were found to have significantly lower levels of microvessel density compared to KM12/WT on immunostaining, but no difference in tumour growth rate. They also noted that KM12/PEDF tumours showed an increase in thrombospondin-1 expression, supporting theories that PEDF can upregulate thrombospondin-1 (Guan et al. 2004). Furthermore, treatment with cyclophosphamide resulted in fewer lung metastases in mice bearing KM12/PEDF tumours compared with KM12/WT, with confirmation achieved by immunostaining. Similar findings were confirmed by Li *et al* (2012); the PEDF gene was delivered by cRGD-PEG-PEI (synthesized polyethyleneglycol-polyetherimide coupled with cyclic

RGD peptide) and was shown to suppress tumour growth and decrease microvessel density in nude mice bearing SW620 human colorectal xenografts.

In summary, studies to date have shown that PEDF expression in colorectal cancer is reduced compared to normal tissue, and declines with worsening prognostic factors. In colorectal cancer cellular functional studies, VEGF expression directly correlates with PEDF expression, with PEDF expression lower in KRAS mutation and evidence of p63 and p73, but not p53, downregulating PEDF expression. In colorectal tumour xenografts, vector delivered PEDF was found to decrease microvessel density but with conflicting results on its effect on tumour growth rate. There is evidence to support that administration of exogenous PEDF in other solid tumours can result in a decline in cellular proliferation, inhibit cellular migration and invasion and induce apoptosis in cancer cells. There is limited evidence on the role PEDF plays in colorectal cancer cellular function but it is logical to hypothesise that these findings may be similar to that of other solid tumours.

1.5 Wound Healing

1.5.1 The anti-inflammatory role of PEDF

As discussed in section 1.2, not only does PEDF have anti-angiogenic and anti-tumorigenic effects, but also immune-modulating effects. There is evidence to support the theory that PEDF expression declines in the presence of inflammation. Zhang *et al* (2006b) observed significantly lower expression levels of PEDF in both the retina and plasma of rats with acute endotoxin-induced uveitis, suggesting that PEDF is a negative acute phase protein. They also found that retinal capillary endothelial

cells, monolayer endothelial permeability was significantly increased by VEGF and blocked by PEDF, suggesting that PEDF inhibited VEGF-induced endothelial permeability by blocking dysregulation of tight junction protein.

Further studies have confirmed similar findings of PEDF expression inversely correlating with pro-inflammatory factors in differing pathologies. Shin *et al* (2014) found that lung endothelial cells from PEDF deficient mice expressed higher levels of pro-inflammatory markers and fibronectin compared to PEDF wild-type mice. Park *et al* (2011) found the levels of pro-inflammatory factors were significantly lower in PEDF transgenic mice (express human PEDF driven by β-actin promoter) compared to wild-type mice, suggesting that overexpression of PEDF inhibits retinal inflammation.

One mechanism of a direct binding site for this anti-inflammatory action has been proposed, with Matsui *et al* (2013) demonstrating that PEDF binds to caveolin-1, a protein component of caveolae (involved in the progression of atherosclerosis), in endothelial cells, thus potentially blocking the inflammatory effects of caveolin-1.

The link between PEDF treatment and its effect on inflammation has also been investigated. Zha *et al* (2016) conducted an *in vivo* experiment on mice with chronic ovalbumin-induced asthma treated with recombinant PEDF and found that PEDF administration significantly inhibited eosinophilic airway inflammation and suppressed VEGF expression in lung tissue.

The above studies highlight that PEDF appears to exhibit anti-inflammatory effects, which may be of additional benefit in the treatment of other pathological conditions where inflammation plays a role, such as chronic wounds.

1.5.2 Novel biological therapies for treatment of chronic wounds

The majority of wounds progress through the normal stages of the wound healing process, at an appropriate time. Yet, roughly 1% of the general population suffer from chronic wounds (defined as a wound of more than 4 weeks duration) (Sen et al. 2009). This burden will inevitably rise with an ever-increasingly co-morbid population. The management of these chronic wounds is a significant financial drain on national healthcare systems with an estimated cost of £2.5m-£3m per 100,000 population (Drew et al. 2007). However these financial costs fail to reflect the personal costs to the patient, such as a reduction in a patient's ability to work and reduction in quality of life.

Many chronic wounds remain stuck in the inflammation stage of the wound healing process (as discussed in section 1.1.1) and therefore many novel biological therapies are directly targeted to address this biochemical imbalance within the wound bed.

Recombinant growth factors (PDGF, FGFb, human epidermal growth factor (EGF) and granulocyte macrophage colony-stimulating factor (GM-CSF)) have been proposed for use in treatment of wounds (Barrientos et al. 2008; Buchberger et al. 2010). However it has been suggested that it is important to limit lifetime use due to concerns over tumorigenesis (Fu et al. 2005). Becaplermin (PDGF) is the only growth factor product licensed for use to date, and has been proven to be safe for use in

diabetic foot ulcers (Mulder et al. 2009; Blume et al. 2011). It's use in diabetic foot ulcers has been evaluated in three randomised control trials; no difference was found when used in combination with gauze dressings when compared to gauze dressings alone (Landsman et al. 2010), whilst it was found to be inferior to an acellular dermal matrix use (Brigido. 2006), but superior to placebo gel (Wieman et al. 1998).

Another novel area of targeted therapy is aimed at the excessive protease levels, which can often be found in chronic wounds (Cullen et al. 2002; Gibson et al. 2010). Excessive protease levels can result in degradation of growth factors, and addressing this may prevent this degradation. Conversely treatment to address excessive protease levels on wounds that do not have excessive protease levels can result in negative wound healing affects, highlighting the complex balance of biochemical imbalances and the individual approach that is required for each wound. It has been suggested that addressing excessive protease levels can be achieved by either the use of collagen-based dressings that reduce protease activity (Cullen et al. 2002) or by inhibition of MMP synthesis by the use of polyhydrates ionogen (Pirayesh et al. 2007). A randomised control trial investigated the use of a collagen/oxidised regenerated cellulose dressing compared to standard treatment in the management of diabetic foot ulcers and found no difference in terms of wound closure rates at 12 weeks follow-up between both treatment arms (Veves et al. 2002). Collagen/oxidised regenerated cellulose dressings have been combined with silver therapy (anti-microbial properties) and its use has been assessed in a randomised control trial in patients with diabetic foot ulcers, comparing to standard therapy (Gottrup et al. 2013). Results showed significantly more patients had a >50%

reduction in wound area at 4 weeks follow-up in the treatment arm (79% vs. 43%, p=0.035) suggesting that the combination of collagen/oxidised regenerated cellulose/silver both normalises the wound microenvironment and protects against infection. To date, polyhydrates iongen use has not been assessed in level 1 evidence in chronic wounds.

There is some limited evidence from a randomised control trial to support the combined treatment with protease-modulating matrix and autologous growth factors via a gravitational platelet separation system in the treatment of chronic diabetic foot ulcers is superior to treatment arms with either protease-modulating matrix or autologous growth factors as monotherapy (Kakagia et al. 2007).

The use of stem cells have also been proposed for treatment in chronic wounds, and are thought to migrate to wounded tissue and secrete chemokines and growth factors in order to promote angiogenesis and ECM remodelling (Blumberg et al. 2012). They can be categorised into allogenic and autologous stem cells, based on their source. Allogenic stem cells include placental or amnion-derived mesenchymal and embryonic stem cells. Autologous stem cells include bone marrow derived endothelial progenitor cells, bone marrow derived mesenchymal, haematopoietic and adipose-derived stem cells. Although the use of stem cells is promising from animal studies, only one randomised control trial has investigated the use of stem cells in diabetic foot ulcers. Lu *et al* compared bone marrow mesenchymal stem cells with bone marrow-derived mononuclear cells and found the healing rate was significant less with the bone marrow mesenchymal stem cells (Lu et al. 2011). However, further work is certainly required to determine their use in human subjects.

Many clinical trials assessing wound healing have trial sample sizes that often appear underpowered (Martí-Carvajal et al. 2015), therefore casting some doubts over the conclusions of some studies. Nonetheless, these novel therapies show some early promise for the treatment of correcting the biochemical imbalance within chronic wounds. It is critical to recognise that each of the above proposed novel therapies are not applicable for the entirety of non-healing wounds, but rather for non-healing wounds that are caused by that particular biochemical imbalance. The difficulty faced by the clinician, can be the identification of the wounds that will respond to a particular treatment, and the development of clinical biomarkers may be beneficial. Other targets of wound imbalances may also exist in chronic wounds, hence the reason why further research into this area is so vital.

1.5.3 The role of PEDF in wound healing

There have been few studies that have directly investigated the link between PEDF expression and function in the clinical setting of wound healing. mRNA expression of PEDF has been shown to be highly positive in two fibroblast cell lines MRC5 (human lung fibroblasts) and IBR3G (transformed immortalized fibroblasts) but not detected in HECV cell lines (endothelial cell line originating from human umbilical vein) in a study by Cai *et al* (2006b). Expression has also been detected in HaCaT (human keratinocyte) cell line (Li et al. 2011).

mRNA detection of PEDF was found in the dermal layer of the skin (Francis et al. 2004), supporting the fact that fibroblasts, the major cell type in the dermis, are highly expressive of PEDF (Sauer 1996). Whereas *in vitro* data supports the theory that keratinocytes in the epidermis express minimal amounts of PEDF (Pignolo et al.

1995). Zhang *et al* (2009) found strongly positive staining on immunohistochemistry within normal skin tissue specimens, in comparison to a loss of staining in melanoma specimens. Abe *et al* (2010) found PEDF was expressed within both the epidermis and dermis on immunohistochemistry staining of normal human skin tissue samples, but was stronger in the epidermis than dermis. However in contrast, Francis *et al* (2004) found PEDF protein localised to the sub-epidermal region determined by immunofluorescence on normal skin tissue specimen. On a cellular level, expression of PEDF protein was found to be localised to the cytoplasm of keratinocytes on immunocytochemistry and immunofluorescence studies (Abe et al. 2010; Li et al. 2011).

PEDF expression has been found to decline dramatically during cellular aging; first noted in late passage cultured W138 human lung fibroblast cell line (Doggett et al. 1992; Pignolo et al. 1993; Pignolo et al. 2003) with similar findings in skin fibroblast cultures (Tresini et al. 1999; Pignolo et al. 2003). This was also the case when Francis *et al* (2004) examined tissue specimens from skin of differing aged donors; the largest decline was witnessed between young and middle aged donors, suggesting that reduction of PEDF expression may be an early aging event that alters the complex homeostatic balance of angiogenic modulators in the skin tissue microenvironment.

Abe *et al*, (2010) found that cultured keratinocytes stimulated with lipopolysaccharide constitutively secrete PEDF (as determined by ELISA analysis of PEDF concentration in the collected media 1 day after stimulation), and the secretion was significantly upregulated in a dose dependent manner, whereas cultured fibroblasts failed to show up-regulation. This suggests that keratinocytes but not

fibroblasts secrete PEDF in a regulated manner in response to inflammation. Furthermore, Sarojini *et al* suggested that conditioned medium (secretome) for mouse mesenchymal stem cells is chemotactic for human fibroblasts, and that PEDF is the predominant fibroblast chemoattractant, with immunofluorescence studies showing staining for PEDF in the cytoplasm, cell surface and interspace between mesenchymal stem cells (Sarojini et al. 2008).

When HaCaT cells were incubated with 50ng/ml of $VEGF_{165}$, western blot analysis showed that PEDF protein levels were dramatically decreased in comparison to those without treatment, therefore highlighting the counterbalance between VEGF and PEDF (Li et al. 2011). Wei *et al* (2011) also assessed the cellular function in HaCaT cells with the addition of recombinant PEDF either 5ng/ml or 50ng/ml compared to no treatment. The findings confirmed that PEDF inhibited HaCaT cellular growth by 4.62% and 23.91% at doses of 5ng/ml and 50ng/ml respectively. Flow cytometry demonstrated that treatment with rhPEDF 50ng/ml for 24 hours increased the percentage of cells in S phase from 13% to 26%, indicating that PEDF may induce S phase accumulation of HaCaT cells (Li et al. 2011). Adhesion assays found a significant increase in the rate of adhesion of HaCaT cells by 29% compared to untreated HaCaT cells with rhPEDF 50ng/ml ($p<0.05$) (Li et al. 2011). This significance was not seen at the lower dose of rhPEDF 5ng/ml. Scratch migration assays showed that PEDF 50ng/ml decreased wound closure rate by 33% and 29% after 24 and 48 hours of incubation, when compared to the control group ($p<0.001$) (no treatment) (Li et al. 2011). Work by Chen & Dipietro (2014) supported these findings of increased adhesion with the treatment of rhPEDF in keratinocytes, with an impairment of

migration rate but with no effect noted on cellular growth. They also found that treatment with inflammatory cytokines (IL-1β, IL-6 and TNF-α) inhibited PEDF expression in isolated skin keratinocytes. In mouse dermal burn wound models, PEDF was discovered to be downregulated at 0 and 2 hours post-wounding but upregulated at 3 and 14 days post-wounding. The authors hypothesised that this early downregulation of PEDF expression may be because of the high rate of inflammatory cytokines, such as IL-1β, IL-6 and TNF-α, in early wound environments (Chen et al. 2010) or due to disruption of the keratinocyte layer.

There is evidence to suggest that PEDF expression is downregulated in chronic inflammatory skin conditions, in keeping with other inflammatory conditions (as discussed in section 1.5.1), with studies evaluating psoriasis and condyloma acuminatum (Abe et al. 2010; Dong et al. 2013). The low levels of PEDF expression in such cases could be inhibiting cellular proliferation and resulting in abnormal proliferation and thickening of the epidermal basal layers. Topical application of low-molecular weight PEDF peptides in mouse models of psoriatic disease led to reduced angiogenesis and epidermal thickness, and suggest that it may be a novel therapeutic strategy for psoriasis (Abe et al. 2010).

In summary, the potential role PEDF may play in the treatment of chronic wounds is conflicting. PEDF expression appears to be downregulated in the initial acute phase after injury, suggesting its upstream interaction with inflammatory factors. PEDF has been shown to exhibit anti-inflammatory effects in other pathological conditions, which may be beneficial for such patients with chronic wounds. There may also be a direct chemoattractant or inhibition action of PEDF for cells important for wound

healing such as fibroblasts or keratinocytes. Abnormal angiogenesis also contributes to chronic wounds. PEDF is selective in its action by discriminating between endothelial cells forming new vessels and those from pre-existing vessels and therefore targeting mainly abnormal angiogenesis with newly forming vessels and avoiding existing vessels (Bouck 2002). It is therefore logical that PEDF inhibits aberrant angiogenesis, which leads to normalisation of healthy vasculature, potentially benefiting chronic wound healing.

1.6. Hypothesis and Aims of the Study

The hypothesis of this study is that the loss of PEDF expression will be associated with worsening prognostic factors in colorectal cancer and that the use of recombinant PEDF may result in the decrease of cellular proliferation, adhesion, migration and/or invasion of treated colorectal cancer cells. The hypothesised role of PEDF in wound healing is less clear, based on previous evidence. The aim of this study is to elucidate more detailed regulatory mechanisms of PEDF in wound healing, and tumour angiogenesis in different subtypes of colorectal cancer and provide evidence to develop PEDF or its fragments as therapeutics for wound healing or colorectal cancer treatment via expression profiling and cellular functional assays.

Chapter 2

General Materials and Methods

2.1 Cell lines

Six colorectal cancer cell lines and four wound healing cell lines were used in this study. Full details of cell origins and characteristics are outlined in Table 2.1.

2.2 Wound tissue collection

Tissue biopsies were performed on a total of 71 patients. All patients had duplex-ultrasound confirmed venous leg ulcers with a wound surface area of at least 4cm^2, that were present for at least six months and deemed non-infected by a clinician within the Wound Healing Research Team, Cardiff and Vale University Health Board. Ethical approval was obtained from Cardiff and Vale ethics committee (reference number SJT/C617/08) and written informed consent was gained from the patients, and has been described previously (Bosanquet et al. 2012). A 6mm punch biopsy was performed from the wound edge with the use of 1% lignocaine local anaesthetic using an aseptic technique. Tissue samples were stored at -80°C before transferring into liquid nitrogen. The patients subsequently had standard treatment for 12 weeks in the form of compression therapy and appropriate dressings. At 12 weeks' follow-up, the biopsies of the patients where the wound had either decreased in size or healed were classed as 'healing' and those that had either not decreased in size or remained static in size or increased were classed as 'non-healing'.

Table 2.1 Cell line origins and characteristics

Cell line	Species	Morphology	Sources and features	Purchase Company
RKO	Homo Sapiens	Epithelial	RKO is a poorly differentiated colon carcinoma cell line	American Type Culture Collection (ATCC, Rockville, Maryland, USA
HT115	Homo Sapiens	Epithelial	Derived from colonic adenocarcinoma	Sigma-Aldrich (Poole, Dorset, UK)
HRT-18	Homo Sapiens	Epithelial	Derived from rectal adenocarcinoma	Sigma-Aldrich (Poole, Dorset, UK)
COLO-201	Homo Sapiens	bipolar, slightly refractile, fibroblast-like cell	COLO-201 is a metastatic Dukes' D colorectal adenocarcinoma cell line, derived from ascites. It is sourced from a 70-year-old Caucasian male	American Type Culture Collection (ATCC, Rockville, Maryland, USA
LS174T	Homo Sapiens	Epithelial	LS 174T is mucinous secreting colorectal adenocarcinoma cell line (Dukes' B). Derived from a 58 years old Caucasian female	American Type Culture Collection (ATCC, Rockville, Maryland, USA)
CCD-33C0	Homo Sapiens	Fibroblast	Colorectal fibroblast cell line derived from a 7 years old Caucasian male	American Type Culture Collection (ATCC, Rockville, Maryland, USA)
HaCaT	Homo Sapiens	Keratinocyte	Derived from 62-year-old Caucasian male	CLS Cell Lines Service GmbH (Eppelheim, Germany)
HECV	Homo Sapiens	Endothelial	Derived from umbilical vein/ vascular endothelium	American Type Culture Collection (ATCC, Rockville, Maryland, USA)
Primary Dermal Fibroblasts (DF)	Homo Sapiens	Fibroblast	Derived from an adult	American Type Culture Collection (ATCC, Rockville, Maryland, USA)
Human Adipose-Derived Stem Cells (HASC)	Homo Sapiens	Human Adipose-Derived Stem Cells		Life Technologies (Paisley, UK)

2.3 Colorectal cancer tissue collection

Colorectal cancer tissue collection for transcript analysis was performed at Beijing Friendship Hospital, China. The cohort consisted of a total of 406 patients undergoing a surgical resection for the management of colorectal cancer. Medical records and histology reports were used for the collation of clinical and pathological data preoperatively and during the immediate postoperative follow-up period. Details of patient demographics, TNM staging, Dukes stage and pathological grade were provided during experimental data analysis. Ethical approval was obtained (Appendix 1) and consent received from all patients included in the cohort.

Colonic cancer tissue microarray (T054b) used for immunohistochemical staining was purchased from US Biomax, Inc. (Rockville, USA). The microarray included 12 cases/24 cores with normal colon tissue as control. Rectal cancer tissue microarray (RE961) used for immunohistochemical staining was purchased from US Biomax Inc. (Rockville, USA). The microarray included 48 cases/ 96 cores with normal colon tissue as control. Specimens were registered and stored according to Human Tissue Act regulations. All specimens were analysed anonymously. Details of patient age and gender, TNM staging, Dukes stage and pathological grade were provided during experimental data analysis. Specimens had diagnoses verified by a Consultant Histopathologist.

2.4 Primers

Table 2.2 outlines all the primers used in this study. All primers were designed using the Beacon Design programme (Biosoft International, Palo Alto, California, USA) and

synthesised by Sigma Aldrich (Poole, Dorset, UK). The software described above features an automated search for reaction conditions and possible homology amplification of other genes. The conventional reverse transcription polymerase chain reaction (RT-PCR) and quantitative PCR (qPCR) paired forward and reverse primers for each gene reside in one of two adjacent exons. Additionally, the amplified genome sequence includes at least one intron boundary. The optimal annealing temperature for all the primers used throughout this study was 55^{o}C.

2.5 Antibodies

The antibodies used throughout this study are detailed below in tables 2.3 and 2.4.

Table 2.2: Primers for conventional RT-PCR and real time qPCR

Gene	Primer name	Primer Sequence (5'-3')	Product size (bps)
PEDF	SERPINF1 F50	ATCCTTTCTTCAAAGTCCCC	324
	SERPINF1 R50	ATTTTATGCGCAGCTTCTTC	324
	PEDFF1	GGTGCTACTCCTCTGCATT	128
	PEDFZR	**ACTGAACCTGACCGTACA**AGAAAGGATCCTCC TCCTC	128
GAPDH	GAPDHF8	GGCTGCTTTTAACTCTGGTA	475
	GAPDHR8	GACTGTGGTCATGAGTCCTT	475
	GAPDHF1	AAGGTCATCCATGACAACTT	87
	GAPDHZR1	**ACTGAACCTGACCGTACA**GCCATCCACAGTCT TCTG	87
PDPL	PDPLF8	GAATCATCGTTGTGGTTATG	-
	PDPLZR	**ACTGAACCTGACCGTACA**CTTTCATTTGCCTAT CACAT	-

ACTGAACCTGACCGTACA *represents the Z sequence*

Table 2.3: Primary antibodies

Name	Species	Supplier and Product Code
Anti-PEDF polyclonal antibody	Rabbit	Santa Cruz Biotechnology, Inc. Sc-25594
Anti-GAPDH polyclonal antibody	Rabbit	Santa Cruz Biotechnology, Inc. Sc-25778

Table 2.4: Secondary antibodies

Name	Species	Supplier and Product Code
Anti- rabbit IgG peroxidase conjugate *	Goat	Sigma-Aldrich A-9169
Vectastain Universal Elite ABC Kit **	Universal	Vector Laboratories PK-6200
Anti- rabbit IgG FITC conjugate ***	Goat	Sigma- Aldrich F1262

** For protein probing*
*** For immunohistochemical studies*
**** For immunofluorescence studies*

2.6 General reagents and solutions

The solutions listed below were used throughout. All products were sourced from Sigma Aldrich (Poole, Dorset, UK) unless otherwise stated.

2.6.1 Solutions for use in tissue culture

Antibiotics (100x)

Antibiotic antimycotic solution (x100) containing 10,000units penicillin, 10mg streptomycin and 25µg amphotericin B per ml was diluted in balanced saline solution (BSS) and split into 5ml aliquots. This was then added directly to 500ml bottles of media.

Balanced Saline Solution

Two grams of Potassium Chloride (KCl), 79.5g Sodium Chloride (NaCl), 2.1g of Potassium Phosphate monobasic (KH_2PO_4) (Fisons Scientific equipment, Loughborough, UK), and 11g of Sodium Phosphate dibasic (Na_2HPO_4) (BDH Chemical Ltd, Poole, UK) were dissolved in 10L of distilled water. The pH was then adjusted to 7.4 by using 1M of Sodium Hydroxide (NaOH).

Ethyl Diamine Tetra-acetic Acid (EDTA) (0.02%)

One gram of KCl (Fisons Scientific equipment, Loughborough, UK) 1g, 5.72g of Na_2HPO_4 (BDH Chemical Ltd, Poole, UK), 40g of NaCl and 1.4g of EDTA (Duchefa Biochemie, Haarlem, The Netherlands) were dissolved in 5L of distilled water and the pH was subsequently adjusted to 7.4. This was then autoclaved and stored at room temperature until use.

Trypsin (25mg/ml)

Trypsin (500µg) was dissolved in 0.02% EDTA, mixed and then filtered through a 0.2µm ministart filter (Sartotirus, Epsom, UK). The solution was then aliquoted into 250µl samples and stored at -20^{o}C until use.

2.6.2 Solutions for use in molecular biology

Diethyl pyroncarbonate (DEPC) water

Two hundred and fifty millilitres of DEPC was added to 4.75ml of distilled water and then subsequently autoclaved and stored until use.

Tris-Boric Acid (TBE) (5x)

A five times stock solution containing 900mM of borate, 1.1M of Tris and 25mM of EDTA at ph8.3, was prepared by dissolving 540g of Tris-HCl (Melford Laboratories Ltd, Suffolk, UK), 275g of boric acid (Melford Laboratories Ltd, Suffolk, UK) and 46.5g of EDTA in 10L of distilled water. NaOH was used to adjust the pH to 8.3. The solution was stored at room temperature until required. For the preparation of agarose gels and DNA electrophoresis the TBE was diluted using distilled water to a 1x concentrate.

2.6.3 Solutions for protein analysis

10% Ammonium Persulfate (APS)

One gram of APS was dissolved in 10ml of distilled water. This solution was stored in 2.5ml aliquots at 4^{o}C until further use.

Cell Lysis buffer

The cell lysis buffer was prepared by dissolving 50mM Tris (0.61g), 5mM EGTA (0.19G), 150mM NaCl (0.87g) and 1ml Triton x100 in 100ml of distilled water. Protease inhibitors (phenylmethylsulfonyl fluoride (PMSF) (100µg/ml in isopropanol), aprotinin (10µg/ml), leupeptin (10µg/ml), sodium fluoride (50mM) and sodium vanadate (5mM)) were added prior to use.

Running buffer (10x) (for SDS-PAGE)

Running buffer (10x) stock solution which contained 0.25M Tris, 1.92M glycine and 1% Sodium dodecyl sulphate (SDS) at pH8.3 was prepared by dissolving 303g of Tris, 1.44kg of glycine (Melford Laboratories Ltd, Suffolk, UK) and 100g of SDS (Melford

Laboratories Ltd, Suffolk, UK) in 10L of distilled water. This solution was further diluted to a 1x concentrate using distilled water for usage.

Transfer buffer

Transfer buffer was made by dissolving 15.5g of Tris and 72g of glycine in 4L distilled water. Following this, 1L of methanol (Fisher Scientific, Leicestershire, UK) was added resulting in a final volume of 5L in distilled water.

Tris Buffered Saline (TBS) (10x)

Tris Buffered Saline (10x) stock solution, which contained 0.5M Tris and 1.38M NaCl, at pH7.4 was prepared by dissolving 24.228g of Tris and 80.06g of NaCl (Melford Laboratories Ltd, Suffolk, UK) in 1L distilled water. The addition of HCl resulted in an adjusted pH of 7.4 and was stored at room temperature until use.

Tris Buffered Saline with Tween 20 (TBST)

Tris Buffered Saline (1x) mixed with 0.05% Tween 20 (Melford Laboratories Ltd, Suffolk, UK).

Blocking Solution

TBST with 10% skimmed milk solution dissolved in the solution.

2.6.4 Solutions used for immunohistochemical studies

Blocking Reagent for staining of tissues

A blocking reagent was used to dilute primary and secondary antibodies (described in section 2.5). The blocking reagent consisted of 10mls of TBS mixed with 0.1% BSA, 0.1% saponin, 0.1% skimmed milk powder, and 2ml horse serum.

Blocking Reagent for staining of cells

A blocking reagent was used to dilute primary and secondary antibodies (described in section 2.5). The blocking reagent consisted of 10mls of TBS mixed with 0.1% BSA and 2ml horse serum.

DAB (diaminobenzidine) substrate

DAB substrate was prepared using 0.5ml aliquot of DAB, 4.5mls TBS and 6µl of hydrogen peroxide (H_20_2) and used immediately after preparation.

2.6.5 Reagents used as treatment in cellular functional studies

Recombinant PEDF

Recombinant PEDF was purchased from R&D Systems Europe Ltd (Abingdon, Oxfordshire, UK) and diluted to 10µg/ml using sterile BSS: 0.1% BSA, then stored at -80 ^{o}C until use.

FAK inhibitor (FAKi)

PF-573228 (Cat no: 3239) **[**3,4-Dihydro-6-[[4-[[[3-(methylsulfonyl)phenyl]methyl]amino]-5-(trifluoromethyl)-2-pyrimidinyl]amino]-2(1*H*)-quinolinone] was purchased from Tocris Bioscience (Bristol, UK) and diluted to 1mM stock solution using sterile DMSO, then stored at 20 ^{o}C until use (Figure 2.1).

c-Met inhibitor (c-Mi)

PHA-66572 (Cat no: 2693) [(2R)-1-[[5-[(Z)-[5-[[(2,6-Dichlorophenyl)methyl]sulfony l]-1,2-dihydro-2-oxo-3H-indol-3-ylidene]methyl]-2,4-dimethyl-1H-pyrrol-3-yl]carbonyl]-2-(1-pyrrolidinylmethyl) pyrrolidine] was purchased from Tocris Bioscience (Bristol, UK) and diluted to 1mM stock solution using sterile DMSO, then stored at 20 ^{o}C until use (Figure 2.2).

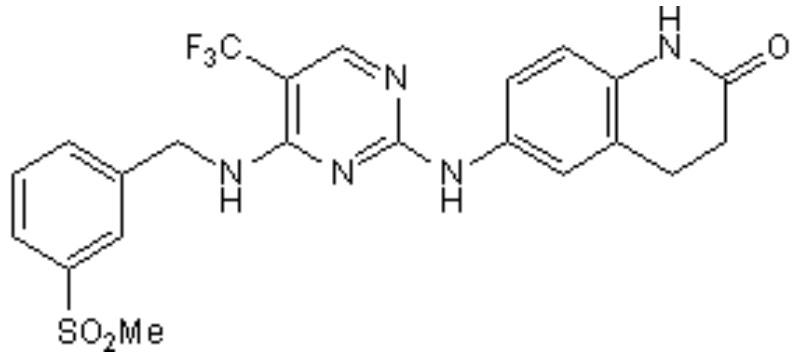

Figure 2.1. PF-573228 **[**3,4-Dihydro-6-[[4-[[[3-(methylsulfonyl)phenyl]methyl]amino]-5-(trifluoromethyl)-2-pyrimidinyl]amino]-2(1*H*)-quinolinone] Chemical Structure.

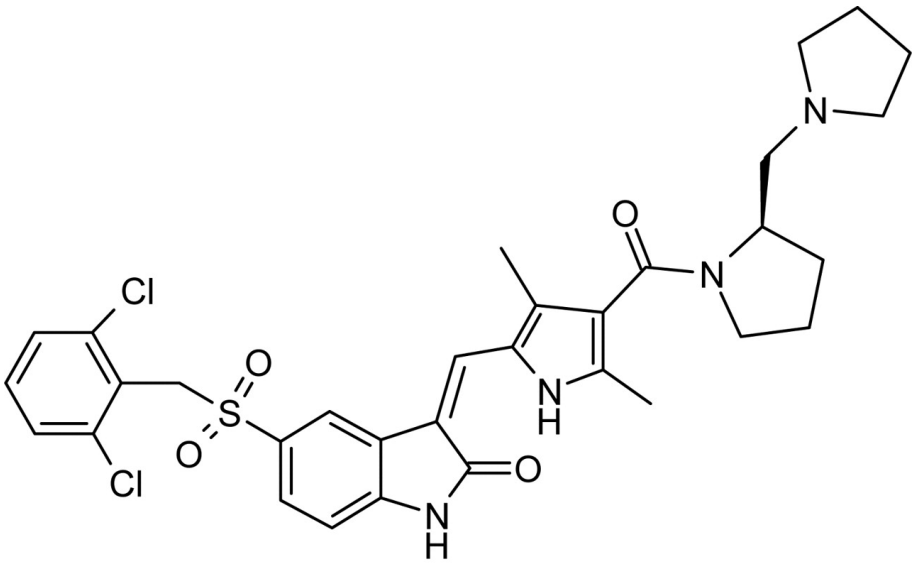

Figure 2.2. PHA-665752 [(2R)-1-[[5-[(Z)-[5-[[(2,6-Dichlorophenyl)methyl]sulfony l]-1,2-dihydro-2-oxo-3H-indol-3-ylidene]methyl]-2,4-dimethyl-1H-pyrrol-3-yl]carbonyl]-2-(1-pyrrolidinylmethyl) pyrrolidine] Chemical Structure.

2.7 Cell maintenance, culture and storage

2.7.1 Preparation of growth medium for maintenance of cells

The culture medium used for each cell line is described in Table 2.5.

2.7.2 Cell Maintenance

All cell lines were maintained in either 25cm^2 or 75cm^2 tissue culture flasks (Greiner Bio-One Ltd, Gloucestershire, UK), within an incubator using the settings as follows; 37^{o}C, 5% CO_2 and 95% humidity. All tissue culture procedures were carried inside a class II laminar flow cabinet whilst adhering to aseptic techniques using autoclaved and sterile equipment. Cells were maintained in the appropriate supplemented media (as described in Table 2.5) and routinely sub-cultured upon reaching 90% confluence. Confluence was determined by assessing the coverage of cells over the surface of the base of the tissue culture flask using a Leica DMi1 inverted light microscope (Leica microsystems Ltd, Milton Keynes, UK) using x100 magnification.

2.7.3 Detachment of adherent cells

The culture medium was aspirated once the cells had reached 90% confluence. Cells were washed in sterile EDTA-BSS buffer to remove any remaining medium, to reduce the inhibitory effect remaining medium would have on the action of trypsin. Adherent cells were detached from the flask by incubating with 5ml of trypsin:EDTA (0.01% trypsin 0.02% EDTA in BSS buffer) and placed back in the incubator at 37^{o}C for roughly ten minutes until the cells had detached. Once the cells were detached from the surface of the base of the tissue culture flask, the cell suspension was placed

in a 30ml universal container (Greiner Bio-One Ltd, Gloucestershire, UK) and centrifuged at 1760rpm for 8 minutes in order to form a cell pellet. The supernatant was aspirated and the cell pellet was resuspended in the appropriate medium.

2.7.4 Cell counting

Cell counting for accurate cell density seeding for immunocytochemical studies and cellular functional assays, was performed using a Neubauer haemocytometer counting chamber (Mod-Fuchs, Rosenthal, Hawksley, UK). This haemocytometer was used in order to calculate the cells per millilitre from the number of cells in a previously known volume. Cell counting took place under a Leica DMi1 inverted light microscope (Leica microsystems Ltd, Milton Keynes, UK) using x100 magnification. The counting chamber has 9 squares on it each with the dimensions 1mm x 1mm x 0.2mm and then further divided into 16 equal small squares. Three of the 1mm x 1mm x 0.2mm squares was counted for representative purposes. The number of cells was calculated by using the equation below:

Cell number/ml= (the sum of the number of cells in each 16 squares /2) x ($1x10^4$)

Table 2.5: Cell line and culture medium used

Cell line	Culture Medium used
RKO	DMEM/Ham's F12 with L-glutamine medium (Sigma-Aldrich, Dorset, UK) with 5ml antibiotics (streptomycin 0.1mg/ml, penicillin 100U/ml, amphotericin 0.25 µg/ml) and 50ml Foetal Calf serum (10%)
HT115	DMEM/Ham's F12 with L-glutamine medium (Sigma-Aldrich, Dorset, UK) with 5ml antibiotics (streptomycin 0.1mg/ml, penicillin 100U/ml, amphotericin 0.25 µg/ml) and 50ml Foetal Calf serum (10%)
HRT-18	DMEM/Ham's F12 with L-glutamine medium (Sigma-Aldrich, Dorset, UK) with 5ml antibiotics (streptomycin 0.1mg/ml, penicillin 100U/ml, amphotericin 0.25 µg/ml) and 50ml Foetal Calf serum (10%)
COLO-201	DMEM/Ham's F12 with L-glutamine medium (Sigma-Aldrich, Dorset, UK) with 5ml antibiotics (streptomycin 0.1mg/ml, penicillin 100U/ml, amphotericin 0.25 µg/ml) and 50ml Foetal Calf serum (10%)
LS174T	DMEM/Ham's F12 with L-glutamine medium (Sigma-Aldrich, Dorset, UK) with 5ml antibiotics (streptomycin 0.1mg/ml, penicillin 100U/ml, amphotericin 0.25 µg/ml) and 50ml Foetal Calf serum (10%)
CCD-33C0	Fibroblast basal medium (ATCC, Rockville, Maryland, USA) with 5ml antibiotics (streptomycin 0.1mg/ml, penicillin 100U/ml, amphotericin 0.25 µg/ml), hydrocortisone (1µg/ml), Basic Fibroblast Growth Factor (FGFb) (5ng/ml), ascorbic acid 50µg/ml), insulin (5µg/ml), glutamine (7.5mM) and 20ml Foetal Calf Serum (2%)
HaCaT	DMEM/Ham's F12 with L-glutamine medium (Sigma-Aldrich, Dorset, UK) with 5ml antibiotics (streptomycin 0.1mg/ml, penicillin 100U/ml, amphotericin 0.25 µg/ml) and 50ml Foetal Calf serum (10%)
HECV	DMEM/Ham's F12 with L-glutamine medium (Sigma-Aldrich, Dorset, UK) with 5ml antibiotics (streptomycin 0.1mg/ml, penicillin 100U/ml, amphotericin 0.25 µg/ml) and 50ml Foetal Calf serum (10%)
Primary Dermal Fibroblasts (DF)	Fibroblast basal medium (ATCC, Rockville, Maryland, USA) with 5ml antibiotics (streptomycin 0.1mg/ml, penicillin 100U/ml, amphotericin 0.25 µg/ml), hydrocortisone (1µg/ml), Basic Fibroblast Growth Factor (FGFb) (5ng/ml), ascorbic acid 50µg/ml), insulin (5µg/ml), glutamine (7.5mM) and 20ml Foetal Calf Serum (2%)
Human Adipose-derived Stem Cells (HASC)	MesenProRS medium (Life Technologies, Paisley, UK) with glutamine (2mM), 20ml Foetal Calf Serum (2%) and with 5ml antibiotics (streptomycin 0.1mg/ml, penicillin 100U/ml, amphotericin 0.25 µg/ml)

2.7.5 Storage of cell stocks in liquid nitrogen

All stocks of low passage (<4) cells were stored in liquid nitrogen. Cells were detached from a tissue culture flask using trypsin:EDTA (as described in section 2.7.3). Following detachment, the cells were resuspended in the required volume (dependant on the number of samples to be frozen) of the cryprotective solution consisting of DMSO (10% of the required volume) in appropriate growth medium. Following resuspension, cells were aliquoted into 1ml volumes in 1.8ml cryotubes (Greiner Bio-One, Germany) and stored overnight in an -80^{o}C freezer. The cryotubes were transferred after 24 hours to liquid nitrogen tanks for longer-term storage.

2.7.6 Cell revival from liquid nitrogen

Cryotubes containing cells were removed from liquid nitrogen tanks when required for use. The cryotubes were thawed, by placing them in a water bath at 37^{o}C. Following thawing, the cell solution was poured into a universal container alongside 10ml of pre-warmed medium thus diluting the DMSO. The universal container was centrifuged at 1760rpm for 8 minutes in order to form a cell pellet. The resultant supernatant was aspirated off and the cell pellet resuspended in 5ml of the appropriate growth medium. The cell solution was then maintained overnight at 37^{o}C in a 25cm^{2} tissue culture flask.

The following day, the surface of the base of tissue culture flask was visualised using a light microscope to confirm viable adherent cells. The medium was aspirated and replaced in order to remove any residual DMSO and non-viable cells. Standard sub-culture techniques, as described in section 2.7.2, were performed as necessary.

2.8 Synthesis of complementary DNA for use in PCR analysis

2.8.1 Total RNA isolation

RNA was extracted according to the TRI Reagent protocol (Sigma-Aldrich). Once cells reached confluence, the medium was aspirated off. 1ml of TRI Reagent was added to the flask in order to induce cell lysis, and a cell scrapper used to facilitate removal. The resultant cell lysate was transferred into a 1.8ml microfuge tube. 0.2ml chloroform was added to the Eppendorf, vigorously shaken for 15 seconds, then centrifuged at 12,000rpm for 15 minutes at 4^0C (Boeco, Wolf Laboratories, York, UK). The upper aqueous phase containing RNA was transferred to a new 1.8ml microfuge tube, followed by the addition of 500µl isopropanol and incubation for 10 minutes at room temperature prior to a centrifuging at 12,000rpm for 10 minutes at 4^OC. Following centrifuging, the supernatant was aspirated off and removed and a pellet at the microfuge tube was visible representing the RNA present in the sample that had precipitated out of the solution. The RNA pellet was washed in 1ml of 75% cold ethanol (Fisher Scientific, Leicestershire, UK) prepared in DEPC water, and then centrifuged at 7,500rpm for 5 minutes at 4^OC. The ethanol was then removed and the microfuge tube placed in a drying oven (Techne Hybridiser HB-1D, Wolf Laboratories, York, UK) for 10 minutes at 55^0C to allow the RNA pellet to dry. The pellet was finally resuspended in 40µl of DEPC water by vortexing.

2.8.2 RNA quantification

Concentration of RNA was measured using an Implen Nanophotometer (Implen, Munich, Germany). This Implen Nanophotometer is configured to detect single

strand RNA (µg/µl) in a 1 in 10 dilution by quantifying the difference in absorbance at 260nm between the RNA sample and a control of DEPC water.

2.8.3 RNA extraction from tissues

Both wound and colorectal tissues sections (60x70µm) were homogenised using a hand-held homogeniser in ice-cold RNA extraction solution. The RNA concentration was determined using UV1101 Biotech Photometer (WPA, Cambridge, UK) and was set to detect single stranded RNA (µg/µl) at 1:10 dilution of the DEPC water control.

2.8.4 Reverse transcription of RNA

RNA was converted into complementary DNA (cDNA) using a high capacity cDNA reverse transcription kit (Applied Biosystems, Manchester, UK). Based on the Nanophotometer reading, PCR water was added to the RNA solution to make up to a total volume of 10µl (standardised values of 250-500ng of RNA and PCR water) with 10µl of RT Mastermix (10x RT buffer (2µl), 25x dNTP mix 100mM (0.8µl), 10x RT random primers (2µl), MultiScibe Reverse transcriptase (1µl), RNase inhibitor (1µl) and Nuclease-free water (3.2µl)) added. The T-cy thermocycler (Creacon Technologies Ltd, Netherlands) settings used were:

Step 1 - 25°C for 10 minutes

Step 2 - 37°C for 120 minutes

Step 3 - 85°C for 5 minutes

Following this reaction, the resultant cDNA was diluted to 1:4 using PCR water and stored at -20°C.

2.8.5 Reverse Transcription Polymerase chain reaction (RT-PCR)

RT-PCR was performed using GoTaq Green master mix (Promega, Madison, USA) and the appropriate primers as described in Table 2.2. The reaction was set up for each sample in a 200µl PCR tube as described in Table 2.6. To prevent contamination, all reactions were run alongside a negative control replacing the cDNA template with nuclease-free water. The PCR tube contents were mixed briefly and placed in a T-Cy thermocycler and set to the following cycling conditions as described in Table 2.7.

Table 2.6 Components for RT-PCR reaction

Component	Volume (µl)
2 x GoTaq Green master mix	8
Forward primer	1
Reverse primer	1
Nuclease-free water (PCR water)	5
cDNA template	1
Total	16

Table 2.7 Cycling conditions used for RT-PCR

Step	Temperature	Time	
Initial denaturing	94^{o}C	5 minutes	
Denaturing	94^{o}C	30 seconds	} 34 cycles
Annealing	55^{o}C	30 seconds	
Extension	72^{o}C	40 seconds	
Final extension	72^{o}C	10 minutes	

2.8.6 Agarose gel electrophoresis

RT-PCR products were run using agarose gel electrophoresis (0.8% gel prepared with 0.4g agarose (Melford Chemicals, Suffolk, UK) and 50mls 1xTBE solution and heated until dissolved then 5µl SYBR safe DNA gel stain (Invitrogen, Manchester, UK) added). This solution was poured into electrophoresis cassette with a comb inserted to form wells. Once the gel had set, the cassette was submerged in 1xTBE buffer and the comb carefully removed. 5µl of 1Kb DNA ladder (Cat No. M106R; GenScript USA Inc.) and 8µl of each sample were loaded into the wells. Settings of 95V and 50W were set on a power pack (Gibco BRL, Life Technologies Inc.) for 45 minutes.

2.8.7 DNA visualisation

Images of the agarose gels were captured using a blue light illuminator in the SyngeneU:Genius 3 system (Geneflow, Elmhurst, Lichfield Staffs). The experiment was repeated at least 3 independent times. Representative images are presented in this study.

2.8.8 Quantitative RT-PCR (qPCR)

Quantitative RT-PCR (qPCR) is a technique first developed in 1992 (Porcher et al. 1992), and its development significantly improved the quantification of nucleic acid samples when compared to RT-PCR, by detecting small amounts of cDNA within a given sample and quantifying with an accurate and reliable transcript copy number. A molecular beacon method for qPCR was performed using the Amplifluor Uniprimer Universal system (Intergen Company, New York, USA). The ampliflour probe consists of a 3’ region specific to the Z-sequence (ACTGAACCTGACCGTACA) present on the

target specific primers (as described in table 2.2) and a 5' hairpin structure labelled with a flourophore (FAM) (Nazarenko et al. 1997). The flourophore hairpin structure is linked to an acceptor moiety (DABSYL) and therefore acts as a fluorescence quencher preventing any signal from being detected. During the qPCR reaction, the uniprobe (Millipore, Watford, UK) becomes incorporated and acts as a template for DNA polymerisation, in which DNA polymerase uses its 5'-3' exonuclease activity to degrade and unfold the hairpin structure. This disrupts the energy transfer between the quencher and flourophore and results in sufficient fluorescence to be emitted and detected. The fluorescent signal emitted during each cycle is directly correlated to the amount of DNA that has been amplified. The degree of fluorescence in a sample was compared to a range of standards of known transcript copy numbers (Figure 2.3). This permits accurate calculation of the transcript copy number in each sample. Detection of GAPDH copy number in the samples was used to allow standardisation and normalisation of each sample tested. The reaction mixture used for qPCR is detailed in Table 2.8. Each sample was loaded (in at least triplicate) into a 96 well plate (Bio-Rad Laboratories, Hemel Hampstead, UK). The standards with copy numbers ranging from 10^8-10^1 was loaded into the first column of the 96 well plate as described in Table 2.9. The 96 well plate was sealed with an optically clear Microseal (Bio-Rad Laboratories, Hemel Hampstead, UK). This was placed in an iCyclerIQ thermocycler (Bio-Rad Laboratories, Hemel Hampstead, UK) to amplify and quantify the cDNA over the cycles detailed in Table 2.10. Specific qPCR primers were verified using a positive control know to express the molecule of interest and a negative control, where PCR water replaced cDNA in a reaction, to rule out contamination before use. Each experiment was repeated at least 3 independent

times and combined data of transcript copy numbers normalised to GAPDH are presented in this study.

Table 2.8 Components for qPCR reaction used for each sample

Component for reactions per well	Volume (µl)
2x mastermix (BioRad iQ Supermix)	5
GAPDH or PEDF Forward primer (10pmol)	0.3
GAPDH or PEDF Reverse Z primer (1pmol)	0.3
Amplifluor probe	0.3
PCR water	3
cDNA	1
Total	10

Table 2.9 Components for qPCR reaction used for standards

Component for standard reaction per well	Volume (µl)
2x mastermix (BioRad iQ Supermix)	5
PDPL Forward primer (10pmol)	0.3
PDPL Reverse primer (1pmol)	0.3
Amplifluor probe	0.3
PDPL standard in water	4
Total	10

Table 2.10 Cycling conditions used for qPCR

Step	Temperature	Time	
Initial denaturing	94^{o}C	5 minutes	
Denaturing	94^{o}C	10 seconds	} 100 cycles
Annealing	55^{o}C	35 seconds	
Final extension	72^{o}C	10 seconds	

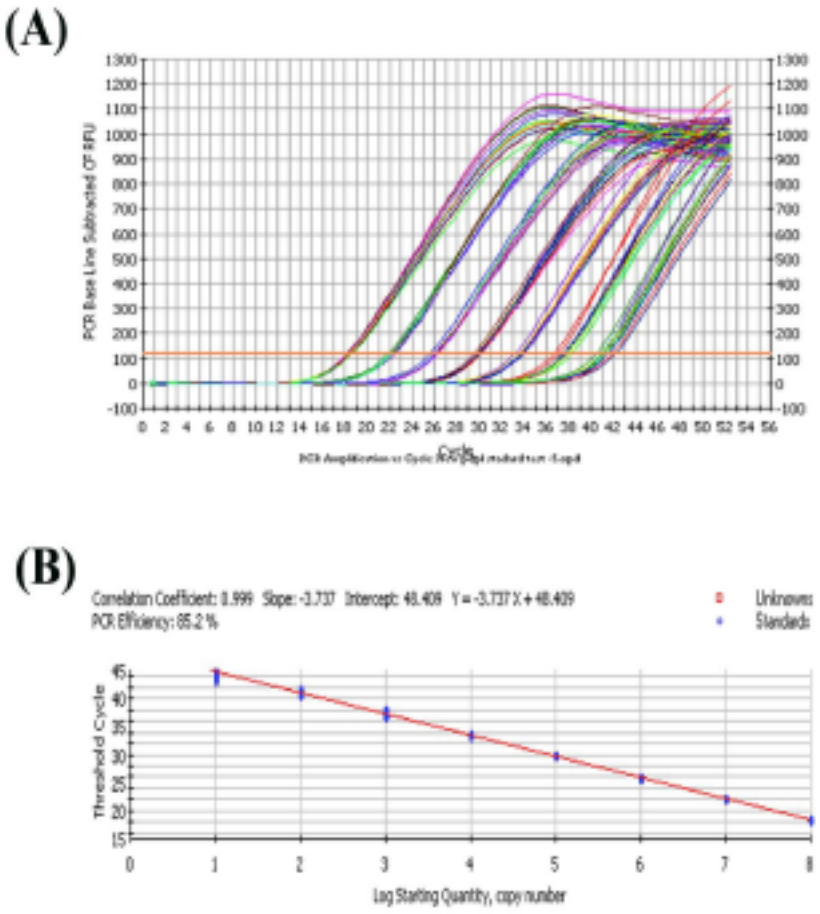

Figure 2.3: qPCR Standards
A) The detection range of the qPCR PDPL standards used throughout this study. Each standard was tested multiple times (n=12, representative data shown) and used to produce a standard curve B).

2.9 SDS-PAGE and Western blotting

2.9.1 Protein extraction and preparation of cellular lysates

Protein extraction was performed once cells reached 70% confluence. The medium was removed, washed 2x PBS and 150µl lysis buffer added. Cells were detached from the flask using a cell scraper and transferred into a 1.8ml Eppendorf. This was placed on ice for 15mins then centrifuged at 13,000rpm for 15mins at 4^{o}C. The supernatant was stored at 20^{o}C.

2.9.2 Protein quantification

Protein quantification was undertaken according to Bio-Rad DC Protein Assay Kit protocol (Hemel Hempstead, UK) in order to standardise the concentration of protein samples prior to use in SDS-PAGE and Western Blotting. A standard curve was created based on the absorbance of the bovine serum albumin (BSA) standards (BSA 50mg/ml serially diluted from 10mg/ml to 0.005mg/ml in lysis buffer). 5 µl of either the standard or the sample was added to wells on a 96 well plate, with the addition of 25 µl of Reagent A' (20 µl of Reagent S per ml of Reagent A) and 200 µl of Reagent B and incubated for 45 minutes at room temperature. Absorbance was subsequently read at 620nm using an ELX800 plate reading spectrophotometer (Bio-Tek, Wolf Laboratories, York, UK). A standard curve was created using an equation to calculate protein quantification from the scatter line graph of spectrophotometer results in Microsoft Excel software (Microsoft, Washington, USA), therefore allowing the sample concentrations to be calculated. Samples were normalised to the desired final concentration of 1.0mg/ml through dilution in lysis buffer and then further

diluted with a 1:1 ratio using 2x Lamelli buffer. Following this the sample was boiled at 100^{o}C for 5 minutes and stored at -20^{o}C.

2.9.3 Sodium dodecyl sulphate polyacrylamide gel electrophoresis (SDS-PAGE)

OmniPAGE VS10 vertical electrophoresis system (Wolf Laboratories, York, UK) was used for SDS-PAGE. The resolving and stacking acrylamide gels were prepared as described in Table 2.11. The resolving gel was poured between two glass plates within the loading cassette, to 1.5cm below the top of the plate. Once set, the stacking gel was poured on top and a comb placed until set. The loading cassette was placed into an electrophoresis tank and filled with 1x running buffer. 8µl of broad range molecular weight marker (Santa Cruz Biotechnology, supplied by Insight Biotechnologies Inc., Surrey, UK) and 18µl of protein sample were loaded into the wells. The proteins were separated using electrophoresis at 120V, 50mA and 50W for 2 hours.

Table 2.11 Components of resolving and stacking acrylamide gels for SDS-PAGE

Component	10% resolving acrylamide gel (ml)	Stacking acrylamide gel (ml)
Distilled water	5.9	3.4
30% acrylamide mix	5.0	0.83
1.5M Tris (pH8.8)	3.8	-
1.0M Tris (pH6.8)	-	0.63
10% SDS	0.15	0.05
10% ammonium persulphate	0.15	0.05
TEMED	0.006	0.005
Total	15	5

2.9.4 Western Blotting

The protein sample gels were transferred to a PVDF membrane using a SD10 SemiDry Maxi System blotting unit (SemiDRY, Wolf Laboratories, York, UK). For this to take place squares of 8cm x 8cm filter paper were pre-soaked in 1x transfer buffer (Whatman International Ltd, Maidstone, UK) and PVDF membrane 7.5cm x 7.5cm (Santa Cruz Biotechnology Inc., UK) pre-soaked in methanol and 1 x transfer buffer. Subsequently these were placed within the SD10 SemiDry Maxi System blotting unit (SemiDRY, Wolf Laboratories, York, UK) as outlined in Figure 2.4. Electroblotting settings were 15V, 500mA, 8W for 45 minutes.

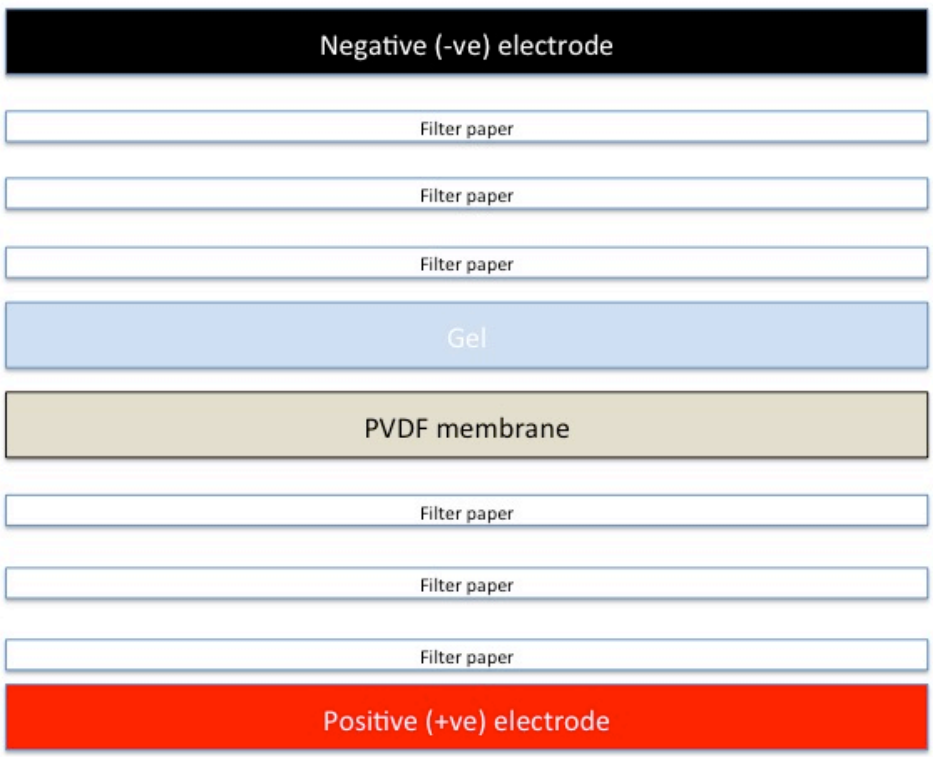

Figure 2.4: Schematic diagram of the layout in the SD10 SemiDry Maxi System blotting unit for the transfer of protein from gel to PVDF membrane

2.9.5 Protein probing

Protein Probing was performed according to the Millipore SNAP i.d. protein detection system protocol (Watford, UK) (Appendix 2). The surface of the blot holder was wet using distilled water and the PVDF membrane was placed with the protein transfer surface downwards and central on the surface of the blot holder. Air bubbles were extracted from the posterior surface of the membrane using a roller. A spacer was placed on top of the posterior surface and rolled again prior to closure of the blot holder. Blocking solution was applied to each well and the vacuum activated. Following suction of all visible blocking solution the primary antibody solution (as described in section 2.5) was added to each well and incubated for 10 minutes at room temperature. The concentration used for primary antibodies was 1:150 for Anti-PEDF polyclonal antibody and 1:400 for Anti-GAPDH polyclonal antibody. The vacuum was activated and washed 3 times using TBST. The secondary antibody solution (as described in section 2.5) was added to each well and incubated for 10 minutes at room temperature. The concentration used for the secondary anti- rabbit IgG peroxidase conjugate concentration was 1:500. The vacuum was once again reactivated and washed 3 times using TBST. Following suction of all visible wash buffer solution the membrane was removed ready for chemiluminescent protein detection.

All volumes used for solutions outlined above were titrated to well size as per the Millipore SNAP i.d. protein detection system protocol (Millipore, Watford, UK) (Appendix 2).

2.9.6 Chemiluminescent protein detection

To permit protein detection 1ml of chemiluminescence detection kit reagent was applied to the membrane and incubated for 5 minutes (Luminata, Millipore, Watford, UK). The solution was drained from the membrane prior to placement in the UVITech Imager (UVTechInc, Cambridge, UK). The chemiluminescent signal was detected at varying exposure times until protein bands were visible using a GAPDH was used as a loading control.

2.10 Immunohistochemical studies

2.10.1 Immunohistochemical staining of tissues

Immunohistochemistry was performed using Vector ABC kit (Vector Laboratories, Burlingame, California, USA) as described previously (Wang et al. 2016). The cryosections were removed from the -80^{o}C freezer and allowed to come to room temperature for 15 minutes. The slides (Menzel-Glaser Superfrost ® Plus, Thermo Scientific, Leicestershire, UK) were fixed in acetone (Fisher Scientific, Leicestershire, UK) for 15 minutes and allowed to air dry at room temperature for 15 minutes then subsequently washed three times with TBS. A ring of wax was applied around each section on the slide. Incubation with the Blocking Reagent for staining of tissue (as described in section 2.6.4) was performed for 1 hour in a humidified box, followed by incubation with the primary antibody for a further hour. Primary antibody used was PEDF rabbit monoclonal antibody at a 1:50 concentration diluted using Blocking Reagent for staining of cells, as described in section 2.5 and 2.6.4. The slides were washed three times with TBS followed by incubation with the secondary antibody for

30 minutes. Secondary antibody used was ABC Biotinylated secondary antibody (5ml of blocking reagent with 100µl of biotinylated antibody stock) (as described in section 2.5). The slides were washed three times with TBS followed by incubation of the ABC reagent for 30 minutes. ABC reagent used consisted of 5ml of blocking reagent with 100µl of reagent A and 100µl of reagent B (Cat no. PK-6200; Vectastain Universal Elite ABC Kit, Vector Laboratories, Burlingame, California, USA). The slides were once again washed three times in TBS and subsequently developed in DAB substrate for 6 minutes. The slides were briefly washed in tap water prior to counterstaining with Hematoxylin Gill's Formula (Vector Laboratories, Burlingame, California, USA) for 10 minutes. The slides were then dehydrated for 5 minutes in each of 50% ethanol (Fisher Scientific, Leicestershire, UK), 70% ethanol (Fisher Scientific, Leicestershire, UK), 90% ethanol (Fisher Scientific, Leicestershire, UK), 100% ethanol (Fisher Scientific, Leicestershire, UK), 100% ethanol (Fisher Scientific, Leicestershire, UK), 50% ethanol/50% xylene (Fisher Scientific, Leicestershire, UK), and finally 100% xylene (Fisher Scientific, Leicestershire, UK). The samples were mounted with DPX Mountant and a coverslip (Fisher Scientific, Leicestershire, UK).

All samples were run against a negative control for comparison purposes. The samples were visualised using a Leica DM 1000 LED microscope (Leica Microsystems Ltd, Milton Keynes, UK) at x100 magnification. Software used capture images was LAS EZ (Leica Application Suite, Milton Keynes, UK). Representative images were shown in this study.

2.10.2 Immunocytochemical staining of cells

The methods used for immunocytochemical staining has been described previously (Martin et al. 2004). Cells were seeded at a seeding density of 2.5 x10^4 cells per 300µl and were cultured in 8-well chamber slides (Millipore, Watford, UK) and incubated in appropriate growth medium overnight at 37^{o}C, 5% CO_2 and 95% humidity. Following incubation, the medium was removed and the cells were fixed with ice-cold 70% ethanol at -20^{o}C for at least 20 minutes. The cells were rehydrated with BSS followed by permeabilisation with 0.1% Triton X-100 for 5 min. After washing with BSS, the cells were blocked with Blocking Reagent for staining of cells, as described in 2.6.4, for 1 hour in a humidified box, followed by incubation with the primary antibody for a further hour. Primary antibody used was PEDF rabbit monoclonal antibody at a 1:50 concentration (Santa Cruz Biotechnology Inc., UK) diluted using blocking reagent, as described in section 2.5 and 2.6.4. The slides were washed three times with TBS followed by incubation with the secondary antibody for 30 minutes. Secondary antibody used was ABC Biotinylated secondary antibody (5ml of blocking reagent with 100µl of biotinylated antibody stock) (as described in section 2.5). The slides were washed three times with TBS followed by incubation of the ABC reagent for 30 minutes. ABC reagent used consisted of 5ml of blocking reagent with 100µl of reagent A and 100µl of reagent B (Cat no. PK-6200; Vectastain Universal Elite ABC Kit, Vector Laboratories, Burlingame, California, USA). The slides were one again washed three times in TBS and subsequently developed in DAB substrate for 6 minutes. The slides were briefly washed in tap water prior to counterstaining with Hematoxylin Gill's Formula (Vector Laboratories, Burlingame, California, USA) for 10 minutes. The

slides were then dehydrated for 5 minutes in each of 50% ethanol (Fisher Scientific, Leicestershire, UK), 70% ethanol (Fisher Scientific, Leicestershire, UK), 90% ethanol (Fisher Scientific, Leicestershire, UK), 100% ethanol (Fisher Scientific, Leicestershire, UK), 100% ethanol (Fisher Scientific, Leicestershire, UK), 50% ethanol/50% xylene (Fisher Scientific, Leicestershire, UK), and finally 100% xylene (Fisher Scientific, Leicestershire, UK). The samples were mounted with DPX Mountant and a coverslip (Fisher Scientific, Leicestershire, UK).

All samples were run against a negative control for comparison purposes. The samples were visualised using a Leica DM 1000 LED microscope (Leica Microsystems Ltd, Milton Keynes, UK) at x100 magnification. Software used capture images was LAS EZ (Leica Application Suite, Milton Keynes, UK). Representative images were shown in this study.

2.11 Immunofluorescence staining of cells

Cells were seeded at a density of 2.5 $x10^4$ cells per 300µl, were cultured in 8-well chamber slides (Millipore, Watford, UK) and incubated in appropriate growth medium overnight at 37^oC, 5% CO_2 and 95% humidity. Following incubation, the medium was removed and the cells were fixed with ice-cold 70% ethanol at -20^oC for at least 20 minutes. The cells were rehydrated with BSS followed by permeabilisation with 0.1% Triton X-100 for 5 min. After washing with BSS, the cells were blocked with Blocking Reagent for staining of cells, as described in 2.6.4, for 1 hour in a humidified box, followed by incubation with the primary antibody for a further hour. Primary antibody used was PEDF rabbit monoclonal antibody at a 1:50 concentration diluted

using blocking reagent, as described in section 2.5 and 2.6.4. The slides were washed three times with TBS followed by incubation with the secondary antibody for 30 minutes. Secondary antibody used was anti- rabbit IgG FITC conjugate at a 1:250 concentration (as described in section 2.5). The slides were one again washed three times in TBS. The samples were mounted with Floursave Reagent (Millipore, Watford, UK) and a coverslip (Fisher Scientific, Leicestershire, UK).

All samples were run against a negative control for comparison purposes. The samples were visualised using an Olympus BX51 polarising microscope at x40 magnification (Olympus KeyMed Group of Companies, Essex, UK). Software used to capture images was cellSens dimension (OIympus KeyMed Group of Companies, Essex, UK). Representative images were shown in this study. All images were normalised against the comparison image using Adobe Photoshop software (Adobe Systems Inc., California, USA).

2.12 Cellular functional assays

For all cellular functional assays, cells were detached on establishing 90% confluence and cell count was performed as described previously (section 2.7.3 and 2.7.4). Cell volumes were calculated in 100µl, unless otherwise stated. The additional 100µl was a 2x concentrate of either treatment made in appropriate growth medium or growth medium alone used as a control.

2.12.1 *In vitro* cellular growth assay

The technique for cellular growth assay was carried out as previously described (Jiang et al. 1995a). Cells were seeded into three 96 well plates at a density of $3x10^3$

cells/100µl, and then the cell solution was supplemented with 100µl of either treatment or control. The plates were incubated for 1,3 and 5 days respectively at 37^{o}C, 5% CO_2 and 95% humidity. After incubation, the medium was removed from the plates and the cells were fixed using 4% formaldehyde in BSS for at least 15 minutes before staining with 0.5% crystal violet in distilled water, for 10 minutes. The crystal violet staining was then washed with water and the plates were left to dry for at least 24 hours at room temperature.

Analysis was performed using an ELX-800 plate reading spectrophotometer (Bio-Tek, Wolf Laboratories, York, UK). Prior to reading, the dye was solubilised in 200µl of 10% acetic acid. Cell density was determined measuring absorbance set at 540nm.

Cell growth rates were presented as a percentage increase for both 3 and 5-day incubation periods compared against the baseline, absorbance measured at day 1 incubation. At least three wells were prepared for each treatment concentration and control. The entire experimental procedure was repeated a minimum of three independent times. Data from all repeated experimental procedures were combined and presented.

2.12.2 *In vitro* cellular adhesion assay

Cellular adhesion was assessed using one of the two methods described overpage, dependent on cell line behaviour.

2.12.2.1 Electric Cell-Substrate Impedance Sensing (ECIS) assay

ECIS is a technique that measures the rate of cells initial attachment and then repopulation of an area following electrical wounding, by using gold electrodes within a well plate to measure changes in resistance and impedance over time (Figure 2.5 and 2.6) (Keese et al. 2004). Stabilisation of the 96 well ECIS electrode array plate (Applied Biophysics Inc., New York, USA) in contact with the ECIS Zθ 96W Array Station (Applied Biophysics Inc., New York, USA) in an incubator at 37°C was performed using 200µl of normal medium in each well. Once stabilisation was complete, the normal medium was aspirated and a solution containing $10x10^4$ cells per 150µl was prepared. 150µl of cell solution was placed in each well of the 96 well ECIS electrode array plate with a further 150µl of either treatment with varying concentrations of rhPEDF or normal medium added. The plate was then reconnected to the ECIS Zθ 96W Array Station. Once all wells had reached confluence (determined by a stable resistance of all wells), a wound command was performed, running 3000µA through the electrode for 30s. Further wounds were performed at least 10 hours after the initial wounds, once the resistance across the electrode surface had returned towards baseline. Throughout this time, the resistance across the electrode was constantly measured in real-time. The change in resistance for each period was calculated by subtracting the baseline resistance from the measured resistance at hourly intervals. At least four wells were prepared for each treatment concentration and control, and the wounding was performed in triplicate. The entire experimental procedure was repeated a minimum of three independent times. Data from all

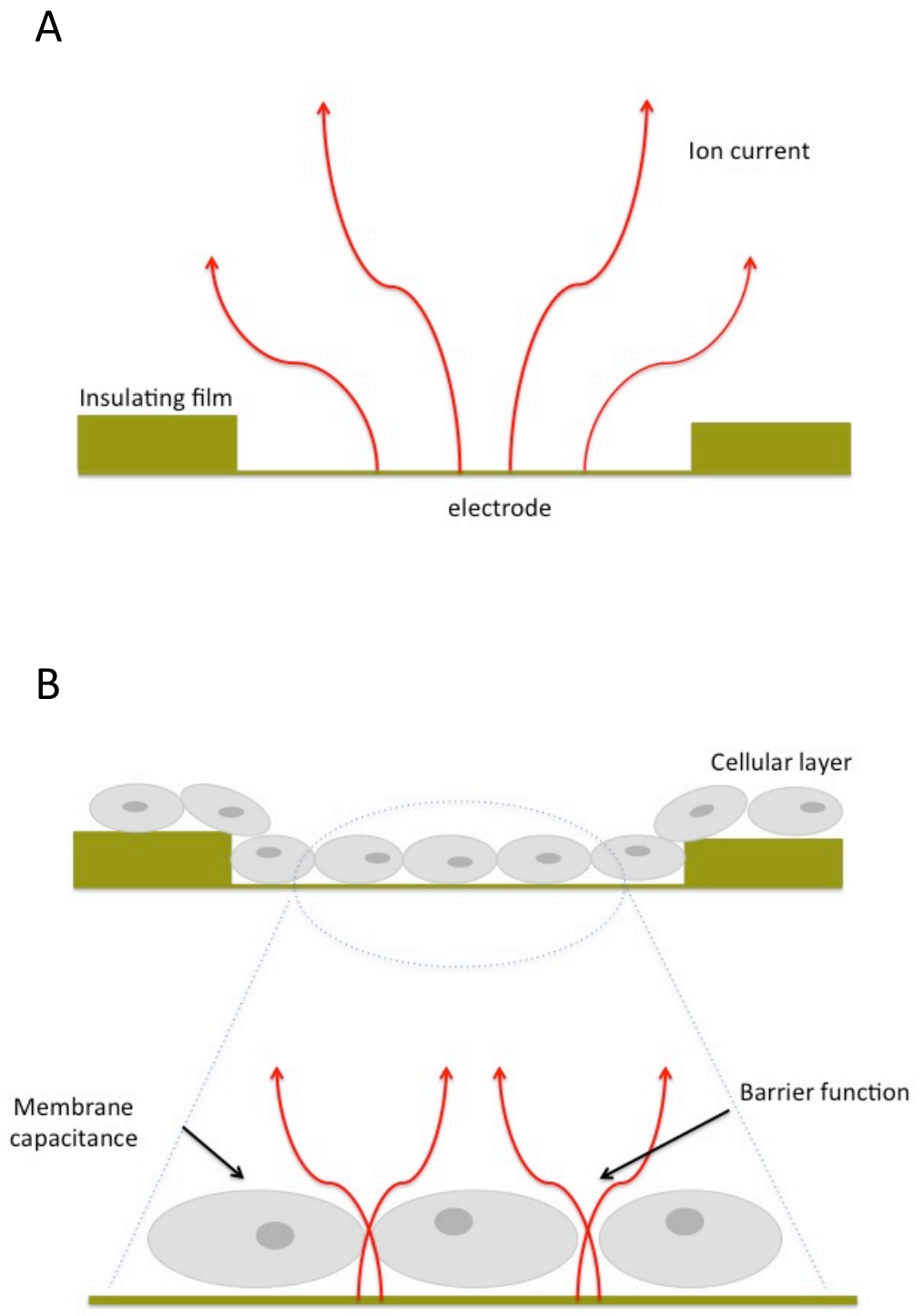

Figure 2.5. Outline of the ECIS process.

A) When there are no cells attached to the electrode the current flows in the solution B) At lower AC frequencies (as used in this study) most of the current flows in the solution channels underneath and between the cells described as the 'barrier function' (as indicated by the red arrows). Adapted from http://biophysics.com/ecis-theory.php

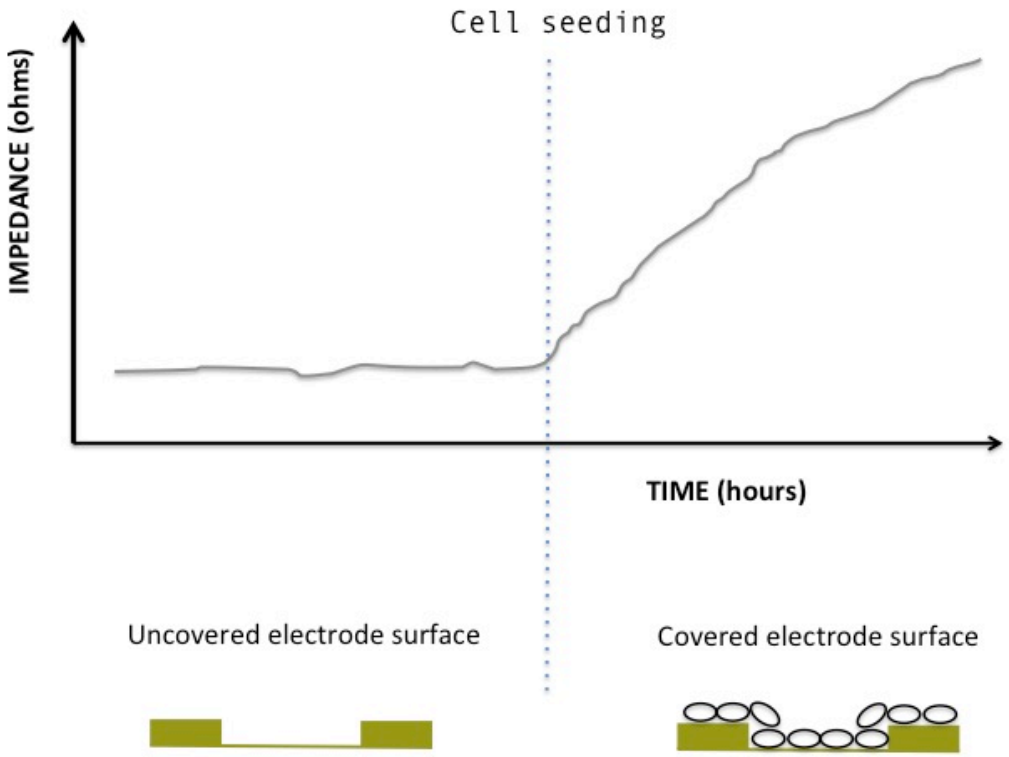

Figure 2.6. Graphical outline of the ECIS process.

Following cell seeding as cells attach to the electrode they act as insulators and therefore increase impedance. As cells proliferate the electrode coverage increases, resulting in a therefore increase in impedance. Adapted from http://biophysics.com/ecis-theory.php

repeated experimental procedures were combined and presented as change over resistance over a 3-hour period, for attachment data.

2.12.2.2 *In vitro* tumour cell Matrigel adhesion assay

A technique using an *in vitro* Matrigel adhesion assay that assessed the ability of tumour cells to adhere to an artificial Matrigel basement membrane has been previously described (Jiang et al. 1995b). This technique has been slightly modified for the purpose of this study and is described below.

5µg of Matrigel in serum free medium was applied to each well of a 96 well plate. The plate was placed in a drying oven set at 55^0C until fully dry, roughly 2 hours. The Matrigel membrane was rehydrated in 100µl of serum free medium for 45 minutes at room temperature. After this time, the serum free medium was aspirated. A solution containing $4.5x10^4$ cells per 100µl was prepared and seeded into each well. An extra 100µl of either treatment or control medium was added to each well. The plate was left to incubate at 37^oC with 5% CO_2 for 45 minutes to allow cells to adhere to the Matrigel.

Removal of the medium took place following incubation and wells were washed with 150µl of BSS solution to remove non-adherent cells. Each well was fixed using 4% formaldehyde in BSS for at least 15 minutes before staining with 0.5% crystal violet in distilled water, for 10 minutes. The crystal violet staining was then washed with water and the plates were left to dry for at least 24 hours at room temperature.

Analysis was performed using an ELX-800 plate reading spectrophotometer (Bio-Tek, Wolf Laboratories, York, UK). Prior to reading, the dye was solubilised in 200µl of 10% acetic acid and transferred to a new 96 well plate keeping the same well plate layout. Cell density was determined measuring absorbance set at 540nm.

At least four wells were prepared for each treatment concentration and control. The entire experimental procedure was repeated independently a minimum of three times. Data from all repeated experimental procedures were combined and absorbance levels were presented as a marker of cell density.

2.12.3 *In vitro* cellular motility assay

Cellular motility was assessed using one of the two methods described below, dependent on cell line behaviour; ECIS was performed as the preferable method were possible due to ease of use and accuracy of data readings, however it is noted that certain cell lines will not migrate following wounding and therefore if ECIS was not possible then in-vitro scratch migration assay was performed.

2.12.3.1 Electric Cell-Substrate Impedance Sensing (ECIS) assay

ECIS was performed as described above in section 2.12.2.1. The entire experimental procedure was repeated a minimum of three independent times. Data from all repeated experimental procedures were combined and presented as changeover resistance over a 6-hour period, for migration data.

2.12.3.2 *In vitro* scratch migration assay

A technique for *in vitro* scratch migration assay has been previously described (Sasi et al. 2014). The methods used in this study have been modified and are described below. Cells were seeded into a 24-well plate at a density of $3x10^5$ cells/500µl, and were incubated for 24 hours at 37^0C with 5% CO_2. After incubation, a straight-line scratch was made to the cellular monolayer using the end of a sharpened 200µl pipette tip down the midpoint of each well. The medium was then removed from the plates carefully and replaced with 500µl of either treatment or control.

Analysis was performed using EVOS cell imaging system (Life Technologies, Paisley, UK) and images were captured every 60 minutes for a total of 6 hours. Migration distances were measured using Image-J software (National Institutes of Health, USA) (Figure 2.7). The entire experimental procedure was repeated a minimum of three independent times. Data from all repeated experimental procedures were combined and presented.

2.12.4 *In vitro* cellular invasion assay

The methods used to determine the invasive ability of the cells in this study have been previously described (Fernando et al. 2010). This technique has been modified from the originally described method (Albini et al. 1987; Parish et al. 1992) to measure cells capacity to invade through an artificial basement membrane and migrate through 8µm pores.

Transwell inserts with 8µm pores (Falcon, pore size 8µm, 24 well format, Greiner Bio-One, Germany) were used in wells of a 24 well plate (NUNC, Greiner Bio-One,

Germany). Each of the transwell inserts was coated with in 50µg of Matrigel (BD Matrigel Matrix, Matrigel Basement Membrane Matrix, Biosciences) in serum free medium. These inserts were left to dry at 55^{o}C for 2 hours then rehydrated in 100µl of serum free medium at room temperature for 40 minutes. Following rehydration, the serum free medium was removed. In order to maintain any cells that invaded through the insert 1ml of normal medium was placed in the base of the well containing the Transwell insert. Then 3 x 10^4 cells/100µl solution plus 100µl of treatment or normal medium were added to each insert. These were incubated for 72 hours at 37^{0}C, 5% CO_2 and 95% humidity.

Following incubation, the inserts were removed from the well plate, the solution containing the cells was removed and the inside of the insert was cleaned with a cotton swab in order to remove non-invaded cells and matrigel. The inferior aspect of the insert was then placed in 4% formaldehyde in BSS for 10 minutes then stained in 0.5% crystal violet solution in distilled water for another 10 minutes. The crystal violet solution was thoroughly washed off and the inserts left to dry at room temperature for at least 24 hours. The inserts were placed back in the wells of a 24 well plate, which contained 500µl of 10% acetic acid for 10 minutes. 100µl of the acetic acid from each well was transferred to a 96 well plate in order for analysis to be performed using an ELX-800 plate reading spectrophotometer (Bio-Tek, Wolf Laboratories, York, UK). Cell density was determined measuring absorbance set at 540nm. The entire experimental procedure was repeated a minimum of three independent times. Data from all repeated experimental procedures were combined and presented.

A

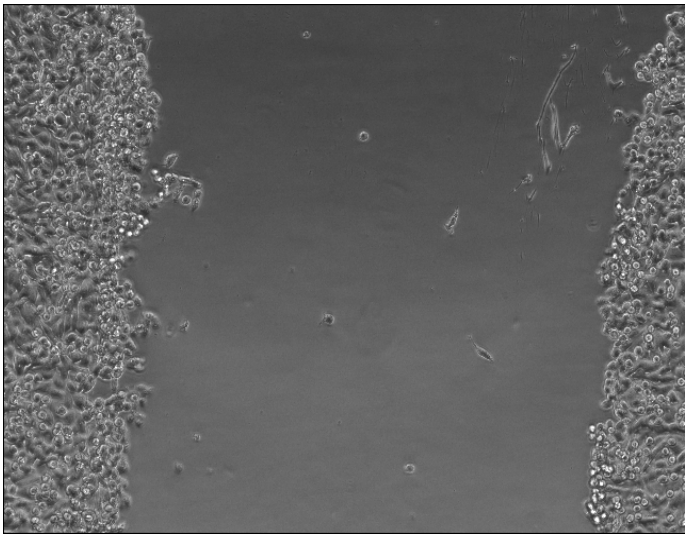

B

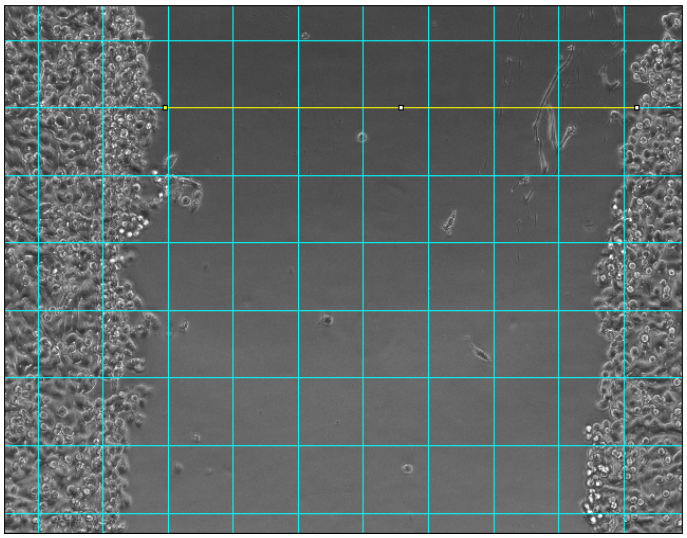

Figure 2.7: Calculating migration distance following scratch assay

A) Image captured on EVOS of HRT-18 cells following scratch, with the leading edges on both sides.

B) Using Image-J software to measure migration distance

2.13 Antibody Array

Two 75cm^2 flasks of confluent cells were incubated with 2% serum medium overnight. Each 75cm^2 flask of cells was treated with either treatment of 50ng/ml rhPEDF or with normal medium for 2 hours prior to the preparation of cell lysates. Cells washed in PBS were scraped into a 1.8ml eppendorf and centrifuged for 10 minutes at 2,000 rpm until a cell pellet formed. 500µl lysis buffer (100mM Tris Buffer, 10% 2-ME, 1% NP-40, 50mM NaFI and protease inhibitor cocktail tablet (Roche, Basel, Switzerland)) was added and rotated on blood wheel for 60 minutes at 4^{0}C. Protein quantification was then performed as described in Section 2.9.2.

Samples were shipped to Kinex^{TM} Screening Services (Kinexus Bioinformatics Corporation, Vancouver, Canada). Testing was performed for detection of protein changes on the KAM-880 antibody microarray (Kinexus Bioinformatics Corporation, Vancouver, Canada).

2.14 Statistical analysis

All experiments were repeated at least three independent times (with a new flask of cells used). Statistical analysis was performed using Sigma plot 11.0 statistical software (Systat software Inc.). Statistical analysis was performed using Student T-test for parametric data and Mann-Whitney U test for non-parametric data, where two variables were present. Where multiple variables or comparisons were present one of either two tests were performed. The significance of associations between PEDF mRNA levels and clinicopathological variables and for functional cellular assays (except adhesion (ECIS) and migration assays) were assessed by Kruskal-Wallis one-

way analysis of variance on ranks test, and pairwise multiple comparison procedure (Dunn's method). Two-way analysis of variance was performed for adhesion (ECIS) and migration assay data. The significance of associations between positive or negative PEDF expression on immunohistochemistry for colorectal cancer samples and clinicopathological variables were assessed by chi-squared test. Parametric data was presented as mean values with error bars depicting standard error of the mean (SEM). Non-parametric data was presented, were possible as boxplots, with median values and interquartile range (IQR), with error bars depicting 95% confidence intervals. Differences were considered to be statistically significant at $p \leq 0.05$.

Chapter 3

Expression profile of PEDF in colorectal cancer

3.1 Introduction

PEDF is one of the most potent endogenous inhibitors of angiogenesis (Dawson et al. 1999; Duh et al. 2002). PEDF expression has been found to be lower in solid tumour tissue when compared to normal tissue from the same organ, suggesting that loss of PEDF expression may play a crucial role in tumorigenesis (Cai et al. 2006b; Zhou et al. 2010; Zhang et al. 2006a; Cheung et al. 2006; Guan et al. 2003; Zhang et al. 2009). PEDF expression also declines with worsening oncological prognostic factors, such increased tumour size (Zhou et al. 2010), increased pathological grade (Guan et al. 2003), lymph node involvement (Cai et al. 2006b; Fitzgerald et al. 2012), distant metastasis (Cai et al. 2006b; Zhou et al. 2010; Fitzgerald et al. 2012; Uehara et al. 2004; Dass et al. 2008; Halin et al. 2004) and local recurrence (Cai et al. 2006b; Zhou et al. 2010).

Similar to the results from other solid tumour tissues, lower levels of PEDF expression were found within serum samples of colorectal cancer patients compared to healthy controls (Wågsäter et al. 2010; Ji et al. 2013) with lower levels correlating with advanced TNM stage, distance metastasis and significantly shorter overall survival, and was an independent risk factor for colorectal cancer prognosis (Ji et al. 2013). Interestingly patients with mucinous adenocarcinoma patients displayed higher PEDF serum levels than adenocarcinoma patients (Ji et al. 2013).

Studies examining protein levels for PEDF expression within colorectal cancer tissue showed conflicting results; Ji *et al* (2013) found lower PEDF protein levels in colorectal cancer tissue compared to normal tissue, whereas Wågsäter *et al* (2010) found no difference or association between clinicopathological outcomes. Low levels

of mRNA expression of PEDF were found in colorectal cancer tissue when compared to matched adjacent tissue, and low levels correlated with advanced clinical stage, lymph node involvement, distant metastasis and shorter disease-free survival (Ji et al. 2013), and mRNA expression of PEDF appeared to be higher for tissue from rectal tumours when compared to tissue from colonic tumours (Díaz et al. 2008).

Immunohistochemistry studies for PEDF expression in tissue samples found contrasting results, with Uhlen (2005) commenting on nuclear staining of colorectal cancer cells, whereas Ji *et al* (2013) noted cytoplasm and cell membrane staining with weaker expression seen in tumour compared to normal mucosa. Uhlen (2005) did however comment that the expression might have appeared stronger in cancer cells nuclei as it reflects the fact that cancer cell nuclei are larger, contain more nucleic acids and have a higher rate of transcription and metabolism.

The aims of this section of the study were to determine the expression profile of PEDF in a range of colorectal cell lines and within colorectal cancer tissue and its association with clinical and pathological data.

3.2 Materials and Methods

3.2.1 Cell lines

Six cell lines were screened for PEDF expression as part of this study; RKO, HT115, HRT-18, COLO-201, LSI74T and CCD-33C0. RKO and HT115 are cell lines derived from colonic adenocarcinoma. HRT-18 is a cell line derived from rectal adenocarcinoma. COLO-201 is a cell line derived from metastatic Dukes' D colorectal adenocarcinoma and sourced from ascites. LS174T is a mucin secreting colorectal adenocarcinoma.

CCD-33C0 is a cell line derived from normal colorectal fibroblasts. Full details of cell lines are described in Table 2.1. Cells were maintained in medium as described previously in section 2.7.1.

3.2.2 Colorectal tissue

Colorectal cancer tissue collection for qPCR was performed at Beijing Friendship Hospital, China as described in section 2.3. Colonic cancer tissue microarray (T054b) and rectal cancer tissue microarray (RE961) purchased from US Biomax Inc. (Rockville, USA) were used for immunohistochemical staining and these microarrays included normal tissue and cancer adjacent normal tissue as described in section 2.3.

3.2.3 RNA isolation, cDNA synthesis, RT-PCR and qPCR

RNA isolation was performed using TRI reagent kit as described in section 2.8.1. Following this, reverse transcription was carried out using a high capacity RT kit. RT-PCR products were separated electrophorectically on an agarose gel. RT-PCR representative images are presented, normalised against GAPDH. qPCR was performed as described in section 2.8.8. All results presented were normalised against GAPDH and represent combined results from at least 3 independent repeats.

3.2.4 Immunohistochemical staining of tissues

Tissue arrays used are described in section 3.2.2. Immunohistochemistry was performed using Vector ABC Kit as is described in full detail in Section 2.10.1. The primary antibody used was rabbit monoclonal antibody against PEDF at a 1:50 concentration as described in section 2.5. All specimens were analysed anonymously.

Details of demographical and clinicopathological associations were provided during experimental data analysis. Representative images are shown in this study.

3.2.5 Immunocytochemical staining of cells

RKO, HT115 and HRT-18 cell lines were used for immunocytochemistry, as representative cell lines for colorectal cancer. Immunocytochemistry was performed as described in Section 2.10.2. The primary antibody used was rabbit monoclonal antibody against PEDF at a 1:50 concentration and secondary antibody used was Vector ABC Kit as described in section 2.5. Representative images are shown in this study.

3.2.6 Immunofluorescence staining of cells

RKO, HT115 and HRT-18 cell lines were used for immunofluorescence staining of cells. Immunofluorescence staining was performed as described in section 2.11. The primary antibody used was rabbit monoclonal antibody against PEDF at a 1:50 concentration and the secondary antibody used was anti- rabbit IgG FITC conjugate at a 1:250 concentration as described in section 2.5. Representative images are shown in this study.

3.3 Results

3.3.1 Colorectal cancer cell lines expression screening for PEDF

PEDF transcript expression using RT-PCR was high in the CCD-33C0 colorectal fibroblast cell line when compared to all other colorectal cancer cell lines used; RKO, HT115, HRT-18, COLO-201 and LS174T (Figure 3.1).

qPCR confirmed that CCD-33C0 showed higher expression of PEDF compared to the RKO, HT115, HRT-18, COLO-201 and LS174T colorectal cell lines (Table 3.1). Lowest expression was seen in the COLO-201 metastatic cell line. However, these results were not found to be statistically significant (p=0.58).

Immunofluorescence and Immunocytochemistry showed a tendency towards cytoplasmic staining more so than nuclear staining for RKO, HT115 and HRT-18 colorectal cancer cell lines (Figures 3.2 to 3.7). However, expression appeared to be lower for the HRT-18 cell line compared with the RKO and HT115 cell lines.

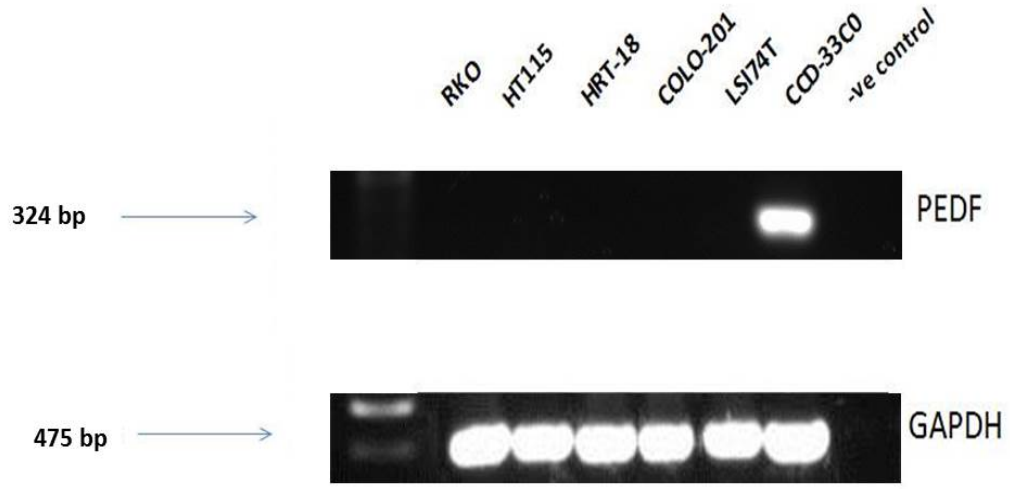

Figure 3.1. Transcript expression levels in PEDF in colorectal cell lines. Control= Nuclease free water and all gels were run with a molecular weight marker used to identify band sizes.

Table 3.1. qPCR expressional analysis of PEDF within colorectal cell lines.

Cell lines	Median transcript copy number	IQR	P value
RKO	45.8	10.3 - $6.5x10^4$	
HT115	8.4	0.3 - 17.0	
HRT-18	11.5	0.36 - $3.8x10^5$	
COLO-201	0.1	$6.5x10^{-7}$ - 3.78	
LS174T	0.2	$3.4x10^{-6}$ - 34.7	
CCD-33C0	$8.5x10^5$	0.02 - $1.3x10^7$	0.58

Relative transcript copy number was calculated based on internal standard. Median data from at least 6 independent repeats are shown

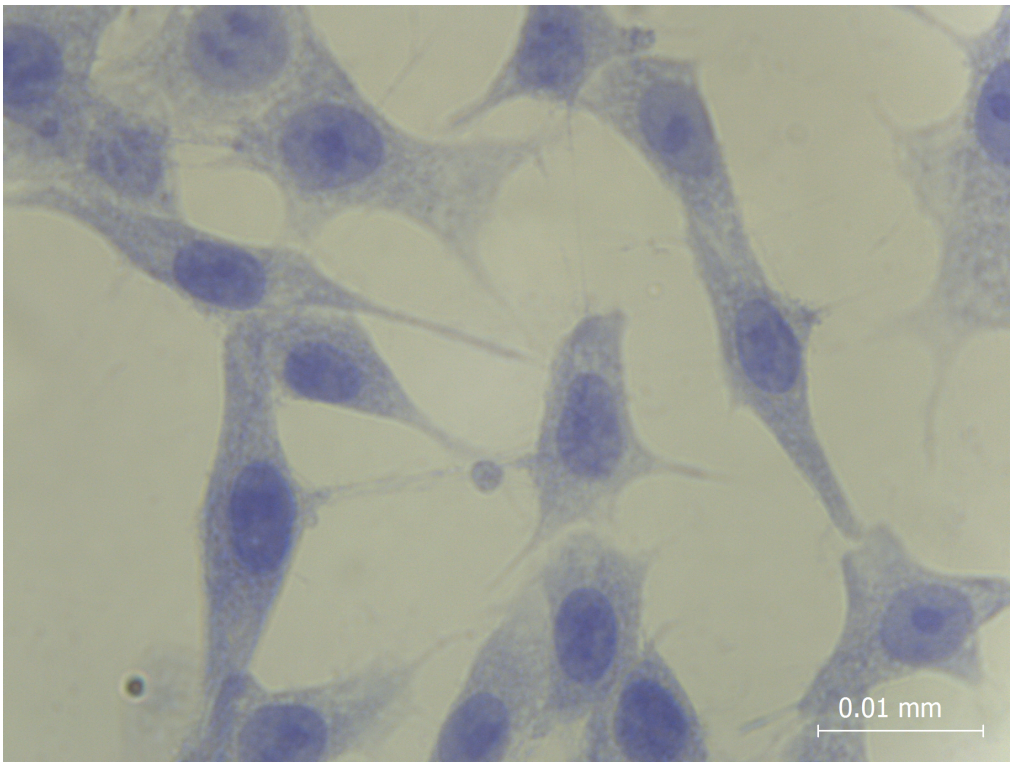

Negative control

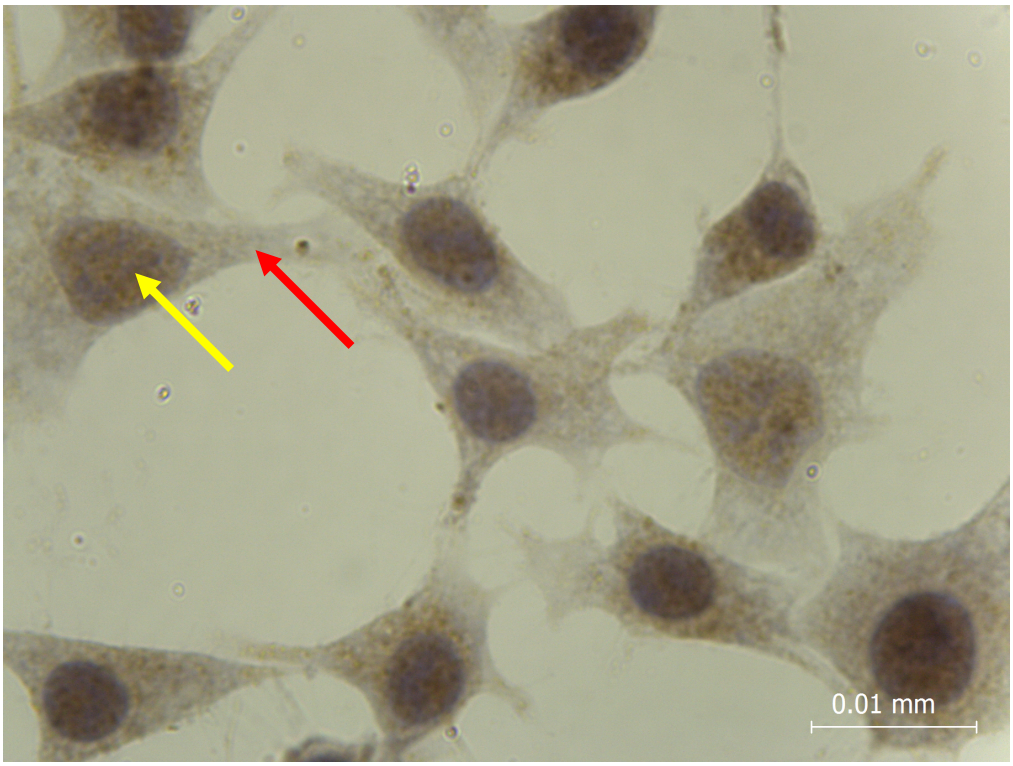

Figure 3.2. Representative immunocytochemistry images for RKO cell line. X100 magnification used. Scale bar represents 10µm. Red arrow shows weakly positive cytoplasmic staining and yellow arrow shows weakly positive nucleic staining.

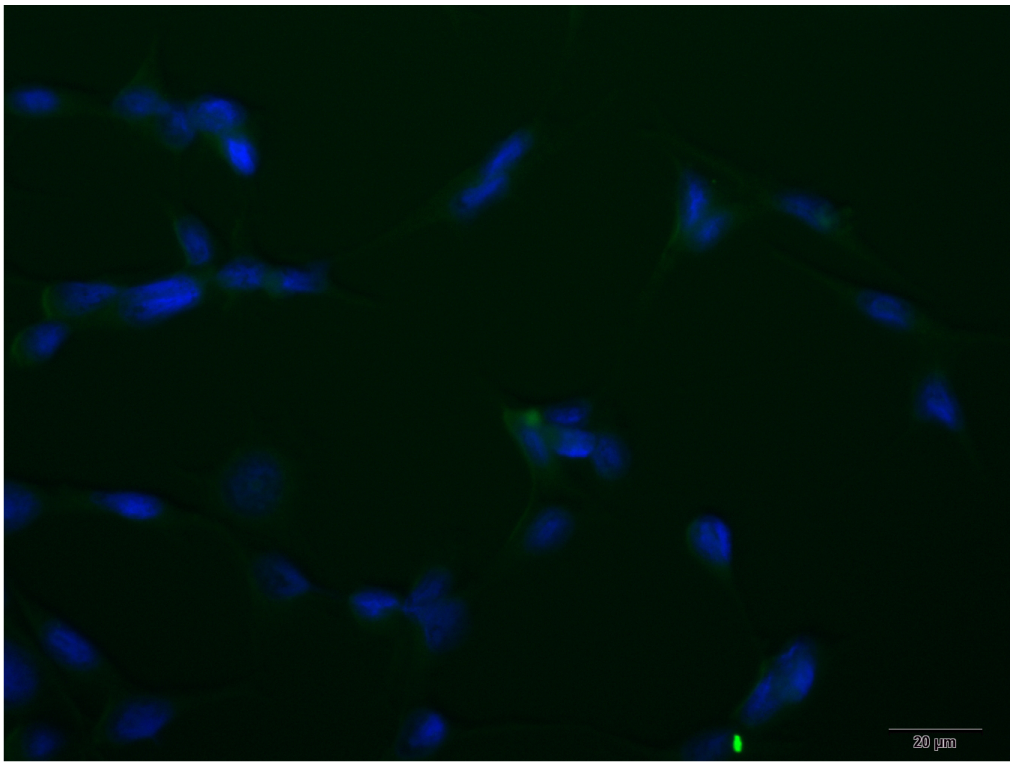

Negative control

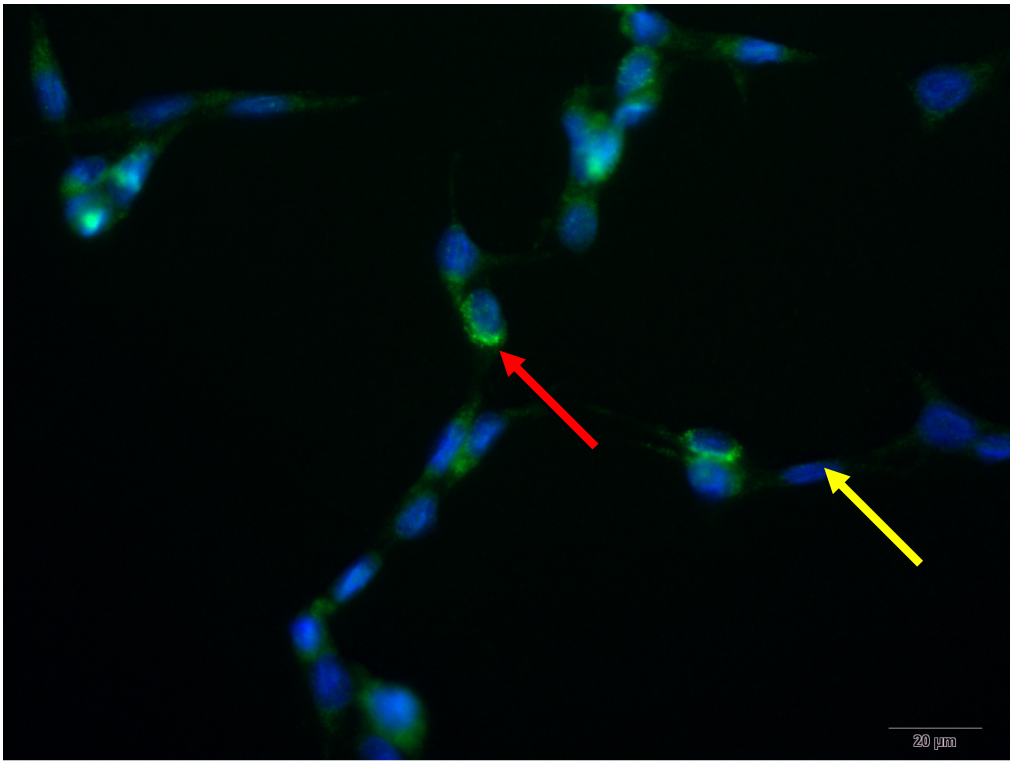

Figure 3.3. Representative immunofluorescence images for RKO cell line. X40 magnification used. Scale bar represents 20µm. Red arrow shows strongly positive cytoplasmic staining. Yellow arrow shows minimal nuclear staining.

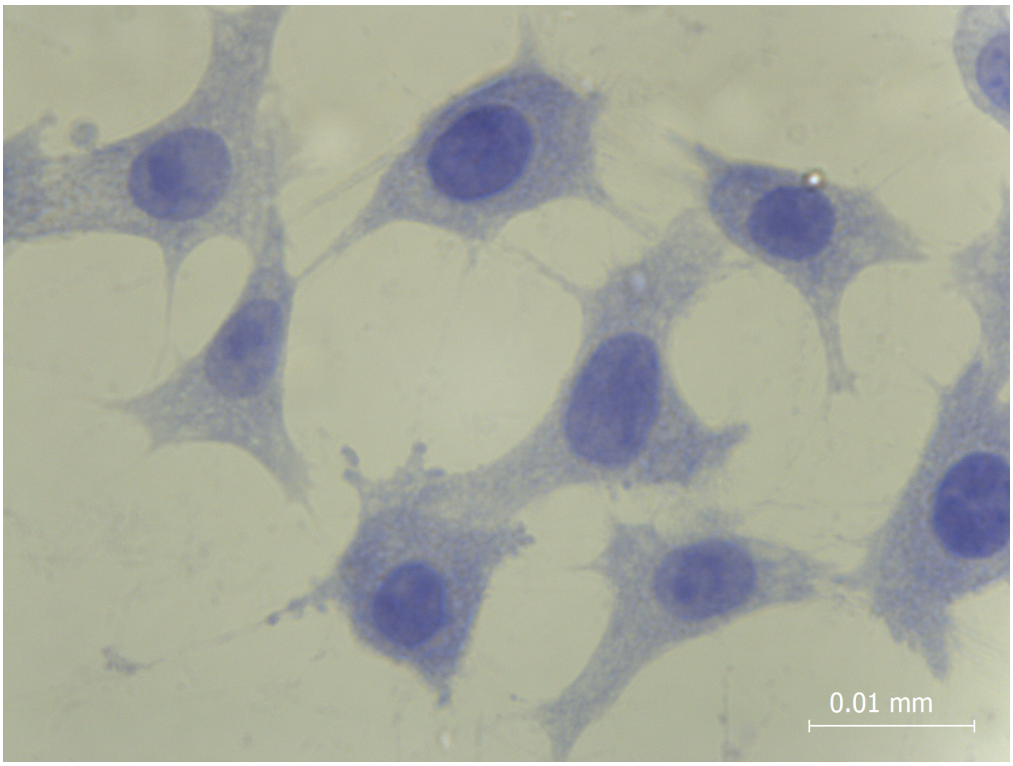

Negative control

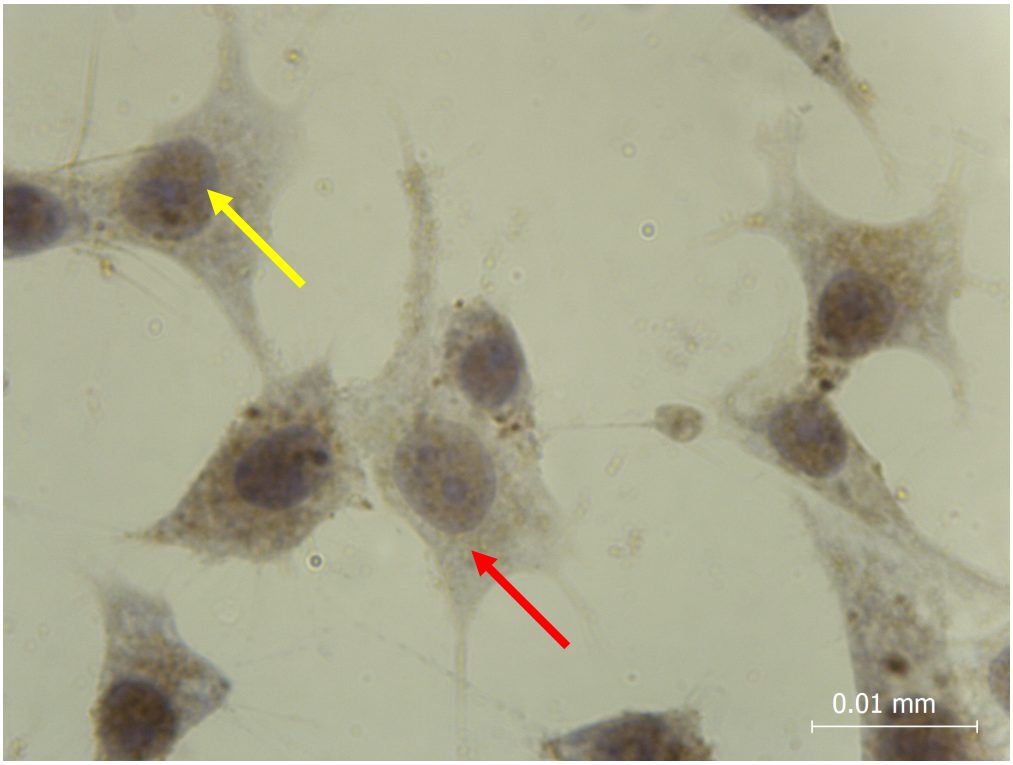

Figure 3.4. Representative immunocytochemistry images for HT115 cell line. X100 magnification used. Scale bar represents 10µm. Red arrow shows weakly positive cytoplasmic staining and yellow arrow shows weakly positive nucleic staining.

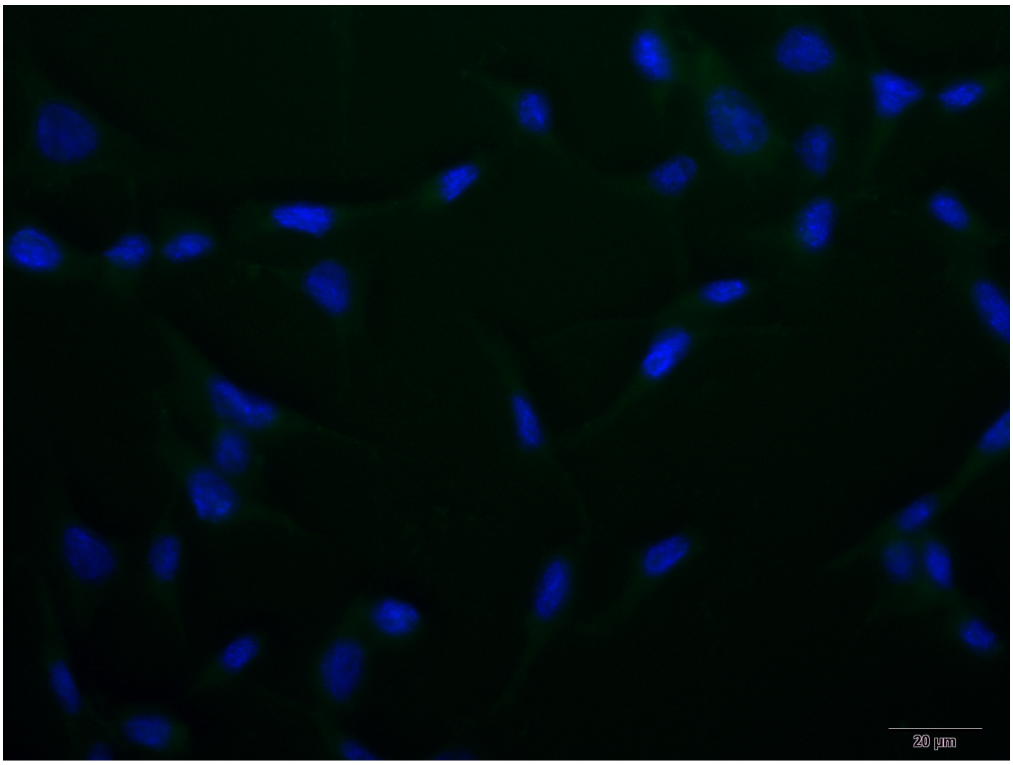

Negative control

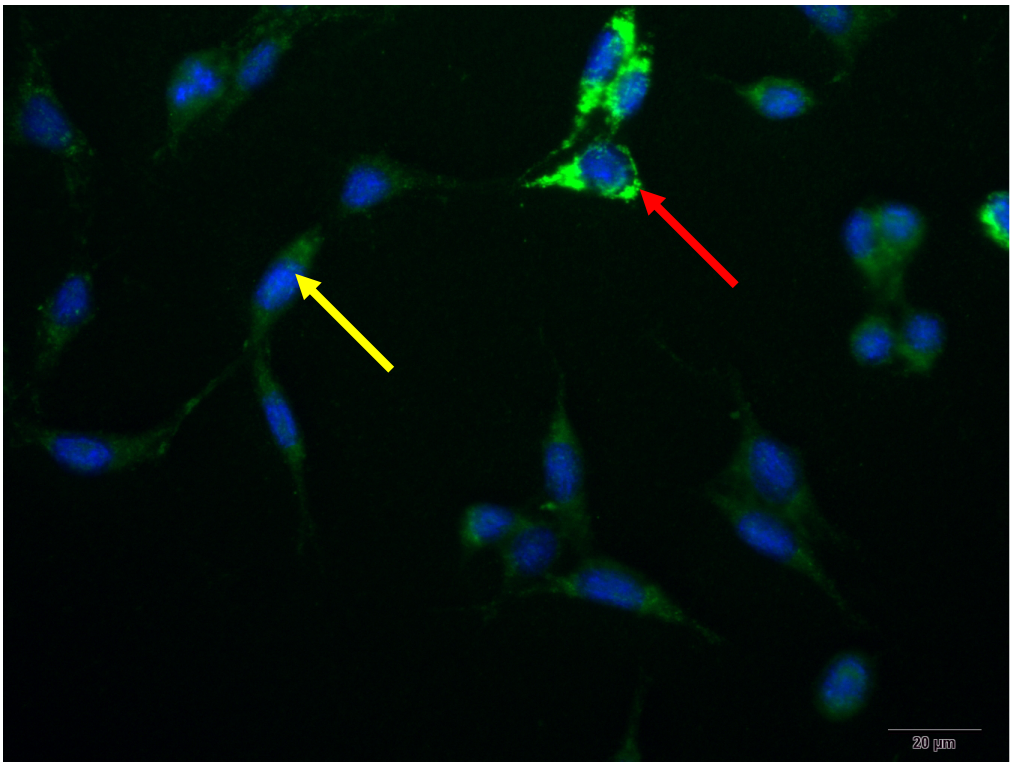

Figure 3.5. Representative immunofluorescence images for HT115 cell line. X40 magnification used. Scale bar represents 20µm. Red arrow shows strongly positive cytoplasmic staining. Yellow arrow shows minimal nucleic staining.

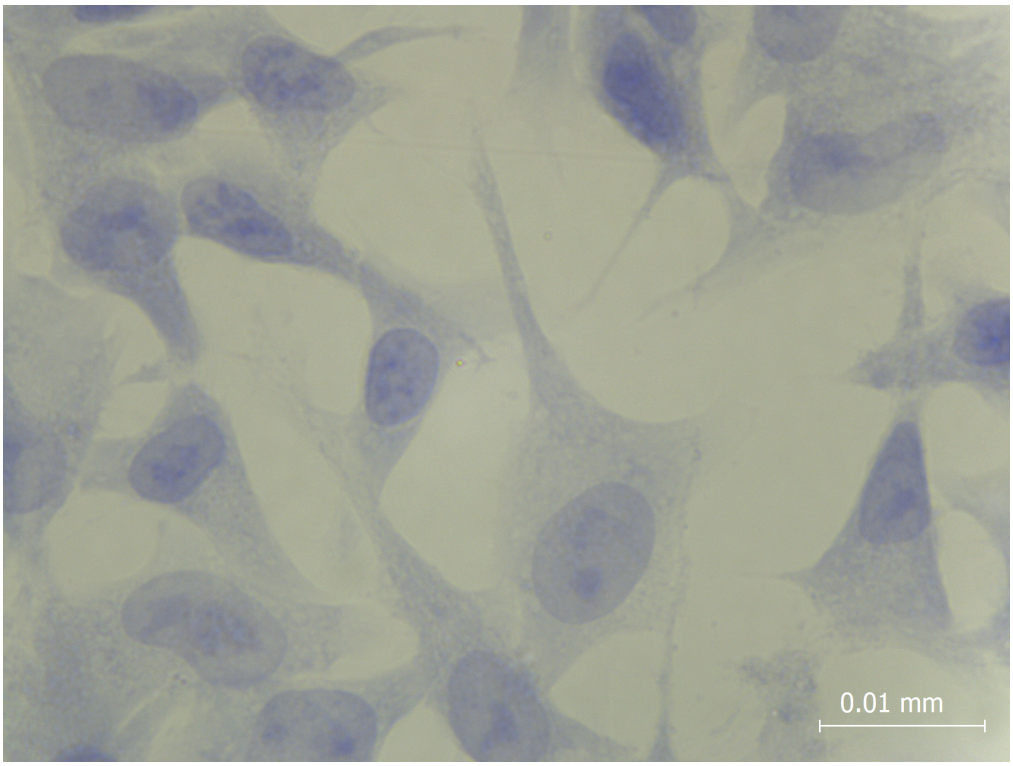

Negative control

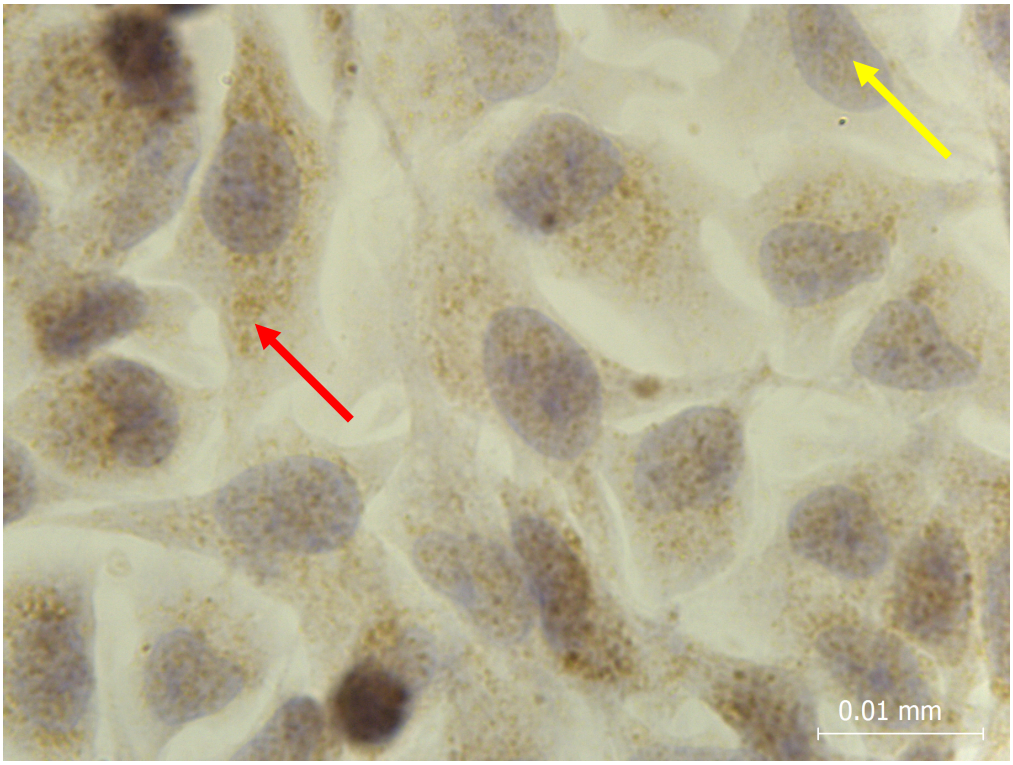

Figure 3.6. Representative immunocytochemistry images for HRT-18 cell line. X100 magnification used. Scale bar represents 10µm Red arrow shows weakly positive cytoplasmic staining. Yellow arrow shows minimal nucleic staining.

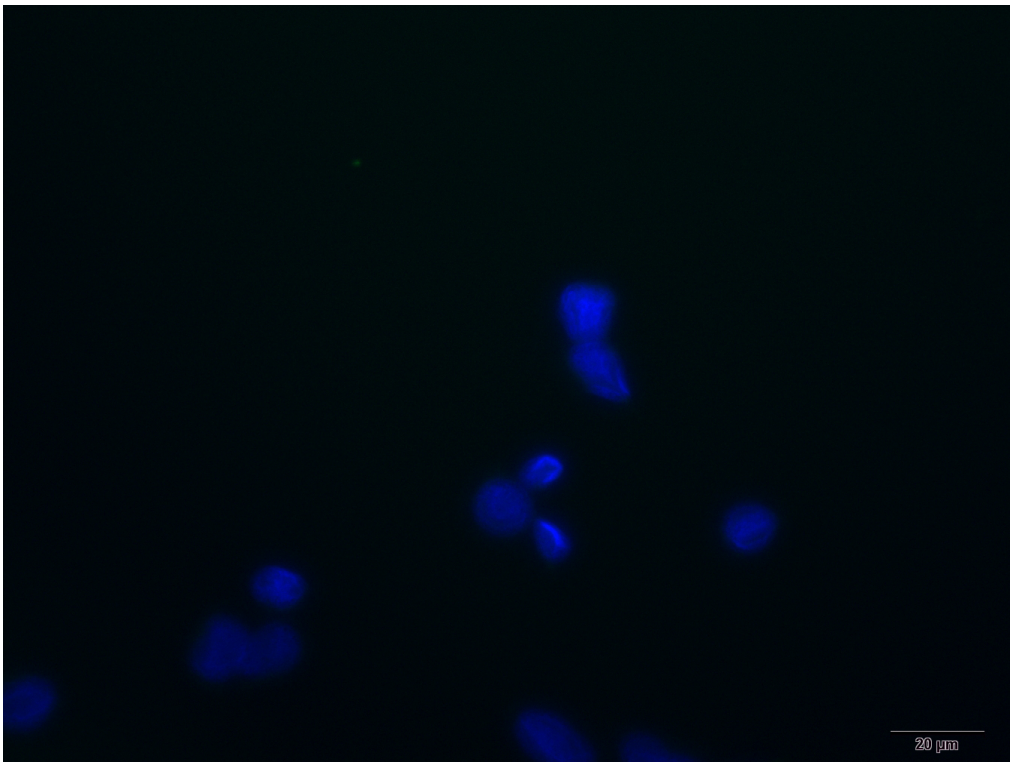

Negative control

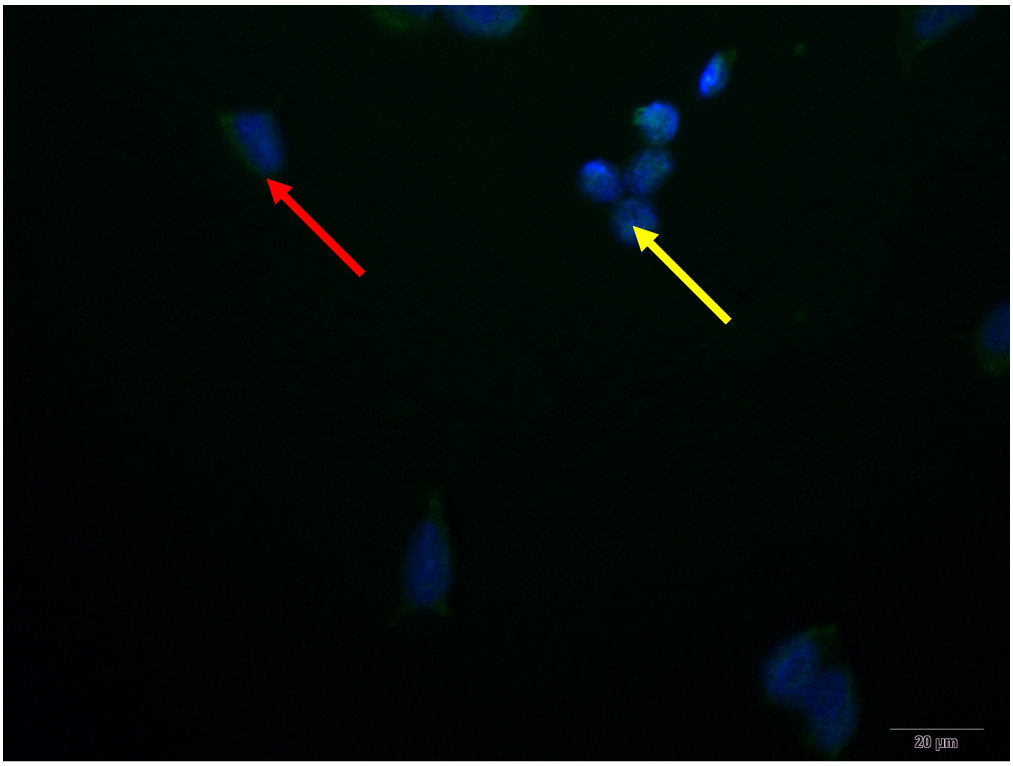

Figure 3.7. Representative immunofluorescence images for HRT-18 cell line. X40 magnification used. Scale bar represents 20µm. Red arrow shows no cytoplasmic staining. Yellow arrow shows minimal nucleic staining.

3.3.2 Expression of PEDF in human colorectal cancer tissues and the association with clinicopathological characteristics

The cohort used for qPCR consisted of 221 male patients and 185 female patients, who underwent resectional surgery for treatment of their colorectal cancer; with normal matched colorectal tissue, available for additional analysis from 209 of these patients. This demonstrated that mRNA expression of PEDF was lower in colorectal tumour tissue when compared to matched normal colorectal tissue from colorectal cancer patients ($p<0.001$) (Table 3.2). Interestingly, PEDF was more highly expressed in females with colorectal cancer within this cohort when compared to males with colorectal cancer ($p=0.01$), and in rectal tumours compared with colonic tumours ($p<0.001$). Whilst there was an obvious decline in mRNA expression of PEDF with worsening tumour grade, this trend was not found to be significant ($p=0.187$). No other demographic or clinicopathological association were found to be statistically significant. Unfortunately, survival data was not available due to the short follow-up period of this cohort.

On immunohistochemical staining highest expression of PEDF was seen within smooth muscle, endothelial cells and fibroblasts (Figure 3.8). Tumour expression of PEDF was more pronounced in well-differentiated mucinous adenocarcinomas when compared to poorly differentiated mucinous adenocarcinomas and all grades of adenocarcinoma (Figure 3.9 and 3.10). There was a significant decrease in expression with worsening tumour grade in both adenocarcinomas and mucinous adenocarcinomas ($p=0.008$ and $p<0.001$, respectively). There was no difference seen in expression in tumour location (colon vs. rectum), Dukes Stage or TNM Stage. There

was some slight cytoplasmic staining seen within cancer adjacent and normal colorectal tissue, however there was poor expression overall (Figure 3.11).

Table 3.2. Correlation between PEDF expression and clinical parameters in colorectal cohort

	N	Median transcript copy number	IQR	P value
Tumour	406	$3.64x10^{-5}$	$1.05x10^{-9}$ - $4.40x10^{-3}$	
Normal matched tissue	209	$1.05x10^{-3}$	$6.84x10^{-9}$ - $4.18x10^{-2}$	<0.001 *
Female	185	$1.54x10^{-4}$	$3.95x10^{-8}$ - $1.02x10^{-2}$	
Male	221	$1.51x10^{-5}$	$2.52x10^{-10}$ - $2.36x10^{-3}$	0.01 *
Aged 64 years or younger	163	$8.78x10^{-6}$	$1.17x10^{-12}$- $3.46x10^{-3}$	
Aged 65 years or older	184	$1.04x10^{-6}$	$1.17x10^{-12}$-$1.36x10^{-3}$	0.645
Female aged 64 years or younger	75	$1.08x10^{-5}$	$1.17x10^{-12}$- $4.18x10^{-3}$	
Male aged 64 years or younger	88	$4.39x10^{-6}$	$2.45x10^{-12}$- $1.44x10^{-3}$	0.729
Female aged 65 years or older	84	$1.47x10^{-5}$	$1.17x10^{12}$-$2.29x10^{-3}$	
Male aged 65 years or older	100	$5.63x10^{-7}$	$1.17x10^{-12}$-$7.25x10^{-4}$	0.107
Smoker	95	$1.78x10^{-5}$	$8.34x10^{-11}$ - $3.02x10^{-3}$	
Non-smoker	239	$6.44x10^{-5}$	$1.31x10^{-10}$ - $3.92x10^{7}$	0.70
History of other cancers	17	$4.02x10^{-5}$	$6.54x10^{-7}$ - $2.79x10^{-3}$	
No history of other cancers	375	$5.32x10^{-5}$	$9.62x10^{-10}$ - $4.50x10^{-3}$	0.617
Family history of colorectal cancer	47	$1.85x10^{-5}$	$1.69x10^{-10}$- $1.15x10^{-3}$	
No family history of colorectal cancer	344	$6.93x10^{-5}$	$4.09x10^{-9}$ - $5.25x10^{-3}$	0.382

Tumour location				
Colon	263	$2.91x10^{-6}$	$5.00x10^{-14}$ - $4.78x10^{-3}$	
Rectum	143	$1.25x10^{-4}$	$4.44x10^{-6}$ - $3.40x10^{-3}$	<0.001 *
Tumour differentiation				
Well differentiation	84	$1.31x10^{-4}$	$3.36x10^{-7}$ - $4.00x10^{-3}$	
Moderately differentiation	231	$2.49x10^{-5}$	$1.97x10^{-10}$ - $3.31x10^{-3}$	
Poorly differentiation	37	$9.69x10^{-7}$	$1.31x10^{-11}$ - $1.83x10^{-3}$	0.187
Tumour type				
Adenocarcinoma	307	$6.44x10^{-5}$	$9.62x10^{-10}$ - $3.67x10^{-3}$	
Mucinous adenocarcinoma	49	$4.92x10^{-5}$	$4.45x10^{-10}$ - $2.41x10^{-3}$	0.98
Duke's stage				
A	22	$1.94x10^{-4}$	$3.17x10^{-6}$ - $5.03x10^{-3}$	
B	170	$1.63x10^{-5}$	$4.78x10^{-11}$ - $3.33x10^{-3}$	
C	156	$1.29x10^{-4}$	$2.45x10^{-8}$ - $6.66x10^{-3}$	
D	30	$5.12x10^{-5}$	$2.24x10^{-9}$ - $2.25x10^{-3}$	0.16
Pathological T Stage				
T1	0			
T2	34	$1.65x10^{-4}$	$3.09x10^{-7}$ - $4.37x10^{-3}$	
T3	201	$2.66x10^{-5}$	$3.55x10^{-10}$ - $2.51x10^{-3}$	
T4	148	$5.78x10^{-5}$	$1.50x10^{-10}$ - $7.76x10^{-3}$	0.45

No nodal involvement	201	$2.77x10^{-5}$	$2.25x10^{-10}$ - $3.46x10^{-3}$	
Nodal involvement	181	$7.30x10^{-5}$	$7.21x10^{-9}$ - $5.33x10^{-3}$	0.23
No metastatic disease	273	$6.04x10^{-5}$	$9.42x10^{-11}$ - $3.69x10^{-3}$	
Metastatic disease	31	$1.45x10^{-5}$	$1.09x10^{-9}$ - $2.11x10^{-3}$	0.54
Radical surgery	341	$6.48x10^{-5}$	$4.09x10^{-9}$ - $4.42x10^{-3}$	
Palliative surgery	45	$1.51x10^{-5}$	$1.50x10^{-12}$ - $5.33x10^{-3}$	0.54

* $p<0.05$

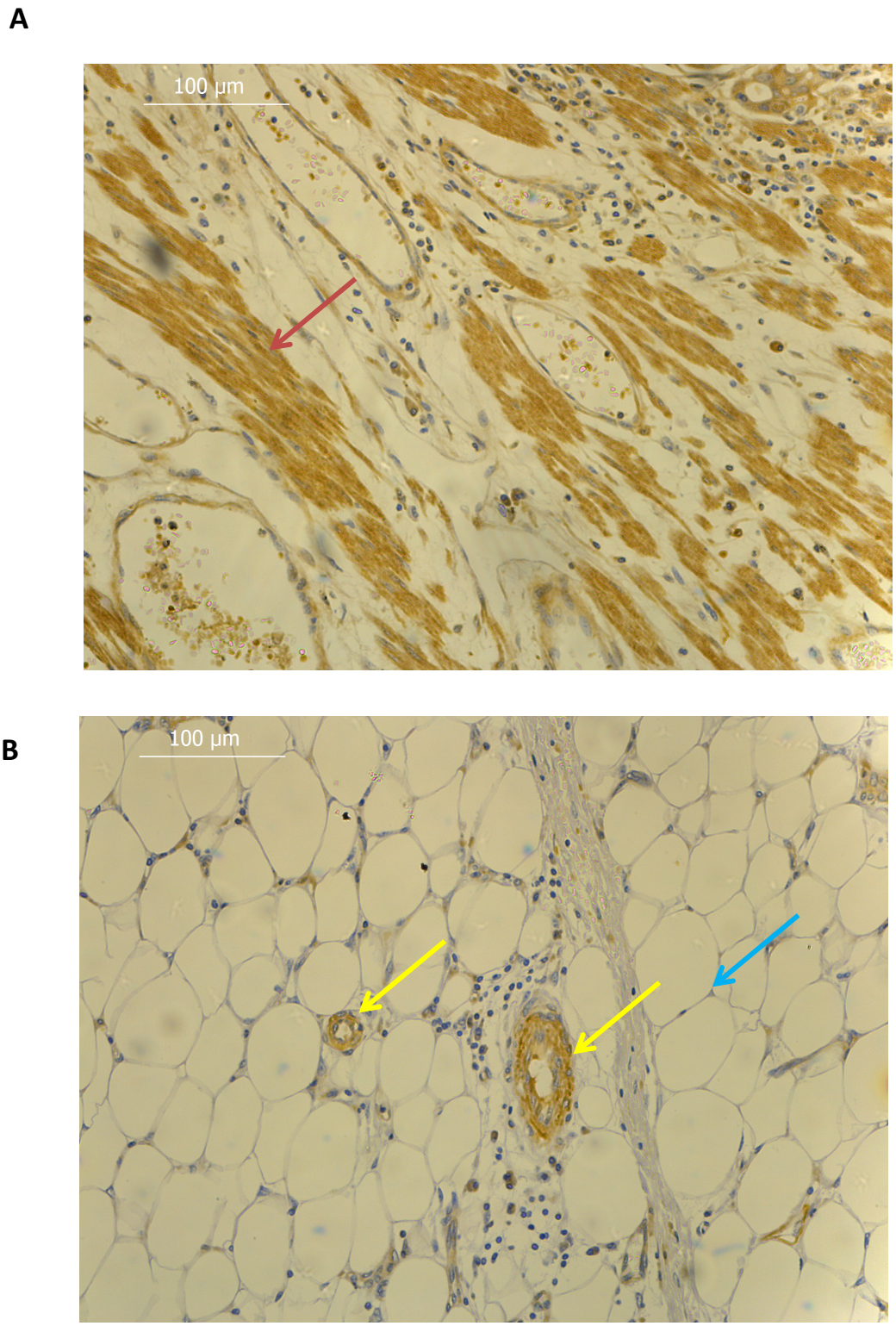

Figure 3.8. Representative immunohistochemistry images for A) smooth muscle and B) adipose tissue. X200 magnification used. Scale bar represents 100µm. Red arrow shows positive staining of muscle. Yellow arrows show positive staining of blood vessels. Blue arrow shows adipose tissue with no staining visible.

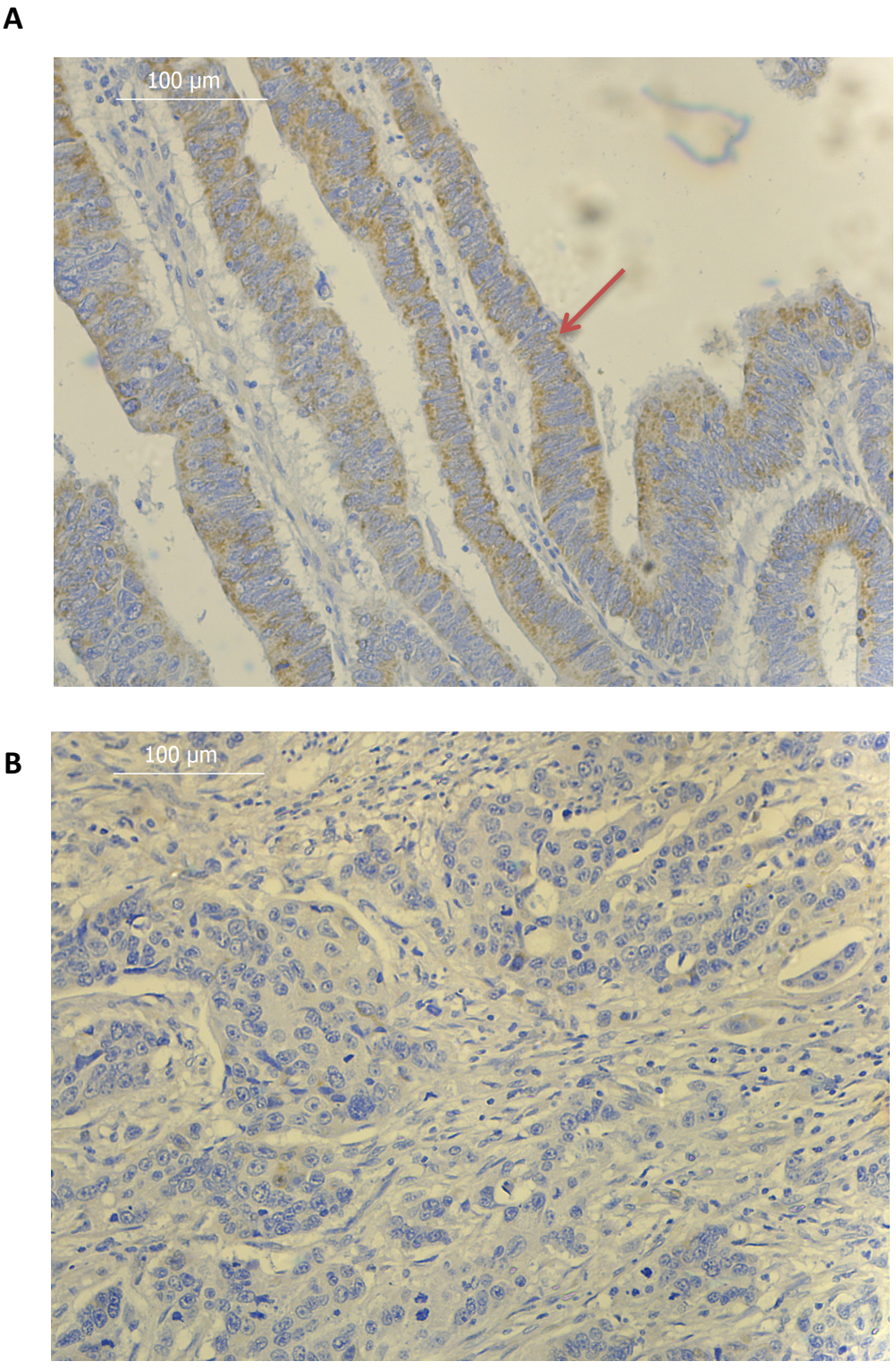

Figure 3.9. Representative immunohistochemistry images for A) well differentiated adenocarcinoma and B) poorly differentiated adenocarcinoma tissue samples. X200 magnification used. Scale bar represents 100µm. Red arrow shows cytoplasmic tumour staining within the well differentiated adenocarcinoma sample. There was no staining evident in the poorly differentiated tissue sample.

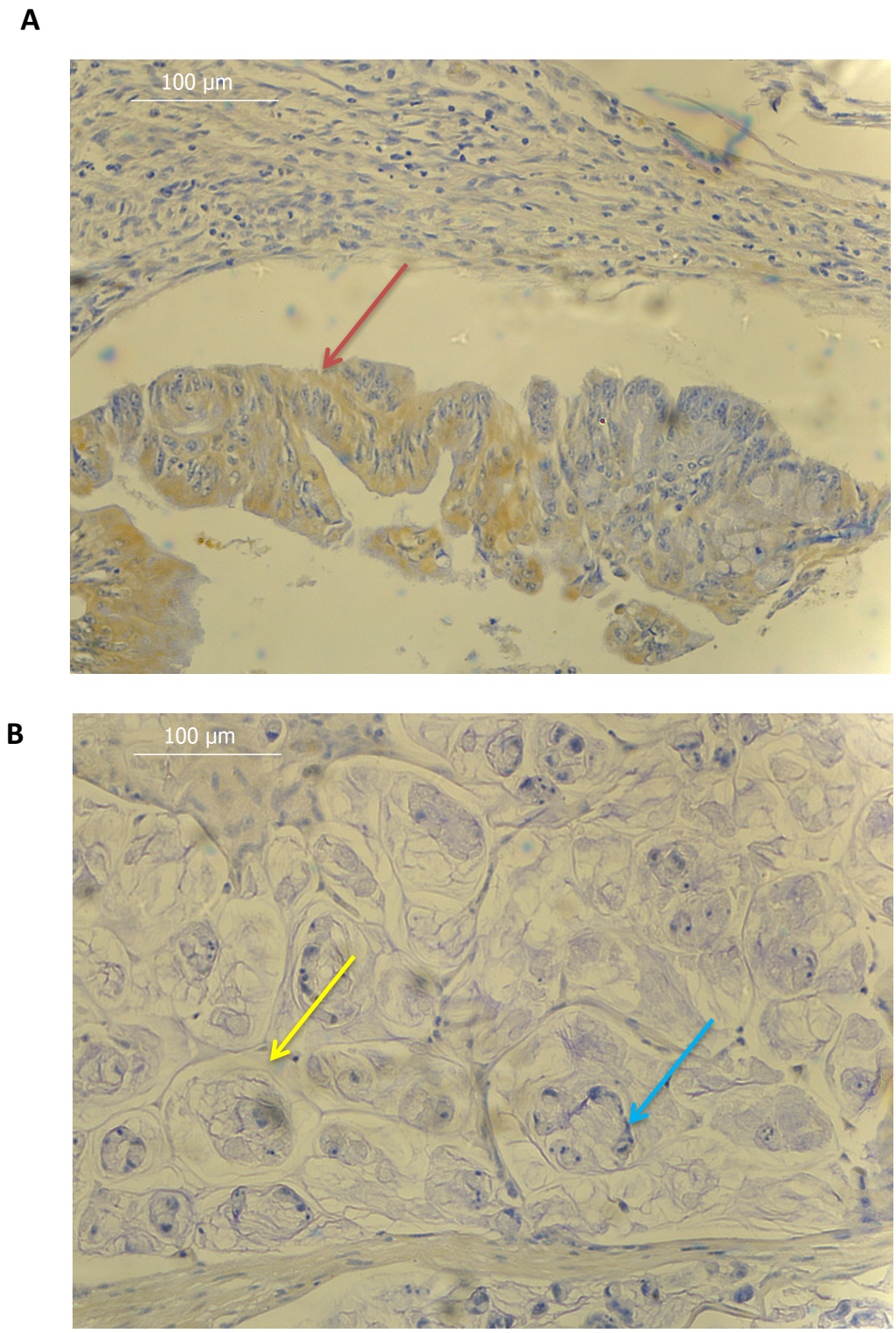

Figure 3.10. Representative immunohistochemistry images for A) well differentiated mucinous adenocarcinoma and B) poorly differentiated mucinous adenocarcinoma tissue samples. X200 magnification used. Scale bar represents 100µm. Red arrow shows positive tumour cell staining in the well differentiated mucinous adenocarcinoma sample. Yellow arrow shows no staining of mucus. Blue arrow shows no staining of tumour cells in the poorly differentiated mucinous adenocarcinoma sample.

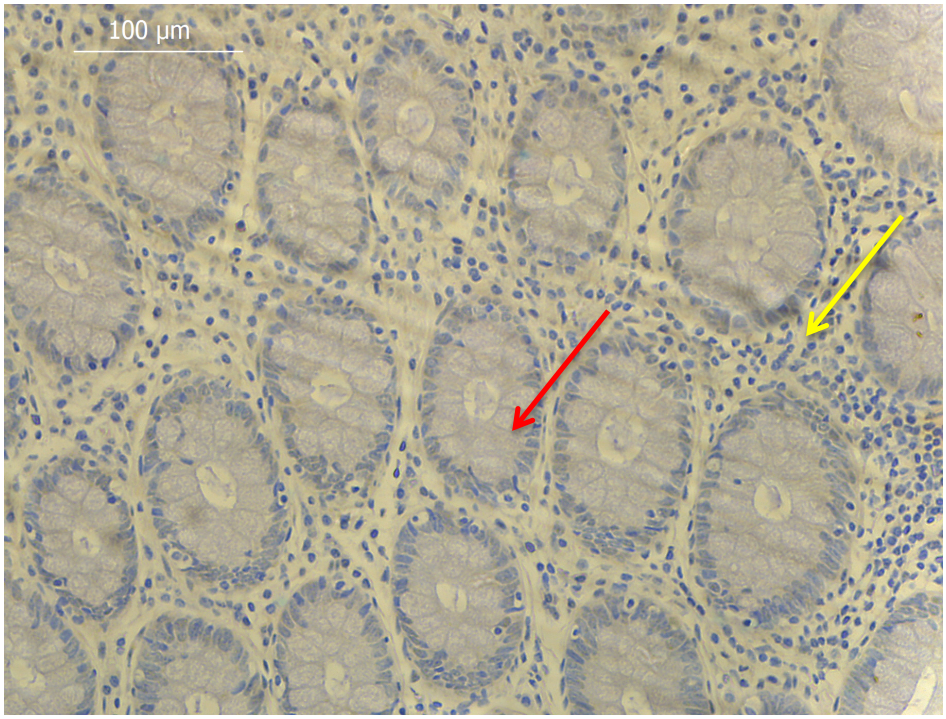

Figure 3.11. Representative immunohistochemistry images for normal colorectal tissue samples. X200 magnification used. Scale bar represents 100µm. Red arrow shows no staining of epithelial cell in an intestinal gland. Yellow arrow shows no staining of stroma.

3.4 Discussion

The results presented in this chapter show that PEDF mRNA expression was lower in colorectal cancer cell lines when compared to normal colorectal fibroblasts and in colorectal cancer tissue compared to normal tissue. These findings support those of Wågsäter *et al* (2010) and Ji *et al* (2013). PEDF expression was found to decline with worsening grade of tumour, as demonstrated by a statistical significance on immunohistochemistry staining and with a trend witnessed in mRNA expression, confirming the association between loss of PEDF expression and worsening oncological prognostic factors; this echoed the findings of Guan *et al* (2003) where decreased expression of PEDF was apparent with worsening tumour grade in glioma tissue. However, there was little evidence from the results presented to support associations between other negative prognostic factors, such as advanced Duke's Stage, T stage or lymph node involvement, and PEDF expression levels; whilst there was a trend towards lower expression in metastatic colorectal cell line, compared to other colorectal cancer cell lines, this did not reach significance, and results from qPCR and immunohistochemistry studies did not support this either.

Interestingly, mRNA expression of PEDF was observed to be higher in female colorectal cancer patients when compared to male colorectal cancer patients. This is contrary to both Yamagishi *et al* (2006) and Wågsäter *et al* (2010) who established that plasma samples from healthy male controls had higher levels of PEDF when compared to healthy female controls, however a similar finding in colorectal cancer patients was either not assessed or demonstrated, in the respective studies. Other

studies evaluating PEDF expression in other solid tumours did not display significance difference between genders (Uehara et al. 2004; Jiang et al. 2010).

A recent population-based analysis study of 164,996 colorectal cancer patients in Germany demonstrated a higher age-adjusted 5-year survival rate in females compared to males (64.5% vs. 61.9%, p<0.0001) (Majek et al. 2013). The survival advantage of women was seen on multivariate analysis after adjusting for tumour staging in women under 65 years of age (Relative Excess Risk 0.86, 95% CI 0.82-0.90) but not in those over the age of 65 years of age (Relative Excess Risk 1.01, 95% CI 0.98-1.04). When analysing patients with advanced stage disease, older women aged >75 years had a worse survival than men. Location of tumour did not seem to affect survival. These findings were comparable to two earlier studies, in patients based in USA and Japan (Hendifar et al. 2009; Koo et al. 2008), with younger women have a survival advantage compared to younger men, but with the opposite pattern noted in older patients. One of the main reasons suggested for this effect is the favourable effect of endogenous female sex hormones (Franceschi et al. 2000). Other reasons include increased bowel cancer screening uptake amongst females and therefore higher proportion of early stages at diagnosis and better prognosis (Stock et al. 2011), however Majek *et al* (2013) found a survival benefit remained after adjusting for tumour staging, therefore making this reason less likely. However, it may be plausible that the gender difference in expression of PEDF may be responsible for the survival difference seen. In our cohort, we found no difference in PEDF expression comparing both genders in age groups 64 years or less and 65 years and over (p=0.729 and p=0.107, respectively). The outcome in this chapter warrants

further evaluation in future studies into the possible reasons behind a difference in PEDF expression patterns between the genders within colorectal cancer.

Rectal tumour tissue appeared to express higher mRNA levels of PEDF when compared to colonic tumour tissue, however this was not confirmed on immunohistochemistry or in cell line studies. Díaz *et al* (2008) detected a similar difference with higher mRNA expression of PEDF in tissue from rectal tumours when compared to tissue from colonic tumour. Cai *et al* (2006b) found conflicting results on a cellular level with stronger PEDF expression in HT115 colonic adenocarcinoma cell line and weaker expression in HRT-18 rectal adenocarcinoma cell line, however our results showed little difference in the expression of these two cell lines and therefore there may be other cellular factors in these cell lines that may be responsible for the expression levels shown.

Mucinous adenocarcinoma tissue showed more positive tumour expression when compared to adenocarcinoma tissue on immunohistochemical staining. This is consistent with work from Ji *et al* (2013) where patients with mucinous adenocarcinoma displayed higher PEDF plasma levels than adenocarcinoma patients. This is perhaps a slightly surprising result, as mucinous adenocarcinoma of the colon or rectum is well recognised to have a poorer survival rate when compared to non-mucinous adenocarcinoma (Numata et al. 2012) and hence there must be other influences, yet to be identified, that are specific to mucin producing tumours that are responsible for the higher expression levels of PEDF.

Immunofluorescence, immunocytochemistry and immunohistochemistry studies showed a tendency towards cytoplasmic staining more so than nucleic staining for

colorectal tumour cells, comparable to findings from Ji *et al* (2013). Certainly, this provides some evidence to support the association between PEDF and critical cell activities such as cellular differentiation, cell growth and cell cycle control, which typically take place in the cytoplasm in eukaryotic organisms.

In conclusion, our results confirmed that PEDF expression was higher in normal colorectal tissue and cells compared to cancer tissue and cells, confirming the inverse correlation between PEDF levels and pathological angiogenesis. It is therefore logical to suggest that normalisation of PEDF levels to their baseline may be responsible for halting such processes.

Chapter 4

Role of PEDF on cellular function in colorectal cancer

4.1 Introduction

Over recent decades, significant advances in the early detection and treatment for colorectal cancer have been made. In early detection, these include the introduction of national bowel cancer screening programmes and the improvement of radiological imaging. Through large scale clinical trials there has been advancement in both chemotherapy and radiotherapy regimes that can be offered to patients with colorectal cancer, including the wide spread adoption of neo-adjuvant chemo-radiotherapy for locally advanced rectal cancers to down stage tumours prior to surgical resection. Surgical practice has also focused on the achievement of good oncological resections of tumour such as the gold standard total mesorectal excision for low rectal tumours.

Despite these advances, the overall 5 year survival rate from colorectal cancer in the UK is still as low as 58.7% and there are approximately 16,000 deaths secondary to colorectal cancer per annum (Cancer Research UK. 2016; http://www.cancerresearchuk.org). It is for this reason that the search for novel therapies for the treatment of colorectal cancer remains an urgent priority.

Many proposed novel therapies focus on the cessation of tumorigenesis and have been targeted at various angiogenic factors such as VEGF and EGFR (as discussed in section 1.3.1). However, in the UK, their licensed use in the treatment of colorectal cancer has been limited to KRAS wild-type expressing tumours, following evaluation of level 1 clinical evidence.

PEDF has been demonstrated to inhibit cellular growth, adhesion, migration and invasion in a range of solid tumours, and consequently may present an exciting cancer therapeutic option. However, the evidence investigating the role of PEDF in colorectal cell line function has been limited; therefore the aim of this section of the study was to investigate the effect of treatment with recombinant PEDF on cellular function within colorectal cell lines.

4.2. Methods and Materials

4.2.1 Cell lines

RKO, HT115 and HRT-18 cell lines were chosen for this part of the study as representative cell lines for colorectal adenocarcinoma. Cells were maintained as described in section 2.7.1 and 2.7.2.

4.2.2 Treatment

All cellular functional assays were performed using normal medium as described in section 2.7.1 as a control. Treatment with rhPEDF was performed at doses of 10ng/ml, 50ng/ml and 100ng/ml (Section 2.6.5). These varying doses were chosen based on a previous study which used 100ng/ml of rhPEDF for treatment (Cai et al. 2006a) and the manufacturers guidance.

4.2.3 *In vitro* cellular growth assay

Cells were seeded into three 96 well plates at a seeding density of $3x10^3$ cells/100µl, supplemented with 100µl of either treatment or control medium. The plates were then incubated for 1,3 and 5 days, respectively, as described in full detail in section

2.12.1. After incubation, cells were fixed using 4% formaldehyde (v/v) then stained with 0.5% crystal violet (v/v). Analysis was performed at 540nm using a spectrophotometer. Prior to reading the dye was solubilised using 10% acetic acid. Data from at least 3 repeated experimental procedures were combined and presented in this chapter.

4.2.4 *In vitro* tumour cell Matrigel adhesion assay

Cells were seeded into matrigel-coated wells at a seeding density of $4.5x10^4$ cells/100µl, supplemented with 100µl of either treatment or control medium. The plate was then incubated for 45 minutes to allow cells to adhere to the Matrigel as described in full detail in section 2.12.2. After incubation, cells were fixed using 4% formaldehyde (v/v) then stained with 0.5% crystal violet (v/v). The dye was solubilised using 10% acetic acid and analysed using a spectrophotometer at 540nm. Data from at least 3 repeated experimental procedures were combined and presented in this chapter.

4.2.5 *In vitro* cellular scratch migration assay

Cells were seeded into a 24-well plate at a seeding density of $3x10^5$ cells/500µl, and were incubated for 24 hours, as described in full detail in section 2.12.3.2. After incubation, a straight-line scratch was made to the cellular monolayer down the midpoint of each well. The medium was then removed from the plates carefully and replaced with 500µl of either treatment or control medium. Analysis was performed using EVOS cell imaging system (Life Technologies, Paisley, UK) and images were captured every 60 minutes for a total of 6 hours. Data from at least 3 repeated

experimental procedures were combined and presented as migration distance in this chapter.

4.2.6 *In vitro* cellular invasion assay

Cells were seeded into a 24-well plate containing matrigel-coated Transwell inserts at a seeding density of 3 x 10^4 cells/100µl supplemented with 100µl of treatment or control medium as described in section 2.12.4. Following 72 hours' incubation, the inferior aspect of the insert was fixed in 4% formaldehyde (v/v) then stained in 0.5% crystal violet (v/v). The dye was solubilised using 10% acetic acid and analysed using a spectrophotometer at 540nm. Data from at least 3 repeated experimental procedures were combined and absorbance levels as a marker of cell density presented in this chapter.

4.3 Role of PEDF on cellular function in colorectal cancer cell lines

4.3.1 Effect of PEDF on colorectal cancer cell growth

In the RKO cell line, after both day 3 and day 5 of incubation there was no statistically significant decrease in cellular proliferation with varying doses of rhPEDF when compared to control group (p=0.259 and p=0.283 respectively for day 3 and day 5) (Figure 4.1).

There was no statistically significant difference seen after both 3 and 5 days of incubation of HT115 cell line comparing control with varying concentrations of rhPEDF (p=0.830 and p=0.260 respectively) (Figure 4.2).

In the HRT-18 cell line, after day 3 and day 5 of incubation there was no statistically significant difference seen between the control group and the varying rhPEDF concentrations (p=0.197 and 0.151 respectively) (Figure 4.3).

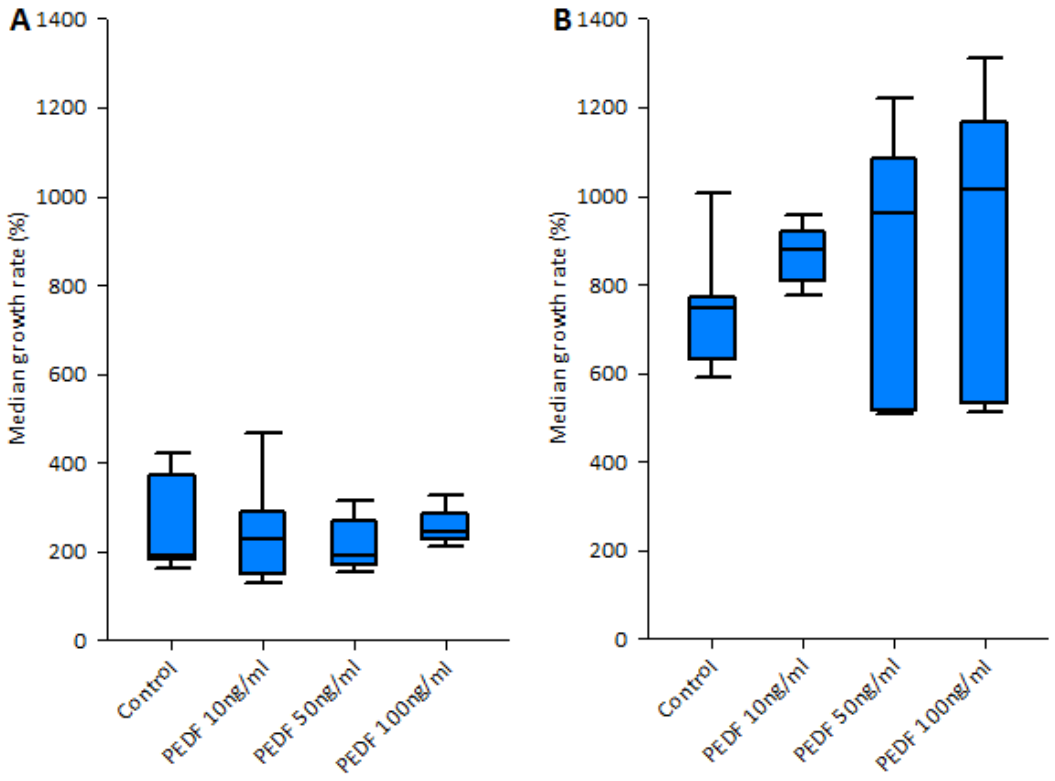

Figure 4.1. Impact of rhPEDF on cellular growth after 3 days (A) and 5 days (B) of incubation, in response to varying concentrations of rhPEDF in RKO cells. Median values of 3 independent repeats are shown. The absorbance of Day 1 was used as a baseline to normalise data.

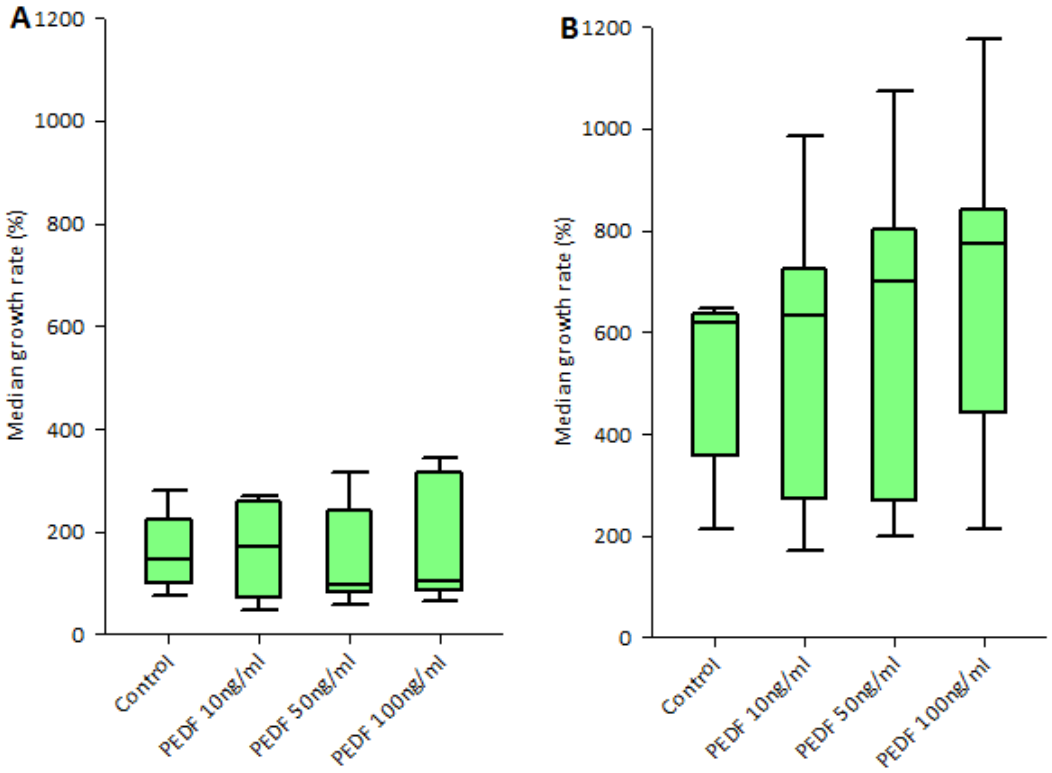

Figure 4.2. Impact of rhPEDF on cellular growth after 3 days (A) and 5 days (B) of incubation, in response to varying concentrations of rhPEDF in HT115 cells. Median values of 3 independent repeats are shown. The absorbance of Day 1 was used as a baseline to normalise data.

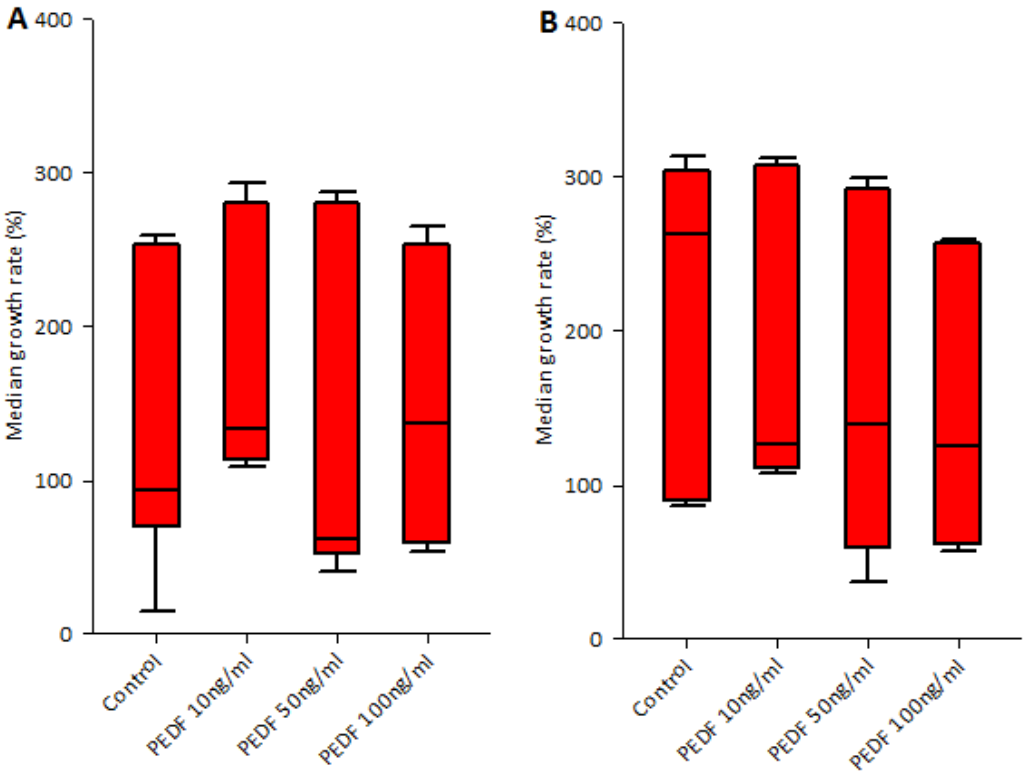

Figure 4.3. Impact of rhPEDF on cellular growth after 3 days (A) and 5 days (B) of incubation, in response to varying concentrations of rhPEDF in HRT-18 cells. Median values of 3 independent repeats are shown. The absorbance of Day 1 was used as a baseline to normalise data.

4.3.2 Effect of PEDF on colorectal cancer cell adhesion

There was no difference observed in the attachment of RKO cells with any of the treatment doses of rhPEDF compared to the control (p=0.603) (Figure 4.4).

There was a statistical significant increase in the attachment of HT115 with the treatment of rhPEDF 100ng/ml when compared to the control (p=0.003); however, this significant increase was not observed with either treatment doses of rhPEDF at 10ng/ml or 50ng/ml (Figure 4.5).

No difference was demonstrated in the attachment of HRT-18 cells with the treatment of rhPEDF compared to the control (p=0.810) (Figure 4.6).

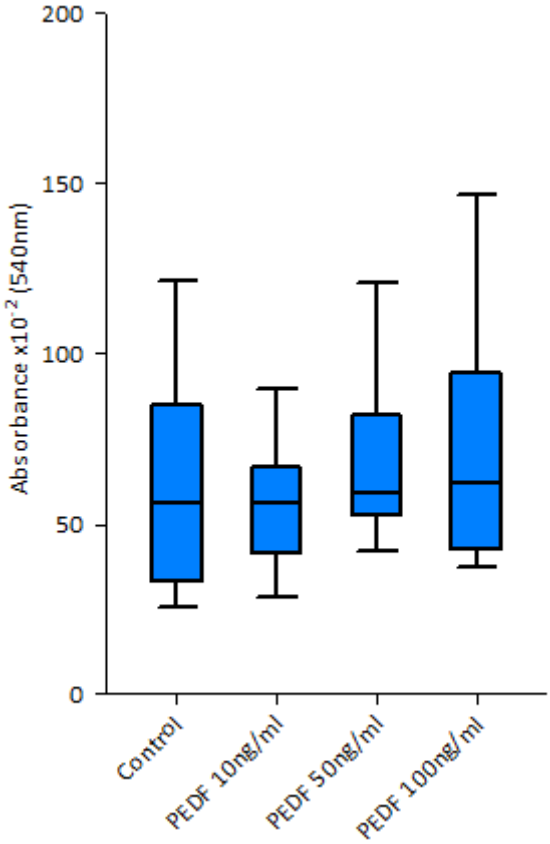

Figure 4.4. Impact of rhPEDF on cellular attachment in RKO cells. Absorbance $x10^{-2}$ (540nm) readings used as a marker of cellular attachment, in response to varying concentrations of rhPEDF. Median values and IQR of 3 independent repeats are shown. Error bars represent 95% confidence intervals

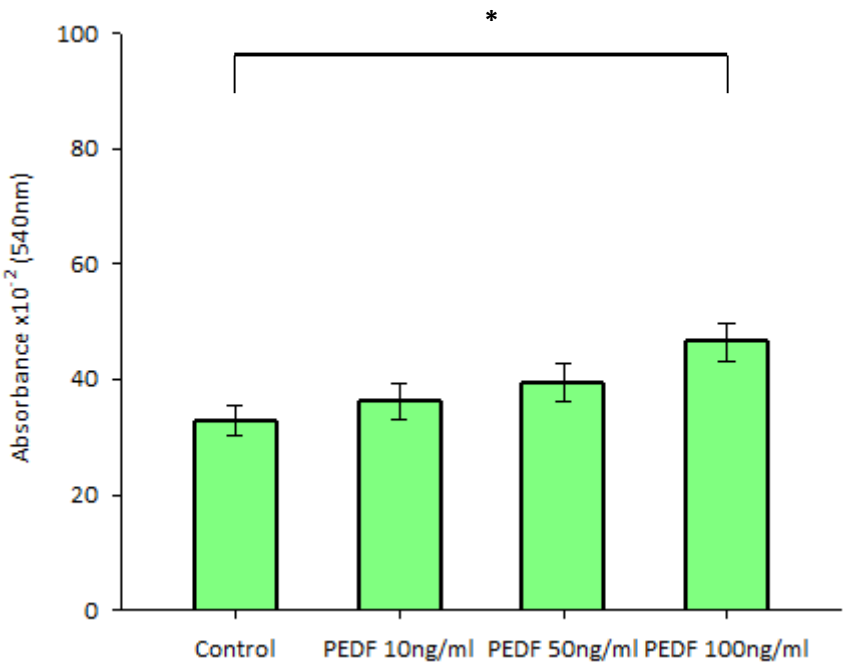

Figure 4.5. Impact of rhPEDF on cellular attachment in HT115 cells. Absorbance $x10^{-2}$ (540nm) readings used as a marker of cellular attachment, in response to varying concentrations of rhPEDF. Mean values of 3 independent repeats are shown. Error bars represent SEM * $p<0.05$

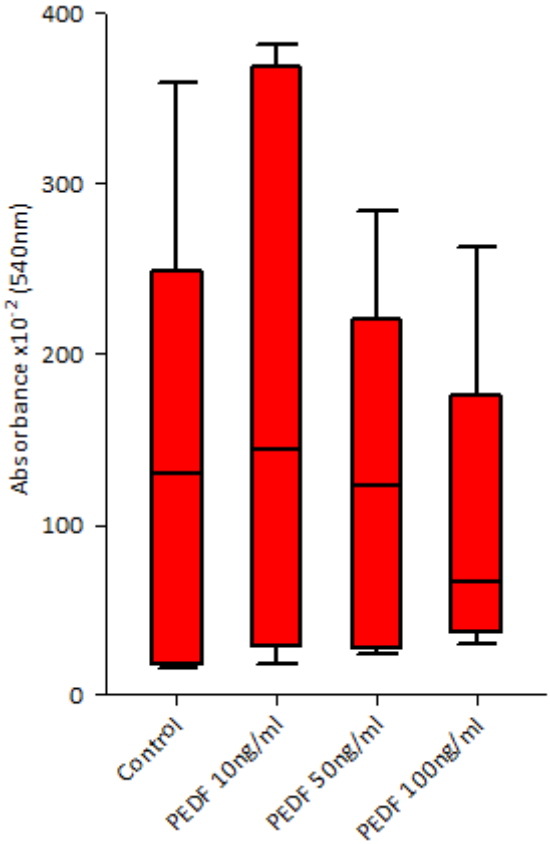

Figure 4.6. Impact of rhPEDF on cellular attachment in HRT-18 cells. Absorbance $x10^{-2}$ (540nm) readings used as a marker of cellular attachment, in response to varying concentrations of rhPEDF. Median values and IQR of 3 independent repeats are shown. Error bars represent 95% confidence intervals

4.3.3 Effect of PEDF on colorectal cancer cell migration

Under the influence of rhPEDF treatment, there was a statistically significant decrease in HT115 migration rate over a 6-hour period. This significant decrease in migration rate was evident for both 50ng/ml and 100ng/ml rhPEDF treatment doses ($p=0.007$ and $p<0.001$, respectively), when compared to untreated HT115 cells and 10ng/ml rhPEDF treatment dose (Figure 4.7). There was also a significantly significant decrease when comparing 10ng/ml rhPEDF treatment compared to both 50ng/ml and 100ng/ml ($p=0.006$ and $p<0.001$, respectively).

A similar effect was demonstrated in the HRT-18 cell line; a statistically significant decrease in HRT-18 migration rate over a 6-hour period, with treatment of rhPEDF. This significant decrease in migration rate was evident for all doses of rhPEDF compared to untreated HRT-18 cells. (rhPEDF 10ng/ml vs control $p= 0.002$, rhPEDF 50ng/ml $p<0.001$, rhPEDF 100ng/ml $p<0.001$) (Figure 4.8).

Unfortunately, RKO cellular behaviour did not permit migration assay to be performed, as when a scratch was performed the entire cellular layer would peel off in a ‘sheet- like’ manner thus not allowing further migration to be assessed.

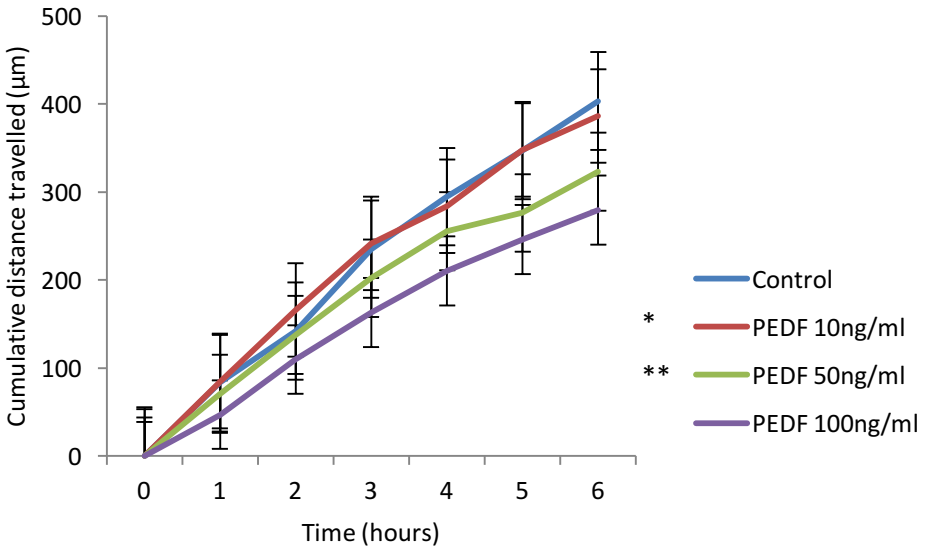

Figure 4.7. Impact of rhPEDF on HT115 cellular migration assessed through scratch migration assay. Cumulative distance travelled following scratch is shown and taken as representative of migration in HT115 cells compared to control and varying doses of rhPEDF. Mean values of 3 independent repeats are shown. Error bars represent SEM. *p<0.05 ** p<0.001

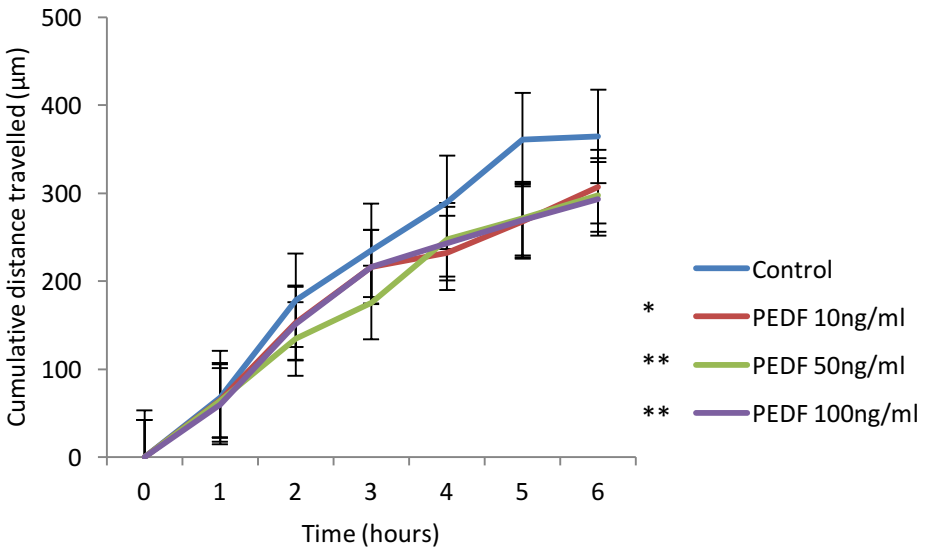

Figure 4.8. Impact of rhPEDF on HRT-18 cellular migration assessed through scratch migration assay. Cumulative distance travelled following scratch is shown and taken as representative of migration in HRT-18 cells compared to control and varying doses of rhPEDF. Mean values of 3 independent repeats are shown. Error bars represent standard error of the mean. *p<0.05 ** p<0.001

4.3.4 Effect of PEDF on colorectal cancer cell invasion

Under the influence of treatment with rhPEDF 100ng/ml, there was a statistically significant decrease in RKO cellular invasion when compared to control medium ($p=0.025$); however, this difference was not witnessed under the influence of the lower doses of rhPEDF treatments (10ng/ml and 50ng/ml) (Figure 4.9).

No difference was noticed in the cellular invasion when comparing all treatment doses of rhPEDF compared to control medium in HT115 cells ($p=0.865$) (Figure 4.10).

Whilst there was an observed trend towards a decrease in HRT-18 cellular invasion with the treatment of all doses of rhPEDF when compared to control medium, this was not found to be significant on statistical analysis ($p=0.352$).

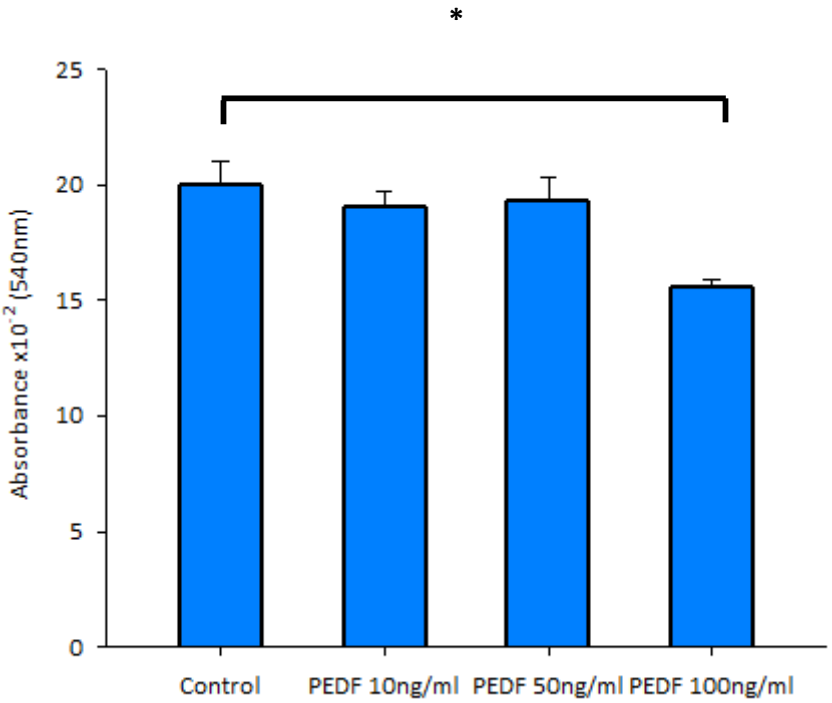

Figure 4.9. Impact of rhPEDF on cellular invasion in RKO cells. Absorbance $x10^{-2}$ (540nm) readings used as a marker of cellular density, in response to varying concentrations of rhPEDF. Median values and IQR of 3 independent repeats are shown. Error bars represent 95% confidence intervals. * $p<0.05$

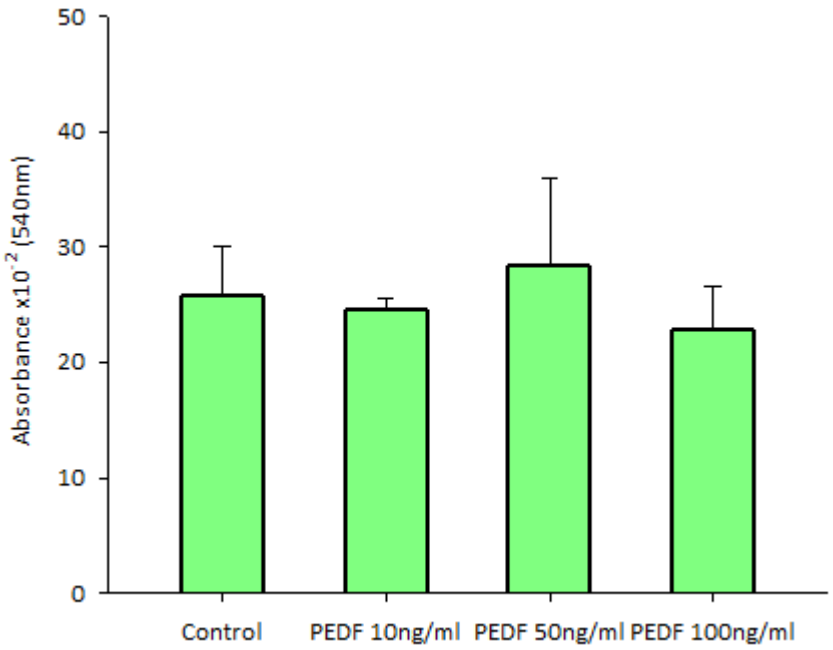

Figure 4.10. Impact of rhPEDF on cellular invasion in HT115 cells. Absorbance $x10^{-2}$ (540nm) readings used as a marker of cellular density, in response to varying concentrations of rhPEDF. Median values and IQR of 3 independent repeats are shown. Error bars represent 95% confidence intervals.

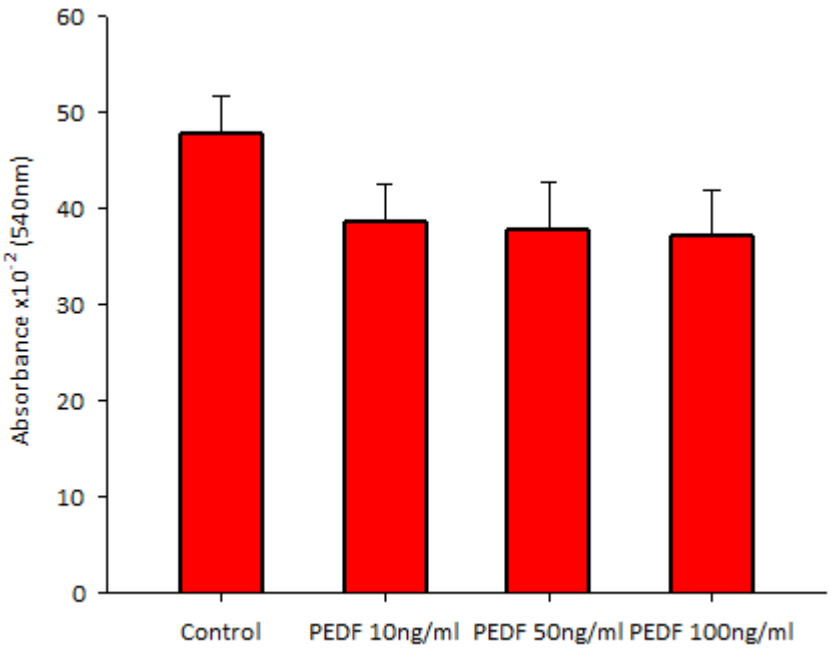

Figure 4.11. Impact of rhPEDF on cellular invasion in HRT-18 cells. Absorbance $x10^{-2}$ (540nm) readings used as a marker of cellular density, in response to varying concentrations of rhPEDF. Median values and IQR of 3 independent repeats are shown. Error bars represent 95% confidence intervals.

4.4 Discussion

Mortality from colorectal cancer is frequently related to metastatic spread, most commonly affecting the liver or lungs. Treatments aimed at preventing the metastatic spread of colorectal cancer cells could therefore prove highly beneficial for the survival of such patients. A number of studies have demonstrated that the decreased expression of PEDF is associated with the increased incidence of metastases in a range of solid tumours (Uehara et al. 2004; Halin et al. 2004; Cai et al. 2006b; Dass et al. 2008; Zhou et al. 2010; Fitzgerald et al. 2012; Ji et al. 2013). It is therefore logical to hypothesise that administration of PEDF may suppress metastases formation. Tumour metastasis depends on several cancer cell characteristics including cellular proliferation, adhesion, invasion and migration, and hence the capability to adapt to *in vivo* environments and outcompete with normal cells for resources necessary for survival. To date, the exact mechanisms of PEDF on colorectal cancer metastases remain poorly understood.

In this section of the study, treatment with rhPEDF in both the HT115 and HRT-18 colorectal cancer cell lines appeared to significantly decrease the rate of cellular migration. This effect was visible in HT115 cells with the higher doses used of rhPEDF, 50ng/ml and 100ng/ml vs control ($p=0.007$ and $p<0.001$, respectively), and in HRT-18 cells with all doses of rhPEDF vs control (10ng/ml $p=0.002$, 50ng/ml $p<0.001$, 100ng/ml $p<0.001$), when compared to normal control medium. Similarly, invasion studies showed a significant decrease in the rate of cellular invasion within the RKO colorectal cancer cell line, with treatment of 100ng/ml rhPEDF compared to normal

control medium (p=0.025), and whilst not significant there was a similar trend noticed in the HRT-18 colorectal cell line (p=0.352).

To date, the effect of rhPEDF on cellular function has not been studied in colorectal cell lines, but has been reported in a number of other solid tumours. Hong *et al* (2014) investigated the effect of the human breast cancer cell line MDA-MB-231 transfected with PEDF plasmid, compared to a control group. The results of their *in vitro* cellular migration and invasion studies confirmed a significant decrease in both tumour cell migration and invasion, and found that PEDF inhibited breast cancer cell migration and invasion by down-regulating fibronectin and subsequent MMP2/MMP9 reduction via p-ERK and p-AKT signalling pathways. Correspondingly, Tan *et al* (2010) found a 20% decrease in cellular invasion in PEDF treated chondrosarcoma cell when compared to control cells. These findings support our results presented in this chapter.

In the adhesion studies presented in this chapter, treatment with 100ng/ml rhPEDF resulted in an increase in cellular attachment in HT115 colorectal cancer cell lines (p=0.003). Tan *et al* (2010) found a similar finding when examining chondrosarcoma cells, with PEDF treatment significantly enhancing cellular adhesion to collagen-1 coated surfaces by 204% when compared to untreated cells. Increased adhesion certainly presents a beneficial effect in the prevention of metastatic progression, by contributing to a decreased ability for the cancer cells to invade and migrate.

Unlike other studies investigating the effect of PEDF treatment on cellular proliferation in other solid tumour cell lines (Abe et al. 2004; Matsumoto et al. 2004; Cheung et al. 2006; Guan et al. 2007; Dass et al. 2008; Chen et al. 2009; Hong et al.

2014), we found no significant different in cellular growth rates for any of the colorectal cancer cell lines examined. However many of these studies that demonstrated decreased cellular proliferation with PEDF used differing methods from the ones used in this study; in particular Hong *et al* (2014) used animal models and Matsumoto *et al* (2004) studied human umbilical vein endothelial cells treated with cultured media from PEDF transfected hepatocellular cancer cells and compared to control media. This provides a limitation in the comparison of the findings from these studies to those presented in this chapter.

In conclusion, the findings in this chapter suggest that PEDF administration confers an inhibitory effect on the migration and invasion of colorectal cancer cells. Future studies should examine the effect on a range of colorectal cancer cell lines (including metastatic and mucinous adenocarcinoma) and to explore the effect of cellular function in *in vivo* models using colorectal tumour xenografts within animal models.

Chapter 5

Expression profile of PEDF in wounds

5.1 Introduction

In order for optimal wound healing to take place, it is crucial that normal neovascularisation occurs during the proliferation stage of wound healing (Harding et al. 2002). During a normal wound healing process, the many soluble mediators released by macrophages initiate this stage. The process of neovascularisation is delicate and maintained by the fine balance of both pro-angiogenic and anti-angiogenic mediators, with any imbalance increasing the risk of a chronic wound.

PEDF has been found to be one of the most potent natural inhibitors of angiogenesis (Dawson et al. 1999; Duh et al. 2002) and exerts anti-angiogenic activities by arresting VEGF- or FGFb-mediated endothelial cell proliferation, migration and inducing apoptosis in activated endothelial cells (Dawson et al. 1999; Volpert et al. 2002; Bouck 2002).

PEDF has also been shown to be highly expressed in fibroblasts (Francis et al. 2004; Cai et al. 2006b), and less so in keratinocytes (Pignolo et al. 1995). There is evidence from immunohistochemistry studies that suggests that PEDF is produced within both the human epidermis and dermis (Abe et al. 2010; Francis et al. 2004) and that there is strongly positive staining for PEDF in normal skin tissue samples (Zhang et al. 2009; Abe et al. 2010).

The aim of this section of work was to determine the expression profile of PEDF within wound healing cell lines. An additional aim was to determine the expression profile within chronic wound tissue samples and to correlate the expression profile with clinical outcomes.

5.2 Materials and Methods

5.2.1 Cell lines

Four cell lines were screened for PEDF expression as part of this study; HASC (human adipose stem cells), DF (primary dermal fibroblasts), HaCaT (human keratinocytes) and HECV (Human endothelial vascular cell line). These cells were chosen as they are cell types that are known to play a role in wound healing. Cells were maintained in medium as described previously in section 2.7.1.

5.2.2 Wound tissue

Wound tissue collection and storage for qPCR and immunohistochemistry staining was performed at Wound Healing Research Unit, Cardiff and Vale University Health Board as described in section 2.2**.** For the purposes of analysis, the biopsies of the patients where the wound had either decreased in size or healed at 12 weeks' follow-up were classed as 'healing' and those that had either not decreased in size or remained static in size or increased were classed as 'non-healing'.

5.2.3 RNA isolation, cDNA synthesis, RT-PCR and qPCR

RNA isolation was performed using TRI reagent kit as described in section 2.8.1. Following this reverse transcription was carried out using a high capacity RT kit. RT-PCR products were separated electrophorectically on an agarose gel. RT-PCR representative images are presented, normalised against GAPDH.

qPCR was performed as described in section 2.8.8. All results presented were normalised against GAPDH and represent combined results from at least 3 independent repeats.

5.2.4 Protein isolation, SDS-PAGE and Western blotting

The method for isolating protein lysates has been described in section 2.9.1. Following SDS-PAGE, the protein was transferred onto PVDF membranes and probed with specific primary antibody (anti-GAPDH and anti-PEDF) and corresponding peroxidase conjugated secondary antibodies. Antibodies used are described in full detail in section 2.5 and concentrations described in section 2.9.5. Chemiluminescent protein detection kit was used to visualise protein bands as described in section 2.9.6. A representative image following 3 repeats has been presented.

5.2.5 Immunohistochemical staining of tissues

Immunohistochemistry was carried out using Vector ABC Kit as described in section 2.10.1. The primary antibody used was rabbit monoclonal antibody against PEDF at a 1:50 concentration as described in section 2.5. All specimens were analysed anonymously. Details of demographical and clinicopathological associations were provided during experimental data analysis. Representative images are shown in this study.

5.2.6 Immunocytochemical staining of cells

HaCaT, DF, HECV and HASC cell lines were used for immunocytochemistry, as representative cell lines for wound healing. Immunocytochemistry was performed as

described in section 2.10.2. The primary antibody used was rabbit monoclonal antibody against PEDF at a 1:50 concentration and the secondary antibody used was Vector ABC Kit as described in section 2.5. Representative images are shown in this study.

5.2.7 Immunofluorescence staining of cells

HaCaT, DF, and HECV cell lines were used for immunofluorescence staining of cells, as representative cell lines for wound healing. Immunofluorescence staining was performed as described in section 2.11. The primary antibody used was rabbit monoclonal antibody against PEDF at a 1:50 concentration and the secondary antibody used was anti-rabbit FITC conjugate at a 1:250 concentration as described in section 2.5. Representative images are shown in this study.

5.3 Results

5.3.1 Wound healing cell lines expression screening for PEDF

PEDF transcript expression using RT-PCR was detected in HASC, DF and HaCaT cell lines (Figure 5.1); with PEDF being more highly expressed in HASC compared with DF, HaCaT and HECV cell lines.

qPCR showed that HASC and DF cell lines had higher expression of PEDF when compared to HaCaT and HECV cell lines ($p<0.05$) (Figure 5.2).

With western blotting, HASC demonstrated higher expression of PEDF protein bands, when compared to HaCaT, DF and HECV (Figure 5.3).

Immunofluorescence and immunocytochemistry showed a tendency towards nucleic staining for the DF, HECV and HASC cell lines and cytoplasmic staining for the HaCaT cell line (Figures 5.4 to 5.10). Due to the HASC cell line only remaining viable for a low number of passages it was not possible to perform immunofluorescence studies.

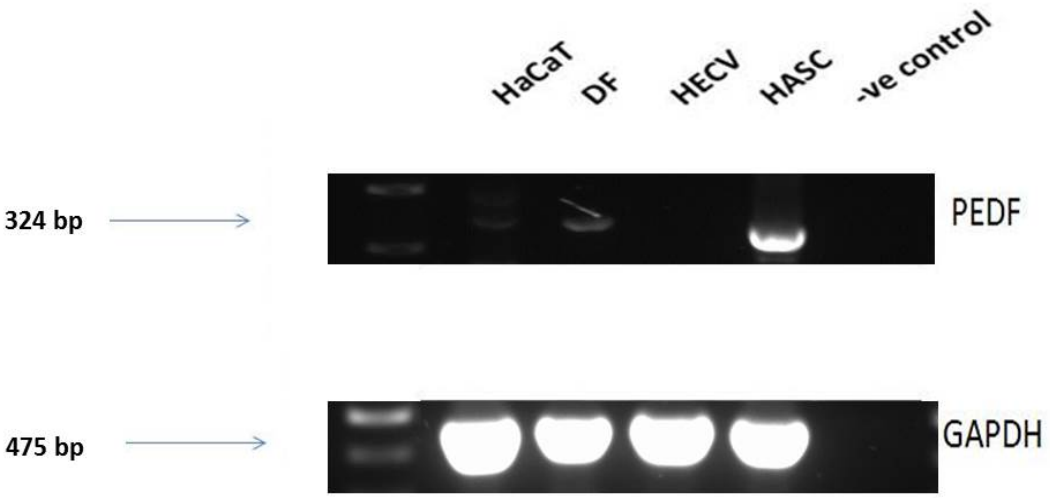

Figure 5.1. Transcript expression levels in PEDF in wound healing cell lines Control= Nuclease free water and all gels were run with a molecular weight marker used to identify band sizes.

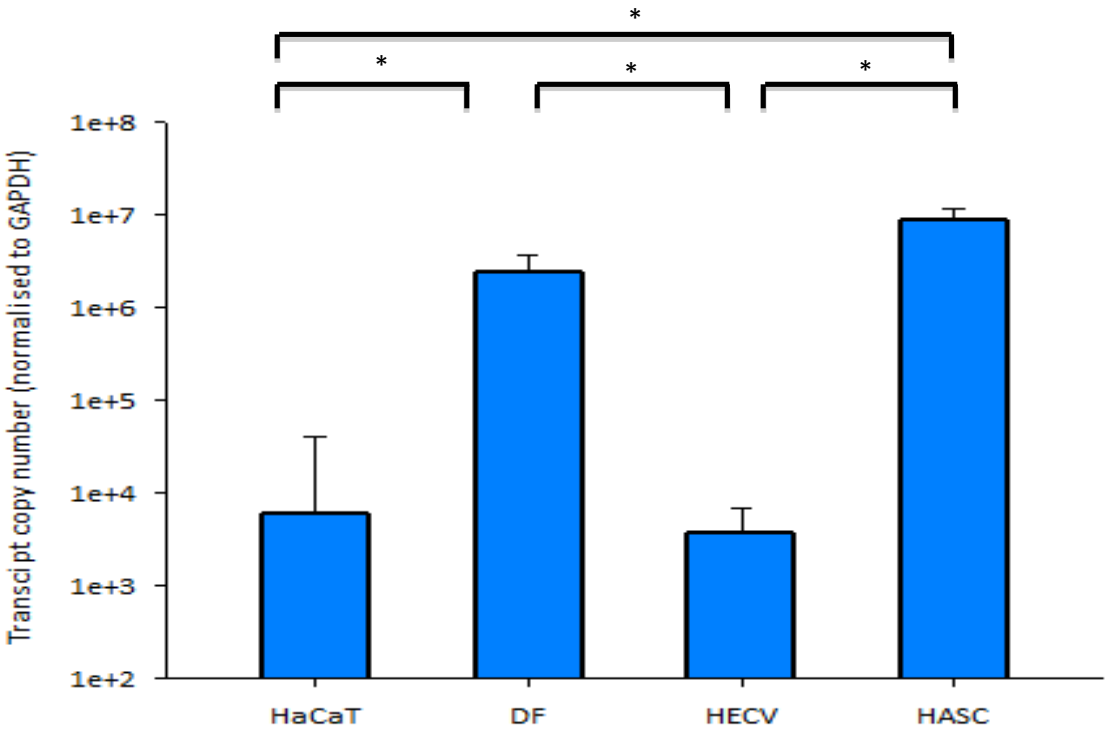

Figure 5.2. qPCR expressional analysis of PEDF within wound healing cell lines. Relative transcript copy number was calculated based on internal standard. Median data from 3 independent repeats are shown. Error bars represent IQR. * $p<0.05$

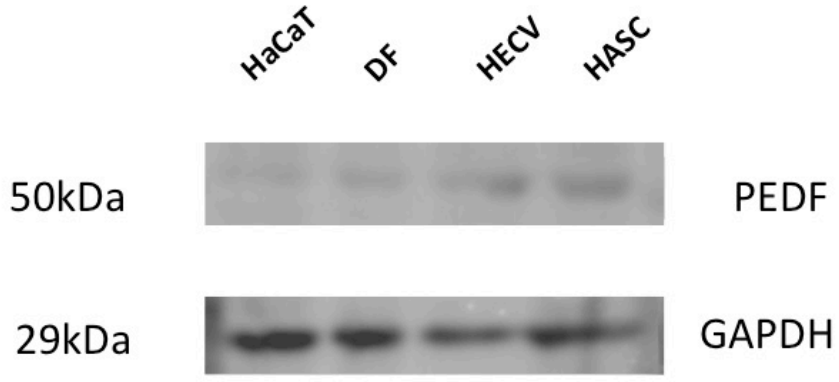

Figure 5.3. Confirmation of PEDF protein bands in wound healing cell lines

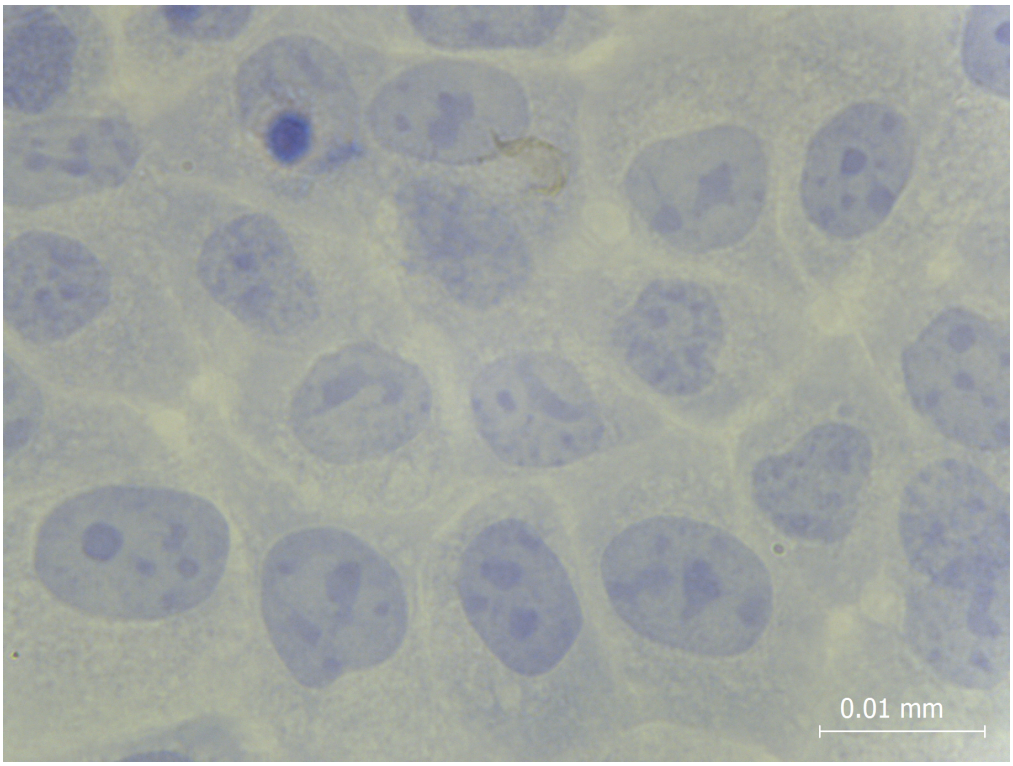

Negative control

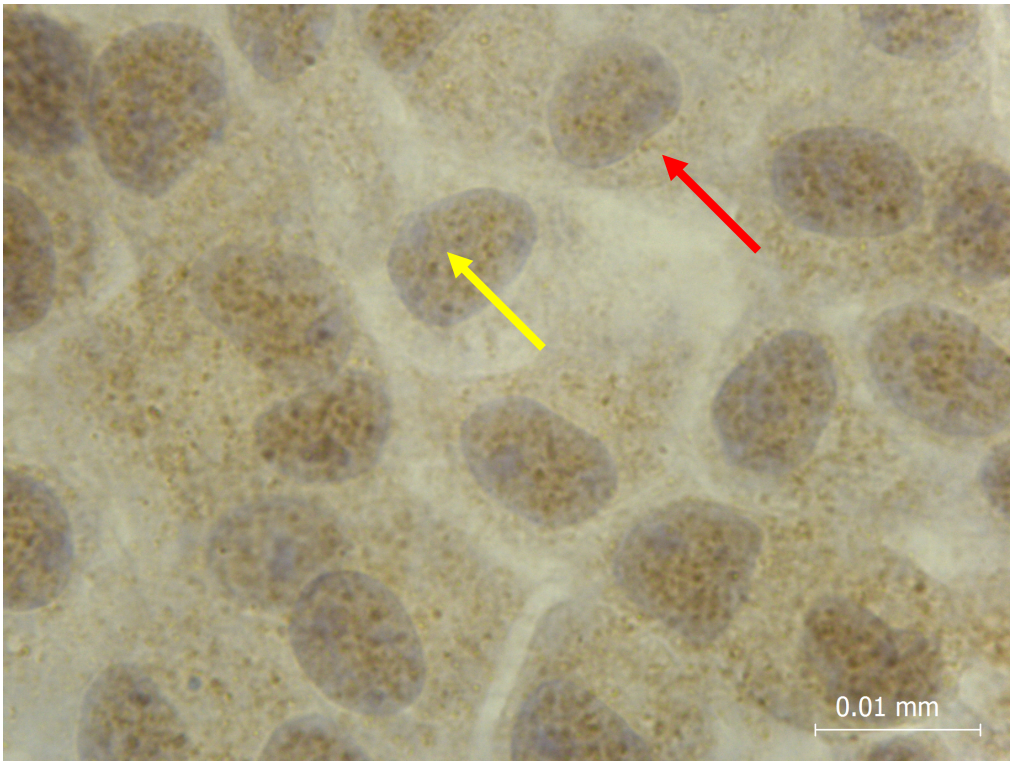

Figure 5.4. Representative immunocytochemistry images for HaCaT cell line. X100 magnification used. Scale bar represents 10µm. Red arrow shows weakly positive cytoplasmic staining and yellow arrow shows minimal nucleic staining.

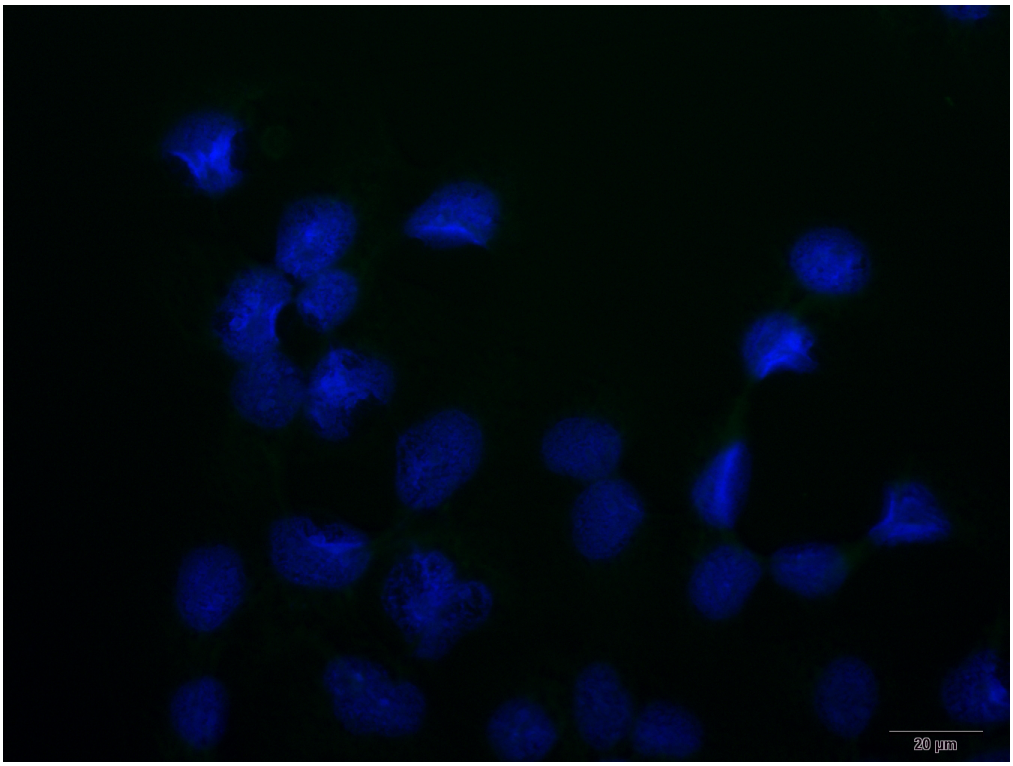

Negative control

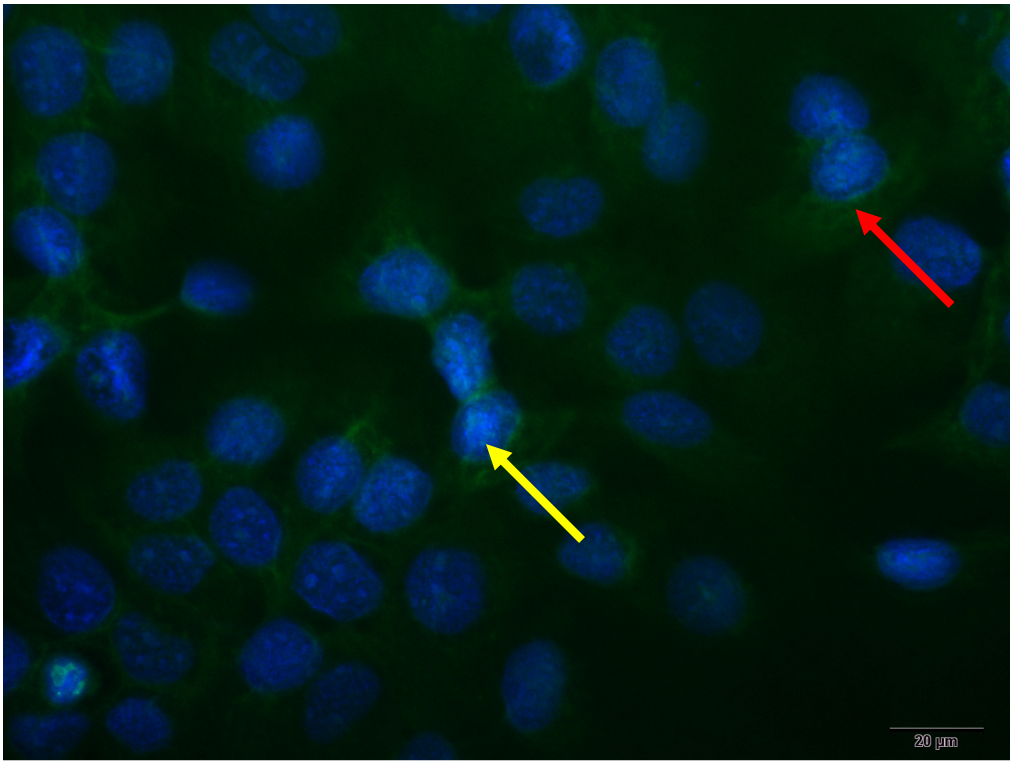

Figure 5.5. Representative immunofluorescence images for HaCaT cell line. X40 magnification used. Scale bar represents 20µm. Red arrow shows weakly positive cytoplasmic staining. Yellow arrow shows moderately positive nucleic staining.

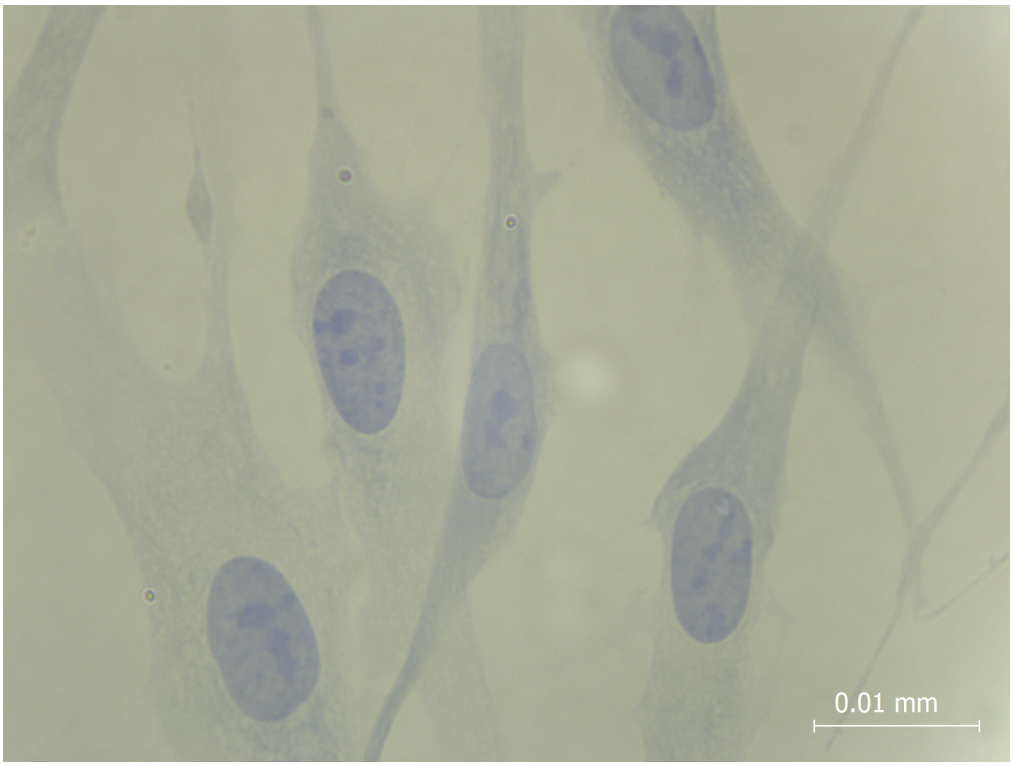

Negative control

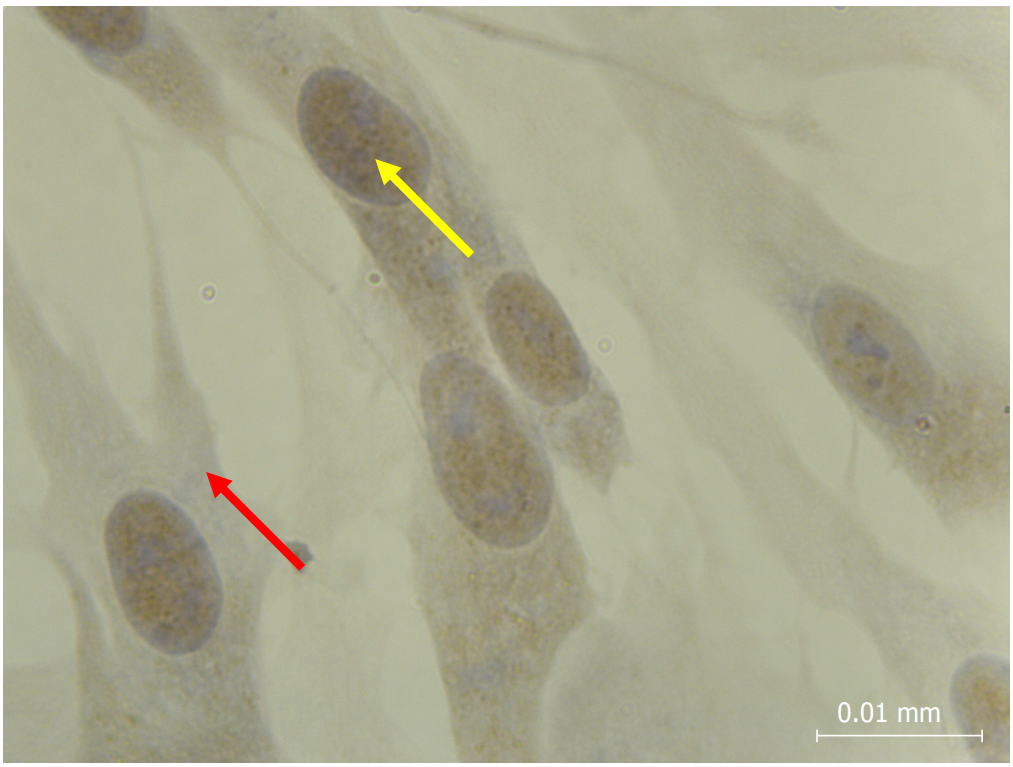

Figure 5.6. Representative immunocytochemistry images for DF cell line. X100 magnification used. Scale bar represents 10µm. Red arrow shows minimal cytoplasmic staining and yellow arrow shows weakly positive nucleic staining.

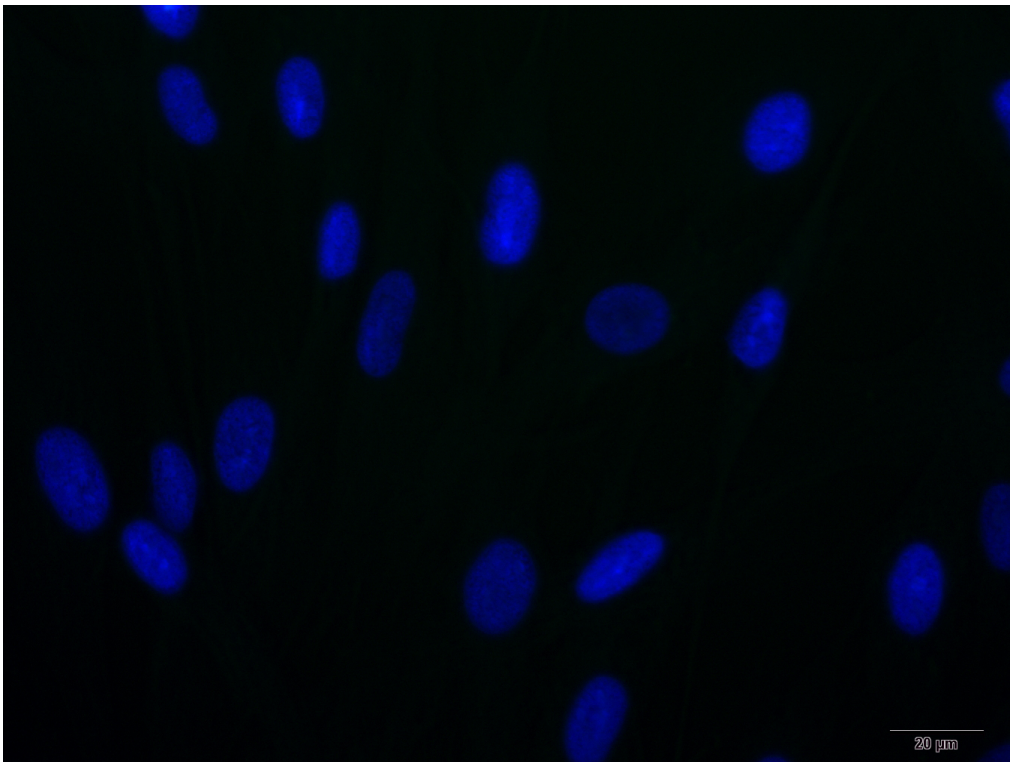

Negative control

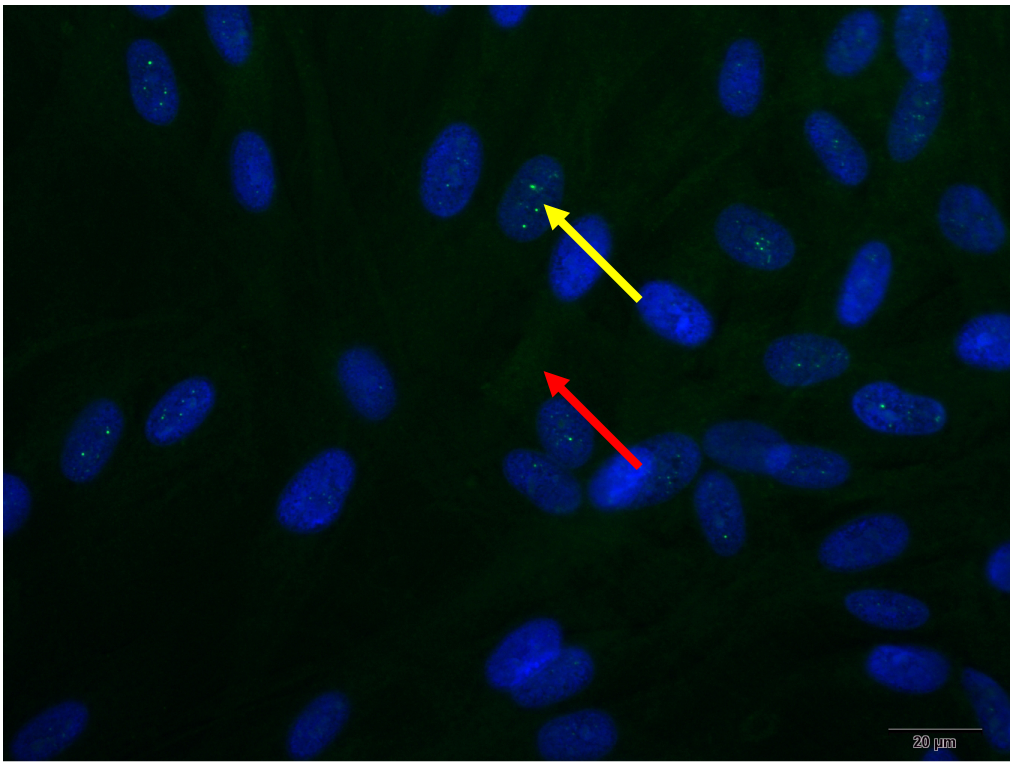

Figure 5.7. Representative immunofluorescence images for DF cell line. X40 magnification used. Scale bar represents 20µm. Red arrow shows weakly positive cytoplasmic staining and yellow arrow shows weakly positive nucleic staining.

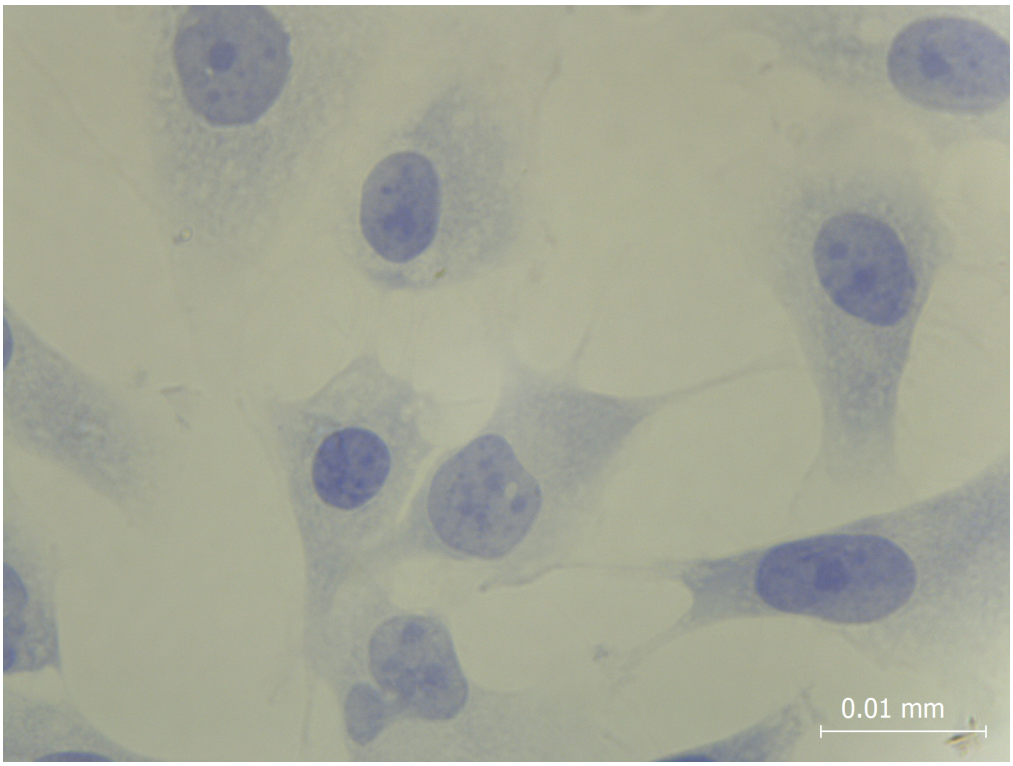

Negative control

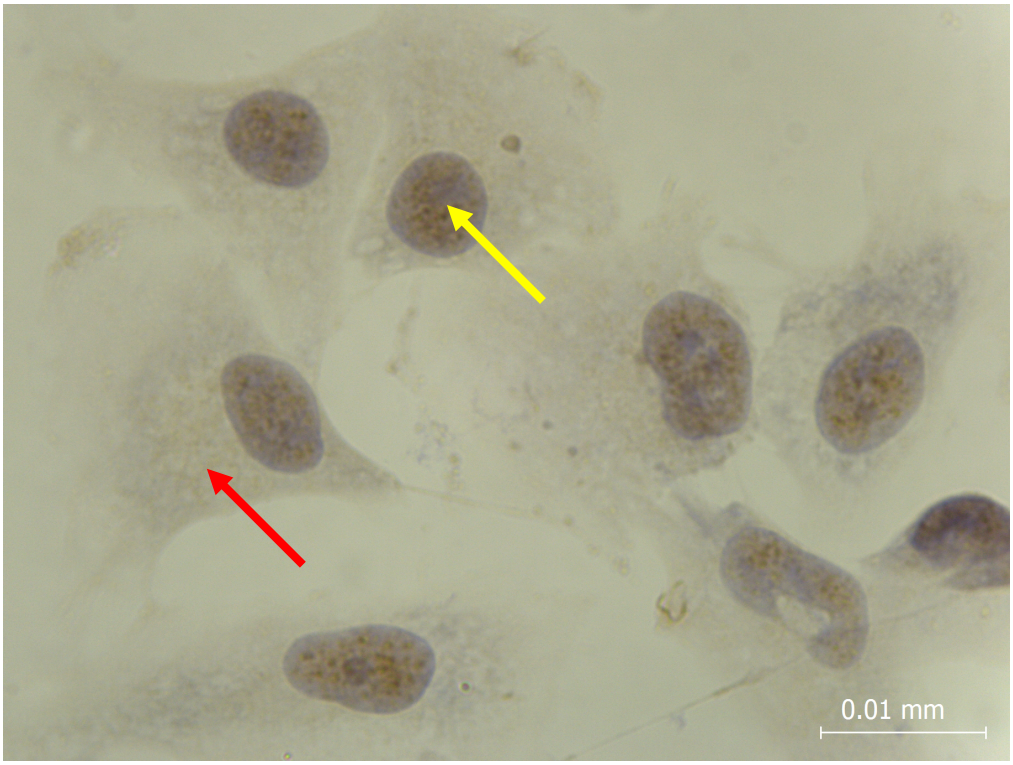

Figure 5.8. Representative immunocytochemistry images for HECV cell line. X100 magnification used. Scale bar represents 10µm. Red arrow shows minimal cytoplasmic staining and yellow arrow shows moderately positive nucleic staining.

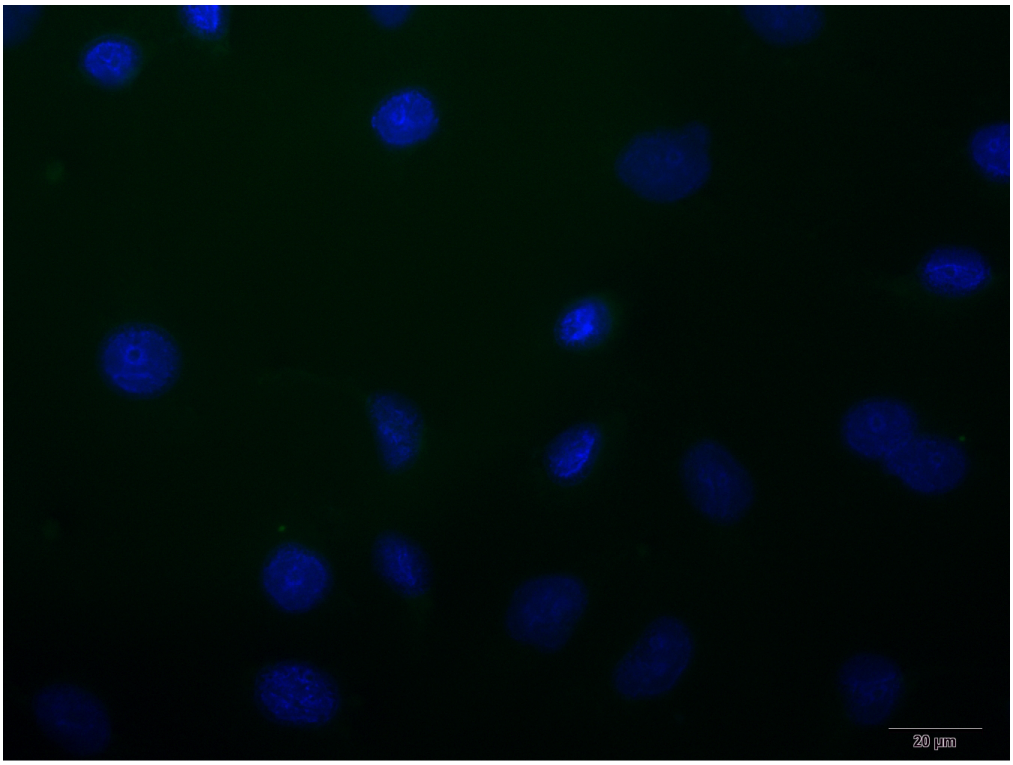

Negative control

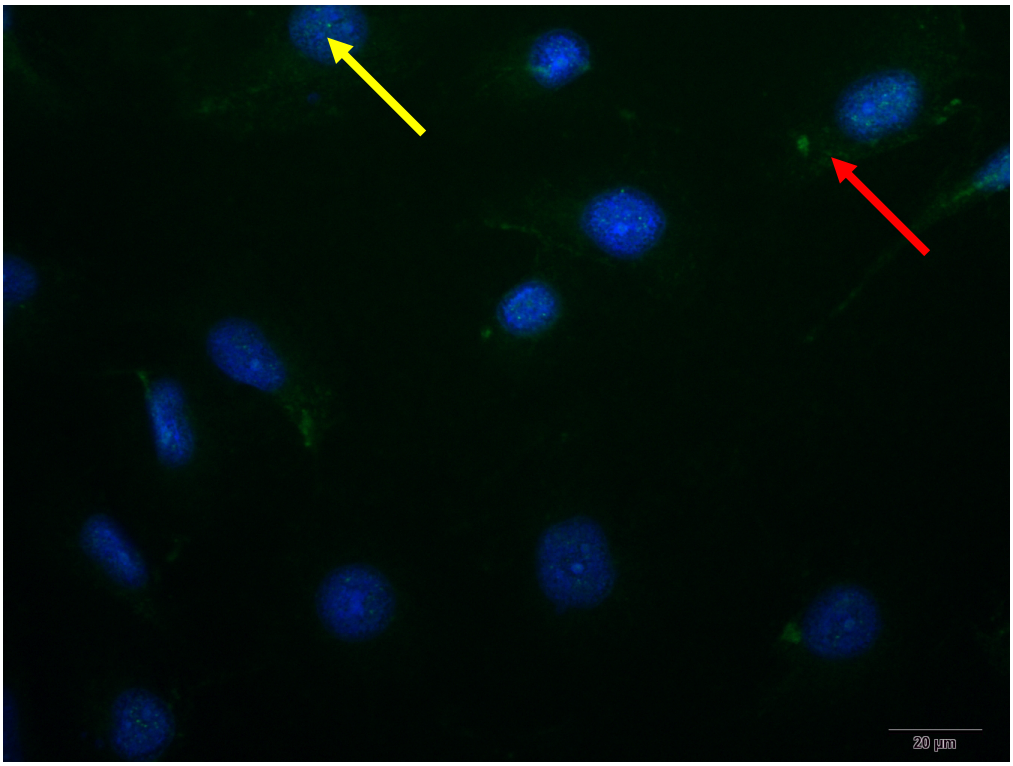

Figure 5.9. Representative immunofluorescence images for HECV cell line. X40 magnification used. Scale bar represents 20µm. Red arrow shows weakly positive cytoplasmic staining and yellow arrow shows weakly positive nucleic staining.

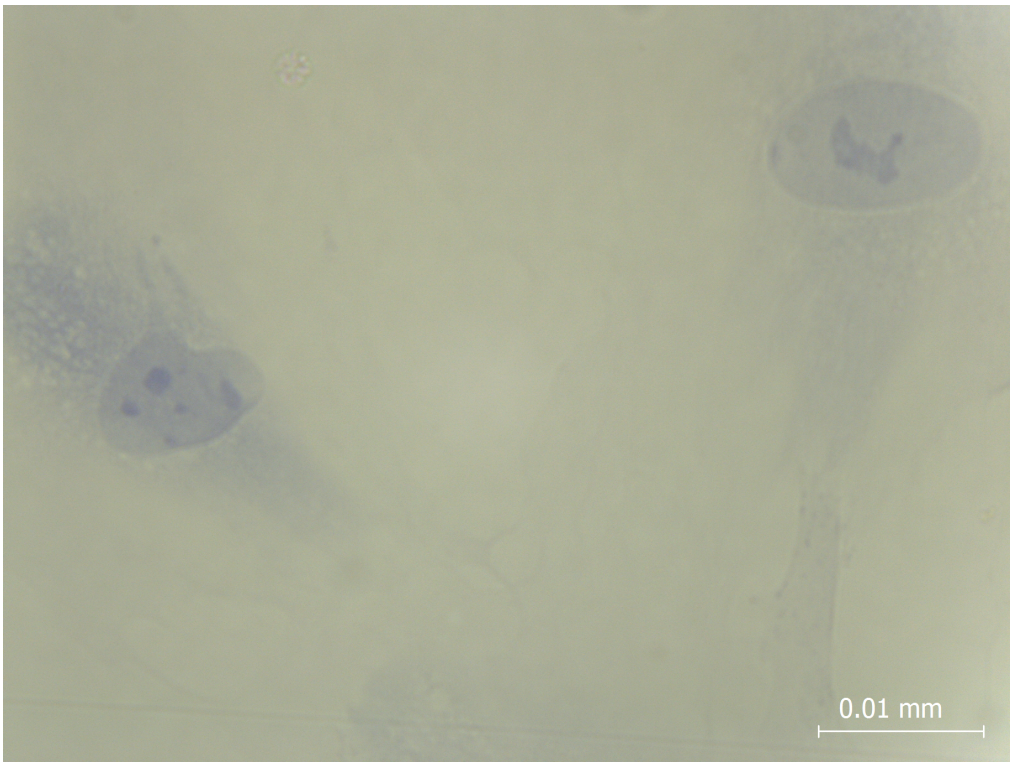

Negative control

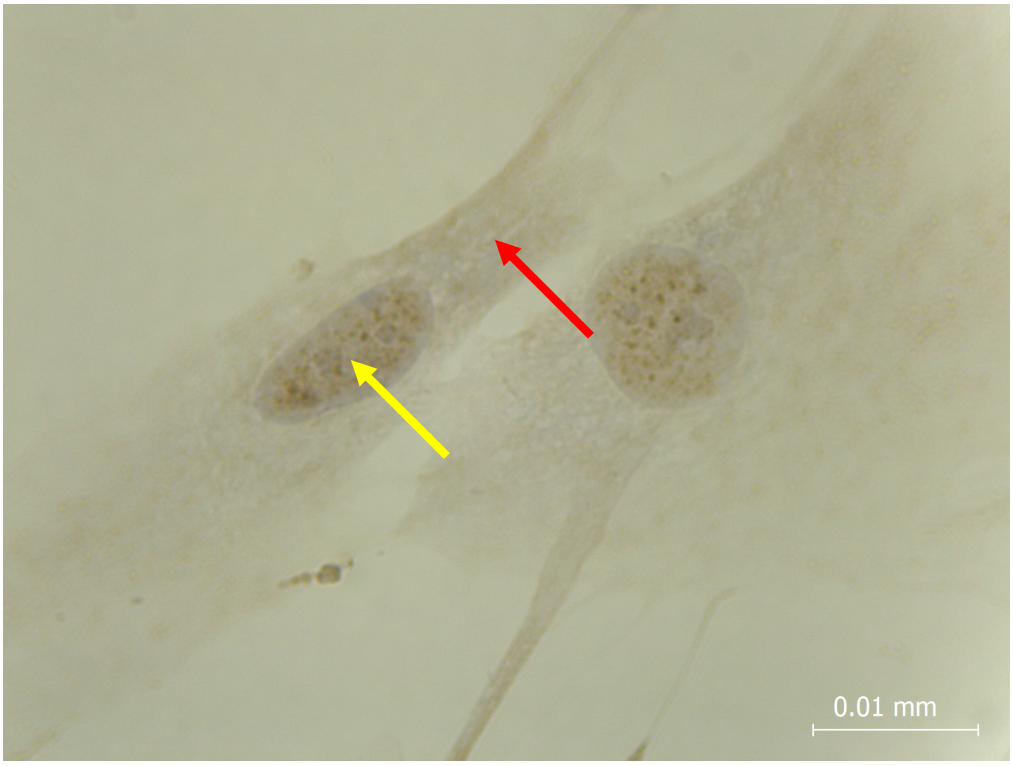

Figure 5.10. Representative immunocytochemistry images for HASC cell line. X100 magnification used. Scale bar represents 10µm. Red arrow shows weakly positive cytoplasmic staining and yellow arrow shows weakly positive nucleic staining.

5.3.2 Expression of PEDF in human chronic wound tissues and the association with clinicopathological characteristics

The demographical data for the cohort of patients with chronic wound tissue samples can be seen in Table 5.1. Within chronic wound tissue samples, there was higher expression in non-healing wounds compared to healing wounds, however this was not found to be statistically significant (p = 0.21) (Table 5.2).

Table 5.1. Clinical cohort of chronic venous leg ulcer patient demographics

	Healing	**Non-healing**
Number of patients	20	51
Age (mean ± SD)	72.6 ± 6.2	73.2 ± 7.1
Male: Female	4:16	13:38
Diabetes	3	9

Table 5.2. qPCR expressional analysis of PEDF within chronic wound samples.

	N	**Median transcript copy number**	**IQR**	**P value**
Non-healed	51	$2.1x10^{7}$	$6.0x10^{11}$	
Healed	20	$1.6x10^{5}$	$1.9x10^{8}$	0.21

Immunohistochemical staining of chronic wound samples showed PEDF expression in the dermis in the majority of chronic wound tissue samples studied (Figure 5.11 and 5.12). There was also evidence of high PEDF expression at the dermal/epidermal junction (Figure 5.11) as well as blood vessel (smooth muscle and endothelial cells) and fibroblast staining in most of the chronic wounds. There was a tendency for increased PEDF expression at the leading wound edge in 'healing' wounds when

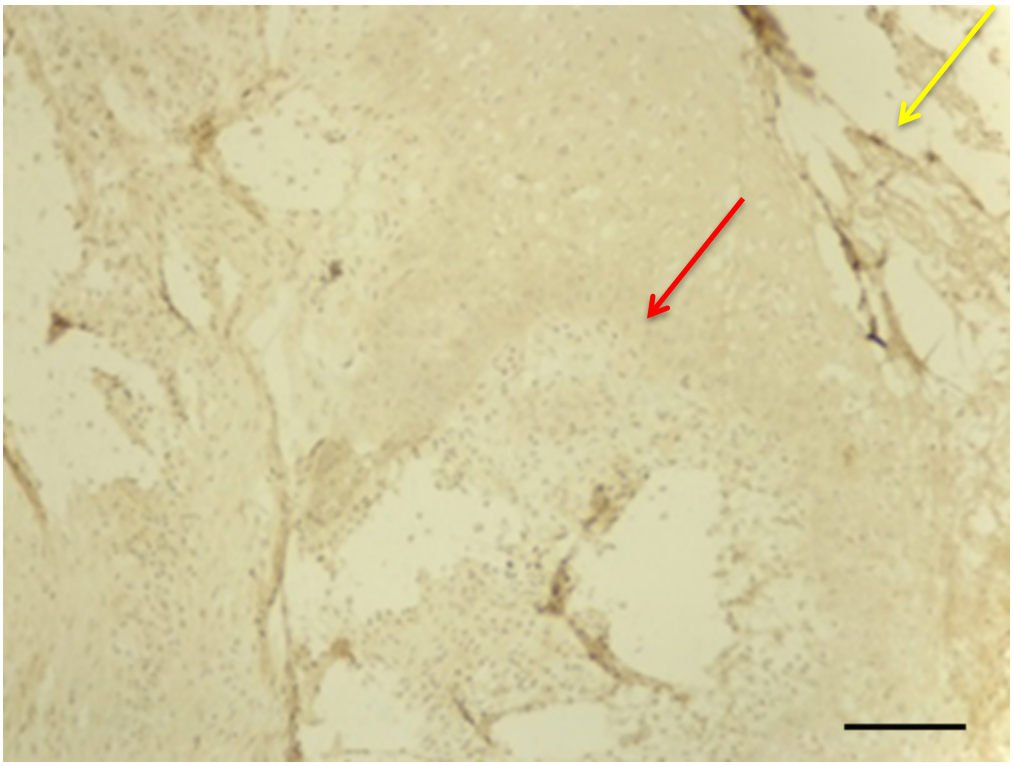

Negative control

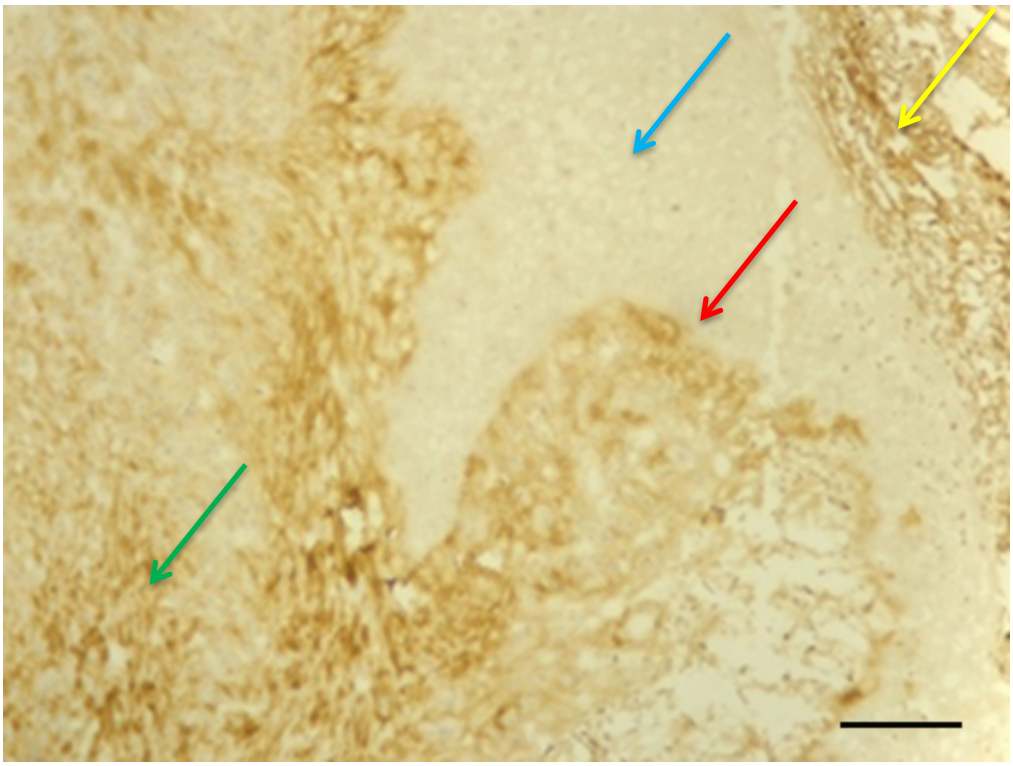

Figure 5.11. Representative immunohistochemistry images for healing chronic wound tissue samples. X100 magnification used. Scale bar represents 50µm. Red arrow shows the dermal/ epidermal junction, with evidence of positive staining compared to the negative control. Yellow arrows show the leading wound edge, with evidence of positive staining compared to the negative control. Blue arrow shows the epidermis with minimal staining. Green arrow shows the dermis with positive staining.

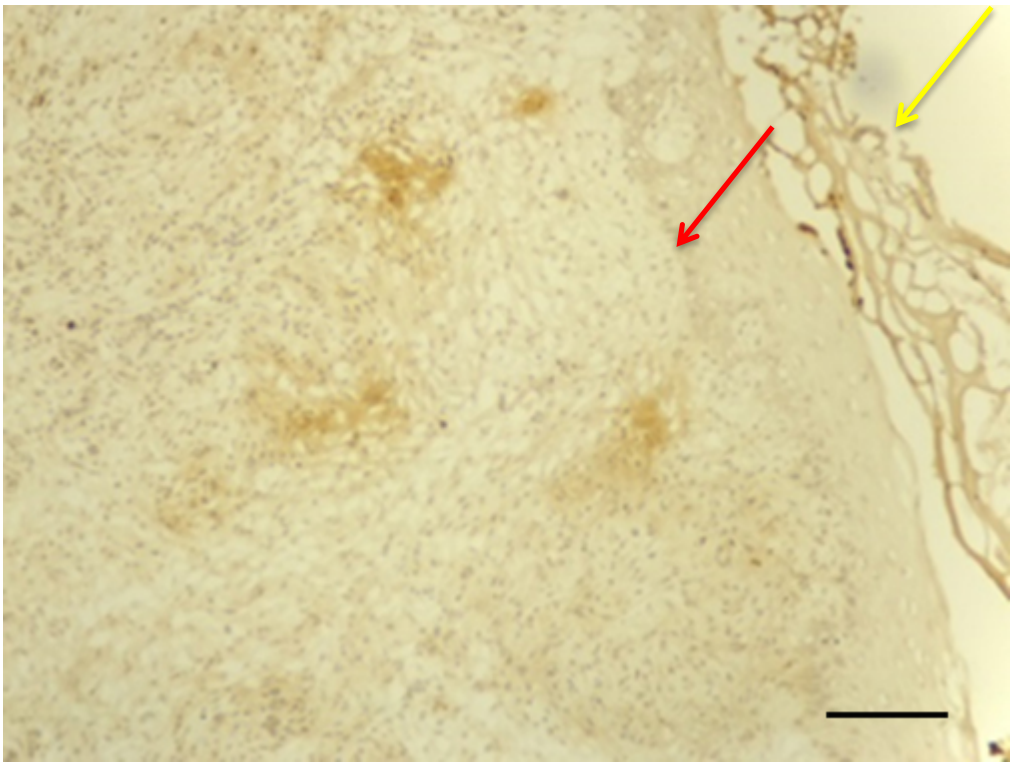

Negative Control

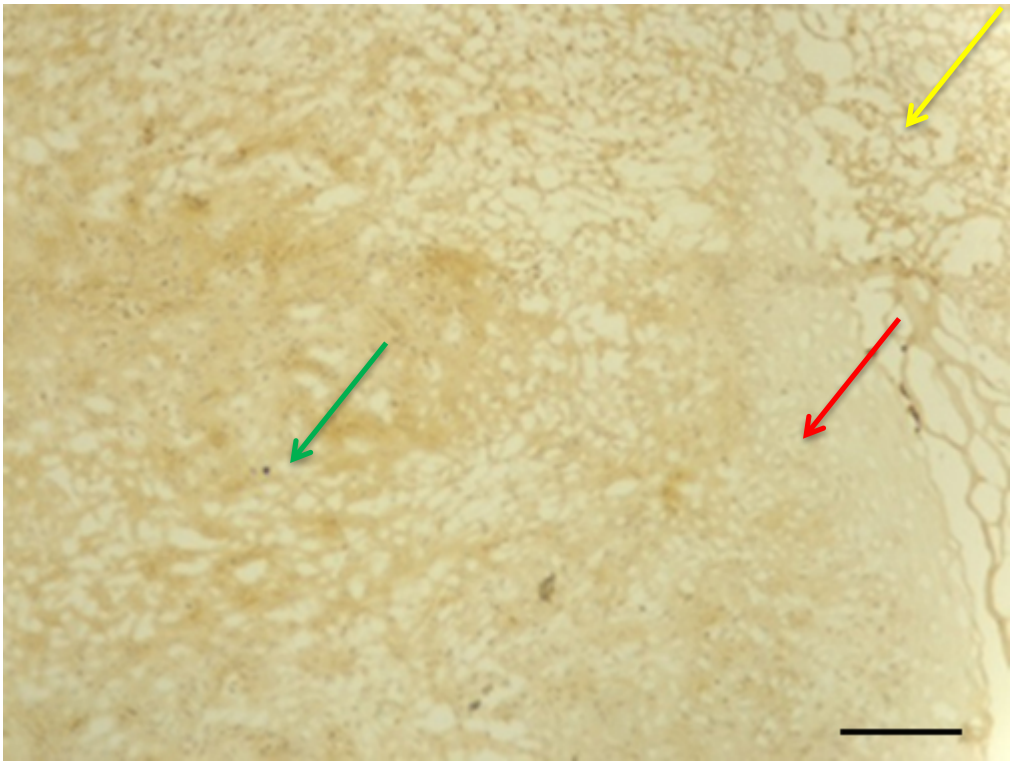

Figure 5.12. Representative immunohistochemistry images for non-healing chronic wound tissue samples. X100 magnification used. Scale bar represents 50µm. Red arrows show the dermal/epidermal junction, with no difference in staining seen. Yellow arrows show the leading wound edge, with no difference in staining seen. Green arrow shows some staining of the dermis compared to the negative control.

compared to 'non-healing' wounds (Figure 5.11 and 5.12).

5.4 Discussion

The results presented in this chapter show that PEDF mRNA expression was higher in human adipose stem cells (HASC) and primary dermal fibroblasts (DF) when compared to HaCaT keratinocyte and HECV endothelial cell line. This was also confirmed by protein expression with western blotting. These findings support those of Francis *et al* (2004) and Cai *et al* (2006b), who demonstrated high mRNA expression of PEDF in fibroblasts. It has also been shown that there was no mRNA expression in HECV cell lines in a study by Cai *et al* (2006b) and some expression detected in the HaCaT cell line in a study by Wei *et al* (2011), which again agrees with the findings presented in this chapter. However, to date, the expression profile of PEDF in stem cells has not been studied.

Immunofluorescence and immunocytochemical staining of cells found a tendency towards cytoplasmic staining in a HaCaT cell line. This correlates with previous studies that demonstrated that expression of PEDF protein was found to be localised to the cytoplasm of keratinocytes on immunocytochemistry and immunofluorescence studies (Abe et al. 2010; Li et al. 2011). As described previously in section 3.4, cytoplasmic staining supports the association between PEDF and critical cell activities such as cellular differentiation, cell growth and cell cycle control. The other cell lines used in this study (DF, HASC and HECV) showed a tendency towards nucleic staining; with evidence to support that PEDF in the nucleus may be associated with an inhibition of gene expression (Irving et al. 2002).

In chronic wound tissue samples, there was no statistical difference found between the mRNA expression in those classified as 'healing' and 'non-healing' wounds, however there was an obvious trend seen with higher expression in the 'non-healing' wounds. This may relate to the fact that 'healing' wounds require the presence of keratinocytes in order to complete the healing process and it is suggested that their lower expression of PEDF may be the reason for the witnessed trend.

On immunohistochemical staining studies, PEDF expression was observed in the dermis layer, blood vessels and fibroblasts on both 'healing' and 'non-healing' chronic wound samples. There was a tendency for higher expression at both the epidermal/dermal junction and the leading wound edge in the 'healing' wounds. The observation of higher PEDF expression in the epidermis compared to dermis was found by Abe *et al* (2010), which contrasts to the results presented here. The results somewhat conflict with the cellular findings of mRNA and protein expression in this chapter. However, in our study we have not examined the expression profile of melanocytes or taken into account the presence of epidermal skin stem cells, which may be responsible for the higher expression seen in the epidermal/dermal junction or leading wound edge. The positive staining of blood vessels and fibroblasts was previously observed in immunohistochemical staining studies of colorectal cancer tissue as described in section 3.3.2.

In conclusion, PEDF expression was highest within the stem cell and fibroblast cell lines used in this section of the study. There was no difference in the mRNA expression of PEDF between chronic wound tissue samples deemed to be 'healing' compared to 'non-healing'.

Chapter 6

Role of PEDF on cellular function in keratinocytes

6.1 Introduction

The management of chronic wounds is responsible for a significant financial drain on national healthcare systems, with a prevalence of approximately 1% of the general population (Sen et al. 2009; Drew et al. 2007). There are a number of factor leading wounds to fail to progress through the normal wound healing stages. However, the majority of chronic wounds fail to progress beyond the inflammation stage, leaving wounds in a state of chronic inflammation. Many novel therapies have attempted to target various factors responsible for progressing to the proliferation stage of wound healing, therefore resulting in re-epithelisation of the wound following keratinocyte proliferation and migration.

The results presented in Chapter 5 confirmed that PEDF expression was higher in fibroblasts compared with keratinocytes. Abe *et al* (2010) demonstrated that cultured keratinocytes stimulated with lipopolysaccharide would secrete PEDF (in response to inflammation), but the same effect was not seen in cultured fibroblasts. This highlights the interplay that exists between both fibroblasts and keratinocytes and suggesting that not only do fibroblasts upregulate keratinocytes, but that in turn keratinocytes may also upregulate fibroblasts.

Keratinocyte cellular function has previously been assessed in response to treatment with PEDF. Wei *et al* (2011) found that treatment with recombinant PEDF inhibited cellular proliferation, increased adhesion and inhibited cellular migration, findings also described by Chen & Dipietro (2014).

The aim of this section of the study was to investigate the effect of treatment with recombinant PEDF on cellular function of keratinocytes. A secondary aim was to explore the cellular signalling pathways that may be responsible for any effects witnessed with PEDF treatment.

6.2 Materials and Methods

6.2.1 Cell line

HaCaT, a human keratinocyte immortalised cell line was used for this part of the study. Cells were maintained in medium as described previously in section 2.7.1.

6.2.2 Treatment

All cellular functional assays were performed using normal medium as described in section 2.7.1 as a control. Treatment with rhPEDF (as described in section 2.6.5) was performed at doses of 10ng/ml, 50ng/ml and 100ng/ml. These varying doses were chosen based on a previous study which used 100ng/ml of rhPEDF for treatment (Cai et al. 2006a) and the manufacturers guidance.

Additional treatments with both Focal Adhesion Kinase inhibitor (FAKi) and c-Met tyrosine kinase inhibitor (c-Mi) were also used further in this chapter (as described in section 2.6.5). The doses of both FAKi and c-Mi at 10nM were chosen based on previously publications (Cai et al. 2010; Christensen et al. 2003).

6.2.3 *In vitro* cellular growth assay

HaCaT cells were seeded into three 96 well plates at a seeding density of $3x10^3$ cells/100µl, supplemented with 150µl of either treatment or control. The plates were then incubated for 1,3 and 5 days, respectively as described in full detail in section 2.12.1. After incubation, cells were fixed using 4% formaldehyde (v/v) then stained with 0.5% crystal violet (v/v). Analysis was performed at 540nm using a spectrophotometer. Prior to reading the dye was extracted using 10% acetic acid. Data from at least 3 repeated experimental procedures were combined and are presented in this chapter.

6.2.4 Electric Cell-Substrate Impedance Sensing (ECIS) assay

ECIS measures the rate of cells initial attachment and then repopulating an area following electrical wounding, by using gold electrodes within a well plate to measure changes in resistance and impedance over time and is described in full detail on section 2.12.2.1. HaCaT cells were seeded at a seeding density of $10x10^4$/150µl with an additional 150µl of either treatment with varying concentrations of rhPEDF or normal medium added. Electrical wounding was performed in triplicate. Data from at least 3 repeated experimental procedures were combined and presented as the change in resistance over a 3 and 6-hour period, for attachment and migration data respectively.

6.2.5 Antibody Array

Overnight, serum-starved HaCaT cells were treated either with or without 50ng/ml rhPEDF for 2 hours prior to the preparation of cell lysates (as described in section

2.13). Samples were shipped to Kinex™ Screening Services (Kinexus Bioinformatics Corporation, Vancouver, Canada). Testing was performed for detection of protein changes on the KAM-880 antibody microarray. Results are presented as percentage change from control to treatment with rhPEDF in HaCaT cells. Top 20 down-regulating and up-regulating phospho-specific antibodies are shown in this study.

6.3 Role of PEDF in keratinocyte cellular function

6.3.1 Effect of PEDF on keratinocyte cell growth

After 3 days of incubation with rhPEDF, the dose at 10ng/ml resulted in an initial statistically significant increase in HaCaT cell proliferation compared to all other tested concentrations of rhPEDF and the untreated HaCaT cells (control group) ($p=0.002$). However, after 5 days of incubation, there were no significant effects evident on HaCaT cells following treatment with all concentrations of rhPEDF($p=0.249$) (Figure 6.1). The initial significant increase in HaCaT cells demonstrated with 10ng/ml after day 3 of incubation was no longer apparent after 5 days incubation.

6.3.2 Effect of PEDF on keratinocyte cell adhesion

There was no difference demonstrated in the rate of attachment of HaCaT cells with all tested concentrations of treatments with rhPEDF and the untreated HaCaT cells over a 3-hour period ($p=0.193$) (Figure 6.2).

6.3.3 Effect of PEDF on keratinocyte cell migration

Under the influence of rhPEDF treatment, there was a statistically significant increase in HaCaT migration rate over a 6-hour period. This significant increase in migration rate was evident for both 10ng/ml, 50ng/ml and 100ng/ml rhPEDF treatment doses ($p<0.001$), when compared to untreated HaCaT cells. However, this significant increase in HaCaT cell migration with treatment of rhPEDF was not dose dependent (Figure 6.3).

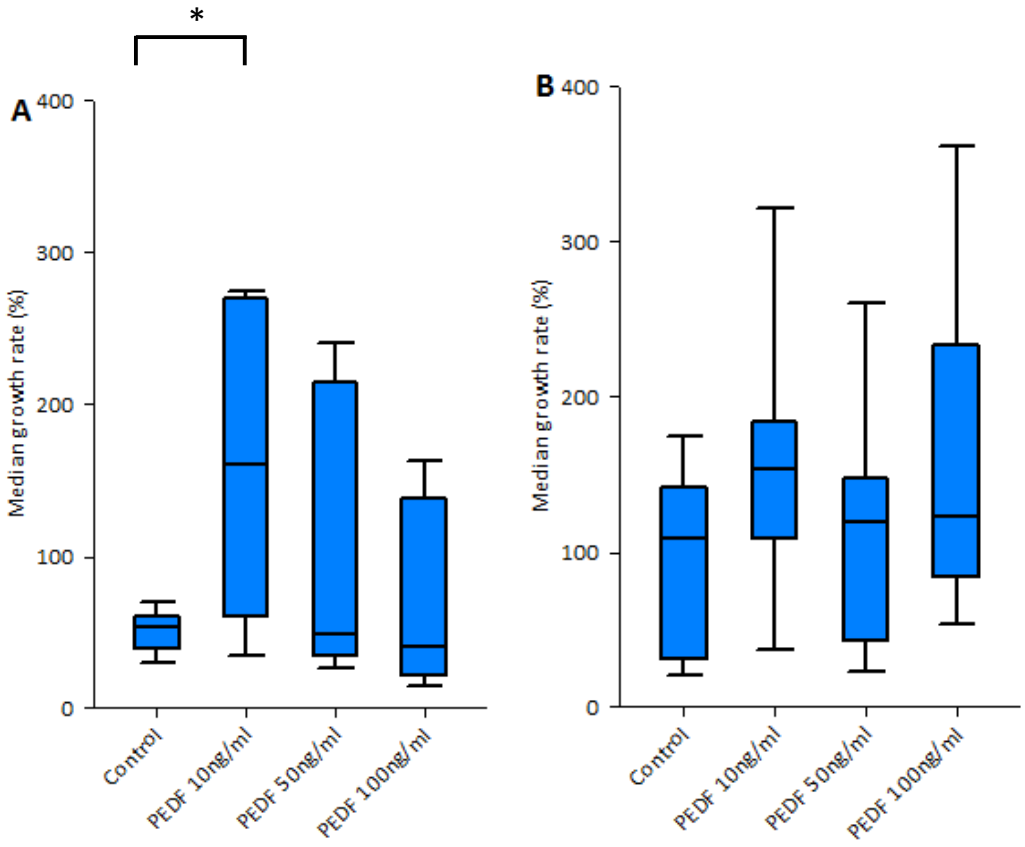

Figure 6.1. Impact of rhPEDF on cellular growth after 3 days (A) and 5 days (B) of incubation, in response to varying concentrations of rhPEDF in HaCaT cells. Median values of 3 independent repeats are shown. The absorbance of Day 1 was used as a baseline to normalise data. * $p<0.05$

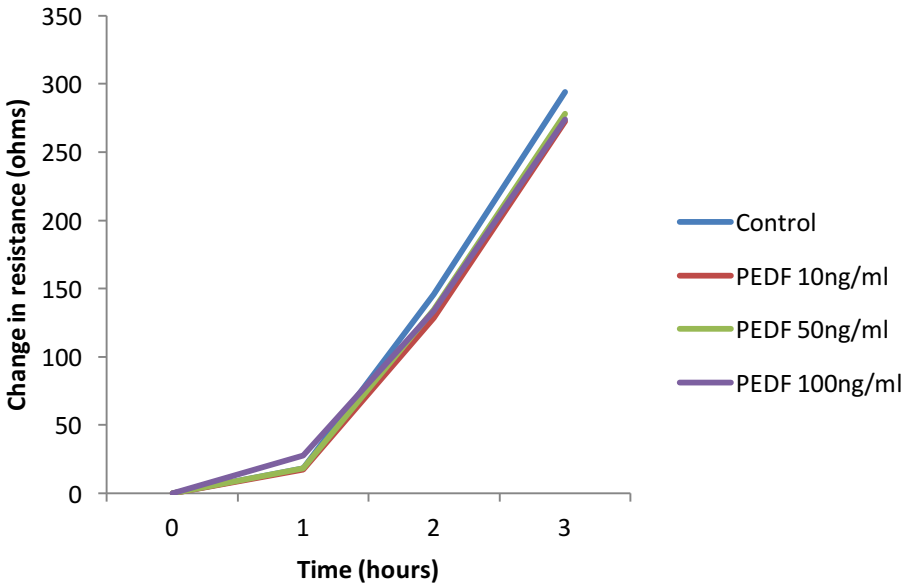

Figure 6.2. Impact of rhPEDF on cellular attachment assessed through ECIS assay. Change in electrode resistance from baseline is shown and taken as representative of attachment, in response to varying concentrations of rhPEDF in HaCaT cells. Mean values of 3 independent repeats are shown.

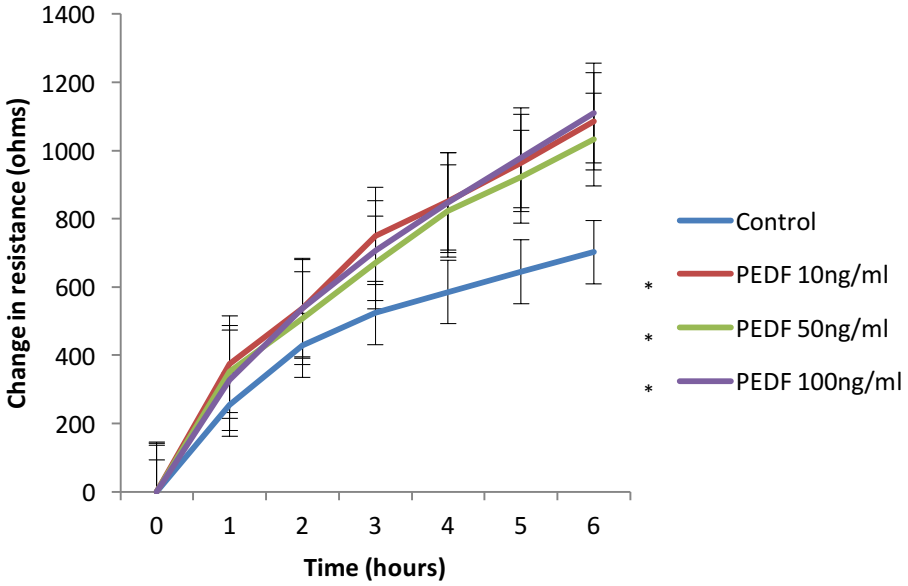

Figure 6.3. Impact of rhPEDF on cellular migration assessed through ECIS assay. Change in electrode resistance from post-wounding baseline is shown and taken as representative of migration, in response to varying concentrations of rhPEDF in HaCaT cells. Mean values of 3 independent repeats are shown. Error bars represent standard error of the mean. *p <0.001

6.4 Antibody array results

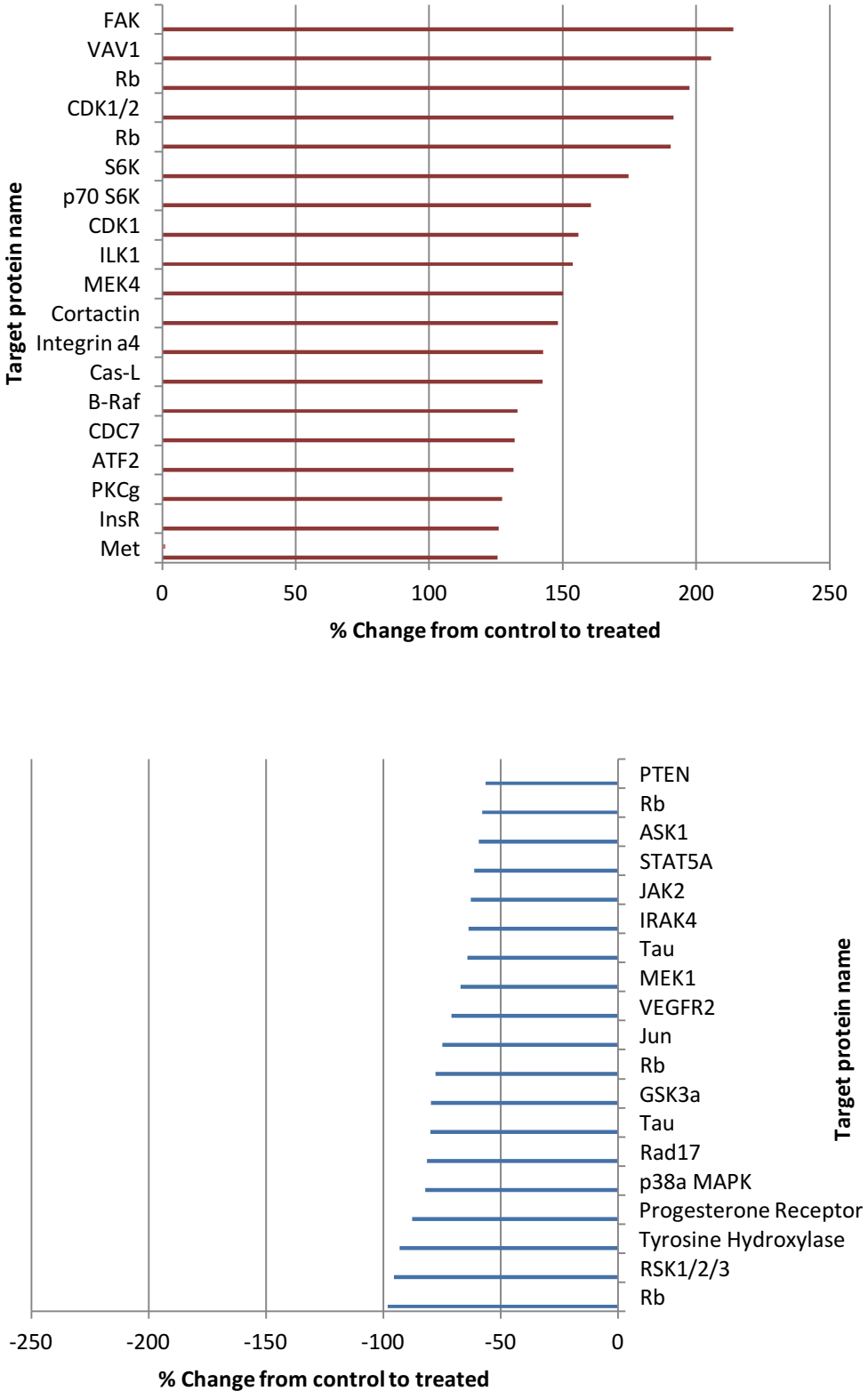

Figure 6.4. Antibody micro array results. Percentage change from control to treatment with rhPEDF in HaCaT cells. Top 20 down-regulating and up-regulating phospho-specific antibodies shown.

Two of the phospho-specific antibodies shown in Figure 6.4 were chosen for further investigation; Both Focal adhesion kinase (FAK) and hepatocyte growth factor receptor (Met) were found to be significant up-regulators and have been extensively studied in our unit previously (Cai et al. 2010; Christensen et al. 2003).

6.5 Role of Focal Adhesion Kinase in keratinocyte cellular function

For this part of the study, 50ng/ml rhPEDF was chosen as a further comparison based on the results of the earlier functional cellular assays performed on HaCaT cells with treatment of varying concentrations of rhPEDF (described in sections 6.3.1, 6.3.2 and 6.3.3). These results did not demonstrate a dose-dependent relationship.

Focal adhesion kinase inhibitor (FAKi) dose of 10nM was chosen following previous work published from our unit (Cai et al. 2010). Two treatments of FAKi were used in this part of the study, 10nM alone and 10nM used in combination with rhPEDF 50ng/ml. These three treatments (rhPEDF 50ng/ml; FAKi 10nM; FAKi 10nM plus rhPEDF 50ng/ml) were run alongside a control of normal growth medium.

6.5.1 Effect of Focal Adhesion Kinase inhibitor on growth in keratinocytes

There was no significant increase seen in HaCaT cell growth after both 3 and 5 days of incubation with all treatments compared to untreated HaCaT cells; p= 0.205 and 0.260 respectively (Figure 6.5).

6.5.2 Effect of Focal Adhesion Kinase Inhibitor on adhesion in keratinocytes

There was no difference exhibited in the rate of attachment of HaCaT cells with all tested treatments with FAKi in comparison to the untreated HaCaT cells over a 3-hour period (Figure 6.6).

6.5.3 Effect of Focal Adhesion Kinase Inhibitor on migration in keratinocytes

There was a significantly significant increase in the cellular migration of HaCaT cells with all treatments compared to control over a 6-hour time period (Figure 6.7). This increase was most notable for rhPEDF 50ng/ml combined with FAKi 10nM ($P<0.001$), but was also evident for both rhPEDF 50ng/ml and FAKi 10nM alone ($p<0.005$).

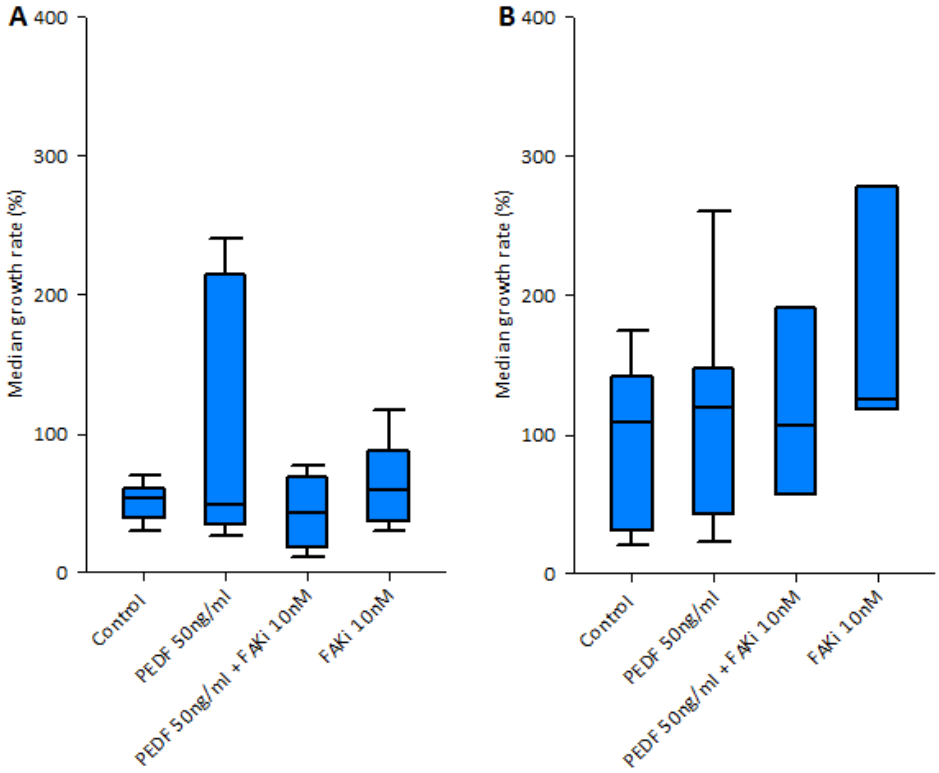

Figure 6.5. Impact of FAKi and FAKi/rhPEDF on cellular growth after 3 days (A) and 5 days (B) of incubation, in HaCaT cells compared to control and rhPEDF 50ng/ml. Median values of 3 independent repeats are shown. The absorbance of Day 1 was used as a baseline to normalise data.

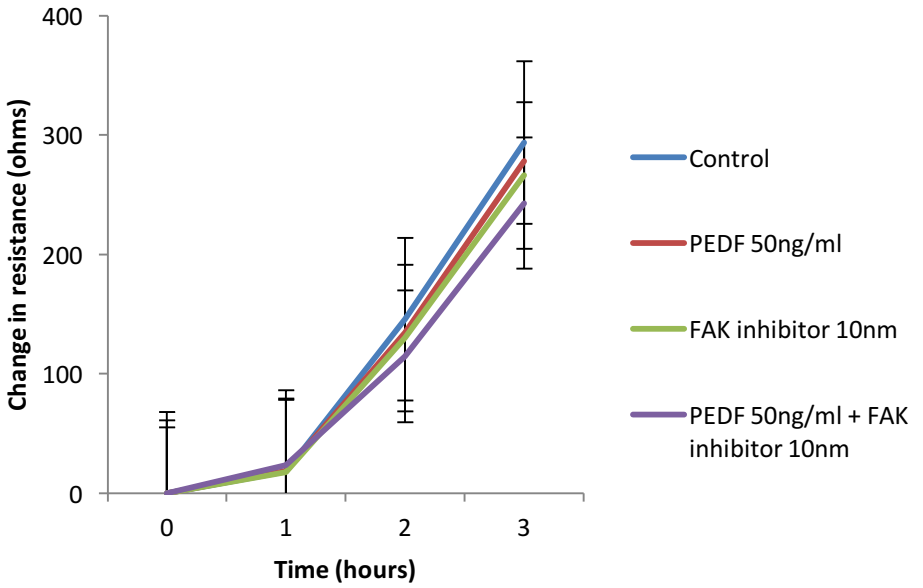

Figure 6.6 Impact of FAKi and FAKi/rhPEDF on cellular attachment assessed through ECIS assay. Change in electrode resistance from baseline is shown and taken as representative of attachment in HaCaT cells compared to control and PEDF 50ng/ml. Mean values of 3 independent repeats are shown.

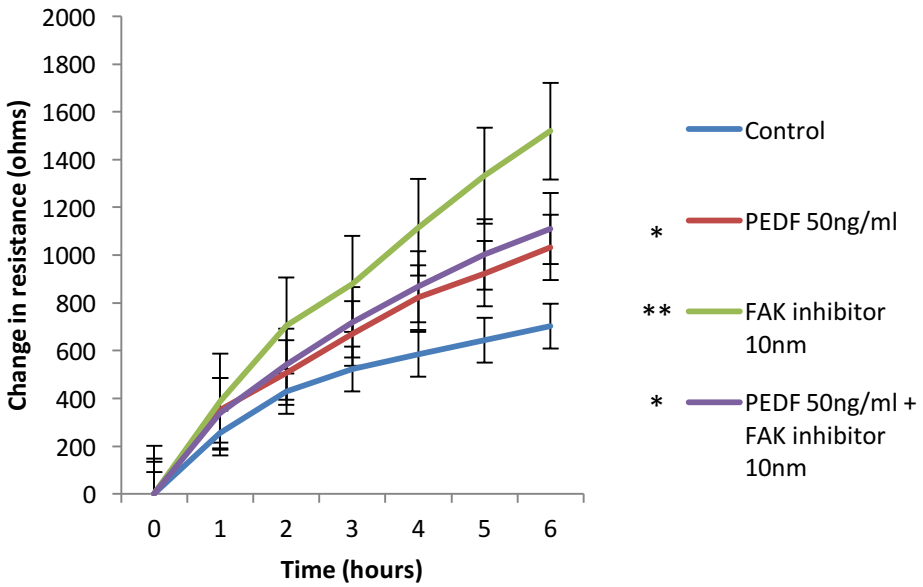

Figure 6.7 Impact of FAKi and FAKi/rhPEDF on cellular migration assessed through ECIS assay. Change in electrode resistance from post-wounding baseline is shown and taken as representative of migration, in HaCaT cells compared to control and PEDF 50ng/ml. Mean values of 3 independent repeats are shown. Error bars represent standard error of the mean. *p <0.005 ** p<0.001

6.6 Role of c-Met in keratinocyte cellular function

For this part of the study, 50ng/ml rhPEDF was chosen as a further comparison based on the results of the earlier functional cellular assays performed on HaCaT cells with treatment of varying concentrations of rhPEDF (described in sections 6.3.1, 6.3.2 and 6.3.3). These results did not demonstrate a dose dependent relationship.

c-Mi dose of 10nM was chosen based on previously published work (Christensen et al. 2003). Two treatments of c-Mi were used in this part of the study, 10nM alone and 10nM used in combination with rhPEDF 50ng/ml. These three treatments (rhPEDF 50ng/ml, c-Mi 10nM, C-mi 10nM plus rhPEDF 50ng/ml) were run alongside a control of normal growth medium.

6.6.1 Effect of c-Met inhibitor on growth in keratinocytes

There was no significant difference in HaCaT cell growth after 3 and 5 days of incubation with c-Mi 10nm or PEDF50ng/ml with c-Mi 10nm; p= 0.387 and 0.218 respectively (Figure 6.8).

6.6.2 Effect of c-Met Inhibitor on adhesion in keratinocytes

There was no difference exhibited in the rate of attachment of HaCaT cells with all tested treatments with c-Mi in comparison to the untreated HaCaT cells over a 3-hour period (Figure 6.9).

6.6.3 Effect of c-Met Inhibitor on migration in keratinocytes

There was a significant increase in cellular migration of HaCaT cells with treatment of both rhPEDF 50ng/ml and rhPEDF 50ng/ml in combination with cMi 10nM

compared to the control over a 6-hour time period ($p<0.005$) (Figure 6.10). There was no increase in cellular migration witnessed with the use of cMi 10nM alone.

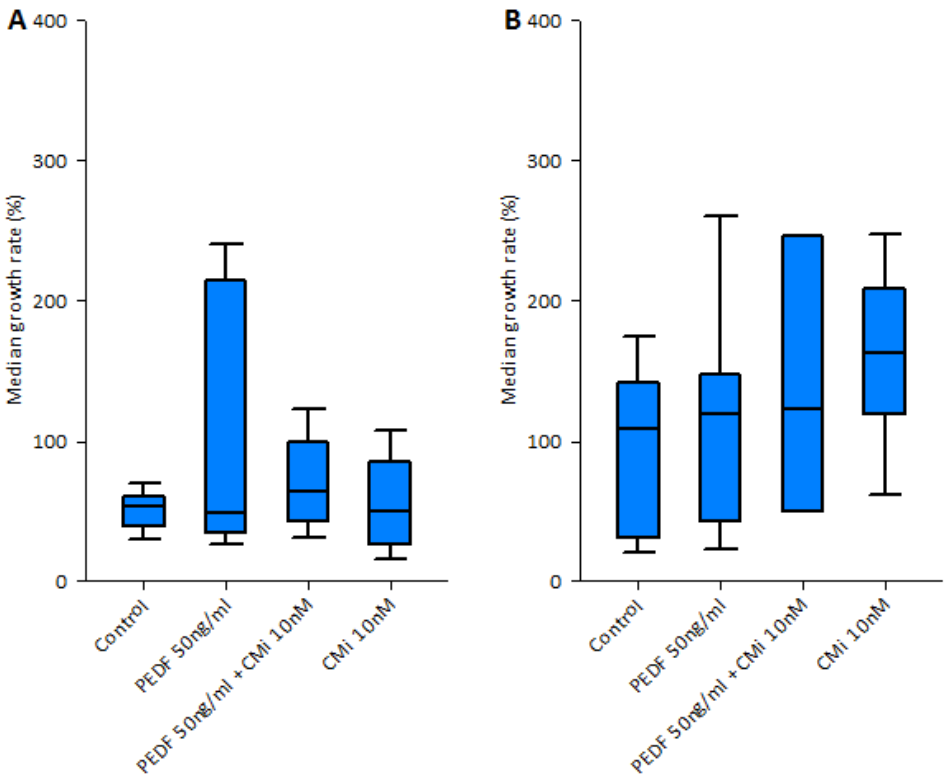

Figure 6.8. Impact of c-Mi and c-Mi/rhPEDF on cellular growth after 3 days (A) and 5 days (B) of incubation in HaCaT cells compared to control and rhPEDF 50ng/ml. Median values of 3 independent repeats are shown. The absorbance of Day 1 was used as a baseline to normalise data.

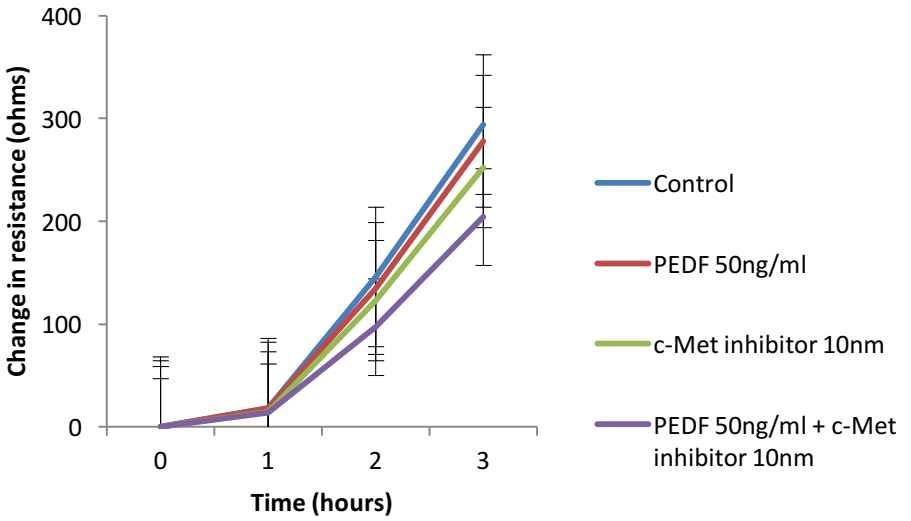

Figure 6.9. Impact of c-Mi and c-Mi/rhPEDF on cellular attachment assessed through ECIS assay. Change in electrode resistance from baseline is shown and taken as representative of attachment in HaCaT cells compared to control and PEDF 50ng/ml. Mean values of 3 independent repeats are shown.

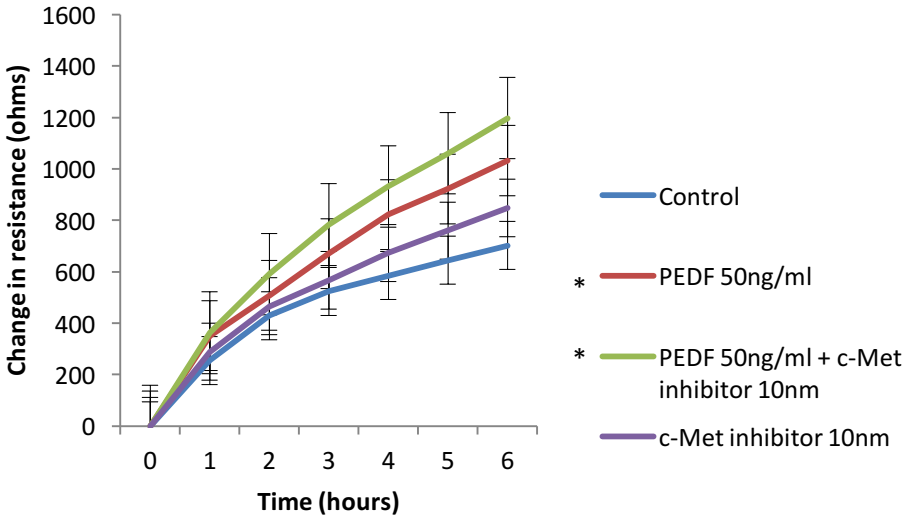

Figure 6.10. Impact of c-Mi and c-Mi/rhPEDF on cellular migration assessed through ECIS assay. Change in electrode resistance from post-wounding baseline is shown and taken as representative of migration, in HaCaT cells compared to control and PEDF 50ng/ml. Mean values of 3 independent repeats are shown. Error bars represent standard error of the mean. *p <0.005

6.7 Discussion

The results presented in this chapter showed that the treatment of recombinant PEDF significantly increased the migration of the HaCaT (immortalised human keratinocyte) cell line as assessed by ECIS assay. Whilst there was an initial significant increase in cellular growth comparing the lower treatment dose of rhPEDF (10ng/ml) with control medium at 3 days incubation, this effect was not seen at 5 days incubation or in any of the higher treatment doses of rhPEDF (50ng/ml or 100ng/ml). There was no difference demonstrated in cellular adhesion with any treatment dose of rhPEDF compared to the control. These results are conflicting with previous similar studies. Wei *et al* (2011) reported an inhibitory effect of rhPEDF treatment on HaCaT cellular growth using both 5ng/ml and 50ng/ml doses of rhPEDF; on HaCaT cellular migration (using scratch migration assay) using a 50ng/ml dose of rhPEDF, and an increased cellular adhesion effect was observed. The methods differ slightly when comparing those presented in this chapter, scratch migration assay compared to ECIS assay, however we would not expect these two methods to produce differing results and ECIS has previously been validated against scratch migration assay (Jiang. 2012). However it is unsurprising that in the Wei *et al* (2011) study, if cellular adhesion was increased that it would result in decreased migration due to the 'sticky' cells becoming less mobile.

There is certainly evidence to suggest that different fragments of PEDF are responsible for different mechanisms of action such as 34-mer fragment of PEDF exhibiting anti-angiogenic effects and 44-mer fragment exhibiting neurotrophic

effects (Filleur et al. 2005). Whilst human recombinant PEDF is full length, folding may play a role in the proper function.

Antibody micro array showed multiple up-regulating and down-regulating phosphor-specific antibodies. Two of the up-regulating antibodies (Met and FAK) showing >100% increase from control to treated were chosen for further investigation based on the unit's previous experience.

c-Met tyrosine kinase is the receptor for HGF. HGF is known to increase migration of keratinocytes (Bevan et al. 2004). HGF has a higher concentration in chronic wounds compared to acute wounds, whereas c-Met is virtually undetectable in keratinocytes in chronic wound edges, in contrast to acute wounds (Conway et al. 2007). PHA-66572 is a second-generation C-met inhibitor that inhibits enzymatic activity of c-Met tyrosine kinase. Our results demonstrated that HaCaT migration was significantly increased when recombinant PEDF (50ng/ml) was combined with c-Met inhibitor (10nM). This effect can be somewhat explained by the fact that inhibiting c-Met may result in a higher concentration of HGF which is known to increase the migration of keratinocytes, however this effect was only visible when cMi was combined with rhPEDF and not when used alone. It is likely that PEDF treatment results in c-Met expression, with cMi blocking c-Met, therefore these two opposite actions in the system results in the net outcome described above. It also highlights that PEDF may have a stronger direct action on keratinocyte migration by some other means.

FAK protein is encoded by PTK2 gene with evidence that it is required for keratinocyte migration (Gates et al. 1994). PF573228 is a potent and selective inhibitor of FAK and blocks fibronectin-directed migration and decreases focal

adhesion turnover *in vitro.* Our results showed that surprisingly, HaCaT migration was significantly increased when recombinant PEDF (50ng/ml) was combined with FAK inhibitor (10nM). This again suggests that there is likely to be another downstream cellular signalling pathway(s) involved, responsible, for this effect or a direct action of PEDF in keratinocyte migration, which requires further investigation.

In summary, treatment with recombinant PEDF increases the migration of keratinocytes in this study, in contrary to earlier published work. This may be explained by the potential for different PEDF fragments to have different mechanisms of action. Inhibiting c-Met and FAK in combination with recombinant PEDF increased migration further, and the exact mechanisms for this effect are, to date, unknown. Further work is proposed to investigate the other cellular signalling pathways involved and to assess the cellular functional effects on fibroblasts, endothelial cells and stem cells.

Chapter 7

General Discussion

7.1 Thesis aims

The main aims of this thesis were to elucidate, in more detail the regulatory mechanisms of PEDF in wound healing, and in tumour angiogenesis related to different subtypes of colorectal cancer, by examining the expression profiles of PEDF in colorectal cancer and wounds and investigating its role of cellular function in colorectal cancer and wounds with the treatment of recombinant PEDF. This was in order to provide evidence to potentially develop PEDF or its fragments as a therapeutic agent for colorectal cancer and/or wound healing treatments.

7.2 The role of PEDF in angiogenesis

There are many similarities between wound repair and cancer development, and it is well recognised that the stroma of an epithelial tumour has a similar composition to the granulation tissue of healing skin wounds (Dvorak. 1986). Epithelial tumours stimulate the formation of the stroma by activation of the wound healing process, but in contrast to the acute healing of wounds the process is not self-limiting and results in uncontrolled cell proliferation, invasion and metastasis. Angiogenesis is the process of the formation of new blood vessels and controlled by a complex delicate balance between pro-angiogenic and anti-angiogenic mediators. Physiological angiogenesis occurs when this balance is tightly controlled, such as during normal wound healing processes, however pathological angiogenesis occurs when this complex balance goes awry, such as in colorectal cancer or chronic wounds. PEDF is known to be one of the most potent natural inhibitors of angiogenesis (Dawson et al. 1999) and its mechanism of action is to arrest endothelial cell proliferation and

migration. However, PEDF is selective in its action, discriminating between endothelial cells forming new vessels and those from pre-existing vessels and therefore targeting mainly abnormal angiogenesis with newly forming vessels only (Bouck 2002). It is therefore logical that administration of endogenous PEDF can inhibit aberrant angiogenesis leading to restoration of healthy vasculature. PEDF is known to also exhibit neurotrophic, neuroprotective, anti-tumorigenic and anti-inflammatory effects, demonstrating the complex range of interactions and mechanisms of action PEDF appears to possess.

7.3 Main conclusions from this study

7.3.1 The role of PEDF in colorectal cancer

In this study, PEDF expression was found to be downregulated in colorectal cancer cell lines compared to normal colorectal fibroblast cell lines and mRNA expression of PEDF found to be lower in colorectal tumour tissue when compared to matched normal colorectal tissue from colorectal cancer patients. These findings are similar to those of Wågsäter *et al* (2010) and Ji *et al* (2013) confirm the inverse correlation between PEDF levels and pathological angiogenesis. There was also a significant decrease in the expression of PEDF with worsening tumour grade, suggesting a possible tumour suppressor role and may indicate a potential inhibitory role in primary tumour growth. It is therefore logical to suggest that elevation of PEDF levels to their baseline may be responsible for halting such processes. Though PEDF expression was not associated with worsening Duke's Stage, or the presence of nodal involvement or metastasis.

Interestingly, our study found higher PEDF expression in mucinous adenocarcinoma when compared to adenocarcinoma, higher PEDF expression in rectal tumours when compared to colonic tumours and higher PEDF expression in tumour tissue from female colorectal cancer patients when compared to male colorectal cancer patients. Ji *et al* (2013) results are in agreement with those presented in this study, with patients with mucinous adenocarcinoma displayed higher PEDF plasma levels than those patients with adenocarcinoma; it would be interesting to know whether mucin production is in some manner related to PEDF expression, particularly as mucinous adenocarcinoma tend to have a poorer prognosis and therefore it would seem more likely that PEDF expression should be less. Díaz *et al* (2008) also detected higher mRNA expression of PEDF in tissue from rectal tumours when compared to colonic tumours, however aside from an anatomical difference it is unclear whether the cellular differences are responsible for the difference of PEDF expression between cells from rectum and colon. There are previous studies that have demonstrated the opposite gender difference in expression to our study in normal subjects; with healthy males having higher levels of PEDF in plasma compared to healthy females (Yamagishi et al. 2006; Wågsäter et al. 2010); however, the effect in colorectal cancer patients was either not assessed or observed, respectively. Studies in other solid tumours did not result in any gender difference for expression levels of PEDF (Uehara et al. 2004; Jiang et al. 2010). These outcomes certainly warrant further evaluation in future studies into the possible reasons behind the difference in PEDF expression patterns seen in tumour type (mucin producing vs. non-mucin producing), tumour location and patient gender in colorectal cancer.

Our study established that treatment with recombinant PEDF resulted in a significant decrease in the rate of colorectal cancer cellular migration in both HT115 and HRT-18 cell lines. Similarly, invasion studies showed a decrease in the rate of RKO colorectal cancer cellular invasion with the treatment of recombinant PEDF, and whilst not significant there was a similar trend observed in the HRT-18 colorectal cancer cell line. We also observed an increase in cellular adhesion with treatment of recombinant PEDF in the HT115 colorectal cancer cell line. To date the role of PEDF treatment on colorectal cancer cellular function has not been studied, however published studies relating to breast cancer and chondrosarcoma confirmed decreases in both tumour cell invasion and migration, and increase in cellular attachment with the treatment of recombinant PEDF (Hong et al. 2014; Tan et al. 2010), thus supporting the results of this study. Multiple other studies have found decreased cellular proliferation with the treatment of PEDF in other solid tumour cell lines (Abe et al. 2004; Matsumoto et al. 2004; Cheung et al. 2006; Guan et al. 2007; Dass et al. 2008; Chen et al. 2009; Hong et al. 2014), however this study did not demonstrate any difference in cellular growth for any of the three colorectal cancer cell lines examined perhaps due to the limitation of sensitivity of the assays we chose.

The most frequent cause of mortality from colorectal cancer is related to the effects of metastatic spread, and therefore treatments aimed at its prevention may prove highly beneficial for the long-term survival of colorectal cancer patients. The results from our study show that PEDF administration confers an inhibitory effect on the migration and invasion of colorectal cancer cells and offers a potentially promising novel area of interest in the quest for colorectal cancer treatments. Two approaches

have been suggested as a method of testing PEDF as a therapeutic cancer agent; either as a viral vector (Wu et al. 2012) or direct administration of unmodified PEDF into tumours (Abramson et al. 2003). However, to date there has been limited success due to the need for the continuous delivery of the gene to maintain its expression and the unknown effects of exposure of PEDF to adjacent normal tissues, and hence merits further research.

7.3.2 The role of PEDF in wound healing

This study revealed that PEDF expression was high in cell lines important for wound healing; primary dermal fibroblasts (DF) and human adipose stem cells (HASC), but not in endothelial cells (HECV) and keratinocytes (HaCaT) suggesting that fibroblasts but not keratinocytes secrete PEDF in a regulated manner in response to inflammation. These findings are in agreement with other studies (Pignolo et al. 1995; Francis et al. 2004; Cai et al. 2006b).

The immunohistochemistry findings support this theory, with evidence of staining of fibroblasts and positive staining of dermis and dermal-epidermal junction, which might correlate with fibroblast migration. However, the difference for PEDF expression when comparing healing and non-healing chronic wound tissue samples did not reach statistical significance.

When assessing the role of PEDF in keratinocyte cellular function, it was found that the treatment of recombinant PEDF significantly increased the migration of keratinocytes. This was in contrast to the previously published findings of similar experiments (Wei et al. 2011; Chen & Dipietro. 2014). One plausible explanation is

perhaps due to folding of the human recombinant PEDF that various fragments available were responsible for the differing results.

The addition of either focal adhesion kinase inhibitor or c-Met tyrosine kinase inhibitor in combination with recombinant PEDF increased keratinocyte migration further. The exact mechanisms to explain these results are unclear; PEDF treatment is likely to result in both c-Met and FAK expression (as demonstrated by the antibody micro result results described in section 6.4), but with the blockage of both c-Met and FAK using the respective inhibitors, the net outcome are the results presented. However, they may also be a stronger direct chemoattractant action from PEDF on keratinocyte migration via some other mechanism yet to be identified. The possible cellular signalling pathways involved warrants more investigation as does the effect of recombinant PEDF treatment on other cells important for wound healing, such as fibroblasts and endothelial cell lines.

Human adipose stem cells are a population of pluripotent mesenchymal cells, which can differentiate into various lineages, which have previously been shown to be superior to dermal fibroblast in promoting dermal fibroblasts proliferation (Kim et al. 2007). There has been concerns raised previously regarding the stability and delivery of PEDF treatment, and therefore others have trialled the use of vectors in order to deliver PEDF in a stable manner (Wu et al. 2012). Stem cells may be an effective delivery vector and certainly its role as a delivery method should be investigated in more detail in future studies.

7.4 Future work

The results presented in this thesis have demonstrated the critical role of PEDF in both colorectal cancer and wound healing. Whilst a number of important observations have been identified, an additional number of questions requiring further assessment have been highlighted. These are summarised below:

1. The expression profile of PEDF should be performed comparing normal subjects and those patients with colorectal cancer (with a range of clinicopathological variables including age) to assess for gender differences. This should include assessment of serum levels and mRNA expression from tissue samples in large clinical cohort. If there is a gender difference witnessed in the PEDF expression it may affect potential treatment options available to either gender of patients, or may influence survival differences seen between the genders. It is also worth exploring why the gender differences may exist- are there other factors influencing PEDF expression perhaps related to hormonal differences between genders?

2. The further assessment into the differing expression levels of PEDF comparing mucinous adenocarcinoma in comparison to adenocarcinoma. Is there a factor related to the mucin production that can explain the differing expression levels? And if so what is the clinical relevance?

3. The role of treatment of PEDF on cellular function in mucinous adenocarcinoma and metastatic colorectal cancer cell lines should be investigated. Any potential effect of PEDF treatment may only be applicable to a set subtype of colorectal cancer or early in the cancer stage, prior to metastatic spread.

4. It would be beneficial to investigate the role of PEDF on cellular function in *in vivo* models, using colorectal tumour xenografts in animal models. The next stage of any human treatment development would depend on the successful results beyond cellular models.

5. In order to assess the cellular signalling pathways involved with the mechanism of actions of PEDF on cellular function, it would be appropriate to further assess the other phosphor-specific antibodies identified on antibody micro-array as being either upregulated or downregulated by PEDF administration.

6. To examine how the other wound healing cells fit with regards to cellular function in response to PEDF treatment, it would be sensible to repeat the cellular function experiments described in this study using dermal fibroblasts and endothelial cell lines. There may be other effects of PEDF treatment on these cells that may either enhance or prohibit wound healing processes which need to be explored.

7. A longer-term strategy would be to determine an effective delivery method for treatment of PEDF. It would be prudent to investigate whether human adipose stem cells might be a suitable delivery vector via co-culture method. Human adipose stem cells are relatively easy to extract when compared to stem cells from bone marrow and would be more acceptable to patients.

Despite the questions poised here that are yet to be answered, it is hoped that with the improved knowledge of the interactions between PEDF and pathological processes seen in colorectal cancer and chronic wound healing, it may result in the improvement of outcomes for patient who suffer with these diseases.

Chapter 8

References

Abe R, Shimizu T, Yamagishi S, Shibaki A, Amano S, Inagaki Y, Watanabe H, Sugawara H, Nakamura H, Takeuchi M, Imaizumi T, Shimizu H. 2004. Overexpression of pigment epithelium-derived factor decreases angiogenesis and inhibits the growth of human malignant melanoma. Am J Pathol, 164(4):1225–32.

Abe R, Yamagishi S, Fujita Y, Hoshina D, Sasaki M, Nakamura K, Matsui T, Shimizu T, Bucala R, Shimizu H. 2010. Topical application of anti-angiogenic peptides based on pigment epithelium-derived factor can improve psoriasis. Journal of Dermatological Science, 57(3):183–91.

Abramson L, Stellmach V, Doll J, Cornwell M, Arensman R, Crawford S. 2003. Wilms' tumor growth is suppressed by antiangiogenic pigment epithelium- derived factor in a xenograft model. J Pediatr Surg, 38(3):336–42.

Alberts SR, Sargent DJ, Nair S, Mahoney MR, Mooney M, Thibodeau SN, Smyrk TC, Sinicrope FA, Chan E, Gill S, Kahlenberg MS, Shields AF, Quesenberry JT, Webb TA, Farr GH Jr, Pockaj BA, Grothey A, Goldberg RM. 2012. Effect of oxaliplatin, fluorouracil, and leucovorin with or without cetuximab on survival among patients with resected stage III colon cancer: a randomized trial. JAMA, 307(13):1383-93.

Albini A, Iwamoto Y, Kleinman H, Martin G, Aaronson S, Kozlowski J, McEwan R. 1987. A rapid in vitro assay for quantitating the invasive potential of tumour cells. Cancer Research, 47:3239–45.

Albini A, Sporn MB. 2007. The tumour microenvironment as a target for chemoprevention. Nature Rev Cancer, 7:139-47.

Allavena P, Sica A, Garlanda C, Mantovani A. 2008. The yin-yang of tumor-associated macrophages in neoplastic progression and immune surveillance. Immunol Rev, 222:155-61.

Allegra C, Yothers G, O'Connell M, Sharif S, Petrelli N, Lopa S, Wolmark N. 2013. Bevacizumab in stage II-III colon cancer: 5-year update of the National Surgical Adjuvant Breast and Bowel Project C-08 trial. J Clin Oncol, 31(3):359–64.

Amado R, Wolf M, Peeters M, Van Cutsem E, Siena S, Freeman D, Juan T, Sikorski R, Suggs S, Radinsky R, Patterson S, Chang D. 2008. Wild-type KRAS is required for panitumumab efficacy in patients with metastatic colorectal cancer. Journal of Clinical Oncology, 26(10):1626–34.

Barrientos, S, Stojadinovic O, Golinko M, Brem H, Tomic-Canic M. 2008. Growth factors and cytokines in wound healing. Wound Repair Regen Reg, 16(5):585–601.

Becerra S, Notario V. 2013. The effects of PEDF on cancer biology: mechanisms of action and therapeutic potential. Nat Rev Cancer, 13:258–71.

Bennouna, J, Sastre J, Arnold D, Österlund P, Greil R, Van Cutsem E, von Moos R, Viéitez J, Bouché O, Borg C, Steffens C, Alonso-Orduña V, Schlichting C, Reyes-Rivera I, Bendahmane B, André T, Kubicka S. 2013. Continuation of bevacizumab after first progression in metastatic colorectal cancer (ML18147): a randomised phase 3 trial. Lancet Oncol, 14(1):29–37.

Bevan, D, Gherardi E, Fan T, Edwards D, Warn R. 2004. Diverse and potent activities of HGF/SF in skin wound repair. J Pathol, 203(3):831–8.

Bilak M, Corse A, Bilak S, Lehar M, Tombran-Tink J, Kuncl R. 1999. Pigment epithelium-derived factor (PEDF) protects motor neurons from chronic glutamate-mediated neurodegeneration. J Neuropathol Exp Neurol, 58:719–28.

Blumberg S, Berger A, Hwang L, Pastar I, Warren S, Chen W. 2012. The role of stem cells in the treatment of diabetic foot ulcers. Diabetes Research and Clinical Practice, 96(1):1–9.

Blume P, Driver V, Tallis A, Kirsner R, Kroeker R, Payne W, Wali S, Marston W, Dove C, Engler R, Chandler L, Sosnowski B. 2011. Formulated collagen gel accelerates healing rate immediately after application in patients with diabetic neuropathic foot ulcers. Wound Repair Regen, 19(3):302–8.

Bodnar RJ. 2015. Chemokine regulation of angiogenesis during wound healing. Adv Wound Care (New Rochelle), 4(11):641-50.

Bokemeyer C, Bondarenko I, Makhson A, Hartmann J, Aparicio J, de Braud F, Donea S, Ludwig H, Schuch G, Stroh C, Loos A, Zubel A, Koralewski. 2009. Fluorouracil, leucovorin, and oxaliplatin with and without cetuximab in the first-line treatment of metastatic colorectal cancer. J Clin Oncol, 27:663–71.

Borgstrom P, Hillan K, Sriramarao P, Ferrara N. 1996. Complete inhibition of angiogenesis and growth of microtumors by anti-vascular endothelial growth factor neutralizing antibodies. Novel concepts of angiostatic therapy from intravital videomicroscopy. Cancer Res, 56:4032–9.

Bosanquet D, Harding K, Ruge F, Sanders A, Jiang W. 2012. Expression of IL-24 and IL-24 receptors in human wound tissues and the biological implications of IL-24 on keratinocytes. Wound Repair Regen, 20(6):896–903.

Bouck N. 2002. PEDF: anti-angiogenic guardian of ocular function. Trends Mol Med, 8(7):330–4.

Brigido S. 2006. The use of an acellular dermal regenerative tissue matrix in the treatment of lower extremity wounds: A prospective 16-week pilot study. Int Wound J, 3:181–7.

Browne M, Stellmach V, Cornwell M, Chung C, Doll J, Lee E, Jameson J, Reynolds M, Superina R, Abramson L, Crawford S. 2006. Gene transfer of pigment epithelium-derived factor suppresses tumor growth and angiogenesis in a hepatoblastoma xenograft model. Pediatr Res, 60(3): 282–7.

Buchberger B, Follmann M, Freyer D, Huppertz H, Ehm A, Wasem J. 2010. The importance of growth factors for the treatment of chronic wounds in the case of diabetic foot ulcers. GMS Health Technol Assess, 6:Doc12. doi: 10.3205/hta000090.

Cai J, Jiang W, Grant M, Boulton M. 2006a. Pigment epithelium-derived factor inhibits angiogenesis via regulated intracellular proteolysis of vascular endothelial growth factor receptor 1. Journal of Biological Chemistry, 281(6):3604–13.

Cai J, Parr C, Watkins G, Jiang W, Boulton M. 2006b. Decreased pigment epithelium-derived factor expression in human breast cancer progression. Clinical cancer research : an official journal of the American Association for Cancer Research, 12(11 Pt 1):3510–7.

Cai W, Ye L, Sun J, Mansel R, Jiang W. 2010. Expression of MLN64 influences cellular matrix adhesion of breast cancer cells, the role for focal adhesion kinase. International Journal of Molecular Medicine, 25:573–80.

Cancer Research UK. 2016. One, five and ten year survival rates for bowel cancer. http://www.cancerresearchuk.org/health-professional/cancer-statistics/statistics-by-cancer-type/bowel-cancer/survival#heading-Zero [Last accessed 19th July 2016].

Carmeliet P & Jain RK. 2011. Molecular mechanisms and clinical applications of angiogenesis. Nature, 473: 298-307.

Carrato A, Swieboda-Sadlej A, Staszewska-Skurczynska M, Lim R, Roman L, Shparyk Y, Bondarenko I, Jonker D, Sun Y, De la Cruz J, Williams J, Korytowsky B, Christensen J, Lin X, Tursi J, Lechuga M, Van Cutsem E. 2013. Fluorouracil, leucovorin, and irinotecan plus either sunitinib or placebo in metastatic colorectal cancer: a randomized, phase III trial. J Clin Oncol, 31(10):1341–7.

Carrell R, Travis J. 1985. α1-Antitrypsin and the serpins: variation and countervariation. Trends in Biochemical Sciences, 10(1):20–4.

Chen J, Ye L, Zhang L, Jiang W. 2009. The molecular impact of pigment epithelium-derived factor, PEDF, on lung cancer cells and the clinical significance. Int J Oncol, 35(1):159–66.

Chen L, Arbieva Z, Guo S, Marucha P, Mustoe T, DiPietro L. 2010. Positional differences in the wound transcriptome of skin and oral mucosa. BMC Genomics, 11:471.

Chen L, Dipietro L. 2014. Production and function of pigment epithelium-derived factor in isolated skin keratinocytes. Experimental Dermatology, 23(6):436–8.

Cheung L, Au S, Cheung A, Ngan H, Tombran-Tink J, Auersperg N, Wong A. 2006. Pigment epithelium-derived factor is estrogen sensitive and inhibits the growth of human ovarian cancer and ovarian surface epithelial cells. Endocrinology, 147(9):4179–91.

Christensen J, Schreck R, Burrows J, Kuruganti P, Chan E, Le P, Chen J, Wang X, Ruslim L, Blake R, Lipson K, Ramphal J, Do S, Cui J, Cherrington J, Mendel D. 2003. A selective small molecule inhibitor of c-Met kinase inhibits c-Met-dependent phenotypes in vitro and exhibits cytoreductive antitumour activity in vivo. Cancer Research, 63(21):7345–55.

Coppinger JA, Cagney G, Toomey S, Kislinger T, Belton O, McRedmond JP, Cahill DJ, Emili A, Fitzgerald DJ, Maguire B. 2004. Characterization of the proteins released from activated platelets leads to localization of novel platelet proteins in human atherosclerotic lesions. Blood, 103:2096-104

Conway K, Ruge F, Price P, Harding K, Jiang W. 2007. Hepatocyte growth factor regulation: An integral part of why wounds become chronic. Wound Repair

Regen, 15:683–92.

Crawford T, Alfaro D, Kerrison J, Jablon E. 2009. Diabetic retinopathy and angiogenesis. Curr Diabetes Rev, 5(1):8–13.

Cullen B, Watt P, Lundqvist C, Silcock D, Schmidt R, Bogan D, Light N. 2002. The role of oxidised regenerated cellulose/collagen in chronic wound repair and its potential mechanism of action. Int J Biochem Cell Biol, 34(12):1544–56.

Cunningham D, Lang I, Marcuello E, Lorusso V, Ocvirk J, Shin D, Jonker D, Osborne S, Andre, N, Waterkamp D, Saunders M; AVEX Study Investigators. 2013a. Bevacizumab plus capecitabine versus capecitabine alone in elderly patients with previously untreated metastatic colorectal cancer (AVEX): an open-label, randomised phase 3 trial. Lancet Oncol, 14(11):1077–85.

Cunningham D, Wong R, D'Haens G, Douillard J-Y, Robertson J, Stone A, Van Cutsem E; on behalf of the HORIZON I study group, 2013b. Cediranib with mFOLFOX6 vs bevacizumab with mFOLFOX6 in previously treated metastatic colorectal cancer. Br J Cancer, 108:493–502.

Dass C, Ek E, Choong PF. 2008. PEDF as an emerging therapeutic candidate for osteosarcoma. Curr cancer drug targets, 8(8):683–90.

Dass C, Tran T, Choong PF. 2007. Angiogenesis inhibitors and the need for anti-angiogenic therapeutics. J Dent Res, 86(10):927–36.

Dawson D, Volpert O, Gillis P, Crawford S, Xu H, Benedict W, Bouck N. 1999. Pigment epithelium-derived factor: a potent inhibitor of angiogenesis. Science, 285(5425):245–48.

de Gramont A, Van Cutsem E, Schmoll H, Tabernero J, Clarke S, Moore M, Cunningham D, Cartwright T, Hecht J, Rivera F, Im S, Bodoky G, Salazar R, Maindrault-Goebel F, Shacham-Shmueli E, Bajetta E, Makrutzki M, Shang A, André T, Hoff P. 2012. Bevacizumab plus oxaliplatin-based chemotherapy as adjuvant treatment for colon cancer (AVANT): a phase 3 randomised controlled trial. Lancet Oncol, 13(12):1225–33.

Díaz R, Peña C, Silva J, Lorenzo Y, García V, García J, Sánchez A, Espinosa P, Yuste R, Bonilla F, Domínguez G. 2008. p73 isoforms affect VEGF, VEGF165b and PEDF expression in human colorectal tumors: VEGF165b downregulation as a marker of poor prognosis. Int J Cancer, 123(5):1060–67.

DiPietro L, Polverini P. 1993. Role of the macrophage in the positive and negative regulation of wound neovascularisation. Am J Pathol, 143:678–84.

Doggett D, Rotenberg M, Pignolo R, Phillips P, Cristofalo V. 1992. Differential gene expression between young and senescent, quiescent WI-38 cells. Mech Ageing Dev, 65(2-3):239–55.

Doll J, Stellmach V, Bouck N, Bergh A, Lee C, Abramson L, Cornwell M, Pins M, Borensztajn J, Crawford S. 2003. Pigment epithelium-derived factor regulates the vasculature and mass of the prostate and pancreas. Nat Med, 9(6):774–80.

Dong Y, Li Z., Sun Y, Zhuang L., Wang Y, Su Q. 2013. Downregulation of pigment epithelium-derived factor in condyloma acuminatum. J Int Med Res, 41(2):365–70.

Douillard J, Siena S, Cassidy J, Tabernero J, Burkes R, Barugel M, Humblet Y, Bodoky G, Cunningham D, Jassem J, Rivera F, Kocákova I, Ruff P, Błasiłska-Morawiec M, Smakal M, Canon J, Rother M, Oliner K, Tian Y, Xu F, Sidhu R, Błasińska-Morawiec M, Smak Sidhu R. 2014. Final results from PRIME: randomized phase III study of panitumumab with FOLFOX4 for first-line treatment of metastatic colorectal cancer. Ann Oncol, 25(7):1346–55.

Drew P, Posnett J, Rusling L. 2007. Wound Care Audit Team. The cost of wound care for a local population in England. Int Wound J, 4:149–55.

Duh E, Yang H, Suzuma I, Miyagi M, Youngman E, Mori K, Katai M, Yan L, Suzuma K, West K, Davarya S, Tong P, Gehlbach P, Pearlman J, Crabb J, Aiello L, Campochiaro P, Zack D. 2002. Pigment epithelium-derived factor suppresses ischaemia-induced retinal neovascularization and VEGF-induced migration and growth. Invst Ophthalmol Vis Sci, 43(3):821–9.

Dunham LJ. 1972. Cancer in man at site of prior benign lesion of skin or mucous membrane: a review. Cancer Res, 32:1359-74.

Dvorak HF. Tumors: wounds that do not heal. Similarities between tumor stroma generation and wound healing. 1986. N Engl J Med, 315:1650-59.

Elayappan B, Ravinarayannan H, Pasha S, Lee K, Gurunathan S. 2009. PEDF inhibits VEGF- and EPO- induced angiogenesis in retinal endothelial cells through interruption of P13K/Akt phosphorylation. Angiogenesis, 12:313-24.

Ellis L, Hicklin D. 2008. VEGF-targeted therapy: mechanisms of anti-tumour activity. Nat Rev Cancer, 8(8):579–91.

Eming SA, Martin P, Tomic-Canic M. 2014. Wound repair and regeneration: mechanisms, signalling, and translation. Sci Trans Med 6(265):265sr6.

Eming A, Wynn TA, Martin P. 2017. Inflammation and metabolism in tissue repair and regeneration. Science 356(6342):1026-1030.

Fernando H, Sanders A, Kynaston H, Jiang W. 2010. WAVE3 is associated with invasiveness in prostate cancer cells. Urol Oncol, 28:320–7.

Ferrara N, Hillan K, Gerber H, Novotny W. 2004. Discovery and development of bevacizumab, an anti-VEGF antibody for treating cancer. Nat Rev Drug Discov, 3(5):391–400.

Filleur S, Volz K, Nelius T, Mirochnik Y, Huang H, Zaichuk T, Aymerich M, Becerra S, Yap R, Veliceasa D, Shroff E, Volpert O. 2005. Two functional epitopes of pigment epithelial-derived factor block angiogenesis and induce differentiation in prostate cancer. Cancer Res, 65(12):5144–52.

Fischer C, Mazzone M, Jonckx B, Carmeliet P. 2008. FLT1 and its ligands VEGFB and PlGF: drug targets for anti-angiogenic therapy? Nat Rev Cancer, 8(12):942–56.

Fitzgerald D, Subramanian P, Deshpande M, Graves C, Gordon I, Qian Y, Snitovsky Y, Liewehr D, Steinburg S, Paltán-Ortiz J, Herman M, Camphausen K, Palmieri D, Becerra S, Steeg PS. 2012. Opposing effects of pigment epithelum-derived factor on breast cancer cell versus neuronal survival: implication for brain metastasis and metastasis-induced brain damage. Cancer Res, 72(1):144–53.

Folkman J. 1995. Angiogenesis in cancer, vascular, rheumatoid and other disease. Nat Med, 1:27–31.

Folkman J. 1971. Tumour angiogenesis: therapeutic implications. N Engl J Med, 285(21):1182–6.

Franceschi S, Gallus S, Talamini R, Tavani A, Negri E, La Vecchia C. 2000. Menopause and colorectal cancer. Br J Cancer, 82:1860–2.

Francis M, Appel S, Meyer C, Balin S, Balin A, Cristofalo V. 2004. Loss of EPC-1/PEDF expression during skin aging in vivo. J Invest Dermatol, 122(5):1096–105.

Fu X, Li X, Cheng B, Chen W, Sheng Z. 2005. Engineered growth factors and cutaneous wound healing: Success and possible questions in the past 10 years. Wound Repair Regen, 13:122–30.

Gao G, Li Y, Gee S, Dudley A, Fant J, Crosson C, Ma J. 2002. Down-regulation of vascular endothelial growth factor and up-regulation of pigment epithelium-derived factor: a possible mechanism for the anti-angiogenic activity of plasminogen kringle 5. J Biol Chem, 277(11):9492–7.

Gates R, King L, Hanks S, Nanney L. 1994. Potential role for focal adhesion kinase in migrating and proliferating keratinocytes near epidermal wounds and in culture. Cell Growth Differ, 5(8):891–9.

Giantonio B, Catalano P, Meropol N, O'Dwyer P, Mitchell E, Alberts S, Schwartz M, Benson, A; Eastern Cooperative Oncology Group Study E3200. 2007. Bevacizumab in combination with oxaliplatin, fluorouracil, and leucovorin (FOLFOX4) for previously treated metastatic colorectal cancer: results from the Eastern Cooperative Oncology Group Study E3200. J Clin Oncol, 25(12):1539–44.

Gibson D, Cullen B, Legerstee R, Harding KG, Schultz G. 2010. MMPs made easy. Wounds Int, 1:1-6.

Golebiewska EM, Poole AW. 2015. Platelet secretion: From haemostasis to wound healing and beyond. Blood Rev, 29(3):153-62.

Gottrup F, Cullen B, Karlsmakr T, Bischoff-Mikkelsen M, Nisbet L, Gibson M. 2013. Randomized controlled trial on collagen/oxidzized regenerated cellulose/silver treatment. Wound Repair Regen, 21:216–25.

Greaves NS, Ashcroft KJ, Baguneid M, Bayat A. 2013. Current understanding of molecular and cellular mechanisms in fibroplasia and angiogenesis during acute wound healing. J Dermatol Sci, 72(3):206-17.

Grothey A, Van Cutsem E, Sobrero A, Siena S, Falcone A, Ychou M, Humblet Y, Bouché O, Mineur L, Barone C, Adenis A, Tabernero J, Yoshino T, Lenz H, Goldberg R, Sargent D, Cihon F, Cupit L, Wagner A, Laurent D; Correct Study Group. 2013. Regorafenib monotherapy for previously treated metastatic colorectal cancer (CORRECT): an international, multicentre, randomised, placebo-controlled, phase 3 trial. Lancet, 381(9863):303–12.

Guan M, Jiang H, Xu C, Xu R, Chen Z, Lu Y, 2007. Adenovirus-mediated PEDF

expression inhibits prostate cancer cell growth and results in augmented expression of PAI-2. Cancer Biol Ther, 6:419–25.

Guan M, Pang C, Yam H, Cheung K, Liu W, Li Y. 2004. Inhibition of glioma invasion by overexpression of pigment-epithelium-derived factor. Cancer Gene Ther, 11:325–32.

Guan M, Yam H, Su B, Chan K, Pang C, Liu W, Zhang W, Lu Y. 2003. Loss of pigment epithelium derived factor expression in glioma progession. J Clin Pathol, 56(4):277–82.

Guan Z, Xu J, Luo R, Feng F, Wang L, Shen L, Yu S, Ba Y, Liang J, Wang D, Qin S, Wang J, He J, Qi C, Xu R. 2011. Efficacy and safety of bevacizumab plus chemotherapy in Chinese patients with metastatic colorectal cancer: a randomized phase III ARTIST trial. Chin J Cancer, 30(10):682–9.

Guang-Wu H, Sunagawa M, Jie-En L, Shimada S, Gang Z, Tokeshi Y, Kosughi T. 2000. The relationship between microvessel density, the expression of vascular endothelial growth factor (VEGF), and the extension of nasopharyngeal carcinoma. Laryngoscope, 110(12):2066–9.

Gurtner GC, Werner S, Barrandon Y, Longaker MT. 2008. Wound repair and regeneration. Nature, 453: 314-21.

Haddow A. 1972. Molecular repair, wound healing, and carcinogenesis: tumour production a possible overhealing? Adv Cancer Res, 16:181-234.

Haertel E, Werner S, Schäfer M. 2014. Transcriptional regulation of wound inflammation. Semin Immunol, 26(4):321-8.

Hagman H, Frödin JE, Berglund Å, Sundberg J, Vestermark LW, Albertsson M, Fernebro E, Johnsson A. 2016. A randomized study of KRAS-guided maintenance therapy with bevacizumab, erlotinib or metronomic capecitabine after first-line induction treatment of metastatic colorectal cancer: the Nordic ACT2 trial. Ann Oncol, 27(1):140-7

Halin S, Wikström P, Rudolfsson S, Stattin P, Doll J, Crawford S, Bergh A. 2004. Decreased pigment epithelium-derived factor is associated with metastatic phenotype in human and rat prostate tumors. Cancer Res, 64(16):5664–71.

Hanahan D, Weinburg RA. 2011. Hallmarks of cancer: The next generation. Cell, 144:646-69.

Harding K, Morris H, Patel G. 2002. Healing chronic wounds. Br Med J, 324:160–3.

Hecht JR, Mitchell E, Chidiac T, Scroggin C, Hagenstad C, Spigel D, Marshall J, Cohn A, McCollum D, Stella P, Deeter R, Shahin S, Amado RG. 2009. A randomized phase IIIB trial of chemotherapy, bevacizumab, and panitumumab compared with chemotherapy and bevacizumab alone for metastatic colorectal cancer. J Clin Oncol, 27(5):672-80.

Hecht J, Trarbach T, Hainsworth J, Major P, Jäger E, Wolff R, Lloyd-Salvant K, Bodoky G, Pendergrass K, Berg W, Chen B, Jalava T, Meinhardt G, Laurent D, Lebwohl D, Kerr D. 2011. Randomized, placebo-controlled, phase III study of first-line oxaliplatin-based chemotherapy plus PTK787/ZK 222584, an oral vascular endothelial growth factor receptor inhibitor, in patients with metastatic

colorectal adenocarcinoma. J Clin Oncol, 29(15):1997–2003.

Hegewisch-Becker S, Graeven U, Lerchenmüller CA, Killing B, Depenbusch R, Steffens CC, Al-Batran SE, Lange T, Dietrich G, Stoehlmacher J, Tannapfel A, Reinacher-Schick A, Quidde J, Trarbach T, Hinke A, Schmoll HJ, Arnold D. 2015. Maintenance strategies after first-line oxaliplatin plus fluoropyrimidine plus bevacizumab for patients with metastatic colorectal cancer (AIO 0207): a randomised, non-inferiority, open-label, phase 3 trial. Lancet Oncol, 16(13):1355-69.

Heidenreich R, Rocken M, Ghoreschi K. 2009. Angiogenesis drives psoriasis pathogenesis. Int J Exp Pathol, 90(3):232–48.

Heinemann V, von Weikersthal LF, Decker T, Kiani A, Vehling-Kaiser U, Al-Batran SE, Heintges T, Lerchenmüller C, Kahl C, Seipelt G, Kullmann F, Stauch M, Scheithauer W, Hielscher J, Scholz M, Müller S, Link H, Niederle N, Rost A, Höffkes HG, Moehler M, Lindig RU, Modest DP, Rossius L, Kirchner T, Jung A, Stintzing S. 2014. FOLFIRI plus cetuximab versus FOLFIRI plus bevacizumab as first-line treatment for patientswith metastatic colorectal cancer (FIRE-3): a randomised, open-label, phase 3 trial. Lancet Oncol, 15(10):1065-75.

Hendifar A, Yang D, Lenz F, Lurje G, Pohl A, Lenz C, Ning Y, Zhang W, Lenz HJ. 2009. Gender disparities in metastatic colorectal cancer survival. Clin Cancer Res, 15:6391–7.

Ho T, Chen S, Yang Y, Liao C, Cheng H, Tsao Y. 2007. PEDF induces p53-mediated apoptosis through PPAR gamma signallin in human umbilical endothelial cells. Cardiovasc Res, 76(2):213–23.

Hoff P, Hochhaus A, Pestalozzi B, Tebbutt N, Li J, Kim T, Koynov K, Kurteva G, Pintér T, Cheng Y, van Eyll B, Pike L, Fielding A, Robertson J, Saunders M. 2012. Cediranib plus FOLFOX/CAPOX versus placebo plus FOLFOX/CAPOX in patients with previously untreated metastatic colorectal cancer: a randomized, double-blind, phase III study (HORIZON II). J Clin Oncol, 30(29):3596–603.

Hollstein M, Soussi T, Thomas G, von Brevern M, Bartsch. 1997. P53 gene alterations in human tumors: perspectives for cancer control. Recent Results Cancer Res, 143:369–89.

Hong H, Zhou T, Fang S, Jia M, Xu Z, Dai Z, Li C, Li S, Li L, Zhang T, Qi W, Bardeesi A, Yang Z, Cai W, Yang X, Gao G. 2014. Pigment epithelium-derived factor (PEDF) inhibits breast cancer metastasis by down-regulating fibronectin. Breast Cancer Res Treat, 148(1):61–72.

Hurwitz H, Fehrenbacher L, Novotny W, Cartwright T, Hainsworth J, Heim W, Berlin J, Baron A, Griffing S, Holmgren E, Ferrara N, Fyfe G, Rogers B, Ross R, Kabbinavar F. 2004. Bevacizumab plus irinotecan, fluorouracil, and leucovorin for metastatic colorectal cancer. N Engl J Med, 350(23):2335–42.

Irving J, Shushanov S, Pike R, Popova E, Brömme D, Coetzer T, Bottomley S, Boulynko I, Grigoryev S, Whisstock J. 2002. Inhibitory activity of a heterochromatin-associated serpin (MENT) against papain-like cysteine proteinases affects chromatin structure and blocks cell proliferation. J Biol Chem, 277:13192–201.

Iwamoto S, Takahashi T, Tamagawa H, Nakamura M, Munemoto Y, Kato T, Hata T, Denda T, Morita Y, Inukai M, Kunieda K, Nagata N, Kurachi K, Ina K, Ooshiro M, Shimoyama T, Baba H, Oba K, Sakamoto J, Mishima H. 2015. FOLFIRI plus bevacizumab as second-line therapy in patients with metastatic colorectal cancer after first-line bevacizumab plus oxaliplatin-based therapy: the randomized phase III EAGLE study. Ann Oncol, 26(7):1427–33.

Ji D, Li M, Zhan T, Yao Y, Shen J, Tian H, Zhang Z, Gu J. 2013. Prognostic role of serum AZGP1, PEDF and PRDX2 in colorectal cancer patients. Carcinogenesis, 34(6):1265–72.

Jia L, Waxman D. 2013. Thrombospondin-1 and pigment epithelium-derived factor enhance responsiveness of KM12 colon tumor to metronomic cyclophosphamide but have disparate effects on tumor metastasis. Cancer Lett, 330(2):241–9.

Jiang W. 2012. Electric Cell-Substrate Impendance Sensing and Cancer Metastasis, London: Springer.

Jiang W, Hiscox S, Hallett M, Horrobin D, Mansel R, Puntis M. 1995a. Regulation of the Expression of E-Cadherin on Human Cancer Cells by γ -Linolenic Acid (GLA). Cancer Res, 55(21):5043–8.

Jiang W, Hiscox S, Hallett M, Scott C, Horrobin D, Puntis M. 1995b. Inhibtion of hepacyte growth factor-induced motility and in vitro invasion of human colon cancer cells by gamma-linolenic acid. Brit J Cancer, 71:744–52.

Jiang Z, Fang Z, Ding Q. 2010. Prognostic role of pigment epithelium-derived factor in clear cell renal cell carcinoma. Urol Int, 84(3):334–40.

Johnsson A, Hagman H, Frödin JE, Berglund A, Keldsen N, Fernebro E, Sundberg J, De Pont Christensen R, Garm Spindler KL, Bergström D, Jakobsen A. 2013. A randomized phase III trial on maintenance treatment with bevacizumab alone or in combination with erlotinib after chemotherapy and bevacizumab in metastatic colorectal cancer: the Nordic ACT Trial. Ann Oncol, 24(9):2335-41.

Jonker D, O'Callaghan C, Karapetis C, Zalcberg J, Tu D, Au H, Berry S, Krahn M, Price T, Simes R, Tebbutt N, van Hazel G, Wierzbicki R, Langer C,Moore M. 2007. Cetuximab for the treatment of colorectal cancer. N Engl J Med, 357(20):2040–8.

Kabbinavar F, Hurwitz H, Fehrenbacher L, Meropol N, Novotny W, Lieberman G, Griffing S, Bergsland E. 2003. Phase II, ranomized trail comparing bevacizumab plus fluorouracil(FU)/leucovorin(LV) with FU/LV alone in patients with metastatic colorctal cancer. J Clin Oncol, 21(1):60–5.

Kakagia D, Kazakos K, Xarchas K, Karanikas M, Georgiadis G, Tripsiannis G, Manolas C. 2007. Synergistic action of protease-modulating matrix and autologous growth factors in healing of diabetic foot ulcers. A prospective randomized trial. J Diabetes Complications, 21(6):387–91.

Keese C, Wegener J, Walker S, Giaever I. 2004. Electrical wound-healing assay for cells in vitro. Proc Natl Acad Sci USA, 101(6):1554–9.

Kerr RS, Love S, Segelov E, Johnstone E, Falcon B, Hewett P, Weaver A, Church D,

Scuddler C, Pearson S, Julier P, Pezzella F, Tomlinson I, Domingo E, Kerr D. 2016. Adjuvant capecitabine plus bevacizumab versus capecitabine alone in patients with colorectal cancer (QUASAR 2): an open-label, randomised phase 3 trial. Lancet Oncol, 17:1543-57.

Kim K, Li J, Houck K, Winer J, Ferrara N. 1992. The vascular endothelial growth factor proteins: identification of biologically relevant regions by neutralizing monoclonal antibodies. Growth Factors, 7:53–64.

Kim TW, Elme A, Kusic Z, Park JO, Udrea AA, Kim SY, Ahn JB, Valencia RV, Krishnan S, Bilic A, Manojlovic N, Dong J, Guan X, Lofton-Day C, Jung AS, Vrdoljak E. 2016. A phase 3 trial evaluating panitumumab plus best supportive care vs best supportive care in chemorefractory wild-type KRAS or RAS metastatic colorectal cancer. Br J Cancer, 115(10):1206-14.

Kim W, Park B, Sung J, Yang J, Park S, Kwak S, Park J. 2007. Wound healing effect of adipose-derived stem cells: A critical role of secretory factors on human dermal fibroblasts. J Derm Sci, 48:15–24.

Koeberle D, Betticher D, von Moos R, Dietrich D, Brauchli, P, Baertschi D, Matter K, Winterhalder R, Borner M, Anchisi S, Moosmann P, Kollar A, Saletti P, Roth A, Frueh M, Kueng M, Popescu R, Schacher S, Hess V, Herrmann R. 2015. Bevacizumab continuation versus no continuation after first-line chemotherapy plus bevacizumab in patients with metastatic colorectal cancer: a randomized phase III non-inferiority trial (SAKK 41/06). Ann Oncol, 26(4):709–14.

Koo JH, Jalaludin B, Wong SK, Kneebone A, Connor SJ, Leong RW. 2008. Improved survival in young women with colorectal cancer. Am J Gastroenterol, 103:1488–95.

Kuncl R, Bilak M, Bilak S, Corse A, Royal W, Becerra S. 2002. Pigment epithelium-derived factor is elevated in CSF of patients with amyotrophic lateral sclerosis. J Neurochem, 81(1):178–84.

Landsman A, Agnew P, Parish L, Joesph R, Galiano RD. 2010. Diabetic foot ulcers treated with becaplermin and TheraGauze, a moisture-controlling smart dressing: a randomized, multicenter, prospective analysis. J Am Podiatr Med Assoc, 100(3):155–60.

Li C, Li W, Man X, Zhou J, Chen J, Cai S, Zheng M. 2011. Pigment epithelium-derived factor plays an inhibitory role in proliferation and migration of HaCaT cells. Mol Biol Rep, 38:2099–105.

Li J, Qin S, Xu R, Yau T, Ma B, Pan H, Xu J, Bai Y, Chi Y, Wang L, Yeh K, Bi F, Cheng Y, Le A, Lin J, Liu T, Ma D, Kappeler C, Kalmus J, Kim TW; CONCUR Investogators. 2015. Regorafenib plus best supportive care versus placebo plus best supportive care in Asian patients with previously treated metastatic colorectal cancer (CONCUR): a randomised, double-blind, placebo-controlled, phase 3 trial. Lancet Oncol, 16:619–29.

Li L, Yang J, Wang W, Yao Y, Fang S, Dai Z, Hong H, Yang, X, Shuai X, Gao G. 2012. Pigment epithelium-derived factor gene loaded in cRGD-PEG-PEI suppresses colorectal cancer growth by targeting endothelial cells. Int J Pharm, 438(1-

2):1–10.

Lu D, Chen B, Liang Z. 2011. Comparison of bone marrow mesenchymal stem cells with bone marrow-derived mononuclear cells for treatment of diabetic critical limb ischemia and foot ulcer: a double-blind, randomized, controlled trial. Diabetes Res Clin Pract, 92(1):26–36.

Majek O, Gondos A, Jansen L, Emrich K, Holleczek B, Katalinic A, Nennecke A, Eberle A, Brenner H; GEKID Cancer Survival Working Group. Sex differences in colorectal cancer survival: population-based analysis of 164,996 colorectal cancer patients in Germany. PLoS One. 2013 Jul 5;8(7):e68077.

Makanya AN, Hlushchuk R, Djonov VG. 2009. Intussusceptive angiogenesis and its role in vascular morphogenesis, patterning, and remodelling. Angiogenesis, 12(2):113-23.

Martí-Carvajal AJ, Gluud C, Nicola S, Simancas-Racines D, Reveiz L, Oliva P, Cedeño-Taborda J.2015. Growth factors for treating diabetic foot ulcers. Cochrane Database Syst Rev (10):CD008548.

Martin T, Watkins G, Mansel R, Jiang W. 2004. Hepatocyte growth factor disrupts tight junctions in human breast cancer cells. Cell Biology Int, 28:361–71.

Masi G, Salvatore L, Boni L, Loupakis F, Cremolini C, Fornaro L, Schirripa M, Cupini S, Barbara C, Safina V, Granetto C, Fea E, Antonuzzo L, Boni C, Allegrini G, Chiara S, Amoroso D, Bonetti A, Falcone A; BEBYP Study Investigators. 2015. Continuation or reintroduction of bevacizumab beyond progression to first-line therapy in metastatic colorectal cancer: final results of the randomized BEBYP trial. Ann Oncol, 26(4):724-30.

Matsui T, Higashimoto Y, Taira J, Yamagishi S. 2013. Pigment epithelium-derived factor (PEDF) binds to caveolin-1 and inhibits the pro-inflammatory effects of caveolin-1 in endothelial cells. Biochem Biophys Res Commun, 441(2):405–10.

Matsumoto K, Ishikawa H, Nishimura D, Hamasaki K, Nakao K, Eguchi K. 2004. Antiangiogenic property of pigment epithelium-derived factor in hepatocellular carcinoma. Hepatology, 40(1):252–9.

Maughan TS, Adam RA, Smith CG, Meade AM, Seymour MT, Wilson RH, Idziaszczyk S, Harris R, Fisher D, Kenny SL, Kay E, Mitchell JK, Madi A, Jasani B, James MD, Bridgewater J, Kennedy MJ, Claes B, Lambrechts D, Kaplan R, Cheadle JP, on behalf of the MRC COIN Trial Investigators. Addition of cetuximab to oxaliplatin-based first line combination chemotherapy for treatment of advacned colorectal cancer: results of the randomised phase 3 MRC COIN trial. Lancet 2011;377:2103-14.

Miller K, Chap L, Holmes F, Cobleigh M, Marcom P, Fehrenbacher L, Dickler M, Overmoyer B, Reimann J, Sing A, Langmuir V, Rugo H. 2005. Randomized phase III trial of capecitabine compared with bevacizumab plus capecitabine in patients with previously treated metastatic breast cancer. J Clin Oncol, 23(4):792–9.

Mulder G, Tallis A, Marshall V, Mozingo D, Phillips L, Pierce G, Chandler L, Sosnowski B. 2009. Treatment of nonhealing diabetic foot ulcers with a

platelet-derived growth factor gene-activated matrix (GAM501): results of a phase 1/2 trial. Wound Repair Regen, 17(6):772–9.

Nazarenko I, Bhatnagar S, Hohman R. 1997. A closed tube format for amplification and detection of DNA based on energy transfer. Nucleic Acids Res, 25(12):2516–21.

Ng E, Adamis A. 2005. Targeting angiogenesis, the underlying disorder in neovascular age-related macular degeneration. Can J Ophthalmol, 40(3):352–68.

NICE. 2010. Bevacizumab in combination with oxaliplatin and either fluorouracil plus folinic acid or capecitabine for the treatment of metastatic colorectal cancer. NICE technology appraisal guidance [TA212]. https://www.nice.org.uk/guidance/ta212 [last accessed 16th July 2016].

NICE. 2009. Cetuximab for the first-line treatment of metastatic colorectal cancer. NICE technology appraisal guidance [TA176]. https://www.nice.org.uk/guidance/TA176/chapter/1-Guidance [last accessed 16th July 2016].

NICE. 2012. Cetuximab, bevacizumab and panitumumab for the treatment of metastatic colorectal cancer after first-line chemotherapy: Cetuximab (monotherapy or combination chemotherapy), bevacizumab (in combination with non-oxaliplatin chemotherapy) and panitumumab (mo. https://www.nice.org.uk/guidance/ta242 [last accessed 16th July 2016].

Numata M, Shiozawa M, Watanabe T, Tamagawa H, Yamamoto N, Morinaga S, Watanabe K, Godai T, Oshima T, Fujii S, Kunisaki C, Rino Y, Masuda M, Akaike M. 2012. The clinicopathological features of colorectal mucinous adenocarcinoma and a therapeutic strategy for the disease. World J Surg Oncol, 10:109.

Ogata N, Matsuoka M, Matsuyama K, Shima C, Tajika A, Nishiyama T, Wada M, Jo N, Higuchi A, Miniamino K, Matsunaga H, Takeda T, Matsumura M. 2007. Plasma concentration of pigment epithelium-derived factor in patients with diabetic retinopathy. J Clin Endocrinol Metab, 92(3):1176–9.

Ohta M, Konno H, Tanaka T, Baba M, Kamiya K, Syouji T, Kondoh K, Watanabe M, Terada H, Nakamura S. 2003. The significance of circulating vascular endothelial growth factor (VEGF) protein in gastric cancer. Cancer Lett, 192(2):215–5.

Passardi A, Nanni O, Tassinari D, Turci D, Cavanna L, Fontana A, Ruscelli S, Mucciarini C, Lorusso V, Ragazzini A, Frassineti GL, Amadori D. 2015. Effectiveness of bevacizumab added to standard chemotherapy in metastatic colorectal cancer: final results for first-line treatment from the ITACa randomized clinical trial. Ann Oncol, 26:1201-7.

Parish C, Jakobsen K, Coombe D. 1992. A basement membrane permeability assay which correlates with the metastatic potential of tumour cells. Int J Cancer, 52:378–83.

Park K, Jin J, Hu Y, Zhou K, Ma J. 2011. Overexpression of pigment epithelium-

derived factor inhibits retinal inflammation and neovascularization. Am J Pathol, 178(2):688–98.

Peeters M, Price T, Cervantes A, Sobrero A, Ducreux M, Hotko Y, Andre T, Chan E, Lordick F, Punt C, Strickland A, Wilson G, Ciuleanu T, Roman L, Van Cutsem E, Tian Y, Sidhu R. 2014. Final results from a randomized phase 3 study of FOLFIRI {+/-} panitumumab for second-line treatment of metastatic colorectal cancer. Ann Oncol, 25(1):107–16.

Petersen S, Valnickova Z, Enghild J. 2003. Pigment-epithelium-derived factor (PEDF) occurs at a physiologically relevant concentration in human blood: purification and characterization. Pigment-epithelium-derived factor (PEDF) occurs at a physiologically relevant concentration in human blood: puri. Biochem J, 371(1):199–206.

Pignolo R, Cristofalo V, Rotenberg M. 1993. Senescent WI-38 cells fail to express EPC-1, a gene induced in young cells upon entry into the G0 state. J Biol Chem, 268:8949–57.

Pignolo R, Kay Francis M, Rotenberg M, Cristofalo V. 2003. Putative role for EPC-1/PEDF in the G0 growth arrest of human diploid fibroblasts. J Cell Physiol, 195(1):12–20.

Pignolo R, Rotenberg M, Cristofalo V. 1995. Analysis of EPC-1 growth state-dependent expression, specificity, and conservation of related sequences. J Cell Physiol, 162(1):110–8.

Pirayesh A, Dessy L, Rogge F, Hoeksema H, Sinove Y, Dall Antonia A, Jawad M, Gilbert P, Rubino C, Scuderi N, Blondeel R, Monstrey S. 2007. The efficacy of a polyhydrated ionogen impregnated dressing in the treatment of recalcitrant diabetic foot ulcers: a multi-centre pilot study. Acta Chir Belg, 107(6):675–81.

Porcher C, Malinge M, Picat C, Grandchamp B. 1992. A simplified method for determination of specific DNA or RNA copy number using quantitative PCR and an automatic DNA sequencer. Biotechniques, 13:106–14.

Presta L, Chen H, O'Connor S, Chisholm V, Meng Y, Krummen L, Winkler M, Ferrara N. 1997. Humanization of an Anti-Vascular Endothelial Growth Factor Monoclonal Antibody for the Therapy of Solid Tumors and Other Disorders. Cancer Res, 57(20):4593–99.

Price TJ, Peeters M, Kim TW, Li J, Cascinu S, Ruff P, Suresh AS, Thomas A, Tjulandin S, Zhang K, Murugappan S, Sidhu R. 2014. Panitumumab versus cetuximab in patients with chemotherapy-refractory wild-type KRAS exon 2 metastatic colorectal cancer (ASPECCT): a randomised, multicentre, open-label, non-inferiority phase 3 study. Lancet Oncol, 15(6):569-79.

Radisky DC, Kenny PA, Bissell MJ. 2007. Fibrosis and cancer: do myofibroblasts come also fro epithelial cells via EMT? J Cell Biochem, 101:830-9.

Reed J, Albino A, McNutt N. 1995. Human cutaneous mast cells express bFGF. Lab Invest, 72:215–22.

Ribatti D. 2006. Genetic and epigenetic mechanisms in the early development of the vascular system. J Anat, 208:139–52.

Ribatti D, Crivellato E. 2012. "Sprouting angiogenesis', a reappraisal. Dev biol, 372(2):157-65.

Rychil K, Kaun C, Hohensinner P, Dorfner A, Pfaffenberger S, Niessner A, Bauer M, Dietl W, Podesser B, Maurer G, Huber K, Wojta J. 2010. The anti-angiogenic factor PEDF is present in the human heart and is regulated by anoxia in cardiac myocytes and fibroblasts. J Cell Mol Med, 14(1-2):198–205.

Saltz L, Clarke S, Díaz-Rubio E, Scheithauer W, Figer A, Wong R, Koski S, Lichinitser M, Yang T, Rivera F, Couture F, Sirzén F, Cassidy J. 2008. Bevacizumab in combination with oxaliplatin-based chemotherapy as first-line therapy in metastatic colorectal cancer: a randomized phase III study. J Clin Oncol, 26(12):2013–9.

Saltz L, Badarinath S, Dakhil S, Bienvenu B, Harker WG, Birchfield G, Tokaz LK, Barrera D, Conkling PR, O'Rourke MA, Richards DA, Reidy D, Solit D, Vakiani E, Capanu M, Scales A, Zhan F, Boehm KA, Asmar L, Cohn A. 2012. Phase III trial of cetuximab, bevacizumab, and 5-fluorouracil/leucovorin vs. FOLFOX-bevacizumab in colorectal cancer. Clin Colorectal Cancer, 11(2):101-11.

Sandler A, Gray R, Perry M, Brahmer J, Schiller J, Dowlati A, Lilenbaum R, Johnson D. 2006. Paclitaxel-carboplatin alone or with bevacizumab for non-small-cell lung cancer. N Engl J Med, 355(24):2542–50.

Sarojini H, Estrada R, Lu H, Dekova S, Lee M, Gray R, Wang E. 2008. PEDF from mouse mesenchymal stem cell secretome attracts fibroblasts. J Cell Biochem, 104(5):1793–802.

Sasaki Y, Naishiro Y, Oshima Y, Imai K, Nakamura Y, Tokino T. 2005. Identification of pigment epithelium-derived factor as a direct target of the p53 family member genes. Oncogene, 24:5131–6.

Sasi W, Ye L, Jiang W, Sharma A, Mokbel K. 2014. In vitro and in vivo effects of suppressor of cytokine signalling 7 knockdown in breast cancer: The influence on cellular response to hepacyte growth factor. Biomed Res Int, 2014:648040.

Sauer G, Hall J. 1996. Manual of Skin Diseases. Philadelphia: Lippincott-Raven Publishers

Sawant S, Aparicio S, Tink A, Lara N, Barnstable C, Tombran-Tink J. 2004. Regulation of factors controlling angiogenesis in liver development: A role for PEDF in the formation and maintenance of normal vasculature. Biochem Biophys Res Commun, 325:408–13.

Schäfer M, Werner S. 2008. Cancer as an overhealing wound: an old hypothesis revisited. Nat Rev Mol Cell Biol, 9:628-38.

Schmoll H, Cunningham D, Sobrero A, Karapetis C, Rougier P, Koski S, Kocakova I, Bondarenko I, Bodoky G, Mainwaring P, Salazar R, Barker P, Mookerjee B, Robertson J, Van Cutsem E. 2012. Cediranib with mFOLFOX6 versus bevacizumab with mFOLFOX6 as first-line treatment for patients with advanced colorectal cancer: a double-blind, randomized phase III study (HORIZON III). J Clin Oncol, 30(29):3588–95.

Schroff R, Foon K, Beatty S, Odham R, Morgan A. 1985. Human anti-murine

immunoglobulin response in patients receiving monoclonal an tibody therapy. Cancer Res, 45:879–85.

Schruefer R, Sulyok S, Schymeinsky J, Peters T, Scharffetter-Kochanek K, Walzog B. 2006. The proangiogenic capacity of PMN delineated by microarray technique and by measurement of neovascularisation in wounded skin of CD-18-deficient mice. J Vasc Res, 43:1–11.

Sen C, Gordillo G, Roy S, Kirsner R, Lambert L, Hunt T, Gottrup F, Gurtner G, Longaker M. 2009. Human skin wounds: a major and snowballing threat to public health and the economy. Wound Repair Regen, 17:763–71.

Seo Y, Baba H, Fukuda T, Takashima M, Sugimachi K. 2000. High expression of vascular endothelial growth factor is associated with liver metastasis and a poor prognosis for patients with ductal pancreatic adenocarcinoma. Cancer, 88(10):2239–45.

Seymour M, Brown S, Middleton G, Maughan T, Richman S, Gwyther S, Lowe C, Seligmann J, Wadsley J, Maisey N, Chau I, Hill M, Dawson L, Falk S, O'Callaghan A, Benstead K, Chambers P, Oliver A, Marshall H, Napp V, Quirke P. 2013. Panitumumab and irinotecan versus irinotecan alone for patients with KRAS wild-type, fluorouracil-resistant advanced colorectal cancer (PICCOLO): A prospectively stratified randomised trial. Lancet Oncol, 14(8):749–59.

Shin E, Sorenson C, Sheibani N. 2014. PEDF expression regulates the proangiogenic and proinflammatory phenotype of the lung endothelium. Am J Physiol Lung Cell Mol Physiol, 306(7):L620–34.

Siu L, Shapiro J, Jonker D, Karapetis C, Zalcberg J, Simes J, Couture F, Moore M, Price T, Siddiqui J, Nott L, Charpentier D, Liauw W, Sawyer M, Jefford M, Magoski N, Haydon A, Walters I, Ringash J, Tu D, O'Callaghan C. 2013. Phase III randomized, placebo-controlled study of cetuximab plus brivanib alaninate versus cetuximab plus placebo in patients with metastatic, chemotherapy-refractory, wild-type K-RAS colorectal carcinoma: the NCIC Clinical Trials Group and AGITG CO.20 Trial. J Clin Oncol, 31(19):2477–84.

Sobrero A, Maurel J, Fehrenbacher L, Scheithauer W, Abubakr Y, Lutz M, Vega-Villegas M, Eng C, Steinhauer E, Prausova J, Lenz H, Borg C, Middleton G, Kröning H, Luppi G, Kisker O, Zubel A, Langer C, Kopit J, Burris H. 2008. EPIC: phase III trial of cetuximab plus irinotecan after fluoropyrimidine and oxaliplatin failure in patients with metastatic colorectal cancer. J Clin Oncol, 26(14):2311–9.

Stathopoulos G, Batziou C, Trafalis D, Koutantos J, Batzios S, Stathopoulos J, Legakis J, Armakolas A. 2010. Treatment of colorectal cancer with and without bevacizumab: a phase III study. Oncology, 78(5-6):376–81.

Steele F, Chader G, Johnson L & Tombran-Tink J. 1993. Pigment epithelium-derived factor: neurotrophic activity and identification as a member of the serine protease inhibitor gene family. Proc Natl Acad Sci U S A, 90(4):1526–30.

Stintzing S, Fischer von Weikersthal L, Decker T, Vehling-Kaiser U, Jäger E, Heintges T, Stoll C, Giessen C, Modest DP, Neumann J, Jung A, Kirchner T, Schietnauer W, Heinemann V. 2012. FOLFIRI plus cetuximab versus FOLFIRI plus

bevacizumab as first-line treatment for patients with metastatic colorectal cancer–subgroup analysis of patients with KRAS: mutated tumours in the randomised German AIO study KRK-0306. Ann Oncol, 23:1693-9.

Stock C, Ihle P, Schubert I, Brenner H. 2011. Colonoscopy and fecal occult blood test use in Germany: results from a large insurance-based cohort. Endoscopy, 43:771–81.

Su Y, Richmond A. 2015. Chemokine regulation of neutrophil infiltration of skin wounds. Adv Wound Care, 4(11):631-40.

Tabernero J, Yoshino T, Cohn AL, Obermannova R, Bodoky G, Garcia-Carbonero R, Ciuleanu TE, Portnoy DC, Van Cutsem E, Grothey A, Prausová J, Garcia-Alfonso P, Yamazaki K, Clingan PR, Lonardi S, Kim TW, Simms L, Chang SC, Nasroulah F; RAISE Study Investigators. 2015. Ramucirumab versus placebo in combination with second-line FOLFIRI in patients with metastatic colorectal carcinoma that progressed during or after first-line therapy with bevacizumab, oxaliplatin, and a fluoropyrimidine (RAISE): a randomised, double-blind, multicentre, phase 3 study. Lancet Oncol, 16(5):499-508.

Taieb J, Tabernero J, Mini E, Subtil F, Folprecht G, Van Laethem JL, Thaler J, Bridgewater J, Petersen LN, Blons H, Collette L, Van Cutsem E, Rougier P, Salazar R, Bedenne L, Emile JF, Laurent-Puig P, Lepage C; PETACC-8 Study Investigators. 2014. Oxaliplatin, fluorouracil, and leucovorin with or without cetuximab in patients with resected stage III colon cancer (PETACC-8): an open-label, randomised phase 3 trial. Lancet Oncol, 15(8):862-73.

Takahashi Y, Kitadai Y, Bucana C, Cleary K, Ellis L. 1995. Expression of vascular endothelial growth factor and its receptor, KDR, correlates with vascularity, metastasis, and proliferation of human colon cancer. Cancer Res, 55:3964–8.

Takenda K, Yamagishi S, Jinnouchi Y, Nakamura K, Imaizumi T. 2005. Pigment epithelium-derived factor (PEDF)-induced apoptosis and inhibition of vascular endothelial growth factor (VEGF) expression in MG63 human osteosarcoma cells. Life Sci, 77(25):3231–41.

Tan M, Choong P, Dass C. 2010. Anti-chondrosarcoma effects of PEDF mediated via molecules important to apoptosis, cell cycling, adhesion and invasion. Biochem Biophys Res Commun, 398:613–8.

Tebbutt NC, Wilson K, Gebski VJ, Cummins MM, Zannino D, van Hazel GA, Robinsn B, Broad A, Ganju V, Ackland SP, Forgeson G, Cunningham D, Saunders MP, Stockler MR, Chua Y, Zalcberg JR, Simes RJ, Price TJ. 2010. Capecitabine, Bevacizumab, and Mitomycin in First-Line Treatment of Metastatic Colorectal Cancer: Results of the Australasian Gastrointestinal Trials Group Randomized Phase III MAX Study. J Clin Oncol, 28(19):3191-8.

Tol J, Koopman M, Cats A, Rodenburg CJ, Creemers GJ, Schrama JG, Erdkamp FL, Vos AH, van Groeningen CJ, Sinnige HA, Richel DJ, Voest EE, Dijkstra JR, Vink-Börger ME, Antonini NF, Mol L, van Krieken JH, Dalesio O, Punt CJ. 2009. Chemotherapy, bevacizumab, and cetuximab in metastatic colorectal cancer. N Engl J Med, 360(6):563-72.

Tombran-Tink J, Chader G, Johnson L. 1991. PEDF: a pigment epithelium-derived

factor with potent neuronal differentiative activity. Exp Eye Res, 53(3):411–4.

Tombran-Tink J, Mazuruk K, Rorıguez I, Chung D, Linker T, Englander E, Chader G. 1996. Organization, evolutionary conservation, expression and unusual Alu denisty of the human gene for pigment epithelium-derived factor, a unique neurotrophic serpin. Mol Vis, 2:11.

Tombran-Tink J, Pawar H, Swaroop A, Rodriguez I, Chader G. 1994. Localization of the gene for pigment epithelium-derived factor (PEDF) to chromosome 17p13.1 and expression in cultured human retinoblastoma cells. Genomics, 19(2):266–72.

Tournigand C, Chibaudel B, Samson B, Scheithauer W, Vernerey D, Mésange P, Lledo G, Viret F, Ramée JF, Tubiana-Mathieu N, Dauba J, Dupuis O, Rinaldi Y, Mabro M, Aucoin N, Latreille J, Bonnetain F, Louvet C, Larsen AK, André T, de Gramont A. 2015. Bevacizumab with or without erlotinib as maintenance therapy in patients with metastatic colorectal cancer (GERCOR DREAM; OPTIMOX3): a randomised, open-label, phase 3 trial. Lancet Oncol, 16(15):1493-505.

Tresini M, Pignolo R, Allen R, Cristofalo V. 1999. Effects of donor age on the expression of a marker of replicative senescence (EPC-1) in human dermal fibroblasts. J Cell Physiol, 179:11–7.

Tveit K, Guren T, Glimelius B, Pfeiffer P, Sorbye H, Pyrhonen S, Sigurdsson F, Kure E, Ikdahl T, Skovlund E, Fokstuen T, Hansen F, Hofsli E, Birkemeyer E, Johnsson A, Starkhammar H, Yilmaz M, Keldsen N, Erdal A, Dajani O, Dahl O, Christoffersen T. 2012. Phase III trial of cetuximab with continuous or intermittent fluorouracil, leucovorin, and oxaliplatin (Nordic FLOX) versus FLOX alone in first-line treatment of metastatic colorectal cancer: the NORDIC-VII study. J Clin Oncol, 30(15):1755–62.

Uehara H, Miyamoto M, Kato K, Ebihara Y, Kaneko H, Hashimoto H, Murakami Y, Hase, R, Takahashi R, Mega S, Shichinohe T, Kawarada Y, Itoh T, Okushiba S, Kondo S, Katoh H. 2004. Expression of pigment epithelium-derived factor decreases liver metastasis and correlates with favourable prognosis for patients with ductal pancreatic adenocarcinoma. Cancer Res, 64(10):3533–37.

Uhlen M. 2005. A Human Protein Atlas for Normal and Cancer Tissues Based on Antibody Proteomics. Mol Cell Proteomics, 4(12):1920–32.

USFDA. 2010. Class Labeling Changes to anti-EGFR monoclonal antibodies, cetuximab (Erbitux) and panitumumab (Vectibix): KRAS Mutations. http://www.fda.gov/AboutFDA/CentersOffices/OfficeofMedicalProductsandTobacco/CDER/ucm172905.htm [last accessed 16th July 2016]

Van Cutsem E, Peeters M, Siena S, Humblet Y, Hendlisz A, Neyns B, Canon JL, Van Laethem JL, Maurel J, Richardson G, Wolf M, Amado RG. 2007. Open-label phase III trial of panitumumab plus best supportive care compared with best supportive care alone in patients with chemotherapy-refractory metastatic colorectal cancer. J Clin Oncol, 25(13):1658-64.

Van Cutsem E, Köhne C, Hitre E, Zaluski J, Chang Chien CR, Makhson A, D'Haens G, Pintér T, Lim R, Bodoky G, Roh JK, Folprecht G, Ruff P, Stroh C, Tejpar S,

Schlichting M, Nippgen J, Rougier P. 2009. Cetuximab and chemotherapy as initial treatment for metastatic colorectal cancer. N Engl J Med, 360(14):1408–17.

Van Cutsem E, Bajetta E, Valle J, Köhne C, Hecht J, Moore M, Germond C, Berg W, Chen B, Jalava T, Lebwohl D, Meinhardt G, Laurent D, Lin E. 2011. Randomized, placebo-controlled, phase III study of oxaliplatin, fluorouracil, and leucovorin with or without PTK787/ZK 222584 in patients with previously treated metastatic colorectal adenocarcinoma. J Clin Oncol, 29(15):2004–10.

Van Cutsem E, Tabernero J, Lakomy R, Prenen H, Prausová J, Macarulla T, Ruff P, van Hazel G, Moiseyenko V, Ferry D, McKendrick J, Polikoff J, Tellier A, Castan R, Allegra C. 2012. Addition of aflibercept to fluorouracil, leucovorin, and irinotecan improves survival in a phase III randomized trial in patients with metastatic colorectal cancer previously treated with an oxaliplatin-based regimen. J Clin Oncol, 30(28):3499–506.

Venook AP, Niedzwiecki D, Lenz HJ, Innocenti F, Fruth B, Meyerhardt JA, Schrag D, Greene C, O'Neil BH, Atkins JN, Berry S, Polite BN, O'Reilly EM, Goldberg RM, Hochster HS, Schilsky RL, Bertagnolli MM, El-Khoueiry AB, Watson P, Benson AB 3rd, Mulkerin DL, Mayer RJ, Blanke C. 2017. Effect of First-Line Chemotherapy Combined With Cetuximab or Bevacizumab on Overall Survival in Patients With KRAS Wild-Type Advanced or Metastatic Colorectal Cancer: A Randomized Clinical Trial. JAMA, 317(23):2392-2401.

Veves A, Sheeshan P, Pham H. 2002. A randomised, controlled trial of promogran (a colagen/oxidized regenerated cellulose dressing) vs standard treatment in the management of diabetic foot ulcers. Arch Surg, 137(7):822–7.

Virchow R, Virchow R. Aetiologie der neoplastichen Geschwulste/ Pathologie der neoplastischen Geschwulste. (Verlag von August Hirschwald, Berlin, Germany, 1863).

Volpert O, Zaichuk T, Zhou W, Reiher F, Ferguson T, Stuart P, Amin M, Bouck N. 2002. Inducer-stimulated Fas targets activated endothelium for destruction by anti-angiogenic thrombospondin-1 and pigment epithelium-derived factor. Nat Med, 8(4):349–57.

Wågsäter D, Löfgren S, Zar N, Hugander A, Dimberg J. 2010. Pigment Epithelium-Derived Factor Expression in Colorectal Cancer Patients. Cancer Invest, 28(8):872-7.

Wang S, Ye L, Sanders A, Ruge F, Harding K, Jiang W. 2016. Tumour endothelial marker-8 in wound healing and its impact on the proliferation and migration of keratinocytes. Int J Mol Med, 37(2):293–8.

Warren, R, Yuan H, Matli M, Gillett N, Ferrara N. 1995. Regulation by vascular endothelial growth factor of human colon cancer tumorigenesis in a mouse model of experimental liver metastasis. J Clin Invest, 95:1789–97.

Weiss S. 1989. Tissue destruction by neutrophils. N Engl J Med, 320:365–76.

Wetzler C, Kampfer H, Stallmeyer B, Pfeilschifter J, Frank S. 2000. Large and sustained induction of chemokines during impaired wound healing in the

genetically diabetic mouse: prolonged persistence of neutrophils and macrophages during the late phase of repair. J Invest Dermsatol, 115:245–53.

Wieman TJ, Smiell JM, Su Y. 1998. Efficacy and safety of a topical gel formulation of recombinant human platelet-derived growth factor-BB (becaplermin) in patients with chronic neuropathic diabetic ulcers. A phase III randomized placebo-controlled double-blind study. Diabetes Care, 21(5):822–7.

Wu Q, Gong C, Luo S, Zhang D, Zhang S, Shi H, Lu L, Yan H, He S, Li D, Yang L, Zhao X, Wei Y. 2012. AAV-mediated human PEDF inhibits tumour growth and metastasis in murine colorectal peritoneal carcinomatosis model. BMC Cancer, 12:129.

Xu X, Zhang S, Barnstable C, Tombran-Tink J. 2006. Molecular phylogeny of the antiangiogenic and neurotrophic serpin, pigment epithelium derived factor in vertebrates. BMC Genomics, 7:248.

Yamagishi S, Adahi H, Abe A, Yashiro T, Enomoto M, Furiki L, Hino A, Jinnouchi Y, Takenaka K, Matsui T, Nakamura K, Imaizumi T. 2006. Elevated serum levels of pigment epithelium-derived factor (PEDF) in the metabolic syndrome. J Clin Endocrinol Metab, 91:2447–50.

Yang, H, Xu Z, Iuvone P, Grossniklaus H. 2006. Angiostatin decreases cell migration and vascular endothelium growth factor (VEGF) to pigment epithelium derived factor (PEDF) RNA ratio in vitro and in a murine ocular melanoma model. Mol Vis, 12:511–7.

Yang J, Haworth L, Sherry R, Hwu P, Schwartzentruber D, Topalian S, Steinberg S, Chen H, Rosenberg S. 2003. A randomised trial of bevacizumab, an anti-vascular endothelial growth factor antibody, for metastatic renal cancer. N Engl J Med, 349(5):427–34.

Zaichuk T, Shroff E, Emmanuel R, Filleur S, Nelius T, Volpert O. 2004. Nuclear factor of activated T cells balances angiogenesis activation and inhibtion. J Exp Med, 199:1513–22.

Zha W, Su M, Huang M, Cai J, Du Q. 2016. Administration of Pigment Epithelium-Derived Factor Inhibits Airway Inflammation and Remodeling in Chronic OVA-Induced Mice via VEGF Suppression. Allergy Asthma Immunol Res, 8(2):161–9.

Zhang C, Xiang L, Shen J, Zhang Y, Li J, Zheng Z. 2009. Expression of pigment epithelium-derived factor in human melanocytes and malignant melanoma cells and tissue. Expression of pigment epithelium-derived factor in human melanocytes and malignant melanoma cells and tissue. Dermato-endocrinol, 1(2):108–13.

Zhang L, Chen J, Ke Y, Mansel R, Jiang W. 2006a. Expression of pigment epithelial derived factor is reduced in non-small cell lung cancer and is linked to clinical outcome. Int J Mol Med, 17(5):937–44.

Zhang S, Wang J, Gao G, Shao C, Mott R, Ma J. 2006b. Pigment epithelium-derived factor (PEDF) is an endogenous antiinflammatory factor. FASEB J, 20(2):323–325.

Zhang T, Guan M, Xu C, Chen Y, Lu Y. 2007. Pigment epithelium-derived factor

inhibits glioma cell growth in vitro and in vivo. Life Sci, 81:1256–63.

Zhou, D, Cheng S, Ji H, Wang J, Xu H, Zhang G, Pang D. 2010. Evaluation of protein pigment epithelium-derived factor (PEDF) and microvessel density (MVD) as prognostic indicators in breast cancer. J Cancer Res Clin Oncol, 136(11):1719–1727.

From:

Professor Wen G. Jiang

Head of MARG and Professor of Surgery,
Cardiff University School of Medicine

To:
Professor Zhong Tao Zhang
Beijing Friendship Hospital
Capital Medical University

10th May 2009

Dear Professor Zhang,

It is my pleasure to attach the MTA document covering the use of the tissues collected at You Yi Hospital as part of the agreement/collaboration with Cardiff University.

Yours sincerely,

Wen G. Jiang

Material Transfer Agreement for the Supply of Human Tissue Materials FOR USE where the material is human organs, tissue or cells (other than human gametes or embryos) but NOT where the intended use is transplantation or human application

This Agreement is made by and between:
a) *Beijing Friendship Hospital, Capital Medical University, Beijing, China* > ("the Provider Institution")
and
b) Professor Wen G. Jiang, Cardiff University School of Medicine, Cardiff University, UK ("the Recipient Institution")

This Agreement records the terms under which the Provider Institution will make available to the Recipient Institution the Material identified in Appendix 2 (the "Material"). The term "Material" means material, other than human gametes or embryos, which consists of, or includes human cells and which is considered "Relevant Material" for the purposes of the Human Tissue Act 2004[1] together with related data. The Recipient Institution will hold the Material on the terms of this Agreement and solely for the purpose of *<description of research to be undertaken using the Material>* ("the Study") and as described in Appendix 1, within the research group of *<name of Recipient Scientist>* ("the Recipient Scientist"). The Recipient Institution hereby agrees to comply and procure that the Recipient Scientist and all personnel who work with the Material comply with the following terms and conditions:

[1] The Human Tissue Act 2004 applies to the "authorised activities" principally the removal, storage and use of "Relevant Materials" (as defined under the Act, including human cells, tissue and organs, but not cell lines) which come from a living or deceased person for "Scheduled Purposes" (these are set out in Schedule 1 of the Act, including, but not limited to, "research in connection with disorders, or the function of the human body", "education or training relating to human health", and "transplantation").

2 The Human Tissue (Quality and Safety for Human Application) Regulations 2007 apply to the procurement, testing, processing, storage, distribution, and import or export of tissues and cells (including cell lines). "Cells" mean human cells (whether individually or in an unbound collection) including cell lines, but not including gametes, embryos outside the body, blood or blood components. "Tissue" for the Regulations, means all constituent parts of the human body formed by cells, but not including gametes and embryos outside the body (which are regulated by the Human Fertilisation and Embryology Authority pursuant to the Human Fertilisation and Embryology Act 1990), or organs.

3 Applicable Laws means all laws, rules, regulations, codes of practice, research governance or ethical guidelines, or other requirements of any Regulatory Authority, that may apply to the use of the Material by the Recipient

1. The Recipient Institution will not use the Material for administration to human subjects or human application as that term is defined in the Human Tissue (Quality and Safety for Human Application) Regulations 2007 (or equivalent as each may be replaced or amended from time to time), or for clinical or diagnostic purposes.2
2. The Recipient Institution may use the Material for the purposes of the Study and as described in Appendix 1, from the date of receipt of the Material. The Recipient Institution will comply fully with all applicable environmental, health and safety laws, the Human Tissue Act 2004 and other Applicable Laws3 with respect to its use (including, but not limited to, disposal or return).

Institution from time to time, including (but not limited) the Human Tissue Act 2004 or the Human Tissue (Scotland) Act 2006, the Human Tissue (Quality and Safety for Human Application) Regulations 2007, the Human Fertilisation and Embryology Act 1990 (as amended), the EU Tissues and Cells Directive (2004/23/EC) and Commission Directives 2006/17/EC and 2006/86/EC. The Human Tissue Authority Directions and Codes of Practice, and the Medicines for Human Use (Clinical Trials) Regulations 2004, as updated and amended from time to time and, where relevant, the national implementations of the same.

3. The Provider Institution makes no charge for the Material / the Material is provided subject to the reimbursement by the Recipient Institution to the Provider Institution for its costs of extracting from storage and preparing the Material as set out in Appendix 2. Risk in and responsibility for the Material shall pass to the Recipient Institution once it is loaded onto transport as organised by the Recipient Institution. If so requested by the Provider Institution the Recipient Institution shall provide it with written confirmation of the safe receipt of the Materials promptly after their delivery to the Recipient Institution's laboratory.

4. The Recipient Institution understands that the Material may have hazardous properties, contain infectious agents or pose other health and safety risks. Subject to clause 9, the Provider Institution makes no representations and gives no warranties either express or implied in relation to it: for example (without limitation), no warranties are given about quality or fitness for a particular purpose, or freedom from infection. The Provider Institution will not be liable for any use made of the Material by the Recipient Institution. The Recipient Institution will use the Material in accordance with good laboratory practice standards, all due skill and care and with dignity, sensitivity and respect. The Recipient Institution will comply with all Applicable Laws, approvals, rules, codes of practice and regulations governing the transportation, storage, use and disposal of the Material. The Recipient Institution warrants that it will only use, or permit the use of the Material in work that has ethical approval, as stated in Appendix 1.
5. Except to the extent prohibited by Law and subject to clause 9, the Recipient Institution assumes all liability for damages which may arise from its receipt, use, storage or disposal of the Material. The Provider Institution will not be liable to the Recipient Institution for any loss, claim or demand made by the Recipient Institution, or made against the Recipient Institution by any other party, due to or arising from its use, storage or disposal of the Material by the Recipient Institution, except to the extent the law otherwise requires.
6. The liability of either party for any breach of this Agreement, or arising in any other way out of the subject matter of this Agreement, will not extend to loss of business or profit, or to any indirect or consequential damages or losses.
7. The Recipient Institution agrees to obtain the written consent of the Provider Institution if there is any material change to the proposed use of the Material in the Study as described in Appendix 1.
8. The Recipient Scientist will acknowledge the source of the Material in any publication reporting on its use. If the Recipient Scientist wishes to include in a publication any information which has been provided by the Provider Institution with the Material and which was clearly marked as "confidential" and "proprietary" at the point of disclosure ("Confidential Information"), the Recipient Scientist must obtain written permission from the Provider Institution, providing a copy of the text to allow a reasonable period for review before publication takes place, such permission not to be unreasonably withheld or delayed. If so requested by the Provider Institution, the Recipient Institution shall provide the Provider Institution with a confidential copy of the findings of the Study.
9. The Provider Institution warrants that where required by Applicable Laws the Material has been obtained from humans with the appropriate consent as required by the Human Tissue Act 2004 and with ethical approval and the Provider Institution shall be liable for any claims arising due to the breach of this warranty.

The Provider Institution hereby grants to the Recipient Institution a non-exclusive research licence to use the Material for the Study only. The Provider Institution further warrants that it has not provided any information (and does not intend to provide any information) which has led or may lead to the Recipient Institution being able to identify the person from whom the relevant material came

10. The Recipient Institution undertakes to store the Material in accordance with all Applicable Laws and not to attempt to identify or contact the donor of the Material or to compromise or otherwise infringe the confidentiality of information on the donors and their right to privacy.

11. Nothing included in this Agreement shall prevent the Provider Institution from being able to distribute the Material to other entities as described in Appendix 1. If, as per the details included in Appendix 1, the Material is to be transferred to another institution for the purposes of the Study, the responsibility for compliance with the terms of this Agreement rests with the Recipient Institution.

12. The Provider Institution has the right to terminate this agreement forthwith at any time by means of written notice to Recipient Institution if the ethical approval is withdrawn or if the Recipient Institution is in breach of this Agreement. In the case of any termination, the Recipient Institution shall immediately discontinue all use of the Material and, at the Provider Institution's discretion, promptly return or destroy (at the Recipient Institution's own cost) all unused Material and provide written confirmation that this has been completed. If requested, the Recipient Institution must certify that it has complied in full with any such requirement of the Provider Institution. Should an individual donor or their next of kin rescind their consent, the Provider Institution will require and the Recipient Institution agrees to discontinue using the appropriately identified sample and return or destroy it in accordance with the Provider Institution's instructions.

13. This Agreement shall be governed by English Law, and the English Courts shall have exclusive jurisdiction to deal with any dispute which may arise out of or in connection with this Letter Agreement.

Accepted and Agreed *by an authorised signatory* on behalf of	Accepted and Agreed on behalf of
<Recipient Institution>	*<the Provider Institution>*
Dr Kathryn Pittard Davies Deputy Director and Head of Research Governance and Contracts Research Innovation Services CARDIFF UNIVERSITY	
Name: Prof Wen G. Jiang	Name: Professor Zhong Tao Zhang
09/06/2009	
Position: Professor of Surgery and Head of MARG, Cardiff University	Position: Professor of Beijing Friendship Hospital
Signature	Signature:
Date: 10/05/2009	Date: 10/05/2009

APPENDIX 1: Study description and details of Materials

TO BE COMPLETED BY THE RECIPIENT INSTITUTION'S SCIENTIST:

1. STUDY DESCRIPTION: Evaluation of differential molecule expression between cancerous and non-cancerous human tissues

2. DETAILS OF MATERIALS REQUESTED (type of material, quantity, numbers of material): Wax sections, numbers undetermined

3. DETAILS OF COURIER TO BE USED AND COURIER ACCOUNT CODE: Materials to be brought by Research fellows from Capital Medical University

4. LOCATION OF LABORATORY WHERE MATERIALS ARE TO BE HELD/USED: MARG laboratories, Section of Surgery, 2nd Floor, Main Building, Cardiff University School of Medicine

5. HTA LICENCE / ETHICS APPROVAL:

Complete one of the following:

■ This Study has been given a favourable opinion by an ethics committee which, within the UK, is recognised under the Human Tissue Act 2004. Please provide the reference of the opinion and name of the committee: Ethics Committee of Beijing You Yi Hospital

Or:

☐ The Materials are to be stored in premises licensed by the Human Tissue Authority, until favourable ethical approval has been obtained for the proposed Study at which point the Recipient Scientist shall notify the Provider Institution. Please provide the licence number:

Or:

☐ Where the Materials are supplied by the Provider Institution from a research tissue bank which may be a diagnostic archive and which has been granted REC approval for specific research projects, this REC approval may cover the research Study with the materials at the Recipient Institution. If this is the case, the Designated Individual (or their duly authorised delegate) of the Provider Institution confirms that its REC approval for the tissue bank will cover the proposed Study by signing here:

APPENDIX 2: Delivery and Storage of Materials

TO BE COMPLETED BY THE PROVIDER INSTITUTION:

1. QUANTITY OF MATERIALS TO BE DELIVERED:

Undetermined number of wax embedded human tissue samples.

2. COST OF SAMPLE PREPARATION:

N/A

3. CONDITIONS OF STORAGE

Dry, at room temperature

4. RETURN/DESTRUCTION OF SURPLUS MATERIALS ON COMPLETION OF STUDY

If there are any Materials left over from the Study, the Recipient Institution needs to provide confirmation to the Provider Institution that any remaining Material will be destroyed and that the Recipient Institution needs to provide confirmation to the Provider Institution that this has been completed).

APPENDIX 1: Study description and details of Materials

TO BE COMPLETED BY THE RECIPIENT INSTITUTION'S SCIENTIST:

1. **STUDY DESCRIPTION: Evaluation of differential molecule expression between cancerous and non-cancerous human tissues**

2. **DETAILS OF MATERIALS REQUESTED (type of material, quantity, numbers of material): Wax sections, numbers undetermined**

3. **DETAILS OF COURIER TO BE USED AND COURIER ACCOUNT CODE: Materials to be brought by Research fellows from Peking University**

4. **LOCATION OF LABORATORY WHERE MATERIALS ARE TO BE HELD/USED: MARG laboratories, Section of Surgery, 2nd Floor, Main Building, Cardiff University School of Medicine**

5. **HTA LICENCE / ETHICS APPROVAL:**

Complete one of the following:

■ This Study has been given a favourable opinion by an ethics committee which, within the UK, is recognised under the Human Tissue Act 2004. Please provide the reference of the opinion and name of the committee: Ethics Committee of Beijing Cancer Hospital Ethics number 2006021

Or:

☐ The Materials are to be stored in premises licensed by the Human Tissue Authority, until favourable ethical approval has been obtained for the proposed Study at which point the Recipient Scientist shall notify the Provider Institution. Please provide the licence number:

Or:

☑ Where the Materials are supplied by the Provider Institution from a research tissue bank which may be a diagnostic archive and which has been granted REC approval for specific research projects, this REC approval may cover the research Study with the materials at the Recipient Institution. If this is the case, the Designated Individual (or their duly authorised delegate) of the Provider Institution confirms that its REC approval for the tissue bank will cover the proposed Study by signing here:

APPENDIX 2: Delivery and Storage of Materials

TO BE COMPLETED BY THE PROVIDER INSTITUTION:

1. QUANTITY OF MATERIALS TO BE DELIVERED:

Undetermined number of wax embedded human tissue samples.

2. COST OF SAMPLE PREPARATION:

N/A

3. CONDITIONS OF STORAGE

Dry, at room temperature

4. RETURN/DESTRUCTION OF SURPLUS MATERIALS ON COMPLETION OF STUDY

If there are any Materials left over from the Study, the Recipient Institution needs to provide confirmation to the Provider Institution that any remaining Material will be destroyed and that the Recipient Institution needs to provide confirmation to the Provider Institution that this has been completed).

SNAP i.d.™ OVERVIEW OF PROCEDURE

Before using the SNAP i.d. Protein Detection System, please read the User Guide completely.

1. Open the blot holder lid, taking care not to damage the inner white surface.

2. Thoroughly wet the white surface of the blot holder with Milli-Q® water.
   NOTE: If using only one well of a double or triple well blot holder, the unused well(s) must also be wet.

3. Place the pre-wet blot in the center of the blot holder with the protein side down. The blot membrane should not exceed size specified in the User Guide.

4. Roll blot membrane gently to remove air bubbles.

5. Place the spacer (wetting not necessary) on top of the blot membrane and roll again to ensure contact of spacer with blot membrane.

6. Close the blot holder lid.

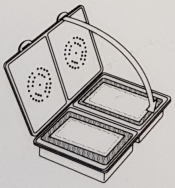

7. Squeeze firmly at base of tab area to secure lid.

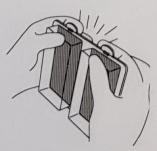

8. Open lid of system and place blot holder in chamber, aligning blot holder tabs with notches of chamber. Close and latch lid.

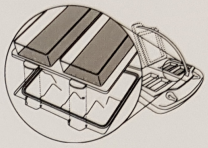

9. Add volume of blocking solution as indicated under **OPTIMIZATION GUIDELINES** on reverse side. Using knobs on the system, apply vacuum until well(s) are completely empty.
   TURN VACUUM OFF.

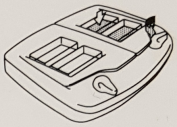

10. Add volume of primary antibody as indicated under **OPTIMIZATION GUIDELINES** on reverse side. Antibody solution must evenly cover ***entire*** blot holder surface.
    Incubate for 10 minutes at room temperature. Solution will be absorbed into the blot holder and surface may appear dry. Apply vacuum.
    IMPORTANT: Do not apply vacuum until after the 10-minute incubation.

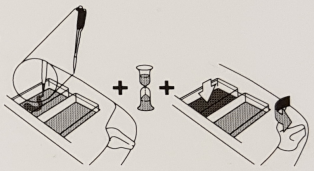

11. With vacuum running continuously, wash 3 times with wash buffer. See **OPTIMIZATION GUIDELINES** on reverse side for volumes.
    TURN VACUUM OFF.

12. Apply appropriate volume of secondary antibody (see **OPTIMIZATION GUIDELINES** on reverse side) evenly across the blot holder surface. Incubate for 10 minutes at room temperature. Again, solution will be absorbed into the blot holder and surface may appear dry. Apply vacuum.
    IMPORTANT: Do not apply vacuum until after the 10-minute incubation.

13. With vacuum on, wash 3 times with buffer. See **OPTIMIZATION GUIDELINES** on reverse side for volumes.
    TURN VACUUM OFF.

14. Remove blot and incubate with the appropriate detection reagent such as Immobilon® HRP, or, if using Millipore fluorescently labeled antibodies, visualize.

00103870 Rev. A, 01/08

SNAP i.d. OPTIMIZATION GUIDELINES

Blocking, Antibody and Wash Recommended Volumes

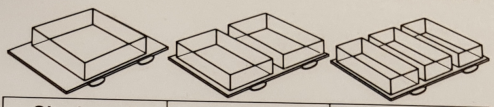

	Single well	Double well	Triple well
Blocking solution volume	30 mL/well	15 mL/well	10 mL/well
Antibody volume	3 mL/well	1.5 mL/well	1 mL/well
Wash buffer* volume	30 mL/well	15 mL/well	10 mL/well

* *Tris or phosphate buffered saline solutions, supplemented with 0.1% Tween® 20 surfactant.*

It is not necessary to use all the wells of double and triple well blot holders, but unused wells must be wet out with Milli-Q water.

Blot Blocking Concentration

- **The use of non-fat/low fat dry milk at concentrations higher than 0.5% is not recommended, as this will result in clogging of the blot holder and prevent reagent flow.**
- Blocking agents should be prepared in tris or phosphate buffered saline solutions containing 0.1% Tween 20 surfactant, to reduce surface tension and ensure even distribution of blocking agent across the blot holder surface.
- The SNAP i.d. system is compatible with the most commonly used blocking agents. Refer to User Guide for complete list with recommended concentrations.
- In order to insure optimal flow through the blot holder, it is essential that blocking solutions be completely solubilized and free of all particulate matter. In some cases, it may be necessary to reduce the concentration of the blocking agent to achieve the required flow.

Antibody Volume and Concentration

- **Most users will be able to use the same amount of antibody, but in 1/3 to 1/5 the volume at 3–5 fold higher concentration.**

	Standard Immunodetection	SNAP i.d. Immunodetection
Mass of antibody required	**1 µg**	**1 µg**
Stock solution	1 mg/mL	1 mg/mL
Diluted stock	1:10,000 (0.1 µg/mL)	1:3,333 (0.33 µg/mL)
Volume required for assay	10 mL	3 mL
Antibody used	0.1 µg/mL × 10 mL = 1 µg	0.33 µg/mL × 3 mL = 1 µg

This guideline is intended as a starting point to develop the final antibody concentration necessary for desired performance. Because each antibody is different, it may be necessary to adjust the blot exposure time, antigen load or both.